UNIVERSIDADE FEDERAL DE MINAS GERAIS
Escola de Engenharia
Programa de Pós-Graduação em Saneamento, Meio Ambiente e Recursos Hídricos

Pâmela Beccalli Vilela

TACKLING ANTIMICROBIAL RESISTANCE VIA SECONDARY WASTEWATER POST-TREATMENT USING SOLAR IRRADIATED OXIDATIVE PROCESSES

Belo Horizonte
2023

Pâmela Beccalli Vilela

TACKLING ANTIMICROBIAL RESISTANCE VIA SECONDARY WASTEWATER POST-TREATMENT USING SOLAR IRRADIATED OXIDATIVE PROCESSES

Thesis presented to the Post-Graduation Program on Sanitation, Environment and Water Resources of the Federal University of Minas Gerais, as an intermediary requirement to obtain the Ph.D. title on Sanitation, Environment, and Water Resources.

Research Field: Environment

Research Line: Characterization, prevention, and control of pollution

Supervisor: Profa. Dra. Camila Costa Amorim

Co-Supervisor: Profa. Dra. Juliana Calábria de Araújo and Profa. Dra. Maria Clara Vieira Martins Starling

Belo Horizonte
2023

Vilela, Pâmela Beccalli.
V699t Tackling antimicrobial resistance via secondary wastewater post-treatment using solar irradiated oxidative processes [recurso eletrônico] / Pâmela Becalli Vilela. -2023.
1 recurso online (220 f. : il., color.) : pdf.

Orientadora: Camila Costa Amorim.
Coorientadoras: Juliana Calábria de Araújo, Maria Clara Vieira Martins Starling.

Tese (doutorado) - Universidade Federal de Minas Gerais, Escola de Engenharia.

Bibliografia: f. 179-220.
Exigências do sistema: Adobe Acrobat Reader.

1. Engenharia sanitária - Teses. 2. Saneamento - Teses. 3. Águas residuais - Tratamento - Teses. 4. Energia solar - Teses. 5. Sulfatos - Teses. 6. Vargem das Flores, Reservatório de - Teses. I. Amaral, Camila Costa de Amorim. II. Araújo, Juliana Calábria. III. Starling, Maria Clara Vieira Martins. IV. Universidade Federal de Minas Gerais. Escola de Engenharia. V. Título.

CDU: 628(043)

Ficha catalográfica elaborada pelo bibliotecário Reginaldo César Vital dos Santos CRB/6 2165
Biblioteca Prof. Mário Werneck, Escola de Engenharia da UFMG

UNIVERSIDADE FEDERAL DE MINAS GERAIS
ESCOLA DE ENGENHARIA
PROGRAMA DE PÓS-GRADUAÇÃO EM SANEAMENTO, MEIO AMBIENTE E RECURSOS HÍDRICOS

FOLHA DE APROVAÇÃO

"Tackling Antimicrobial Resistance Via Secondary Wastewater Post-treatment Using Solar Irradiated Oxidative Processes"

PÂMELA BECALLI VILELA

Tese defendida e aprovada pela banca examinadora constituída pelos Senhores:

Prof. Camila Costa de Amorim Amaral

Prof. Juliana Calábria de Araújo

Prof. Maria Clara Vieira Martins Starling

Prof. Célia Maria Manaia Rodrigues

Prof. Ana Rita Lado Teixeira Ribeiro

Prof. Felipe Piedade Gonçalves Neves

Aprovada pelo Colegiado do PG SMARH

Profa. Priscilla Macedo Moura

Coordenadora

Versão Final aprovada por

Profª. Camila Costa de Amorim Amaral

Orientadora

Belo Horizonte, 05 de setembro de 2023.

Documento assinado eletronicamente por **Ana Rita Lado Teixeira Ribeiro**, **Usuário Externo**, em 05/09/2023, às 12:00, conforme horário oficial de Brasília, com fundamento no art. 5º do Decreto nº 10.543, de 13 de novembro de 2020.

Documento assinado eletronicamente por **Maria Clara Vieira Martins Starling**, **Professora do Magistério Superior**, em 05/09/2023, às 12:23, conforme horário oficial de Brasília, com fundamento no art. 5º do Decreto nº 10.543, de 13 de novembro de 2020.

Documento assinado eletronicamente por **Célia Maria Manaia Rodrigues**, **Usuário Externo**, em 12/09/2023, às 08:45, conforme horário oficial de Brasília, com fundamento no art. 5º do Decreto nº 10.543, de 13 de novembro de 2020.

Documento assinado eletronicamente por **Felipe Piedade Goncalves Neves**, **Usuário Externo**, em 12/09/2023, às 13:44, conforme horário oficial de Brasília, com fundamento no art. 5º do Decreto nº 10.543, de 13 de novembro de 2020.

Documento assinado eletronicamente por **Camila Costa de Amorim Amaral**, **Professora do Magistério Superior**, em 13/09/2023, às 06:06, conforme horário oficial de Brasília, com fundamento no art. 5º do Decreto nº 10.543, de 13 de novembro de 2020.

Documento assinado eletronicamente por **Juliana Calabria de Araujo**, **Professora do Magistério Superior**, em 13/09/2023, às 09:31, conforme horário oficial de Brasília, com fundamento no art. 5º do Decreto nº 10.543, de 13 de novembro de 2020.

A autenticidade deste documento pode ser conferida no site https://sei.ufmg.br/sei/controlador_externo.php?acao=documento_conferir&id_orgao_acesso_externo=0, informando o código verificador **2603160** e o código CRC **8E937CC2**.

Referência: Processo nº 23072.254362/2023-75 SEI nº 2603160

Dedico esta tese às minhas três mães:

À minha mãe do coração, por me ensinar a ser bondosa,
À minha mãe verdadeira, por me ensinar a ser guerreira,
À minha mãe acadêmica, por me ensinar a ir além,
sempre!

AGRADECIMENTOS

Primeiramente, à minha família por sempre acreditar nos meus sonhos. Obrigada pelo apoio incondicional, por todo cuidado e cumplicidade que compartilhamos. Sou grata pelo carinho, confiança e incentivo que vocês sempre me oferecem, mesmo diante das dificuldades enfrentadas. Sem o suporte de vocês, seria impossível alcançar mais essa conquista. Vocês são meu maior exemplo e a minha principal motivação para continuar seguindo em frente, enfrentando desafios e buscando novos sonhos.

Gostaria de expressar minha gratidão à minha orientadora Camila por tudo ... e por tanto. As oportunidades proporcionadas nesses anos de parceria foram fundamentais para o meu aprimoramento e desenvolvimento, pessoal e profissional. Agradeço também pelo constante incentivo, confiança, carinho e amizade cultivados ao longo deste período. Você me ensinou a almejar sempre a excelência e sua orientação inestimável me motivou a superar os desafios de forma contínua, sem desistir JAMAIS. Minha eterna gratidão!

Às minhas coorientadoras, Maria Clara e Juliana, e a professora Renata, cuja colaboração foi essencial para tornar este trabalho tão abrangente e multidisciplinar. Obrigada a todas pela orientação, apoio e confiança, fundamentais para a realização deste trabalho. Agradeço também à UFMG e ao Programa de Pós-Graduação em Saneamento, Meio Ambiente e Recursos Hídricos pela oportunidade. Em especial aos professores, pelo conhecimento transmitido, e pela dedicação ao ensino de qualidade.

Aos meus ICs, em especial Felipe, Giovanna e Victória, sou extremamente grata. Sem o auxílio, companheirismo (mesmo trabalhando até altas horas da noite) e amizade de vocês, este trabalho não seria o mesmo. Afinal, ninguém solta a mão de ninguém! A todos os amigos que o GruPOA e o SIMOA me proporcionaram, agradeço a constante troca de experiências, acadêmicas e de vida. Em especial a Eliz, Adri, Shay, Val, Fê e Rondon por quem eu carrego um imenso carinho, grande admiração e profunda gratidão. À Elayne, por compartilhar seu conhecimento e por ser uma ajuda essencial nos momentos de desespero.

Aos meus trololós e as minhas “sobreviventes”, por estarem sempre presentes, mesmo à distância. Especialmente à Larissa e Drielle, pelo incentivo, carinho e apoio

incondicional em todos os momentos. Ao meu primo Michel, por me avisar desde o princípio que era cilada, e ao meu primo Adriano, por estar presente nos melhores momentos, e por se fazer presente nos piores. À minha amiga Tata, me salvando *since* 1999, seguimos sempre juntas nessa jornada. Obrigada por ouvir minhas crises, por me ensinar o “dogma central” da microbiologia, e por me dar resistência nos momentos essenciais. Ao Ruan agradeço por sempre me desafiar a dar o meu melhor, por ser sempre motivador (e insistente!), e por me mostrar que exercício físico e saúde mental são inseparáveis.

Aos alunos que tive a oportunidade de ensinar, expresso minha gratidão por me mostrarem que eu estava no caminho certo. Obrigado por me inspirarem e por me motivarem a continuar trilhando esse caminho. Vocês foram a minha prova de que o ensino é uma jornada enriquecedora e recompensadora, mesmo que às vezes seja desafiadora. Obrigado por tornarem meu trabalho significativo e por me lembrarem constantemente do impacto positivo que posso ter.

À Minerva e Catarina, minha gratidão, vocês são fontes inesgotáveis de amor e carinho, e sempre serão meu coração fora do peito. Sua presença traz uma alegria indescritível, e minha vida é infinitamente melhor por causa de vocês.

Gostaria de agradecer ao CNPq pela concessão da bolsa de estudos, fundamental no desenvolvimento e na dedicação a esta pesquisa, e à Fundação Bill e Melinda Gates por proporcionar os recursos necessários para elevar o nível do trabalho realizado. Agradeço também à CAPES e a FAPEMIG, assim como a CEMIG/ANEEL, pelos recursos disponibilizados por meio de projetos de pesquisa e extensão, cruciais para o desenvolvimento de pesquisas científicas.

Aos membros da banca examinadora pelo interesse e disponibilidade em avaliar e contribuir com este trabalho.

Por fim, expresso minha gratidão às forças misteriosas que regem esse universo, tão incrível em sua complexidade. E agradeço, imensamente, a todos aqueles que contribuíram direta e indiretamente para a realização deste trabalho.

Meu mais sincero agradecimento a todos vocês!

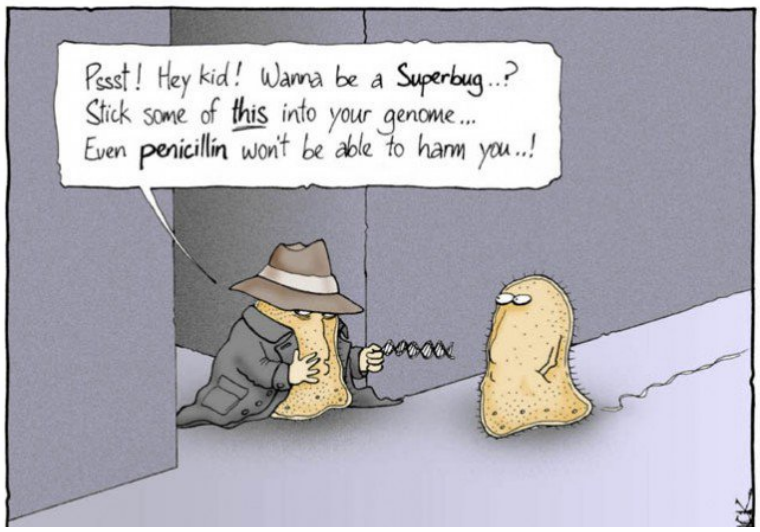

It was on a fateful journey through the wastewater treatment system that Albert was first approached by a member of the Antimicrobial Resistance

RESUMO

O efluente de Estações de Tratamento de Efluentes (ETEs) contém milhares de cepas resistentes à antibióticos, que carregam numerosos genes de resistência, e suas variantes. Consequentemente, a destinação final desse efluente desempenha um papel crítico na disseminação da resistência antimicrobiana (RAM). Portanto, evitar essa propagação é uma preocupação de saúde pública, tornando essencial a desinfecção do efluente de ETEs. No entanto, as tecnologias convencionais (*e.g.* processos de cloração e UV) ou avançadas (*i.e.* ozonização) mostraram-se ineficazes para esse propósito. Em contraste, processos oxidativos avançados são alternativas viáveis, pois os radicais oxidativos formados na reação danificam os constituintes celulares e as estruturas de ácido nucleico por meio de reações de radicais livres. O foto-Fenton constitui um método promissor, promovendo a remoção efetiva de bactérias resistentes a antibióticos (BRA) e dos genes de resistência associados (GRA). No entanto, considerando o pH natural do efluente (6,0 – 7,5), a principal limitação desta aplicação é o pH ideal de operação (2,8 – 3,0). Uma alternativa aplicável é a adição intermitente de ferro, que garante a presença de espécies reativas de Fe^{2+} ao longo do tratamento com pH circunneutro. Essa estratégia tem se mostrado eficaz e é um diferencial neste trabalho. Além disso, o foto-Fenton pode ser realizado sob luz solar, destacando-se sua aplicação em áreas de alta irradiância. Assim, o foto-Fenton solar (FFS) é um tratamento complementar eficiente e ambientalmente sustentável para ETEs. No entanto, enquanto geralmente apenas radicais hidroxila altamente reativos e não seletivos (HO•) são gerados no FFS, o radical sulfato ($SO4^{\bullet-}$) apresenta maior seletividade e um tempo de meia-vida mais longo. No entanto, a eficiência do FFS aprimorado ainda não está clara. Portanto, este trabalho explora o uso de peróxido (H_2O_2), persulfato (PS - $S_2O_8^{-2}$) e um sistema combinado (H_2O_2 e $S_2O_8^{-2}$) como oxidantes. Este trabalho visa combater a RAM por meio do pós-tratamento do efluente secundário de ETEs usando FFS. Os primeiros resultados publicados indicam a eficácia do FFS para a remoção e inativação de plasmídeos que conferem resistência, limitando a descarga desses vetores, que são cruciais para a disseminação da RAM no ambiente. Além disso, embora a maioria dos estudos tenha se baseado exclusivamente em métodos dependentes de cultura, este é o primeiro estudo que investiga o efeito do FFS em BRA e GRAs por meio de análise metagenômica de alto rendimento (16S rDNA e Whole Genome Sequencing). Resultados como remoção efetiva de ARGs, patógenos de alta prioridade e BRA intrinsecamente multidroga foram melhorias alcançadas no combate à RAM.

Palavras-chave: *foto-Fenton solar; radical sulfato; radical hidroxila; métodos dependentes de cultura; análise metagenômica*

ABSTRACT

Municipal Wastewater Treatment Plant Effluent (MWWTPE) contains thousands of resistant strains that carry numerous resistant genes and their variants. Consequently, final outflow plays a critical role in antimicrobial resistance (AMR) dissemination. Ergo, avoiding this spread is one of the most critical public health concerns, making the disinfection of the MWWTPE essential. However, conventional technologies (*e.g.* chlorination and UV processes) or advanced ones (*i.e.* ozonation) proved ineffective. In contrast, advanced oxidative processes are feasible as oxidative radicals damage cell constituents and nucleic acid structures through free radical reactions. Photo-Fenton constitutes an up-and-coming method, promoting the effective removal of antimicrobial-resistant bacteria (ARB) and associated resistance genes (ARG). However, considering the natural pH of MWWTPE (6.0 – 7.5), this application's main limitation is the optimal pH operation (2.8 – 3.0). A feasible alternative is the intermittent iron addition, which assures the presence of reactive Fe^{2+} species throughout circumneutral pH treatment. This strategy has been proven effective and is a differential in this work. Besides that, photo-Fenton may be carried out under sunlight, highlighting its application in areas of high solar irradiance. Thus, solar photo-Fenton (SPF) is an efficient and environmentally sustainable complementary treatment for MWWTP. Yet, while usually only highly reactive and non-selective hydroxyl radicals (HO•) are generated in SPF, sulfate radical ($SO_4^{\bullet -}$) shows higher selectivity and a longer half-life time. Nevertheless, the efficiency of enhanced SPF is still unclear. Therefore, this work explores the use of peroxide (H_2O_2), persulfate (PS), and a combined system (H_2O_2 and $S_2O_8^{-2}$) as oxidants. Accordingly, this work aims to tackle AMR via secondary wastewater post-treatment using enhanced SPF. The first published results indicate the effectiveness of SPF for the removal and inactivation of resistance-conferring plasmids (RCPs), hampering the discharge of these crucial vectors for AMR spread. Moreover, although most studies have relied solely on culture-dependent methods, this is the first study investigating SPF's effect on ARB and ARGs through high throughput metagenomics analysis (16S rDNA and Whole Genome Sequencing). Results such as effective removal of ARGs, high-priority pathogens, and intrinsically multi-drug ARB were improvements achieved in the combat of AMR.

Keywords: *solar photo-Fenton; sulfate radical; hydroxyl radical; culture-dependent methods; metagenomic analysis*

1 INTRODUCTION

The implications of antimicrobial resistance (AMR) dissemination for human and ecological health constitute one of the most critical emerging public health challenges since the resistance acquired by these organisms prolongs, hinders, and prevents the treatment of infected patients by conventional methods (BASSETTI *et al*., 2017; HAVENGA *et al*., 2019; HENDRIKSEN *et al*., 2019). AMR is carried by antimicrobial resistant bacteria (ARB) and expressed through the activation of antimicrobial resistance genes (ARGs). On a global scale, AMR is responsible for approximately 700 thousand (low estimate) deaths per year worldwide (HAQUE *et al*., 2018; NEILL, 2014). If this condition is not adequately managed, the mortality rate will exceed 10 million deaths per year, corresponding to a global economic damage of 100 trillion USD (WORLD BANK GROUP, 2017).

Despite the fact that advances in drug development have provided significant control of diseases, especially those caused by bacterial infections, the excessive and improper use of antimicrobials (more than 70 billion prescriptions per year worldwide) aggravates the development of AMR (AUTA *et al*., 2019; MEDINA; LEGIDO-QUIGLEY; HSU, 2020; TAGLIAFERRI *et al*., 2020; TORRES *et al*., 2021; VIKESLAND *et al*., 2019a). For some drugs, for example, up to 60% of antibiotics may be excreted in their parental or metabolized forms after administration (POLIANCIUC *et al*., 2020). These substances are collected in sewer networks and directed to Municipal Wastewater Treatment Plant (MWWTP), which typically includes a biological stage, which creates a potentially suitable environment for bacterial growth and development (LI *et al*., 2020a; RIZZO *et al*., 2013).

The biological reactors applied as conventional secondary treatment in MWWTP promote a heightened interaction between bacteria originating from different activities (*e.g.*, households, hospitals, industries, animal raising facilities, *etc*.) coupled with continued exposure to antimicrobials (*e.g.*, biocides and antibiotics) in subinhibitory concentrations. Thus, promoting a selective pressure in a constructed environment conducive to the development and selection of resistant organisms (FERNANDES; VAZ-MOREIRA; MANAIA, 2019; VIKESLAND *et al*., 2019a; YIN *et al*., 2019). Furthermore, the high rate of gene exchange mediated by mobile genetic elements

(MGEs) afford contribute to the emergence of new resistance strains (BARANCHESHME; MUNIR, 2018; MANAIA *et al*., 2018; NGUYEN *et al*., 2021). As MWWTP are usually not designed to remove these contaminants, a great variety of ARB and ARGs persist in secondary effluent from MWWTP. Consequently, MWWTP are one of the AMR primary point sources. Hence, the disposal of MWWTP effluent (MWWTPE) plays an essential role in AMR spread to environmental matrices, enhancing human health risks (KARKMAN *et al*., 2018; PAZDA *et al*., 2019).

Therefore, disinfection of MWWTPE is critical to promote the elimination and inactivation of ARB and ARGs before wastewater disposal in order to prevent the spread of these pathogens to the environment (HILLER *et al*., 2019a; KIRCHNER *et al*., 2020; WANG *et al*., 2020b). However, when applied, conventional disinfection technologies (*e.g*. chlorination and UV processes) or advanced ones (*i.e.* ozonation) may be ineffective for this purpose. For instance, chlorine was ineffective for ARB removal and increased intra and extracellular concentrations of ARGs in the effluent (GUO; YUAN; YANG, 2015; HOU *et al*., 2019; JIN *et al*., 2020; LIU *et al*., 2018; WANG *et al*., 2020a). Meanwhile, UV radiation significantly affects the inactivation of various ARB, yet this effect is selective and may increase the abundance of specific ARB. Furthermore, the irradiation dosage applied during treatment does not guarantee the inactivation of ARGs (GUO; YUAN; YANG, 2013, 2015; WANG *et al*., 2020a; ZHANG *et al*., 2020a). Although ozonation significantly reduced both ARB and ARGs, regrowth of ARB and ARGs enrichment was observed in the effluent (MOREIRA *et al*., 2021; IAKOVIDES *et al*., 2019; SOUSA *et al*., 2017).

In contrast, Advanced Oxidative Processes (AOP) are feasible methods for the inactivation of bacteria and elimination of ARGs as oxidative radicals damage cell membrane and DNA structure through free radical reactions (GUO *et al*., 2020; LI *et al*., 2021; MICHAEL-KORDATOU; KARAOLIA; FATTA-KASSINOS, 2018). Among several processes, photo-Fenton constitutes an up-and-coming method for the complementary treatment of MWWTPE, promoting effective removal of ARB and ARGs and inactivating cell-free ARGs present in MWWTPE (MICHAEL-KORDATOU; KARAOLIA; FATTA-KASSINOS, 2018; VILELA *et al*., 2021a; STARLING *et al*., 2021b). In this context, this work is justified as it (i) explores the high potential of solar

photo-Fenton in promoting disinfection as an advanced treatment of secondary effluents; (ii) contemplates the use of solar light as an alternative and sustainable light source in solar photoreactors; (iii) meets the need for the development of alternative, efficient and low-cost technologies for the treatment of MWWTPE, and (iv) promotes advances on the combat of ARB and ARGs present in the MWWTPE, thus advocating towards improvements related to human health and environmental integrity.

2 OBJECTIVES

2.1 General objective

To evaluate the efficiency of solar photo-Fenton using hydrogen peroxide (H_2O_2) and sodium persulfate ($S_2O_8^{-2}$) as oxidants as well as the combination of both in the removal of ARB and ARGs inherent to MWWTPE and treatment impact upon microbiome and resistome profile.

2.2 Specific objectives

The specific objectives of this work are as follows:

- To investigate the elimination and inactivation of free-cell DNA (plasmids) in MWWTPE via solar photo-Fenton;
- To Investigate the effects of solar photo-Fenton upon priority pathogens, bacterial community, and resistome profile present in MWWTPE;
- To investigate the impact of the enhanced solar photo-Fenton upon microbiome diversity, priority pathogens, and resistome profile present in MWWTPE;
- To compare the efficiency of solar photo-Fenton and enhanced solar photo-Fenton by (i) persulfate and (ii) binary oxidants system (H_2O_2 + $S_2O_8^{-2}$) in tackling antimicrobial resistance by removal of ARB and ARGs on bench scale;
- To compare the efficiency of solar photo-Fenton and enhanced solar photo-Fenton by (i) persulfate and (ii) binary oxidants system (H_2O_2 + $S_2O_8^{-2}$) in tackling antimicrobial resistance by removal of ARB and ARGs on pilot-scale.

3 LITERATURE REVIEW

3.1 Antimicrobial resistance in wastewater treatment plants: Critical aspects

AMR is considered a major challenge to human health in 21st-century (BASSETTI *et al*., 2017; MEDINA; LEGIDO-QUIGLEY; HSU, 2020; YADAV; KAPLEY, 2021). Although resistance is an inherently natural process, a wide range of biochemical and physiological mechanisms may be responsible for it. resistance (DAVIES, 1996; EMAMALIPOUR et al., 2020; WELLINGTON et al., 2013). Microbial genome plasticity, facilitated by diverse genetic mechanisms (*e.g.* conjugation, transformation, and transduction), enables microorganisms to evolve, adapt, and persist in antimicrobial-contaminated environments (LEKUNBERRI *et al*., 2017; WELLINGTON *et al*., 2013). Most environmental bacteria become antimicrobial resistant due to the acquisition of ARGs associated with MGEs (*i.e.*, plasmids, transposons, and integrons) (MA *et al*., 2017; SAIMA *et al*., 2019; SZCZEPANOWSKI *et al*., 2009; ZHANG *et al*., 2017). However, it is the selection pressure that determines the occurrence, amplification, and dissemination of ARGs in the environment and pathogenic organisms (DAVIES, 1996; HOLMES et al., 2016; JIANG et al., 2022; SINGH et al., 2022). Consequently, the many years of human overuse and misuse of antimicrobials resulted in the development of generations of antimicrobial-resistant microorganisms and their distribution in environmental. Therefore, AMR can no longer be considered solely a natural process. Instead, it represents a human-induced situation superimposed on nature.

There are two distinct types of AMR in bacteria: acquired AMR and intrinsic AMR (BAEKKESKOV et al., 2020; GIULIERI et al., 2020; GOVINDARAJ VAITHINATHAN; VANITHA, 2018). Intrinsic resistance refers to the existence of genes within bacterial genomes that confer a natural resistance phenotype. Different genera, species, strains, and other bacterial classifications exhibit a spectrum of antibiotic response phenotypes (BAKER-AUSTIN et al., 2006; DAVIES, 1996; JIANG et al., 2022). However, gene amplification represents a common genetic route to enhanced antimicrobial resistance. For instance, many of the bacterial pathogens associated with epidemics of human disease (*e.g. Acinetobacter baumannii, Enterococcus faecium, Klebsiella pneumoniae, Pseudomonas aeruginosa, Helicobacter pylori, Staphylococcus aureus*) have evolved into multidrug-resistant (MDR) forms

subsequent to antibiotic use (BAEKKESKOV et al., 2020; DAVIES, 1996; SINGH et al., 2022). In most cases, bacterial-acquired resistance occurs at a low level, usually limited to one specific antimicrobial agent. Even so, some strains can gain a high ability to become resistant to several antimicrobials (CANTÓN; RUIZ-GARBAJOSA, 2011; HENRIQUES NORMARK; NORMARK, 2002). Infections caused by AMR pathogens result in severe illnesses that necessitate prolonged hospital care and escalated healthcare expenses. Failing to address this issue adequately could result in a mortality rate surpassing 10 million deaths annually, and a corresponding global economic impact of 100 trillion USD (WORLD BANK GROUP, 2017). Consequently, the global spread of AMR endangers public health worldwide.

The World Health Organization (WHO) underlines the multifaceted nature of AMR, highlighting the necessity for comprehensive approaches that involve coherent actions in critical *hotspots* contributing to resistance development (BERENDONK et al., 2015; BRACK et al., 2022; MICHAEL-KORDATOU; KARAOLIA; FATTA-KASSINOS, 2018; MICHAEL et al., 2013; RIZZO et al., 2013). Wastewater Treatment Plants (WWTP) are widely recognized as one of the primary anthropogenic sources responsible for the dissemination of antimicrobial-resistant bacteria (ARB) and antimicrobial resistance genes (ARGs) into the environment. Biological reactors used in WWTP are widely acknowledged to establish an environment that can potentially facilitate the development of AMR (MANAIA et al., 2018; MICHAEL-KORDATOU; KARAOLIA; FATTA-KASSINOS, 2018; MICHAEL et al., 2013; RIZZO et al., 2013).From a microbiological perspective, WWTP serve as collection points for various sources of sewage, mixing human-commensal, environmentally bacterias and recalcitrant natural or synthetic compounds (*i.e.* toxic metals, pharmaceutical residues, pesticides). These substances, including antimicrobial residues and metabolites, can exert various effects on bacteria, acting as stressors. Mainly under significant metabolic activity, the combination of these factors can potentially facilitate horizontal gene transfer (HGT). This mechanism allows for the transmission of genetic elements encoding resistance, including antimicrobial resistance genes (MANAIA et al., 2018; MICHAEL-KORDATOU; KARAOLIA; FATTA-KASSINOS, 2018; MICHAEL et al., 2013; RIZZO et al., 2013). Therefore, MWWTP provide an ideal environment for the proliferation, persistence and development of ARB and ARGs, even in the treated effluent

(FIORENTINO et al., 2019a; MOREIRA et al., 2018; STANTON et al., 2020). Indeed, final MWWTP effluent (MWWTPE) has the potential to disseminate AMR in the environment, posing risk to human health and a long-term threat to environmental ecosystems (HILLER et al., 2019b; MANAIA et al., 2018; MIŁOBEDZKA et al., 2022; NGUYEN et al., 2021; OSIŃSKA et al., 2020; RAZA et al., 2022; RIZZO et al., 2013, 2020; WANG et al., 2020b).

3.2 Addressing Antimicrobial Resistance in Wastewater Treatment Plants: Strategies and Solutions

Municipal Wastewater Treatment Plants (MWWTP) plays a critical role in the emergence, persistence, and proliferation of ARB and ARGs to the environment, consequently, a potential key to AMR dissemination (HILLER *et al*., 2019b; NGUYEN *et al*., 2021; OSIŃSKA *et al*., 2020; RIZZO *et al*., 2013; WANG *et al*., 2020b). Generally, MWWTP involves four main stages: preliminary, primary, secondary, and tertiary treatment. The preliminary stage removes coarse solids and sand particles by physical mechanisms such as racks, screens, and sand chambers. In primary treatment, solids are removed by physical operations, usually sedimentation. In the sequence, biological processes are used to remove biodegradable organic matter. Tertiary treatment consists of additional techniques (*e.g*., ozonation, UV treatment, filtration, adsorption, oxidation, among others) used for the removal of nutrients, persistent organic matter, and/or toxic materials, in addition to promoting the disinfection of the final effluent (METCALF; EDDY, 2013). However, most MWWTP operates only up to the secondary stage, especially in developing countries (COSTA; STARLING; AMORIM, 2021; NOYOLA *et al*., 2012). For instance, the treatment of wastewater in Brazil faces several challenges. Besides being limited to nearly 38% of total domestic sewage generated in the country (STARLING; AMORIM; LEÃO, 2019), some MWWTP operate in inadequate conditions, either for financial or technical reasons (NOYOLA *et al*., 2012; VON SPERLING, 2016).

A diverse variety of wastewater sources (*e.g.* hospitals, households, industries, animal farms, etc.) containing organic, chemical, and microbiological contaminants contribute to the composition of MWW. Thus, resulting in the coexistence of a high diversity of bacteria, mobile genetic elements, and genes in this matrix (KARKMAN *et al*., 2018;

KHAN *et al*., 2020). These contaminants represent a wide range of networks that boost mutation, horizontal gene transfer, and other critical routes of AMR acquisition in the secondary treatment stage (mainly biological reactor) (EMAMALIPOUR *et al*., 2020). In this system, the combination of abiotic factors (*i.e.,* pH, temperature, nutrients, micropollutants) and biotic factors (microbiota, cell permeability, genetic elements) are simultaneously favorable for bacteria reproduction and growth (NGUYEN *et al*., 2021; RIAZ *et al*., 2019). Moreover, subinhibitory concentrations of antimicrobials present in MWW promote selective pressures for resistance transfer and resistant bacteria evolution (ANDERSSON; HUGHES, 2014; HERNANDO-AMADO *et al*., 2019). Besides, chemical contaminants as non-antimicrobial pharmaceuticals, nanomaterials, metals, ionic liquids, and even disinfectants and disinfection by-products, also present in MWW, may increase natural transformation rates of cell-free DNA and facilitate AMR horizontal transfer (MANAIA et al., 2020a; ZHANG et al., 2017). This enables bacteria to evolve rapidly, leading to resistance proliferation to non-resistant bacterial communities (HOFER, 2020; LI *et al*., 2020c; WELLINGTON *et al*., 2013).

In general, the occurrence of a high abundance of ARB and ARG in MWWTPE has been widely disclosed (PAZDA *et al*., 2019; WANG *et al*., 2020b; YIN *et al*., 2019). Yet, more attention should be given to possible treatments for the removal of these contaminants. Although conventional MWWTP can reduce the amount of ARB discharge into the environment, removal efficiencies differ due to different characteristics of MWW and MWWTP operating conditions (LI *et al*., 2016; WANG *et al*., 2020b). Whereas available studies reported limited AMR removal efficiencies for most conventional MWWTP, the pathogenic potential for AMR could not be reduced (HILLER *et al*., 2019b). Besides, the limited number of available studies demonstrates that future research is needed to improve the understanding of AMR removal during various conventional or advanced disinfection treatment processes.

3.3 Application of AOPs on the combat of AMR

Numerous ARB and ARGs have been detected in MWW, MWWTPE, and biological sludge formed during wastewater treatment. Several works point out that the wastewater treatment process leads to a significant increase in the relative abundance of ARB and ARGs (BONDARCZUK; PIOTROWSKA-SEGET, 2019; CHENG *et al*.,

2021; LIU *et al*., 2019; NGUYEN *et al*., 2021; PAZDA *et al*., 2019; RIZZO *et al*., 2013; SHARMA *et al*., 2016). Consequently, investments in developing advanced wastewater treatment strategies that promote the removal of ARB and ARGs from MWWTPE before discharge has increased. The need for the development of new technologies is critical as many studies indicate that conventional disinfection technologies such as chlorination, UV-C, and ozonation are ineffective in removing ARB and ARGs from MWWTPE (DI CESARE *et al*., 2020; LEE *et al*., 2017; NARCISO-DA-ROCHA *et al*., 2018).

In contrast, advanced oxidation processes (AOP) are feasible methods for the inactivation of bacteria and elimination of ARGs as oxidative radicals damage cell constituents (*i.e*., carbohydrates, proteins, and lipids) and nucleic acids structures through free radical reactions (GUO *et al*., 2020; LI *et al*., 2021; MICHAEL-KORDATOU *et al*., 2018). Among AOPs, photo-Fenton constitutes an up-and-coming method for the complementary treatment of MWWTPE. During the photo-Fenton process, highly reactive and non-selective hydroxyl radicals (HO•, E_0 = 1.8–2.7 V) are generated through the reaction between ferrous iron (Fe^{2+}) and hydrogen peroxide (H_2O_2) (Equation 1), and UV-C radiation and H_2O_2 (Equation 2) (GIANNAKIS et al., 2016b; MIRALLES-CUEVAS et al., 2017; RODRÍGUEZ-CHUECA et al., 2019a). Although Fe^{2+} cycling occurs in the dark (Equation 3), it is enhanced under light, and chemical species formed in the system generate an extra route to produce oxidative radicals (Equation 4), thus enhancing treatment effectiveness when compared to the dark Fenton (GIANNAKIS et al., 2016b).

$$Fe^{2+} + H_2O_2 \rightarrow Fe^{3+} + HO\bullet + OH^- \quad (1)$$

$$H_2O_2 + hv\ (254\ nm) \rightarrow 2\ HO\bullet \quad (2)$$

$$Fe^{3+} + H_2O_2 \rightarrow Fe^{2+} + HO_2\bullet + H^+ \quad (3)$$

$$Fe(OH)^{2+} + hv(540\text{-}580\ nm) \rightarrow Fe^{2+} + HO\bullet \quad (4)$$

Since photo-Fenton may be carried out under sunlight, its investigation to improve MWWTPE quality in areas of high solar irradiance (*i.e.* tropical developing countries) must be further stimulated. Therefore, solar photo-Fenton stands out as an environmentally sustainable treatment that effectively removes ARB and ARGs

(GIANNAKIS *et al*., 2018a; IOANNOU-TTOFA *et al*., 2019a; POLO-LÓPEZ; SÁNCHEZ PÉREZ, 2021; STARLING *et al*., 2021b; VILELA *et al*., 2021a, 2021b). Yet, one of the main limitations of photo-Fenton treatment is the optimal pH of operation (2.8 – 3.0). Considering the natural pH of MWWTPE (6.0 – 7.5), different strategies have been investigated to apply photo-Fenton at a neutral pH level (CLARIZIA *et al*., 2017). A feasible alternative for this purpose is the intermittent iron addition strategy which assures the presence of soluble and reactive Fe^{2+} species throughout treatment (CARRA *et al*., 2013, 2014; DÍAZ-ANGULO *et al*., 2021). This strategy has been proven effective for disinfection and ARB removal (STARLING *et al*., 2021a; VILELA *et al*., 2021a, 2021b) and is presented as a differential in this work. Therefore, this work explores the high potential of photo-Fenton in promoting disinfection as an advanced treatment of secondary effluents using solar light as a sustainable light source. In addition, treatment was performed at a neutral pH level using the intermittent iron additions, thus exploring some of the gaps present in the literature.

Despite high reactivity of hydroxyl radical and promising results for the removal of ARB and ARGs obtained via solar photo-Fenton using H_2O_2 as an oxidant (DE LA OBRA JIMÉNEZ *et al*., 2019; FIORENTINO *et al*., 2019a; GIANNAKIS *et al*., 2018b, 2018a; IOANNOU-TTOFA *et al*., 2019a; POLO-LÓPEZ; SÁNCHEZ PÉREZ, 2021), AOPs based on sulfate radical ($SO_4^{\bullet-}$, $E_0 = 2.5 - 3.1$ V) have recently attracted significant attention due to longer half-life time (30–40 μs for sulfate radicals *vs*. 20 ns for hydroxyl radicals) and higher selectivity of $SO_4^{\bullet-}$ compared to HO• (OH; DONG; LIM, 2016; ZHOU *et al*., 2020), and for the greater potential for radical formation with less dependence on the operational parameters (*e.g.* pH, wastewater matrix constituents). Unlike other common oxidants, PS can be activated by several routes simultaneously (*e.g.*, heat, transition metals, UV light, visible light, among others), generating sulfate radical ($SO_4^{\bullet-}$) (Equation 5 and 6) (HOU *et al*., 2021; WACŁAWEK *et al*., 2017; YANG *et al*., 2019):

$$S_2O_8^{2-} \xrightarrow{actviator\ (e^-)} SO_4^{\bullet-} + SO_4^{2-} \quad (5)$$

$$SO_4^{2-} \xrightarrow{energy\ input} 2SO_4^{\bullet-} \quad (6)$$

In the PS mediated photo-Fenton process (UV/Fe^{2+}/$S_2O_8^{-2}$), $SO_4^{\bullet -}$ is produced by the disruption of the O-O bonds of persulfate anions ($S_2O_8^{-2}$) catalyzed by Fe^{2+} (Equation 7). Nevertheless, Fe^{2+} excess can lead to radical scavenging (Equation 8) (HOU *et al*., 2021; KOLTHOFF; MEDALIA; RAAEN, 1951; WACŁAWEK *et al*., 2017).

$$S_2O_8^{2-} + Fe^{2+} \rightarrow SO_4^{\bullet -} + Fe^{3+} + SO_4^{2-} \quad (7)$$

$$Fe^{2+} + SO_4^{\bullet -} \rightarrow Fe^{3+} + SO_4^{2-} \quad (8)$$

Despite the known efficiency of sulfate radicals on bacterial cell and DNA damage, very few studies have evaluated the efficiency of these radicals on the removal of ARB and ARGs (GAO *et al*., 2020; QIU *et al*., 2020; STARLING *et al*., 2021a; ZHOU *et al*., 2020), and mechanisms associated with disinfection via sulfate radical-based AOPs are still unclear (XIAO *et al*., 2019). Besides that, less is known about an alternative mechanism for activation of PS involving H_2O_2, which originates both sulfate ($SO_4^{\bullet -}$) and hydroxyl radicals (HO•) (Equation 9) (DEVI; DAS; DALAI, 2016; DOS SANTOS *et al*., 2020).

$$S_2O_8^{2-} + H_2O_2 \rightarrow 2\ SO_4^{\bullet -} + 2\ HO\bullet \quad (9)$$

This mechanism makes the use of a combination of these two oxidants an interesting alternative. However, the combined use of PS and H_2O_2 is not conventional, reported only in some studies (AMANOLLAHI; MOUSSAVI; GIANNAKIS, 2021; CRIMI; TAYLOR, 2007; KHAN *et al*., 2021; MONTEAGUDO *et al*., 2015; YAZICI GUVENC, 2019). To our knowledge, the combination of PS and H_2O_2 for removal of ARB and ARGs has not been assessed yet. Therefore, this work aims to cover these gaps in the literature, investigating both the use of persulfate as an alternative oxidant in solar photo-Fenton, such as the application of both oxidants simultaneously (H_2O_2+$S_2O_8^{-2}$), which is investigated for the first time for the removal of ARB and ARGs in this study.

Another critical differential of this work is the application of standardized analytical techniques to determine the occurrence of AMR and verify removal efficiencies of the solar photo-Fenton treatment. Furthermore, the quantification of ARB and ARGs in MWWTPE samples was assessed either by culture-dependent methods and metagenomic analyses (16S rDNA sequencing and WGS). So far, no previous studies

have set the WGS profile of MWWTPE treated by solar photo-Fenton. In order to quantify AMR in MWWTPE samples, the choice of quantification methods used was based on the pros and cons of commonly applied culture-based and molecular-based detection methods. Besides that, the techniques used in previously published works were taken into account, synthesized in item 3.4.

3.4 Methods applied for the assessment of ARB and ARGs in MWWTPE

Despite several studies associated with the combat of AMR spread through wastewater discharge, the quantification of ARB and ARGs in MWWTPE samples and analysis of treatment impact upon resistome profile are challenging tasks. Most published studies apply culture-dependent methods (IOANNOU-TTOFA *et al*., 2019; MICHAEL *et al*., 2020; MOREIRA *et al*., 2018; RODRÍGUEZ-CHUECA *et al*., 2019), which are significant as they prove the viability of ARB and expression of ARGs after treatment. Yet, culture-dependent methods may be inadequate to analyze treatment effects upon uncultivable organisms, representing public health risks (MANAIA *et al*., 2018; VAZ-MOREIRA *et al*., 2011). In contrast, metagenomic analyses such as 16S rDNA and WGS sequencing show high specificity and sensitivity for all organisms, no matter their viability, and enable the analysis of treatment impact upon microbial community and resistome, which are fairly diverse in MWWTPE (RIZZO *et al*., 2013; ISHII, 2020; RICE *et al*., 2020).

ARB and ARGs are widely distributed and persistent in the environment. Despite challenges, it is essential to choose reliable, precise, and reproducible quantification methods for their identification and quantification in environmental samples. Researchers have adapted methods used in clinical practices, primarily based on pre-established breakpoints to reach the organism classification (BERENDONK *et al*., 2015; KAHLMETER, 2014), to examine ARB and ARGs present in MWWTP. Hence, quantification of ARB and assessment of their resistance patterns performed in studies related to municipal wastewater treatment are more frequently based on culture-dependent methods (IOANNOU-TTOFA *et al*., 2019b; MICHAEL *et al*., 2020; RODRÍGUEZ-CHUECA *et al*., 2019a). However, culture-independent approaches enable the complete analysis of resistome, as well as the identification of all genes present in a sample (GARNER et al., 2021; HENDRIKSEN et al., 2019; JIANG et al.,

2019). Table 1 shows goals, advantages, and limitations usually associated with both groups of methods.

Table 1 - Advantages and limitations of non-cultivable and cultivable methods used for ARB assessment in environmental samples

Method	Goal	Advantage	Limitation
Culture-independent (molecular-dependent)	To identify bacterial lineages and analyze community diversity and richness in an environmental sample or to evaluate treatment impact upon community composition	(i) High specificity and sensitivity. (ii) Do not rely on bacteria viability or cultivability under laboratory conditions. (iii) No need for sample enrichment for direct quantification. (iv) Less laborious when compared to cultivable methods.	(i) The identification of cell-free DNA is tricky. (ii) New genes and gene variants may compromise assay performance. (iii) High costs and possible misdetection and misinterpretation depending on experimental design.
Culture-dependent	To analyze the occurrence and/or removal of cultivable ARB present in environmental samples	(i) Direct proof of the viability of microorganisms and expression of the ARGs present in samples. (ii) Results are easily comparable over time and between different laboratories. (iii) Relatively inexpensive and easy to perform (Cost-effective).	(i) Under representation of nonculturable and non-viable bacteria, only a reduced fraction of existing bacteria is cultivable. (ii) Requires subsequent confirmation regarding the identification of ARGs

Despite challenges, culture-dependent and independent approaches are supported by guidelines developed for clinical microbiology (RIZZO *et al*., 2013). Regarding culture-dependent methods for ARB identification, membrane filtration is used as sample preparation to concentrate the cells for further characterization. Then, selective culture media is applied to enumerate and isolate specific bacterial groups (APHA, 2017). Disk infusion or micro-dilution methods are used to distinguish between resistant and susceptible organisms, detect resistance patterns, define resistance profiles, and calculate resistance rates (CLSI, 2020). Culture-dependent methods may also be used to elucidate the mechanism of ARB inactivation via oxidative treatments. For example, Giannakis *et al*. (2018a) compared the susceptibility of wild-type *E. coli* whit a knock-out clone that does not produce the porin protein to photo-Fenton treatment. As porin enables the transportation of molecules across the cell membrane to the cytoplasm, H_2O_2 influx was limited in porinless bacteria leading to lower inactivation of this clone. These results indicate that the cell inactivation process via photo-Fenton leans on the transportation of oxidative species through proteins present in the cell membrane.

Similarly, the cultivation of catalase enzyme overexpressing *E. coli* compared to a wild-type indicated that catalase produced by the cell is insufficient to protect bacteria against intracellular photo-Fenton reactions (FENG *et al*., 2020).

Selective chromogenic media has also been used to target ARB with high specificity. In this culture-dependent method, specific enzymes produced by bacteria hydrolyze the chromogenic media substrates and release colored dyes resulting in marked colonies, thus enabling accurate detection of related ARB (PERRY; FREYDIÈRE, 2007). Antonelli *et al*. (2015) used a selective chromogenic medium to screen carbapenem-resistant *Enterobacteriaceae* in hospital wastewater and samples mixed with other ARB. The accuracy of the method was validated by conventional polymerase chain reaction (PCR), a non-cultivable method, with favorable results as only one primer, was amplified, thus linking the result to a single *Enterobacteriaceae* isolate. Complimentarily, mass spectrometry was used to identify species within each sample. The authors also described a new class of carbapenem-resistance gene (blaOXA-372) by performing whole-genome sequencing (WGS) of cultured isolates. This is an example of the use of molecular methods (PCR and WGS) to complement results obtained by culture-dependent methods (cultivation in chromogenic media and mass spectrometry), thus leading to further information about isolated colonies and increasing knowledge related to AMR. Hence, complementarily cultivable and non-cultivable methods to grant more comprehensive, enriching, and accurate results. Rizzo *et al*. (2013) reinforced that conventional microbiology and molecular biology methods are complementary when analyzing the presence/absence of pathogens and their genetic targets of antimicrobial resistance.

Nevertheless, practical questions arise when dealing with culture-based methods as only a tiny portion of ARB can be cultivated in vitro (RIESENFELD; SCHLOSS; HANDELSMAN, 2004). Munck *et al*. (2015) estimated that 85%–99% of the bacteria from MWWTPs are not readily cultured using current protocols. Thus, justifying the use of molecular biology methods that detect microorganisms that cannot grow in the laboratory. Molecular-based techniques, such as qPCR and DNA sequencing, offer the great advantage of eliminating biases associated with the non-cultivability of some ARB or the non-expression of ARGs present in some bacterial hosts (OLIVER, 2010).

Consequently, a higher diversity of organisms and ARGs may be detected in environmental samples. Further, genetics-based tests are more accurate than antibiograms in tracking the epidemiological spread of relevant resistance genes.

Although most authors evaluated the reduction of ARGs by qPCR, conventional PCR has also been applied to verify the presence of ARGs. In Giannakis *et al*. (2018a), the presence of blaCTX-M-9 in MWWTP effluent samples was evaluated. Even though the gene was present in the sample taken before solar photo-Fenton, no amplification was observed after 15 min of exposure, thus indicating its removal after the proposed treatment. Although the conventional PCR method allows for the qualitative evaluation of ARG elimination, qPCR is advantageous as it enables identification and quantification. Nevertheless, variation coefficients related to ARG detection between different laboratories worldwide using qPCR techniques were around 30%. This difference may be associated with distinct practices and equipment applied in these laboratories (CACACE *et al*., 2019; ROCHA *et al*., 2020).

Regarding DNA sequencing for bacteria identification in environmental samples, the most common method used to analyze the microbiome is the amplicon analysis of the 16S ribosomal RNA (rRNA) gene. The 16S subunit of the rRNA has hypervariable regions that are flanked by conserved sequences. Primers are designed to recognize specific conserved sequences to amplify hypervariable parts assigned to operational taxonomic units (OTUs) (SANSCHAGRIN; YERGEAU, 2014). OTUs are identified and can also be quantified by analyzing the read depth of each detected OTU. This technique is limited as not all OTUs have hypervariable sequences described in genomic databases. Hence, although distinguishable, not all OUTs can be associated with a taxonomic unit. An alternative approach to the 16S sequencing is WGS sequencing, which consists of sequencing the total genome present in a sample. The main advantage of WGS is that the taxa can be more accurately defined at the species level (RANJAN *et al*., 2016). Apart from taxa accuracy, WGS also gives information about complete genomes and their organization. Despite producing more and highly reliable data, WGS is less cost-effective (ISHII, 2020; RICE *et al*., 2020).

Next-generation sequencing is a valuable tool for studying natural microbial communities, genomes, and transcriptomes. Furthermore, WGS may be used to

identify known and new ARGs, recognized genomic organization structures, integrons, and other structures related to antimicrobial resistance within environmental samples (NESME *et al*., 2014). Deep knowledge of these structures may be helpful for the definition of AMR indicators in environmental samples, which is one of the leading literature gaps on the subject. However, genomic and transcriptomic approaches demand highly curated sequence reference databases and highly qualified personnel. In addition, some papers published using metagenomics either lack submission to databanks or have been registered within incorrect/unavailable accession numbers (ECKERT *et al*., 2020). Another drawback associated with molecular techniques is that they do not distinguish between living and non-viable organisms or expressed and non-expressed genes. As the presence of ARGs in a sample does not necessarily mean they are being expressed in natural conditions in the environment, it is crucial to be cautious when interpreting and reporting results obtained via WGS.

4 METHODOLOGY

The methodology was divided into five stages for the proposed objectives to be achieved, as detailed in the flowchart (Figure 1).

Figure 1 - Flowchart representative of the chapters developed in this work

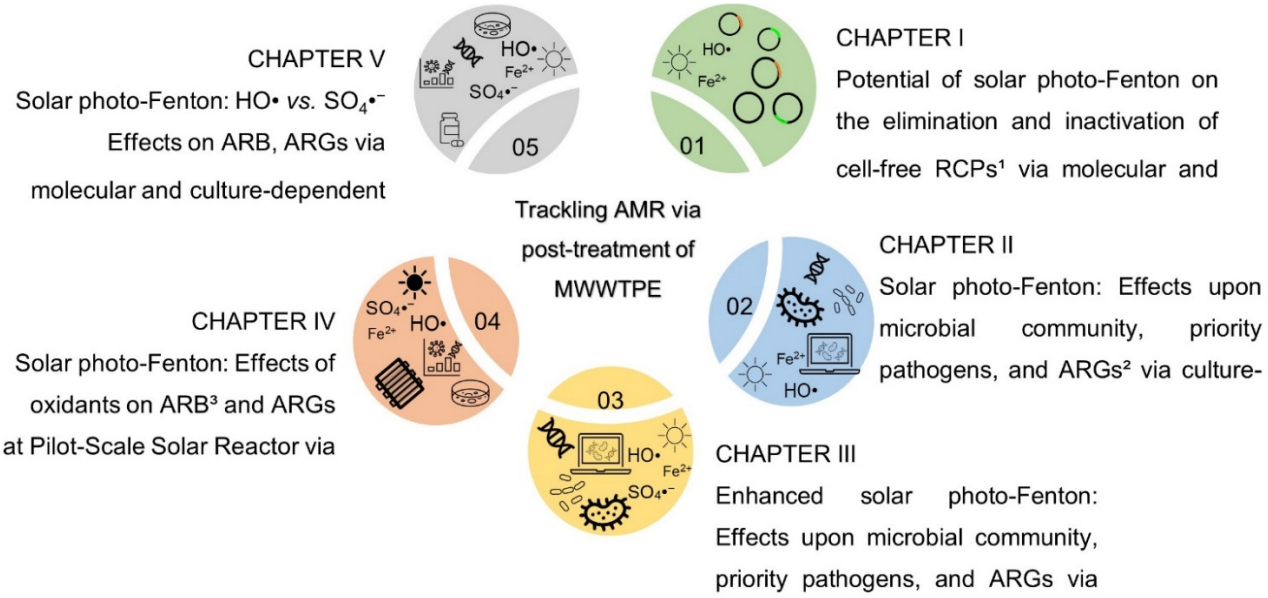

¹RCPs = Resistance-conferring Plasmids; ²ARG = Antimicrobial Resistant Gene; ³ARB = Antimicrobial Resistant Bacteria

4.1 Application of solar photo-Fenton in secondary effluent

The effluent used in this project was sampled in the output of a secondary settling tank from a conventional activated sludge system pertaining to a MWWTP located in Belo Horizonte, in the southeast of Brazil, which receives wastewater from 1.5 million inhabitants (290 m^3 d^{-1}), including hospitals, industries, etc. The collected samples were characterized in terms of Temperature, pH, Conductivity, Turbidity, Chemical Oxygen Demand (COD), Total Solids (TS), Total Fixed Solids (FS), Volatile Solids (VS), and Alkalinity were analyzed as according to APHA (APHA, 2017).

4.2 Solar photo-Fenton treatments

Solar photo-Fenton treatments of MWWTPE performed in steps I, II, III and V were conducted in a solar simulator chamber (SUNTEST) equipped with a Xenon lamp which simulates the solar spectrum. The irradiance was set as 268 W m^{-2} (UVA - 30

W m^{-2}, annual average irradiance in Belo Horizonte/MG, Brazil) at 35°C. Experiments were performed in a glass reactor under continuous magnetic stirring. Solar photo-Fenton treatments performed in step IV were conducted in batch in a semi-pilot solar photoreactor type Compound Parabolic Concentrator (CPC). The CPC reactor contains six borosilicate tubes, totaling a 2.1 m^2 of irradiated area, with 20º of inclination (corresponds to the latitude of Belo Horizonte/MG, Brazil). The reactor was segregated into three independent systems (two tubes and 15 L of total volume each). A global radiometer connected to a data logger is coupled to the CPC, so that incident irradiation (W m^{-2}) is measured during treatment. The experiments were conducted as detailed in Figure 2 and Table 2.

Figure 2 - Flowchart representative of the steps performed in this work

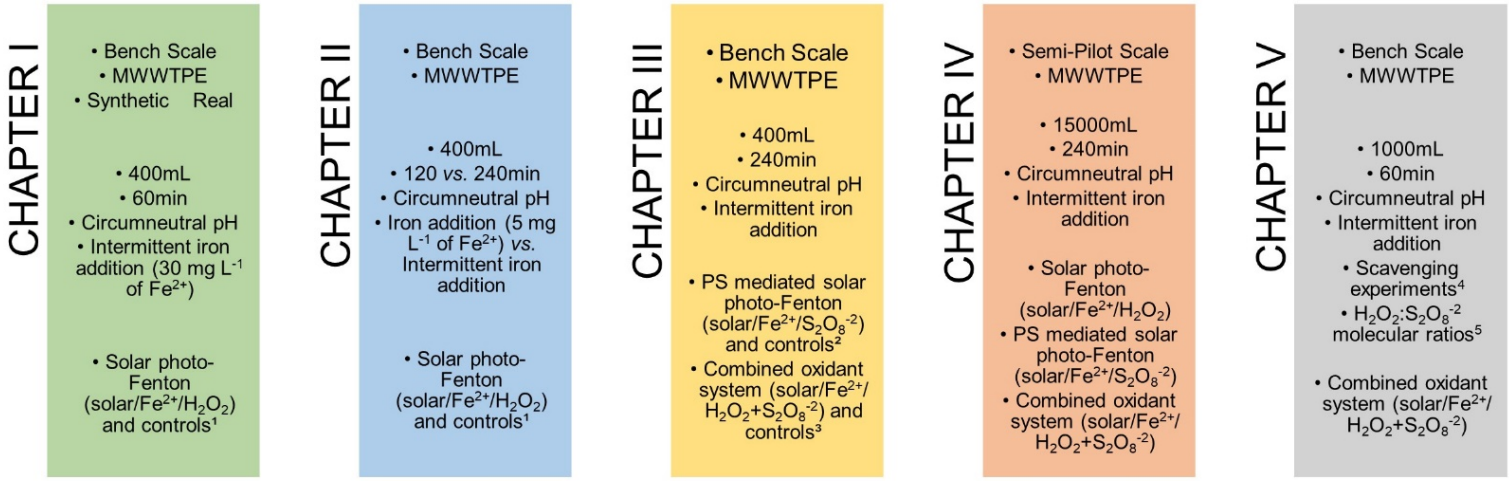

[1]Controls: Fenton (Fe^{2+}/H_2O_2), Solar/Fe^{2+}, Solar/H_2O_2, Fe^{2+}, H_2O_2, Solar; [2]Controls: PS mediated Fenton ($Fe^{2+}/S_2O_8^{2-}$), Solar/Fe^{2+}, Solar/$S_2O_8^{2-}$, Fe^{2+}, $S_2O_8^{2-}$, Solar; [3]Controls: Fenton in the presence of both oxidants ($Fe^{2+}/H_2O_2 + S_2O_8^{2-}$), Solar/$H_2O_2 + S_2O_8^{2-}$, $H_2O_2 + S_2O_8^{2-}$;[4]Tert-butyl alcohol (100mM) for HO• scavenging and methanol (100 mM) for HO• and $SO_4^{\bullet-}$ scavenging; 5Molecular ratios tested for $H_2O_2:S_2O_8^{2-}$ (1:1, 1.5:1 and 1:10).

Table 2 – Oxidants and iron concentration applied in solar photo-Fenton treatments

AOP	Oxidant	Fe^{2+}
Solar photo-Fenton (solar/Fe^{2+}/H_2O_2)	50 mg L^{-1} H_2O_2 (1.5 mM)	Time 0 → 15 mg L^{-1} Time 5 → 5 mg L^{-1} Time 10 → 5 mg L^{-1} Time 15 → 5 mg L^{-1} Total → 30 mg L^{-1} of Fe^{2+} (0.5 mM)
PS mediated solar photo-Fenton (solar/$Fe^{2+}/S_2O_8^{-2}$)	282.27 mg L^{-1} $S_2O_8^{2-}$ (1.5 mM)	
Combined oxidant system (solar/Fe^{2+}/ H_2O_2+$S_2O_8^{-2}$)	25 mg L^{-1} H_2O_2 + 141.135 mg L^{-1} $S_2O_8^{2-}$ (0.75 mM + 0.75 mM)	

Samples were withdrawn during reactions for enabled the quantification of residual $S_2O_8^{2-}$ (LIANG et al., 2008) and residual H_2O_2 (NOGUEIRA; OLIVEIRA; PATERLINI, 2005). For the analysis of iron speciation (Total Fe and Fe^{2+} concentrations) were measured during reactions according to phenanthroline method (APHA, 2017). For molecular, metagenomic and culture-dependent methods, catalase enzyme (460 mg L^{-1} in 0.04M phosphate buffer) and/or ascorbic acid solutions were added to samples prior to these analyses for consumption of residual H_2O_2 (POOLE, 2004) and residual $S_2O_8^{2-}$ (OLMEZ-HANCI; ARSLAN-ALATON; DURSUN, 2014), respectively. For chromatography methods, sodium sulfite (15 mM) was added to samples prior to these analyses for consumption of residual H_2O_2 and residual $S_2O_8^{2-}$.

4.3 Trackling AMR analysis

Chapter I aimed the potential of solar photo-Fenton for elimination and inactivation of RCPs. The elimination was analyzed via molecular analysis (PCR and qPCR) from the plasmid DNA extraction by phenol-chloroform–isoamyl alcohol method (TAKEUCHI et al., 1997). For molecular analysis, primers were designed to recognize specific sequences present in both RCPs to avoid any interference involving the natural occurrence of ARGs in wastewater matrice. The ability of RCPs to induce antimicrobial resistance after solar photo-Fenton was access by cultivation of *E. coli* competent cells and plasmid transformation.

Chapters II and III was dedicated to the analysis of solar photo-Fenton treatments impact upon priority pathogens, resistome, and ARGs, achieved via metagenomic analyses (16S rDNA and Whole Genome Sequencing - WGS) performed from the total DNA extraction performed using FastDNA® Spin Kit for Soil. For library preparation and sequencing samples was shipped to Macrogen (Korea). The taxonomic assignment and ARGs identification were processed by bioinformatics analysis. Furthermore, in Chapter II, the effect of solar photo-Fenton on bacteria community were confirmed by culture-based analysis performed in a non-selective and in an antibiotic enriched medium.

The main goal of Chapter IV was the change from bench to the semi-pilot scale, in order to certify the removal of ARB and ARG via molecular and culture-dependent

methods. For molecular analysis, a selection of primers for ARGs quantification by SYBR-Green based qPCR, included ARGs resistant to β-lactam, macrolides, sulphonamides, streptomycin, erythromycin, and tetracycline. Culture-based analysis was performed to determine the frequency of cultivable ARB. In addition, microbial identification was performed by MALDI-TOF mass spectrometry.

Finally, Chapter V aims to evaluate the mechanisms involved in the combined action of H_2O_2 and $S_2O_8^{-2}$ oxidants upon ARB and ARGs via molecular and culture-dependent methods.

CHAPTER I - Solar photon-Fenton process eliminates free plasmid DNA from wastewater[1]

[1]This chapter was published according to the following reference: VILELA, Pâmela B.; MARTINS, Alessandra S.; STARLING, Maria Clara V. M.; DE SOUZA, Felipe A. R.; PIRES, Giovana F. F.; AGUILAR, Ananda P.; PINTO, Maria Eduarda A.; MENDES, Tiago A. O.; DE AMORIM, Camila C. Solar photon-Fenton process eliminates free plasmid DNA harboring antimicrobial resistance genes from wastewater. Journal of Environmental Management, v. 285, October 2020. DOI: 10.1016/j.jenvman.2021.112204.

1 INTRODUCTION

The implications of antimicrobial resistance (AMR) for human and ecological health constitute one of the most critical emerging public health challenges with worldwide proportions. AMR is carried by antimicrobial-resistant bacteria (ARB) and expressed through the activation of antimicrobial resistance genes (ARGs) (SZCZEPANOWSKI *et al*., 2009; VIKESLAND *et al*., 2019b). Despite being a naturally occurring process, AMR may result from acquired mechanisms, referred to as horizontal gene transfer, mainly driven by MGEs (*i.e.*, plasmids, transposons, and integrons) (LEKUNBERRI *et al*., 2017; PARTRIDGE *et al*., 2009; WELLINGTON *et al*., 2013; XIE *et al*., 2019). Among MGEs, plasmids are extrachromosomal circular DNA that may carry more than one associated ARGs and replicate independently from the host chromosomic DNA. They are transferred horizontally between bacteria or incorporated by bacteria if present as cell-free molecules in the environment (GOKCEZADE; SIENSKI; DUCHEK, 2014; RAHUBE *et al*., 2014; ROSANO; CECCARELLI, 2014; SAN MILLAN, 2018; ZHANG; BROWN; HU, 2019). The acquisition of cell-free plasmids harboring ARGs, or resistance-conferring plasmids (RCPs), enables bacteria to evolve rapidly and is one of the critical routes of global dissemination of AMR (HOFER, 2020; LI *et al*., 2020c; WELLINGTON *et al*., 2013).

Municipal wastewater treatment plants (MWWTP) are among the main hotspots for the development and dissemination of AMR (AMINOV; MACKIE, 2007; BAQUERO; MARTÍNEZ; CANTÓN, 2008; HILLER et al., 2019a; KÜMMERER, 2009a; LUPO; COYNE; BERENDONK, 2012; RIZZO et al., 2013; WANG et al., 2020b). Most of the transformation products and metabolites resulting from the consumption of antimicrobials used as human and veterinary medicine are eliminated by excreta. Consequently, these substances are collected in sewer networks and directed to MWWTP (ADELEYE et al., 2022; FATTA-KASSINOS; MERIC; NIKOLAOU, 2011; KÜMMERER, 2009b; WILKINSON et al., 2017). Thus, MWWTP typically function at a secondary level, primarily in developed countries, and employ biological reactors for effluent treatment. These biological reactors serve as environments that foster genetic evolution due to their high biological connectivity, ability to generate variations, and the presence of specific selection pressures that favors ARB and ARGs. In addition to mutational events, noteworthy genetic variation arises from recombination events,

often facilitated by genetic exchanges among organisms within populations and communities (BERENDONK et al., 2015; CACACE et al., 2019; MANAIA et al., 2016; RIZZO et al., 2013). As wastewater treatment facilities are usually not designed to remove these contaminants, MWWTP effluent (MWWTPE) still contains a great variety of antimicrobials, ARBs, and ARGs. In this matrix, ARGs may be either (i) part of bacteria DNA along with other genes, thus being eliminated during disinfection stages, or (ii) present in suspension in MWWTPE as cell-free DNA carried by RCPs and which may persist in the matrix even after the elimination of bacteria (WOEGERBAUER; BELLANGER; MERLIN, 2020).

Considering the abundance of ARGs, including those carried by RCPs, in MWWTP effluent (MWWTPE), advanced treatment technologies applied to secondary wastewater are critical stages to promote the elimination and inactivation of ARGs from MWWTPE before proper wastewater disposal (BUCKNER; CIUSA; PIDDOCK, 2018; HILLER *et al*., 2019a; LI *et al*., 2018b; SZCZEPANOWSKI *et al*., 2009). Although most published studies focus on the removal of ARGs associated with bacterial DNA (AHMED *et al*., 2020; FIORENTINO *et al*., 2019a; GIANNAKIS *et al*., 2018a; KARAOLIA *et al*., 2017; MOREIRA *et al*., 2018; ZHANG *et al*., 2016), it is also critical to eliminate cell-free RCPs present in MWWTP, as non-resistant bacteria may acquire them in the soil or river after disposal, thus increasing risks of environmental and human contamination as well as AMR spread (LARSSON *et al*., 2018; MA *et al*., 2017; WELLINGTON *et al*., 2013). In recent years, advanced oxidation processes (AOPs) have emerged as effective alternatives for the removal of ARGs from MWWTPE (ARSLAN-ALATON *et al*., 2020; HILLER *et al*., 2019a; LI *et al*., 2019; MOREIRA *et al*., 2018; ZHANG; BROWN; HU, 2019). Yet, only a few studies assess the removal of cell-free ARGs carried specifically by RCPs and present in suspension in MWWTPE (ARSLAN-ALATON *et al*., 2020; NIHEMAITI *et al*., 2020; YOON *et al*., 2017; YOON; DODD; LEE, 2018; ZHANG *et al*., 2019b; FERRO *et al*., 2016). Besides, extensive studies regarding the acquisition and spread of AMR by RCPs are limited to clinical isolates (BUCKNER; CIUSA; PIDDOCK, 2018; HAO *et al*., 2020; TAGLIAFERRI *et al*., 2020; WANG *et al*., 2019a), and only a few studies have addressed their contribution to AMR in the environment.

Solar photo-Fenton is a promising alternative for eliminating RCPs from secondary wastewater since it has been proven effective for eliminating some ARGs (FIORENTINO *et al*., 2019a; GIANNAKIS *et al*., 2018a; KARAOLIA *et al*., 2017). In this process, oxidative radicals, such as hydroxyl radical ($HO^{\bullet}$), are produced during a reaction catalyzed by Fe^{2+} ions in the presence of hydrogen peroxide (H_2O_2). As Fe^{2+} cycling is enhanced under sunlight, chemical species formed in the system generate an extra route to produce oxidative radicals. One of the main limitations of solar photo-Fenton is related to the pH of operation, as the solubility of Fe^{2+} salts is higher at acidic pH. This may be unraveled by using complexing agents that increase the pH range of iron solubility (*i.e.*, ferrioxalate, EDDS, citric acid, etc.), thus enabling process operation at neutral pH. However, the addition of iron complexes has been associated with increased operating costs (CLARIZIA *et al*., 2017; KLAMERTH *et al*., 2013). As an alternative to using complexing agents, Fe^{2+} may be added intermittently to the system to guarantee an extended availability of this reagent even at neutral pH (CARRA *et al*., 2013; STARLING *et al*., 2021a).

In the present study, the potential of solar photo-Fenton (neutral pH, intermittent iron additions) on the elimination and inactivation of RCPs was investigated in synthetic and real MWWTPE. Cell-free RCPs explored in this study carry ARGs that confer resistance to ampicillin and kanamycin. This is unprecedented in the literature as the vast majority of the published studies evaluate the removal of ARGs associated with genomic DNA rather than those carried by RCPs present as cell-free DNA in suspension in MWWTPE (ARSLAN-ALATON *et al*., 2020) and do not assess plasmid activity after treatment (ARSLAN-ALATON *et al*., 2020; ZHANG *et al*., 2019b). Also, most published studies targeting RCPs either apply the proposed treatment in water or a synthetic solution (NIHEMAITI *et al*., 2020; YOON; DODD; LEE, 2018) or to secondary effluent after filtration (YOON *et al*., 2017) and asses their removal by other processes (chlorination, UV-C or just UV/H_2O_2) rather than solar photo-Fenton (ARSLAN-ALATON *et al*., 2020; NIHEMAITI *et al*., 2020; YOON *et al*., 2017; YOON; DODD; LEE, 2018; ZHANG *et al*., 2019b).

2 MATERIAL AND METHODS

2.1 Resistance-conferring Plasmids (RCPs)

The plasmids were obtained from 2019 DNA Distribution Kit plates distributed by International Genetically Engineered Machine (iGEM) Foundation (Cambridge, USA) (https://igem.org/Main_Page). Plasmids pSB1A2 and pSB1K3 were used, and the sequence information of each plasmid is found in the iGEM Registry of Standard Biological Parts (http://parts.igem.org) under the accession numbers BBa_J04450, and BBa_I20260, respectively. Plasmid concentration was measured by spectrophotometry at 260 nm and using Qubit Fluorometric Quantification. The vector pSB1A2 is a high copy plasmid containing an ampicillin resistance gene and red fluorescent protein (RFP) gene reporter under a LacZ promoter. Vector pSB1K3 is a high copy plasmid containing a kanamycin resistance gene and green fluorescent protein (GFP) gene reporter under a constitutive promoter.

2.2 Synthetic secondary wastewater (SWW)

SWW was used as a model matrix for the assessment of treatment efficiency to guarantee the reproducibility of experimental conditions in the different trials as real secondary wastewater may vary according to the sampling campaign. Nutrient solution was prepared by dissolving meat peptone (Kasvi; 160 mg L^{-1}), beef extract (Kasvi; 110 mg L^{-1}), urea (Synth; $CO(NH_2)_2$; 30 mg L^{-1}), NaCl (Sigma-Aldrich; 7 mg L^{-1}), $CaCl_2$ (Synth; 4 mg L^{-1}), $MgSO_4$ (Synth; 2 mg L^{-1}) and K_2HPO_4 (Reagen; 28 mg L^{-1}) in ultra-pure water (OECD, 1992). The physicochemical characterization (APHA, 2017) of the solution was measured after the preparation of SWW (Table I.1).

Table I.1 - Physicochemical characterization of the SWW used as a model matrix (average values; n=3) to assess the removal of RCPs via solar photo-Fenton

Parameter	Unit	SWW
COD	$mgO_2\ L^{-1}$	248 ± 10
pH	-	7.5
DOC	mg L^{-1}	6.3 ± 4.6
Turbidity	NTU	0.3 ± 0.01
TSS	mg L^{-1}	288 ± 111
VSS	mg L^{-1}	129 ± 50
TDS	mg L^{-1}	158 ± 61
Alkalinity	$mgCaCO_3\ L^{-1}$	26 ± 5
Conductivity	µS cm^{-1}	1480.5

Chemical Oxygen Demand (COD), Dissolved Organic Carbon (DOC), Total Suspended Solids (TSS), Volatile Suspended Solids (VSS), Total Dissolved Solids (TDS).

For DOC measurement, a Shimadzu TOC-VCN analyzer was used. DOC was determined in the filtered sample, considering only the organic matter that passed through the filter. The solution was sterilized in autoclave before RCPs addition. RCPs were added to SWW before tests to reach a final concentration of nearly 10^{10} copies mL^{-1} for total plasmid. This concentration was chosen as it is similar to the total concentration of total cell-free DNA present in real wastewater samples (YOON *et al*., 2017).

2.3 Real Municipal Wastewater Treatment Plant Effluent (MWWTPE)

MWWTPE was sampled in the output of a secondary settling tank following an activated sludge reactor in an MWWTP located in Brazil, which receives wastewater from 1.5 million inhabitants (290 $m^3\ d^{-1}$), including hospitals, industries, etc. MWWTPE samples were sterilized before the spike with RCPs to eliminate all biologically active components. Then, also added 10^{10} copies mL^{-1} of total RCPs. The physicochemical characterization (APHA, 2017) before sterilization is shown in Table I.2.

Table I.2 – Physicochemical characterization of the MWWTPE used in solar photo-Fenton experiments performed to remove RCPs

Parameter	Unit	MWWTPE
COD	$mgO_2\ L^{-1}$	255
pH	-	7.4
DOC	$mg\ L^{-1}$	12.81
Turbidity	NTU	63
TSS	$mg\ L^{-1}$	294
VSS	$mg\ L^{-1}$	132
TDS	$mg\ L^{-1}$	161
Alkalinity	$mgCaCO_3\ L^{-1}$	57
Conductivity	$\mu S\ cm^{-1}$	147

Chemical Oxygen Demand (COD), Dissolved Organic Carbon (DOC), Total Suspended Solids (TSS), Volatile Suspended Solids (VSS), Total Dissolved Solids (TDS).

2.4 Solar Photo-Fenton Treatment

Solar photo-Fenton was performed in a glass reactor (400 mL) in bench-scale at a solar simulator chamber (SUNTEST CPS+, ATLAS) containing a Xenon lamp protected by a daylight filter, which emits light in the UV-Vis region (300-800 nm), thus simulating the solar spectrum. The irradiance was set at 268 W m^{-2} (330 to 800 nm) which is equivalent to 30 W m^{-2} (UV-A: 300-400 nm) for 60 minutes (accumulated radiation 5.57 KJ L^{-1}). All reactions were conducted using 50 mg L^{-1} of H_2O_2 (H_2O_2 29%) and 30 mg L^{-1} of Fe^{2+} ($FeSO_4\ 7H_2O$). These concentrations of Fe^{2+} and H_2O_2

were defined according to previous studies (COSTA *et al*., 2020, 2021; STARLING *et al*., 2021a). Experiments were performed at neutral pH using the intermittent iron addition strategy with Fe^{2+} additions at times zero (15 mg L^{-1}), 5 minutes (5 mg L^{-1}), 10 minutes (5 mg L^{-1}), and 15 minutes (5 mg L^{-1}) (STARLING *et al*., 2021a). Control systems consisted of solar/Fe, Fe only, solar/H_2O_2, H_2O_2 alone, and solar irradiation.

During reactions, samples were withdrawn at 30 and 60 minutes to quantify RCPs removal by Real Time PCR (qPCR) using the plasmid DNA extracted. Samples were also withdrawn during all reaction time for iron concentration (Fe^{2+}) by *o*-phenantroline method (ISO 6332:1988). For this purpose, catalase enzyme (460 mg L^{-1} in phosphate buffer) was added for residual hydrogen peroxide consumption once the samples were removed from the reactor. The quantification of residual hydrogen peroxide, using the metavanadate method (NOGUEIRA; OLIVEIRA; PATERLINI, 2005), was done before the addition of catalase. All experiments carried out in SWW and MWWTPE were performed in triplicates.

2.5 Extraction of RCPs

Plasmid DNA extraction was performed using the phenol-chloroform–isoamyl alcohol method adapted from Takeuchi *et al.* (1997). Initially, 300.0 µL of chloroform ($CHCl_3$; Anidrol) and 12.5 µL of isoamyl alcohol ($C_5H_{12}O$; Anidrol) were added to 500 µL of the sample, which was homogenized by inversion and centrifuged at 1200 xg for 5 minutes at 4ºC. The upper phase was recovered, and a 1:1 solution of absolute ethanol (CH_3CH_2OH, Neon) was added, incubated for 10 minutes at 4ºC, and centrifuged at 12000xg for 20 minutes at 4ºC. The supernatant was then discarded, and 100 µL of ethanol, 70%, was added to the sample, homogenized, and centrifuged at 12000 xg for 20 minutes at 4ºC. Once more, the supernatant was discarded, and the final pellet was placed in the oven to dry at room temperature. Finally, the pellet was resuspended with 20 µL of DNA-free water (H_2O, Sigma-Aldrich). The resulting concentration of plasmid DNA was determined in a Nanodrop spectrophotometer at 260 nm.

2.6 Real-time PCR analysis (qPCR)

The number of copies of RCPs per sample was assessed by real-time PCR using the absolute standard curve method. The VF-2 (5'-TGCCACCTGACGTCTAAGAA-3') and

VE-R (5'-ATTACCGCCTTTGAGTGAGC-3') primers were used to quantify both plasmids. These primers were designed to recognize specific sequences present in both RCPs which are not associated with the ARGs carried by these plasmids, thus avoiding any interference involving the natural occurrence of these genes in real matrices. The ability of these primers to amplify the two RCPs was previously checked by conventional PCR. A standard curve using a series of RCP dilutions was constructed to calculate the efficiency of each pair of primer to and quantify both RCPs in synthetic and real effluents. qPCR was prepared with 1µL of genomic DNA template with 10ng of DNA, 5µL of SYBR Premix Ex Taq (Promega, EUA), 1µL of forward and reverse primers, 0.1 µL of dye, and 2.9µL of DNA-free water (Sigma-Aldrich). Amplification was performed in Light Cycler 480 Real-Time PCR System (Applied Science) using the following program: 95°C for 10 min, then 40 cycles (95°C for 30 s and 60°C for 1 min) followed by a gradual denaturation for the elaboration of the melting curve, with an increment of 1°C per minute until the temperature reached 95°C (DE PAIVA *et al*., 2019). This experiment was carried out in triplicates.

2.7 Cultivation of E. coli competent cells and plasmid transformation

As the oxidation of RCPs may result in cell-free DNA containing intact fragments of the PCR amplification region, inactivated plasmids may continue to amplify in PCR even after damage. Therefore, the transformation of non-resistant competent *E. coli,* which did not contain the RCPs explored in this study, was used as a method to evaluate the ability of plasmids present in SWW samples after solar photo-Fenton treatment to induce antimicrobial resistance. This method was only performed for samples obtained during experiments with SWW as it is laborious and qualitative compared to qPCR.

Competent bacteria *E. coli* BL21 were prepared using 0.1M magnesium chloride solution ($MgCl_2$–$CaCl_2$, Sigma-Aldrich). Competent cells were then transformed with 10ng of plasmids by the heat-shock method (CHAN *et al*., 2013). The experiment was performed in biological triplicates and technical duplicates, and the number of colony-forming unit (CFU) was measured in each experiment. The ability of RCP to induce bacteria resistance to antimicrobial and produce GFP and RFP reporter color or fluorescence was also evaluated by microscopy and SpectraMax microplate reader as described in Tagliaferri *et al.* (2020).

2.8 Statistical Analyse

Statistical analyses were performed using GraphPad Prism version 5.0. One-sample Kolmogorov-Smirnoff test was used to evaluate whether the data followed a normal distribution. A nonparametric one-way analysis of variance (ANOVA) test was used to compare the means of each experimental value to time zero (non-treated sample) inside the same experimental group with Bonferroni correction for multiple hypotheses. Differences were considered statistically significant at $p < 0.05$.

3 RESULTS AND DISCUSSION

3.1 Removal of RCP via Solar Photo-Fenton in SWW

To evaluate the efficiency of solar photo-Fenton in RCPs harboring antimicrobial-resistant genes removal from wastewater, the qPCR method was used to quantify RCPs presence in samples before and after treatment and controls. Figure I.1 shows the percentage of RCPs present in SWW samples after 30 and 60 minutes of reaction by Fenton, solar photo-Fenton, and controls. As it may be observed in Figure I.1, qPCR assays did not detect any copies of RCPs (copies mL^{-1}) after one hour of solar photo-Fenton (accumulated radiation 5.75 KJ L^{-1}), thus confirming the efficiency of this process on RCPs carrying resistance genes total elimination. Similar results were found in previous works which assessed the removal of total ARGs (associated with cell-free plasmid DNA and to bacteria DNA) present in MWWTPE by solar photo-Fenton (FIORENTINO *et al*., 2019a; GIANNAKIS *et al*., 2018a; KARAOLIA *et al*., 2017; MOREIRA *et al*., 2018; ZHANG *et al*., 2016). These studies indicated that the removal of total ARGs by solar photo-Fenton varies according to each ARG, matrix composition, and operational conditions (FIORENTINO *et al*., 2019a; GIANNAKIS *et al*., 2018a; ZHANG *et al*., 2016). Also, solar irradiation alone could not remove total DNA (GIANNAKIS *et al*., 2018a), as observed in this study to remove cell-free RCPs (Figure I.1). Besides, Ferro et al. (2016) observed an increase in cell-free ARGs present in suspension in wastewater samples after UV/H_2O_2. Thus, confirming the need for studies targeting cell-free RCPs carrying ARGs to prevent the spread of antimicrobial resistance through wastewater discharge.

Despite the increase observed for cell-free ARGs associated with RCPs present in suspension in MWWTPE samples even after biological treatment, disinfection, and advanced oxidation (DONG *et al*., 2019; FERRO *et al*., 2016; HILLER *et al*., 2019b; LIU *et al*., 2018), no studies have previously targeted specific removal of cell-free ARGs from MWWTPE via solar photo-Fenton as it is done in the present study. The effective removal of cell-free RCPs has only been confirmed for treatments under UV-C irradiation in the presence of oxidants (hydrogen peroxide, peroxymonosulfate, or peroxydisulfate) (ARSLAN-ALATON *et al*., 2020). UV_{254}/H_2O_2 and chlorine were studied to remove and inactivate cell-free ARGs associated with plasmid DNA

(puck4K) from the effluent of a conventional activated sludge process (YOON *et al*., 2017). Arslan-Alaton *et al.* (2020) demonstrated the high efficiency of oxidant/UV-C treatments, which resulted in completely removed genomic and plasmid DNA. In Yoon *et al.* (2017), results indicated that gene structure influences ARGs reduction associated with cell-free DNA via chlorination.

Figure I.1- Percentage of RCPs after 30' and 60' of reaction by Fenton, Solar photo-Fenton, and controls carried out in SWW. The symbol * and * represent significant statistical differences with p < 0.05 and p < 0.001 by nonparametric one-way analysis of variance (ANOVA) test with Bonferroni correction compared to the time 0' for each experimental group, respectively**

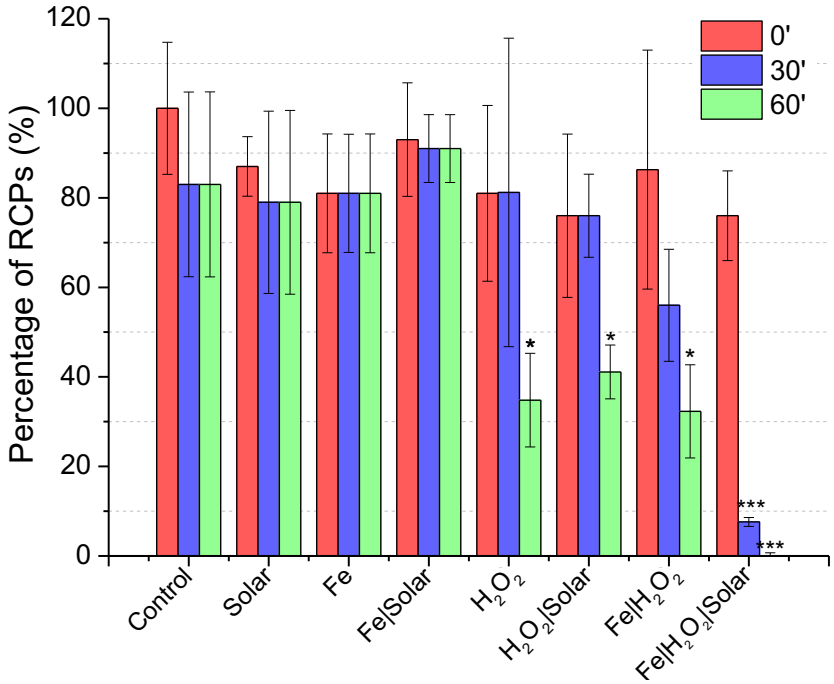

Meanwhile, similar removal rates were observed for different ARGs carried by plasmids under UV_{254} or UV_{254}/H_2O_2 (YOON *et al*., 2017). For instance, a 4-log reduction of ARGs required UV fluences between 60 and 130 mJ cm^{-2}. Besides, UV-induced ARG damage occurred 1.7-fold faster for the cell-free ARGs when compared to intracellular ARGs in filtered MWWTPE, which showed lower organic matter concentrations than the SWW used in this study. Results obtained in the present work are compatible with to results reported in the referred references since the removal of cell-free RCPs was achieved after 30-60 min of treatment. Even so, the use of solar radiation, as proposed in this study, has a range of advantages compared to artificial UV lamps, both from economic and environmental standpoints (OTURAN; AARON, 2014).

Solar irradiation alone, Fe alone, and their combination (Solar + Fe) did not reach any removal of RCPs. This probably occurred because these systems do not generate reactive oxygen species, thus having low reactivity towards RCPs. Solar disinfection (Solar only) and Solar + Fe processes were also ineffective for eliminating ARGs associated with DNA present in MWWTPE (GIANNAKIS, 2018a; GIANNAKIS *et al*., 2018a). However, these were effective for ARB removal due to intra and extracellular ARB damaging processes with loss of protein function. SWW used in the present study did not contain any viable organism as the goal of this study was to analyze the removal of cell-free RCPs present in suspension in MWWTPE rather than ARB. Still, results obtained here and in referred studies indicate that, due to relative stability of DNA, high oxidative potential and extended contact time are usually required for proper elimination of ARGs, thus being more appropriate to use ARGs rather than ARB as indicators to assess the combat of AMR in wastewater samples (SHARMA *et al*., 2016).

Regarding the inactivation of RCPs in control experiments performed in SWW, which was detected by the transformation of *E. coli* with DNA extracted from samples after each treatment, solar and solar + Fe did show a significant reduction of functional resistance to ampicillin and kanamycin (Figure I.2). However, Fe alone was only significantly active towards vector pSB1K3 (kanamycin resistance). These results indicate that, despite not reducing the number of copies of RCPs (Figure I.1), these controls somehow limit the activity of pSB1K3, which also contributes to the reduction of antimicrobial activity. Although there are no previous studies on the matter to elucidate the possible mechanisms of RCP inactivation by Fe alone, it is suspected that RCPs may have complexed with Fe. This hypothesis relies on the fact that plasmid DNA is negatively charged (ROMANOWSKI; LORENZ; WACKERNAGEL, 1991), and iron is highly electronegative. This combination would result in a strong electrostatic attraction between Fe and RCPs (DA SILVA *et al*., 2019). Li *et al.* (2019) obtained excellent removal of extracellular ARGs (*e.g*., plasmid DNA) by pre-coagulation integrated with microfiltration as iron enhanced the aggregation of extracellular DNA. Therefore, it was hypothesized that DNA containing negatively charged phosphate groups bind with positively charged Fe hydroxide colloids through electrostatic adsorption and entrapment during the coagulation process.

Figure I.2 - Number of resistant E. coli to ampicillin (a) and kanamycin (b) recovery after the transformation with total DNA extracted of each control and experimental treatment sample. The symbol *, ** and * represent significant statistical difference with p < 0.05, p < 0.01 and p < 0.001 by nonparametric one-way analysis of variance (ANOVA) test with Bonferroni correction in comparison with the time 0' for each experimental group, respectively**

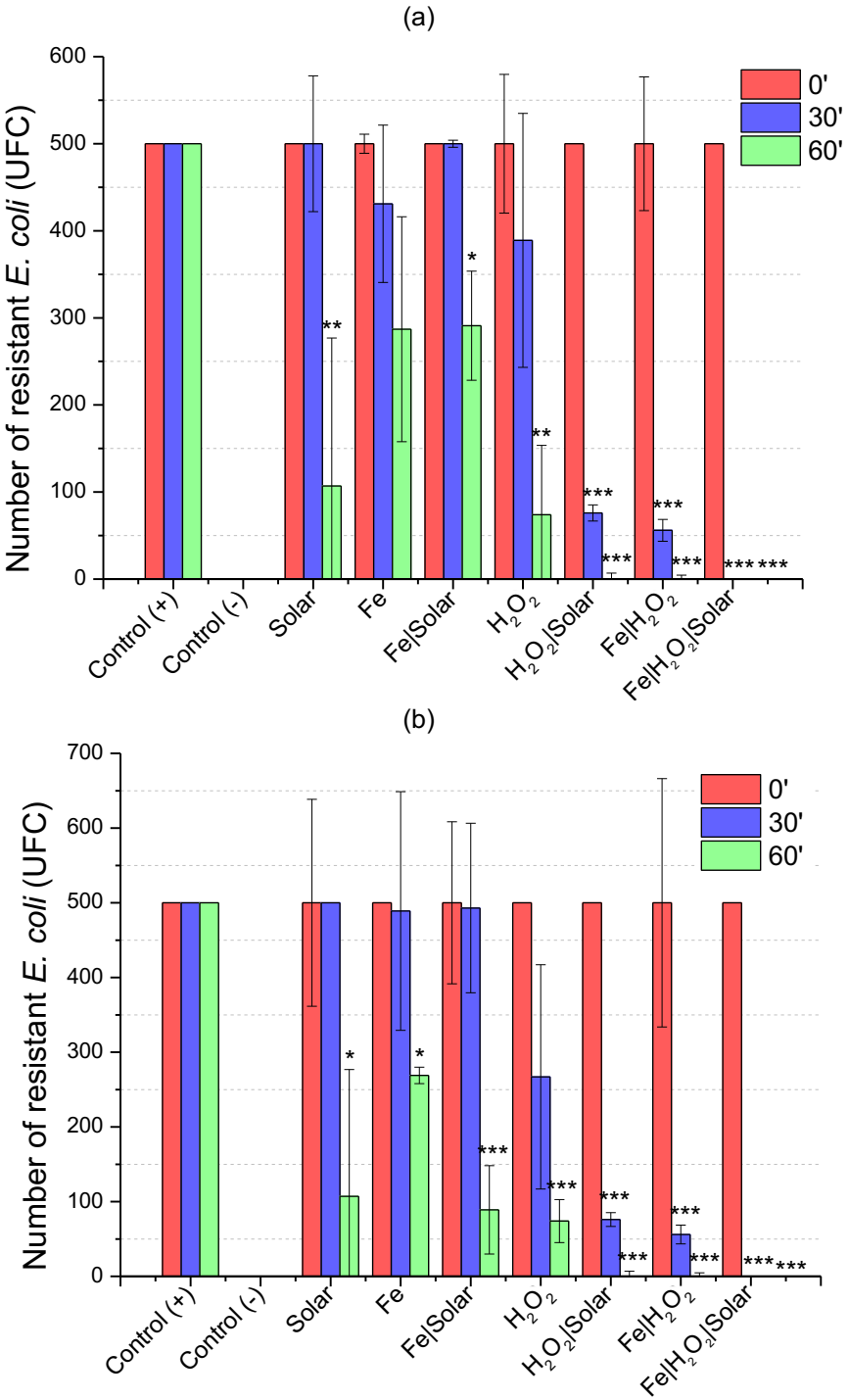

In contrast to results obtained in Yoon *et al.* (2017), who observed no removal of plasmid DNA in the presence of H_2O_2 alone, results shown in Figure I.1 reveal that H_2O_2 alone and solar/H_2O_2 did lead to a significant reduction of RCPs after 1 hour.

This outcome is probably associated with the oxidative potential of H_2O_2 (E^0 = 1.8 V) and with the formation of hydroxyl radicals, as approximately 20-30% of oxidants were consumed in both systems (Figure I.3). Meanwhile, H_2O_2 consumption in the dark Fenton (Fe + H_2O_2) system was nearly 60% (30 minutes; accumulated radiation 2.71 KJ.L^{-1}) (Figure I.3), thus contributing to 40% removal of RCPs when compared to 20% for solar + H_2O_2, as the reaction between Fe and H_2O_2 forms hydroxyl radicals (E^0 = 2.8 V). In the absence of Fe, H_2O_2 consumption probably occurs due to its reaction with organic matter and ions present in SWW (COD of 248 mg L^{-1}).

Figure I.3 - Peroxide consumption, iron concentration after 30' and 60' of reaction by Fenton, Solar photo-Fenton, and controls carried out in SWW

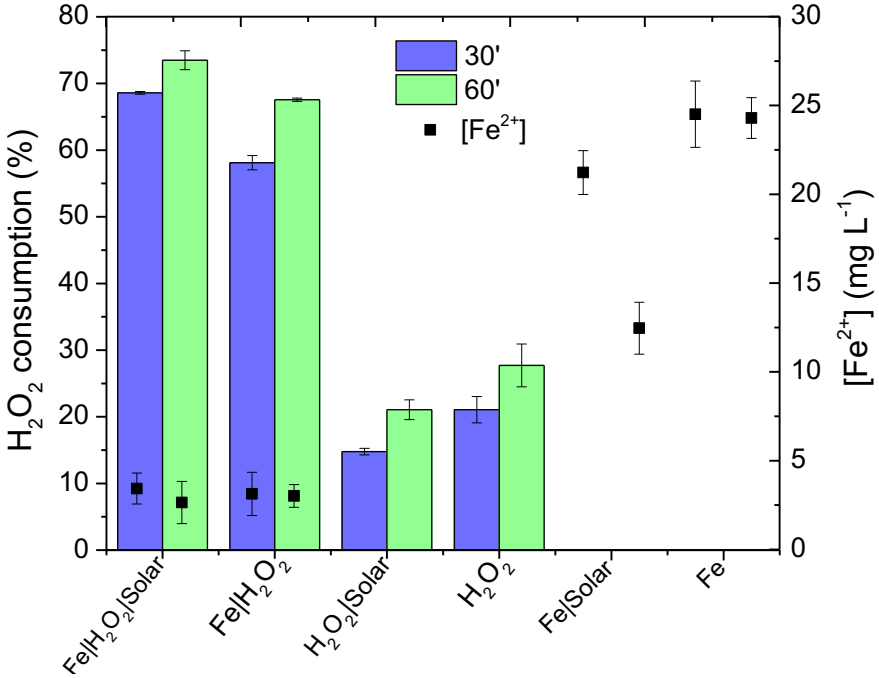

Although H_2O_2 alone, solar + H_2O_2, and Fe + H_2O_2 have the same efficiency of RCP removal (Figure I.1), total inactivation of cell-free RCPs could only be observed for solar + H_2O_2, Fenton, and photo-Fenton processes (Figure I.2). While solar + H_2O_2 and the dark Fenton required one hour to inactivate RCPs completely (Figure I.2), 30 minutes were sufficient for the photo-Fenton system (Figure I.2). This occurs due to higher H_2O_2 consumption in this system (60-70%), thus enhancing the formation of highly reactive species capable of damaging and inactivating cell-free RCPs. Also, as shown in Figure I.3, H_2O_2 consumption was faster in the photo-Fenton process when compared to the dark Fenton, which occurs due to enhanced Fe^{2+} regeneration in the presence of light, leading to increased H_2O_2 consumption (MALATO *et al.*, 2009).

These results show a correspondence between the removal of cell-free RCPs present in suspension in SWW quantified via qPCR and their inactivation, confirmed by bacterial transformation after solar photo-Fenton. Thus, suggesting that the proposed treatment damages the structure of RCPs carrying ARGs and eliminates their potential to induce bacterial resistance by complete inactivation. To confirm the possibility of applying this treatment in MWWTP, it is also essential to evaluate the effect of proposed treatment conditions on removing cell-free RCPs in suspension in real MWWTPE.

3.2 Removal of RCP via Solar Photo-Fenton in MWWTPE

Figure I.4 shows the percentage of cell-free RCPs present in samples after 30 and 60 minutes of reaction by Fenton, solar photo-Fenton, and controls carried out in sterilized MWWTPE. Although real samples are usually more complex and variable, containing several free radical scavenging species (*e.g.* HCO_3^-, Cl^-, Br^-, and NO_3^-) (ABDELRAHEEM; NADAGOUDA; DIONYSIOU, 2020), the SWW used in previous experiments was reasonably consistent with the real MWWTPE applied in this study (Table I.1 and Table I.2).

Figure I.4 - Percentage of RCPs after 30' and 60' of reaction by Fenton, Solar photo-Fenton, and controls carried out in RSWW. The symbol ** represents a significant statistical difference with $p < 0.01$ by nonparametric one-way analysis of variance (ANOVA) test with Bonferroni correction compared with the time 0' for each experimental group

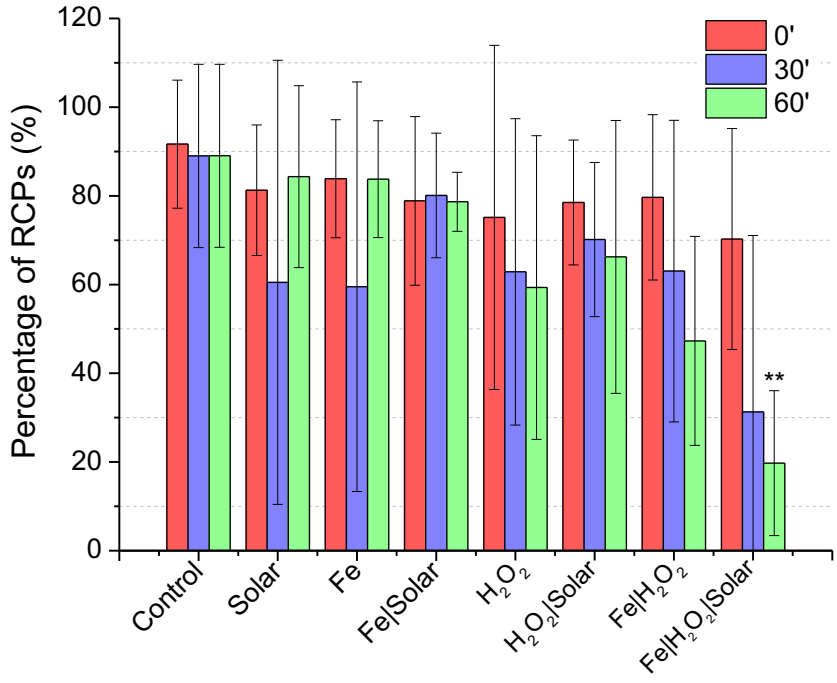

As shown in Figure I.4, solar photo-Fenton efficiency was limited to ~80% RCP removal in MWWTPE compared to total elimination in SWW. Although both matrixes are remarkably similar concerning natural organic matter content, MWWTPE presented higher turbidity and alkalinity. Therefore, the reduced efficiency obtained in the real matrix is probably due to the light scattering effect promoted by turbidity and the scavenging effect promoted by carbonate ions present in higher concentrations in the real matrix. In contrast, Nihemaiti *et al.* (2020) and Yoon *et al.* (2017) observed similar removal of cell-free DNA via UV-H_2O_2 in phosphate buffer compared to real MWWTPE. Yet, the real matrix was filtered before irradiated treatment, thus removing possible effects caused by turbidity. Results obtained in his study for experiments performed in real matrix agree with previous studies, which show that matrix constituents may promote various effects upon reaction kinetics and degradation efficiencies. For instance, Sbardella *et al.* (2019) reported that the removal percentage is reduced by 20-30% due to the scavenging effect of natural components present in secondary effluents under similar treatment conditions. As observed in Figure I.4, it is evident that photo-Fenton was more effective in removing cell-free RCPs in suspension in real MWWTPE than the dark Fenton process and controls. This occurs as photo-generated ferrous ion participates in the photo-Fenton reaction generating additional $HO^{\bullet}$ radicals, thereby accelerating the oxidation process under irradiation when compared to the dark Fenton process (KAVITHA; PALANIVELU, 2004; MOSTEO *et al*., 2020), thus resulting in ~80% RCPs removal under irradiation as compared to ~53% achieved by the dark Fenton process.

Solar irradiation, Fe alone, and Fe + solar, did not reach any removal of RCPs, as these systems do not generate reactive species. Meanwhile, H_2O_2 and H_2O_2 + solar showed a relatively low reduction percentage (41% and 34%) compared to results obtained in SWW (67% and 60%), which is possibly a consequence of quenching and light scattering effects occurring in the real sample as previously explained. For the Photo-Fenton process, the removal of cell-free RCPs was nearly 30% lower in MWWTPE than under the same conditions in SWW. This is justified by the $HO^{\bullet}$ scavenging effect promoted by natural components of real MWWTPE, as H_2O_2 consumption (Figure I.5) was similar for both matrixes (~30% in SWW and ~40% in real MWWTPE). Even though the COD of the SWW (248 mg L^{-1}) is similar to that

observed for MWWTPE (255 mg L^{-1}), its composition is more complex as it contains recalcitrant compounds that are more difficult to degrade than those present in the SWW, thus showing higher consumption of oxidative radicals which decrease the availability of these species for the oxidation of target cell-free RCPs present in solution in MWWTPE.

Figure I.5 - Peroxide consumption and iron concentration after 30' and 60' of reaction by Fenton, Solar photo-Fenton, and controls carried out in RSWW

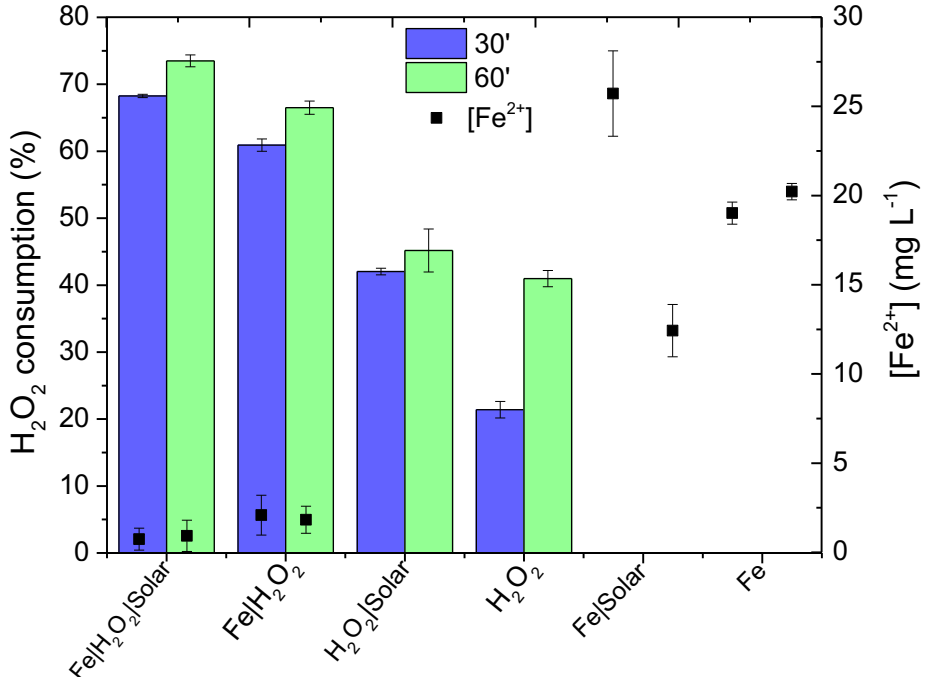

4 CONCLUSIONS

This study reveals the effectiveness of solar photo-Fenton at neutral pH to remove and inactivate cell-free RCPs present in suspension synthetic and real MWWTPE. As these RCPs carry ARGs that non-resistant bacteria may acquire in the environment, results presented here indicate the potential of solar photo-Fenton to combat the spread of AMR related to secondary wastewater disposal. Solar photo-Fenton promoted total elimination and inactivation of RCPs within 30 minutes of reaction in SWW. Meanwhile, 60 minutes were necessary for similar effects in the absence of light. Although Solar + H_2O_2 and H_2O_2 alone showed effective removal of RCPs (>60%) in SWW, these processes could not inactivate RCPs. The role of Fe^{2+} alone on the inactivation of RCP from secondary wastewater must be further elucidated in future studies.

Experiments performed in MWWTPE confirmed the efficiency of the solar photo-Fenton process on the removal (≈ 80%) of cell-free RCPs present in solution in MWWTPE under the same conditions tested in SWW. Results also indicated the influence of matrix composition upon oxidant and hydroxyl radical consumption as only solar photo-Fenton led to significant (>60%) plasmid removal in real samples.

CHAPTER II - Metagenomic analysis of MWWTP effluent treated via solar photo-Fenton at neutral pH: Effects upon microbial community, priority pathogens, and antimicrobial resistance genes[2]

[2]This chapter was published according to the following reference: VILELA, Pâmela B.; MENDONÇA NETO, Rondon P.; STARLING, Maria Clara V. M.; DA S. MARTINS, Alessandra; PIRES, Giovanna F. F.; SOUZA, Felipe A. R.; AMORIM, Camila C. Metagenomic analysis of MWWTP effluent treated via solar photo-Fenton at neutral pH: Effects upon microbial community, priority pathogens, and antibiotic resistance genes. Science of The Total Environment, v. 801, p. 149599, 2021. DOI: 10.1016/j.scitotenv.2021.149599.

1 INTRODUCTION

Antimicrobial resistance (AMR) challenges the treatability of infectious diseases as it decreases the performance of antimicrobials used to treat infected patients. Treatment processes applied in Municipal Wastewater Treatment Plants (MWWTP) play a key role in the spread of antimicrobial-resistant bacteria (ARB) and resistance genes (ARGs) to the environment. The resistome present in Municipal Wastewater Treatment Plants Effluent (MWWTPE) is influenced by the high density and rate of interaction between microbial communities aligned to subinhibitory concentrations of antimicrobials in biological reactors. These factors favor ARG transfer to non-resistant strains resulting in ARB enrichment in the discharged effluent (MURRAY *et al*., 2018; STANTON *et al*., 2020). Therefore, reducing AMR in MWWTP remains a critical challenge (FIORENTINO *et al*., 2019a; VIKESLAND *et al*., 2019b).

The World Health Organization (WHO) highlights that the surveillance of critical hotspots of AMR (*i.e.* MWWTP) is essential. In order to monitor the threat, it is necessary to take a ″One Health″ approach involving coherent and concerted multisectoral (human, animal, and environmental) actions to counter AMR at various levels. Hence, many countries adopt this perspective by tackling the spread of ARB promoted by MWWTPE discharge (COLLIGNON; MCEWEN, 2019). The WHO prioritized ARB on their list of ‘global priority pathogens’ which pose the greatest threat to human health, such as some bacterial species and their accompanying resistome (e.g. Carbapenem-resistant *Acinetobacter baumannii*; Cephalosporin-resistant *Klebsiella pneumonia*; Vancomycin-resistant *Enterococcus faecium*, etc.) (WHO, 2017; Starling *et al*., 2021b). Consequently, investments in the development of advanced wastewater treatment strategies that promote the removal of ARB and ARGs from municipal wastewater (MWW) prior to discharge have increased.

Many studies indicate that tertiary treatment technologies such as chlorination, UV-C, and ozonation are ineffective to remove ARB and ARGs from MWWTPE (DI CESARE *et al*., 2020; LEE *et al*., 2017; NARCISO-DA-ROCHA *et al*., 2018). Chlorination may select ARB favoring their spread and affecting intra and extracellular concentrations of ARGs (GUO; YUAN; YANG, 2015; HOU *et al*., 2019; LIU *et al*., 2018). Recently, ozonation has been associated with the selection of *Pseudomonas aeruginosa*

(MOREIRA *et al*., 2021), a priority pathogen according to the WHO (2017). In contrast, Advanced Oxidation Processes (AOP) are feasible methods for the inactivation of bacteria and elimination of ARGs as oxidative radicals damage cell membrane and DNA structure through free radical reactions (GUO *et al*., 2020; LI *et al*., 2021; MICHAEL-KORDATOU; KARAOLIA; FATTA-KASSINOS, 2018). Even though, regrowth has been observed after some AOP treatments, especially H_2O_2+sunlight (FIORENTINO et al., 2015; MICHAEL et al., 2020; WANG et al., 2021a).

Photo-Fenton has been confirmed to promote effective removal of ARB and ARGs and inactivate cell-free ARGs from MWWTPE (Michael-Kordatou *et al*., 2018; Vilela *et al*., 2021; Starling *et al*., 2021a). Yet, one of the main limitations of photo-Fenton treatment is the optimal pH of operation (2.8 – 3.0). Considering the natural pH of MWWTPE (6.0 – 7.5), different strategies have been investigated to apply photo-Fenton at a circumneutral pH level (CLARIZIA *et al*., 2017). A feasible alternative for this purpose is the intermittent iron addition strategy which assures the presence of soluble and reactive Fe^{2+} species throughout treatment (CARRA *et al*., 2013, 2014; DÍAZ-ANGULO *et al*., 2021). This strategy has been proven effective for disinfection and ARB removal (Starling *et al*., 2021a). Since photo-Fenton may be carried out under sunlight, its investigation for the improvement of MWWTPE quality in areas of high solar irradiance (*i.e.* tropical developing countries) must be further stimulated.

Nevertheless, the quantification of ARB and ARGs in MWWTPE samples and analysis of solar photo-Fenton impact upon resistome profile is still challenging. Most studies apply culture-dependent methods (IOANNOU-TTOFA *et al*., 2019; MICHAEL *et al*., 2020; MOREIRA *et al*., 2018; RODRÍGUEZ-CHUECA *et al*., 2019; STARLING *et al*., 2021a), which are relevant as they prove the viability of ARB and expression of ARGs after treatment. Yet, culture-dependent methods may be inadequate to analyze treatment effects upon uncultivable organisms, which represent public health risks (MANAIA *et al*., 2018; VAZ-MOREIRA *et al*., 2011). In contrast, metagenomic analyses such as 16S rDNA sequencing show high specificity and sensitivity for all organisms, no matter their viability, and enable the analysis of treatment impact upon microbial community and resistome, which are fairly diverse in MWWTPE (RIZZO *et al*., 2013). In addition, Whole Genome Sequencing (WGS) enables identifying all genes present

in a sample using high throughput screening (ISHII, 2020; RICE *et al*., 2020). So far, no previous studies have assessed WGS profile of MWWTPE treated by solar photo-Fenton. Besides, only a few studies analyze treatment efficiency upon some priority pathogens listed by WHO (WHO, 2017) and present in MWWTPE (GIANNAKIS *et al*., 2018b; KARAOLIA *et al*., 2014, 2018; MICHAEL *et al*., 2019). Yet, none of the previous studies encompassed the complete list. The goal of this study was to investigate the effects of the solar photo-Fenton process upon priority pathogens, bacterial community, and ARGs present in MWWTPE by using metagenomic analyses (16S rDNA sequencing and WGS) with a deep examination of the effect of the proposed treatment upon WHO critical priority pathogens and resistome profiles.

2 MATERIAL AND METHODS

2.1 MWWTPE sampling

MWWTPE was sampled in the output of a secondary settling tank from a conventional activated sludge system in an MWWTP located in Belo Horizonte, in the southeast of Brazil, which receives wastewater from 1.5 million inhabitants (290 m^3 d^{-1}), including hospitals, industries, etc. The samples were collected throughout a whole year, comprising wet and dry seasons.

Physicochemical characterization of MWWTPE as presented in Table II.1 (APHA, 2017). For Dissolved Organic Carbon (DOC) and Total Inorganic Carbon (TIC) measurement, a Shimadzu TOC-VCN analyzer was used. DOC was determined in filtered samples, considering only the organic matter that passed through the filter.

2.2 Solar photo-Fenton treatment

Solar photo-Fenton (Fe^{2+} + H_2O_2 + Solar) treatment of MWWTPE was conducted in a solar simulator chamber (SUNTEST CPS+, ATLAS) containing a Xenon lamp protected by a daylight filter, which emits light in the UV-Vis region (300-800 nm), thus simulating the solar spectrum. The irradiance was set at 268 W m^{-2} (330 to 800 nm) which is equivalent to 30 W m^{-2} (UV-A: 300-400 nm) corresponding to the annual average irradiance in Belo Horizonte/MG. The temperature was kept constant at 35°C.

Experiments were performed at neutral pH in a glass container (400 mL) under continuous stirring. Preliminary Fenton and solar photo-Fenton experiments (30 mg L^{-1} of Fe^{2+} and 50 mg L^{-1} of H_2O_2) were conducted for 120 and 240 min to determine the most appropriate reaction length. Then, reactions were performed with 5 mg L^{-1} and 30 mg L^{-1} Fe^{2+} (intermittent additions: 0 min = 15 mg L^{-1}; 5, 10 and 15 min = 5 mg L^{-1}) in the presence of 50 mg L^{-1} of H_2O_2 (240 min) to determine the most appropriate iron concentration. These reagent concentrations were defined according to Vilela *et al*. (2021).

Table II.1 - Physicochemical characterization of MWWTPE

Parameter		2019								2020			$\bar{x} \pm \sigma$
		13/05	27/05	28/05	03/06	03/06	04/06	09/12	12/12	10/02	10/02	10/02	
COD	$mgO_2\ L^{-1}$	45	151	133	70	72	87	74	55	87	60	64	72 ± 32
pH	-	7.2	7.6	7.0	7.4	7.5	7.0	7.4	7.1	7.1	7.0	7.3	7.2 ± 0.2
T	Temp.	24.5	23.0	24.5	23.0	24.0	23.5	24.0	24.0	23.5	23.5	24.5	24 ± 0.6
DOC	$mg\ L^{-1}$	8.133	17.980	-	26.46	-	25.114	12.811	10.33	8.928	7.581	7.928	10.33 ± 7.4
TIC	$mg\ L^{-1}$	59.823	47.72	-	28.24	-	33.48	12.61	16.9	22.45	26.25	28.18	28.45 ± 18
TN	$mg\ L^{-1}$	38.74	45.98	-	42.21	-	49.07	35.145	26.8	22.74	22.52	20.94	37.23 ± 18.9
TU	NTU	10.6	11.4	13.2	53.0	48.5	72.8	22.7	24.3	26.0	24.2	23.4	24.3 ± 19.1
TS	$mg\ L^{-1}$	444	631	583	718	727	267	302	267	370	364	347	347 ± 176
TVS	$mg\ L^{-1}$	148	284	225	346	352	120	132	120	164	156	154	156 ± 80
TFS	$mg\ L^{-1}$	276	347	287	422	382	174	162	146	206	206	206	196 ± 97
A	$mgCaCO_3\ L^{-1}$	168	208	212	211	195	145	157	95	143	145	143	157 ± 47
C	$\mu S\ cm^{-1}$	714	202	215	546	521	645	386	306	535	516	491	461 ± 167

Chemical Oxygen Demand (COD - APHA 5220 D), pH, Temperature (T), Dissolved Organic Carbon (DOC), Total Inorganic Carbon (TIC), Total Nitrogen (TN), Turbidity (TU), Total Solids (TS - APHA 2540 B), Total Volatile Solids (TVS - APHA 2540 E), Total Fixed Solids (TFS - APHA 2540 C), Alkalinity (A - APHA 2320 B), and Conductivity (C - APHA 2510 B).

Solar photo-Fenton was performed using 30 mg L^{-1} Fe^{2+} (intermittent additions) and 50 mg L^{-1} of H_2O_2 for 240 min at neutral pH in all subsequent treatments. Controls consisted of Fenton (Fe^{2+} + H_2O_2), Fe^{2+} alone, Solar + Fe^{2+}, H_2O_2, Solar + H_2O_2 and solar irradiation alone under the same operational conditions. Samples were withdrawn during reactions for residual H_2O_2 (NOGUEIRA; OLIVEIRA; PATERLINI, 2005) and Fe^{2+} quantification (APHA, 2017), and after 240 min of treatment for DNA extraction to later ARB and ARG analysis. Catalase enzyme (460 mg L^{-1} in 0.04M phosphate buffer) was added to consume residual H_2O_2 (POOLE, 2004).

2.3 Culture-based analysis of antimicrobial susceptibility for MIC

The determination of ARB was performed by antimicrobial susceptibility testing for minimum inhibitory concentrations (MIC) (CLI, 2015). A non-selective medium (Plate Count Agar – PCA) was used to evaluate the growth of total heterotrophic bacteria (THB) present in MWWTPE before and after the proposed treatment. At the same time, ARB quantification was performed in PCA medium enriched with Sulfamethoxazole (SMX, 350 mg L^{-1}), Trimethoprim (TMP, 350 mg L^{-1}), Ciprofloxacin (CIP, 4 mg L^{-1}), Tetracycline (TET, 16 mg L^{-1}), and Amoxicillin (AMX, 32 mg L^{-1}). These drugs were chosen as they correspond to different classes of antibiotics which are strongly associated to antimicrobial resistance present in MWWTPE. All plates were performed in triplicate and incubated at 37 ± 1 °C for 48 h, and colony-forming units (CFU) were quantified in each plate.

2.4 DNA extraction, quality control, library preparation, and sequencing

MWWTPE (300 mL) and samples withdrawn after 240 min of treatment (300 mL) were filtered through a standard mixed cellulose filter (0.2 µm; Merck, Millipore). The filters were stored in sterile tubes at -20°C for further analysis. Total DNA extraction was performed using FastDNA® Spin Kit for Soil (MP Biomedicals) following the manufacturer's protocol. DNA concentration and purity were measured by a NanoDrop UV–Vis spectrophotometer (Thermo Fisher Scientific), and structural integrity was determined by 1% agarose gel electrophoresis. Extracted DNA was shipped to Macrogen for library preparation and sequencing. Paired-end fragment libraries with a length of 450nt from the 16S rDNA V3-V4 region were constructed using the primers

338F ACTCCTACGGGAGGCAGCA and 806R GGACTACHVGGGTWTCTAAT. 300nt reads of each end were sequenced from fragments (Illumina MiSeq platform). Entire genomic DNA libraries were produced and sequenced (Illumina HiSeq) in 150nt paired ends reads for WGS.

2.5 Bioinformatics Analysis

2.5.1 Taxonomic Assignment

All pre-processing was carried out using the Micca software (ALBANESE *et al*., 2015). Sequence read pairs were merged, and quality filtering was performed by trimming primer adapters from the concatenated sequences and removing low-quality sequences (0.75% max. error and 400nt min size). Operational Taxonomic Units (OTUs) were generated *de novo* by multiple and global alignments within each sample by grouping those which contained more than 97% identity. Next, resulting OTUs were classified taxonomically (Ribosomal Database Project) (COLE *et al*., 2014). The NAST algorithm globally aligned OTUs to generate phylogenetic profiles. Pre-processed data were used as input in R 3.6.3 (https://www.r-project.org/), Phyloseq (MCMURDIE; HOLMES, 2013), and vegan (Oksanen *et al*., 2019) packages.

A total of 7,486,167 high-quality sequences (> 465 bp) were retained by 16S sequencing analysis. Good's coverage was higher than 99% (GOOD, 1953), indicating that the dataset was representative of the bacterial communities present in samples. Relative abundance in MWWTPE samples was compared by Kruskal-Wallis and Wilcoxon tests (a = 0.05) (SEGATA *et al*., 2011).–Diversity and richness were calculated using rarified and non-rarefied versions of bacterial counts (ROWE; WINN, 2018). Non-rarefied counts were used for further analysis to avoid false positives and data loss (MCMURDIE; HOLMES, 2014). Diversity degrees were accessed by beta-diversity (PCoA) using the Bray-Curtis dissimilarity index. Alpha-diversity analyses ("Observed" index and non-parametric methods "Chao1" and "Ace") were used for estimating the number of species (KIM *et al*., 2017). A phylogenetic tree was drawn (100 bootstraps) containing priority pathogens (WHO, 2017) and other relevant species (MACHADO *et al*., 2020). DESeq2 R packages were used to compare the

abundance of classes present in MWWTPE and treated samples (LOVE; HUBER; ANDERS, 2014).

2.5.2 Identification of ARGs

Sequenced reads were checked for quality (FastQC) (WINGETT; ANDREWS, 2018) and filtered by trimming primer adapters and low-quality sequences (Q<30) using Trimmomatic (BOLGER; LOHSE; USADEL, 2014). Reads were mapped to the ARG reference database Resfinder (BORTOLAIA *et al*., 2020) by Groot software (ROWE; WINN, 2018). All sample reads were partially assembled in de Bruijn graphs MetaCherchant software (OLEKHNOVICH *et al*., 2018) to correlate ARGs with host species by Kraken 2 (WOOD; LU; LANGMEAD, 2019) against the NR database (O'LEARY *et al*., 2016). A heatmap with ARGs abundance, classes, and GC content was plotted using R package pheatmap (https://cran.r-project.org/web/packages/pheatmap/index.html) and Circos (KRZYWINSKI *et al*., 2009). Inhouse perl and R scripts were used to parse data.

Analysis of genes that confer resistance to H_2O_2 (KatA1, KatA2, KatMn, and KatE, AhpCF, Gpx1, Gpx2, and Gpx3) were carried out using filtered reads aligned against catalase (E1S7Y1_HELP9, G0L8N0_ZOBGA, and CATE_ECOLI), hydroperoxidase (Q9RQ72_BACFG), and glutathione peroxidase (GPX1_SYNY3, GPX2_SYNY3 and A0A5P9CBT8_9PSED) peptide sequences through tblastn aligner (CAMACHO *et al*., 2009). Iinhouse bash scripts were used to parse results and measure abundance.

3 RESULTS AND DISCUSSION

3.1 Bacterial community in MWWTPE

Phylogenetic analysis of MWWTPE bacterial community is summarized in Figure II.1. *Proteobacteria* was the dominant phylum in all samples (29.55% ± 10.87% of total sequences), followed by *Actinobacteria* or *Bacteroidetes,* for which occurrence varied seasonally. *Actinobacteria* (20.50 ± 10.78%) prevailed in samples from the dry season, whereas *Bacteroidetes* (19.70 ± 6.83%) were predominant in samples from the wet season. Phyla *Chloroflexi* (11.71 ± 9.68%), *Firmicutes* (3.08 ± 3.38%), and *Acidobacteria* (2.16 ± 1.88%) were also represented in samples.

Figure II.1 - Relative abundance of bacterial phyla in MWWTPE samples (n = 11) during wet and dry seasons. Taxa with an abundance below 1% and unclassified taxa were designated as NA

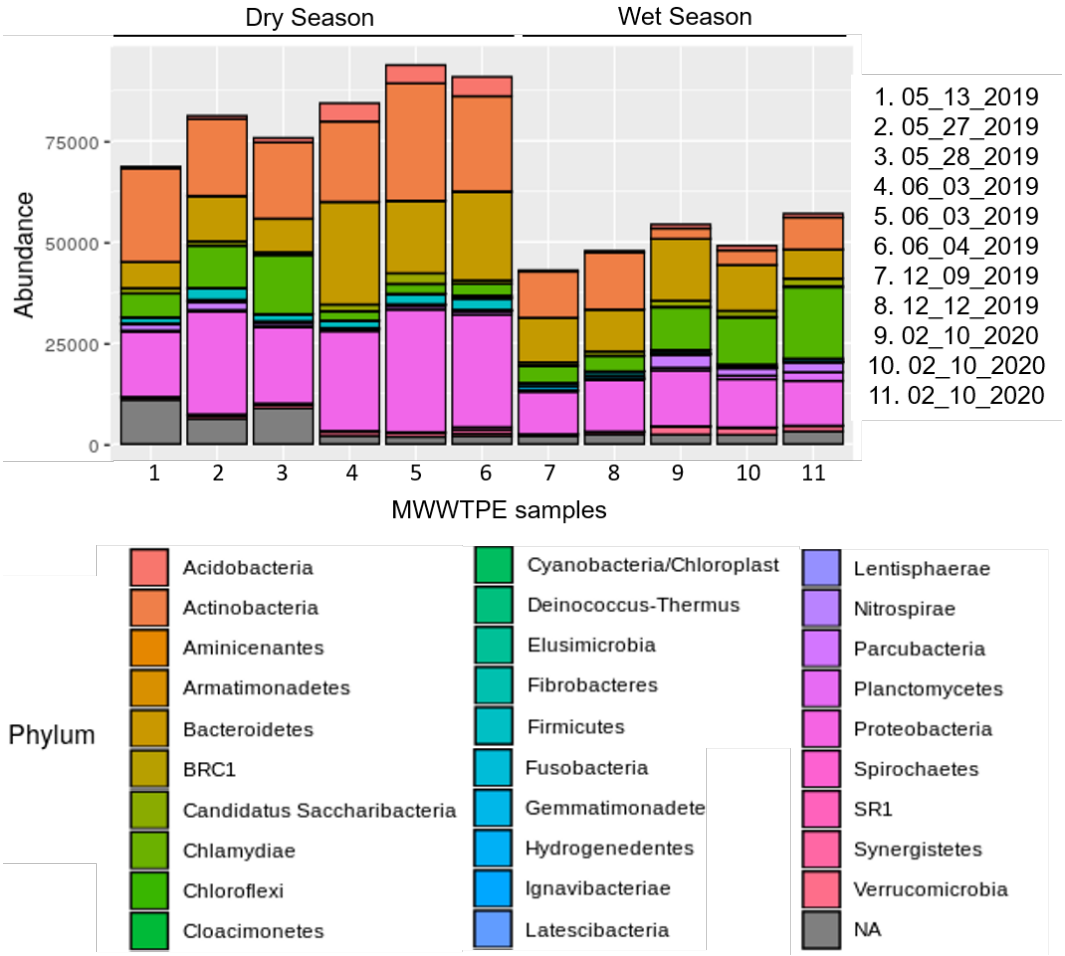

Proteobacteria, along with divergent proportions of *Bacteroidetes, Chloroflexi, Actinobacteria, Acidobacteria,* and *Firmicutes,* were also detected in MWWTPE from activated sludge reactors worldwide (DE CELIS *et al*., 2020; NUMBERGER *et al*.,

2019). No significant differences concerning bacterial composition were detected in the different samples ($p < 0.05$) using a Linear discriminant analysis Effect Size (LEfSe). Specifically, the non-parametric factorial Kruskal-Wallis sum-rank test was used to detect phylum with significant differential abundance. Besides that, biological consistency was investigated using the (unpaired) Wilcoxon rank-sum test (SEGATA *et al*., 2011). This indicates the stability of MWWTPE microbial community and reflects the operational consistency of the activated sludge system applied in the MWWTP.

Although no significant differences concerning bacterial composition were detected, MWWTPE samples present a diverse variety of the occurrence of a high abundance of ARB and ARGs (Figure II.2). For instance, Figure II.2 shows the broad correlation between pathogenic microorganisms and resistance genes from several classes of antimicrobials. Due to the vast and varied bacterial species present in the effluent sample that do not cause disease and are not associated with clinical pathogens, the WHO Global Priority Pathogens List (WHO, 2017) was highlighted. These organisms pose the greatest threat to human health. The WHO list is divided according to the urgency for new antibiotics. The most critical group (*i.e*., *Acinetobacter baumannii*, *Pseudomonas aeruginosa,* and *Enterobacteriaceae*) includes multidrug-resistant bacteria, which bear mainly clinical threat (GOVINDARAJ VAITHINATHAN; VANITHA, 2018).

Figure II.2 shows a high correlation between the different subtypes of multidrug ARGs and *Enterobacteriaceae* species (mainly *Escherichia coli, Enterobacter* spp., and *Serratia* spp.). Another critical point is the strong correlation between the *Enterococcus faecium* and vancomycin-resistant subtypes (priority high by WHO), as well as the relationship between critical priority (*Acinetobacter baumannii* and *Pseudomonas aeruginosa)* and β-lactam resistant subtypes. There is no disinfection stage following the biological process in this MWWTP, so this effluent, with a high diversity of ARB and ARGs, is discharged into the environment. Consequently, this MWWTPE are a great source for AMR spread to environmental matrices, confirming the need for the application of advanced treatments for the elimination of these pathogenic organisms and the ARGs associated with them from MWWTPE.

Figure II.2 - Co-occurrence patterns and contributor network associations between ARG subtypes and microbial community (WHO priority pathogens) present in MWWTPE. The nodes were colored according to ARG types. A connection represents a significant and robust correlation ($p < 0.01$)

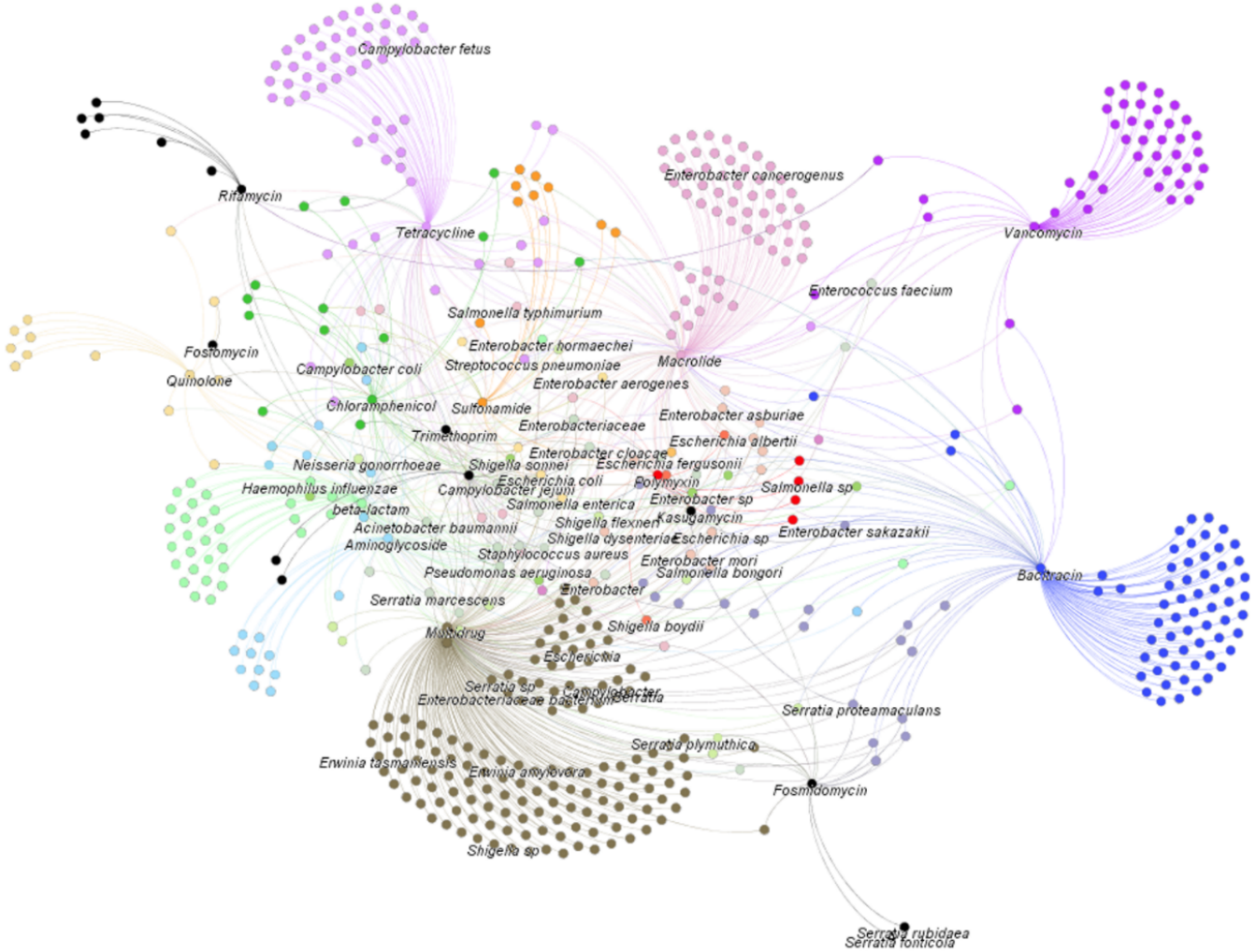

3.2 Effect of solar photo-Fenton on bacteria community

Solar photo-Fenton reaction applied for 240 min (22.28 kJ L^{-1}, 49.5 mg L^{-1} of H_2O_2 consumption) was the most efficient condition for the reduction of microbial community diversity (Figure II.3). In solar processes, treatment efficiency is highly associated with accumulated irradiation during treatment (240 min = 22.28 kJ L^{-1}; 120 min = 11.14 kJ L^{-1}). The incident irradiation used in this study was equivalent to 30 W m^{-2}, which equals average incident irradiation in tropical locations. In this way, reaction time and reactor volume for the application of solar processes must be determined for each site and season after the conduction of scale-up experiments (STARLING *et al.*, 2021b).

Figure II.3 - Principal coordinates analysis (PCoA) based on Bray-Curtis dissimilarity index among the samples of MWWTPE, solar photo-Fenton (Fe_{30mg} + H_2O_2 + solar), and Fenton (Fe_{30mg} + H_2O_2) conducted for 120 or 240 minutes

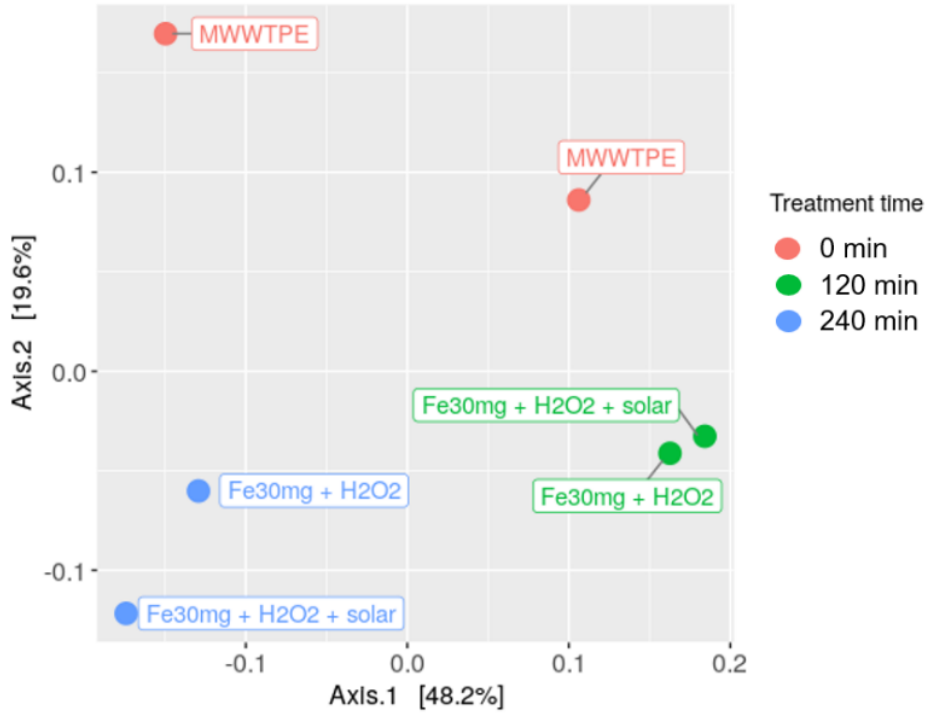

Enhanced disinfection rates are expected to occur after prolonged exposure to irradiation alone. It promotes cell membrane damage and leads to the formation of oxidative radicals from matrix components (GIANNAKIS, 2018b). Additionally, enhanced H_2O_2 consumption during photo-Fenton reactions is associated with a higher generation of oxidative radicals (Equation II.1), thus resulting in exposure of bacteria to highly hostile conditions. Exposition of bacteria to these conditions initially

causes reduced damage, yet prolonged treatment times lead to accumulated injury and eventual cell death (SERNA-GALVIS *et al*., 2019; VERBEL-OLARTE *et al*., 2021).

$$Fe_2^{+} + H_2O_2 \rightarrow Fe^{3+} + HO^{\bullet} + OH^{-} \quad \text{(II.1)}$$

In contrast, recent literature points out the spread and selection of ARB and ARGs after the application of traditional technologies such as Chlorine, ozonation, and UV-C irradiation/oxidant (JIN *et al*., 2020; KIRCHNER *et al*., 2020; LEE *et al*., 2021; MOREIRA *et al*., 2021; SHARMA *et al*., 2019). In addition, ozonation and UV-C irradiated processes are energy-intensive and costly, hindering their application in developing countries. Meanwhile, solar photo-Fenton explores a natural and costless energy source abundant in tropical developing countries.

Solar photo-Fenton using 30 mg L^{-1} of iron (intermittent additions) had a higher impact upon microbial community diversity (640 OTUs) compared with 5 mg L^{-1} of iron (899 OTUs) (Figure II.4a). Higher availability of Fe^{2+} in the system using 30 mg L^{-1} led to greater oxidant consumption (Figure II.4b) in the reaction between iron and H_2O_2 (Equation II.1) and consequently higher generation of hydroxyl radicals ($HO^{\bullet}$) which react quickly with cell components such as DNA (10^8-10^9 M s^{-1}) (NETA *et al*., 1988), thus promoting disinfection and decreasing the diversity of microbial community present in MWWTPE.

The intermittent iron addition strategy ensured the continuous presence of Fe^{2+} during reactions at neutral pH even after 60 min (Figure II.4b), thus being shown to be effectively overcome the limitation associated with optimal pH for the operation of photo-Fenton (CARRA *et al*., 2013, 2014; CLARIZIA *et al*., 2017; DÍAZ-ANGULO *et al*., 2021). Fe^{2+} cycling (Equation II.2) is enhanced in the photo-Fenton system, and an extra route for the formation of $HO^{\bullet}$ (Equation II.3) occurs under UV-A irradiation via light adsorption by iron hydroxides formed in the system (TARR, 2003).

$$Fe^{3+} + H_2O_2 \rightarrow Fe^{2+} + HO_2^{\bullet} + H^{+} \quad \text{(II.2)}$$

$$Fe(OH)^{2+} + hv_{(540\text{-}580\ nm)} \rightarrow Fe^{2+} + HO^{\bullet} \quad \text{(II.3)}$$

Figure II.4 - Comparison of alpha diversity metrics (MWWTPE = 1047 OTUs; Solar photo-Fenton 30 mg L^{-1} = 640 OTUs; solar photo-Fenton 5 mg L^{-1} 898 OTUs; control Fenton mg L^{-1} = 980 and 30 mg L^{-1} of Fe^{2+} = 800 OTUs) (a), dissolved iron concentration, and hydrogen peroxide consumption (b) for solar photo-Fenton and control treatments using 30 or 5 mg L^{-1} of Fe^{2+}

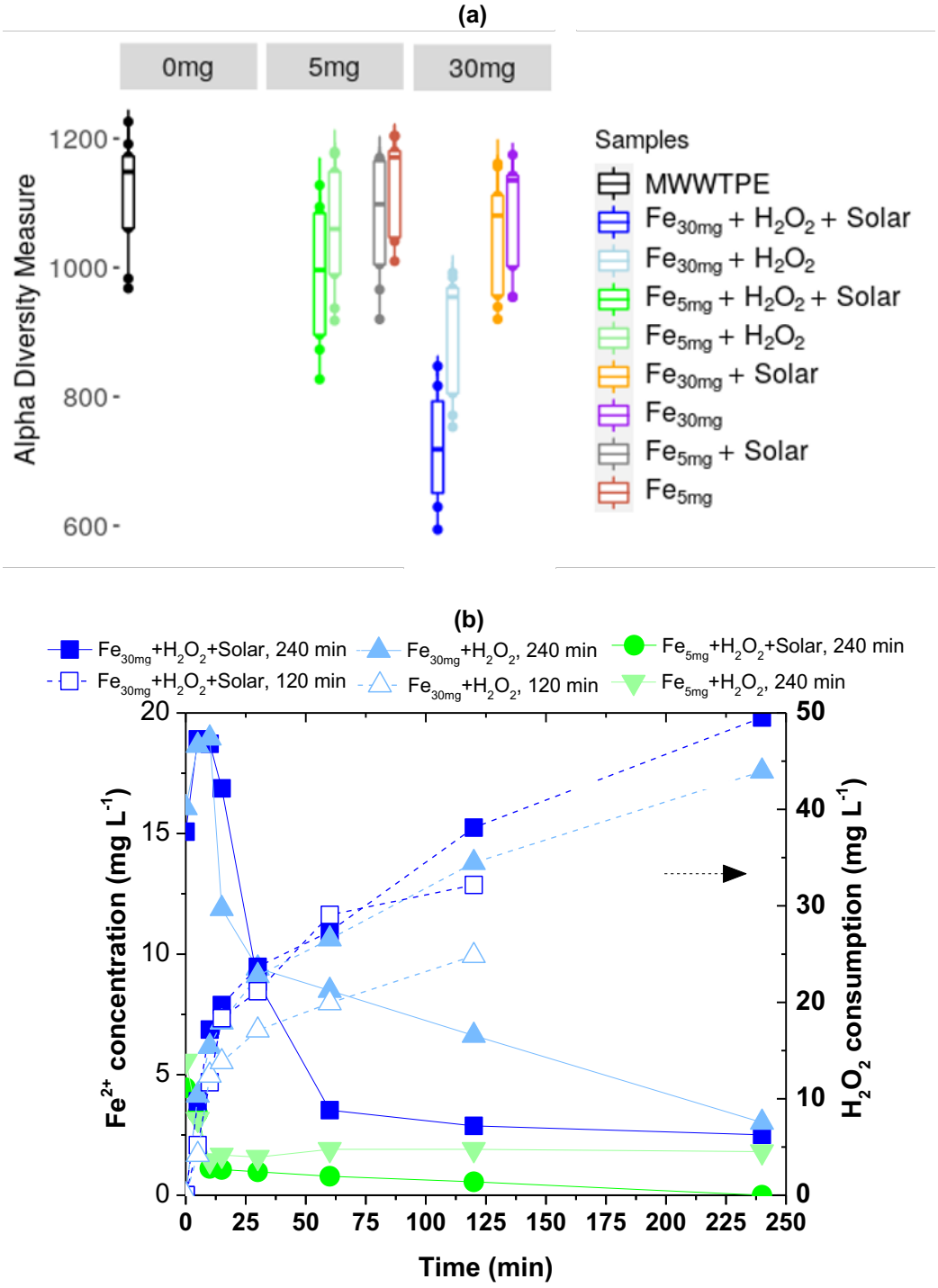

PCoA indicated significant ($p < 0.05$) differences in the taxonomic structure of bacteria community before and after treatment and controls (Figure II.5a). Solar photo-Fenton samples clustered on the bottom left side, showing significant differences in bacterial

community diversity compared with MWWTPE samples (right upper side). The lowest average of microbiome diversity (Chao 1 diversity index) and abundance-based coverage estimator (ACE) (39% below MWWTPE sample) was detected in solar photo-Fenton samples, thus confirming the disinfection potential of this process (Figure II.5b).

Figure II.5 - Beta diversity obtained by PCoA analysis (a), and alpha diversity metrics obtained by non-parametric richness estimator (Chao 1 and ACE) (b) after solar photo-Fenton treatment and controls

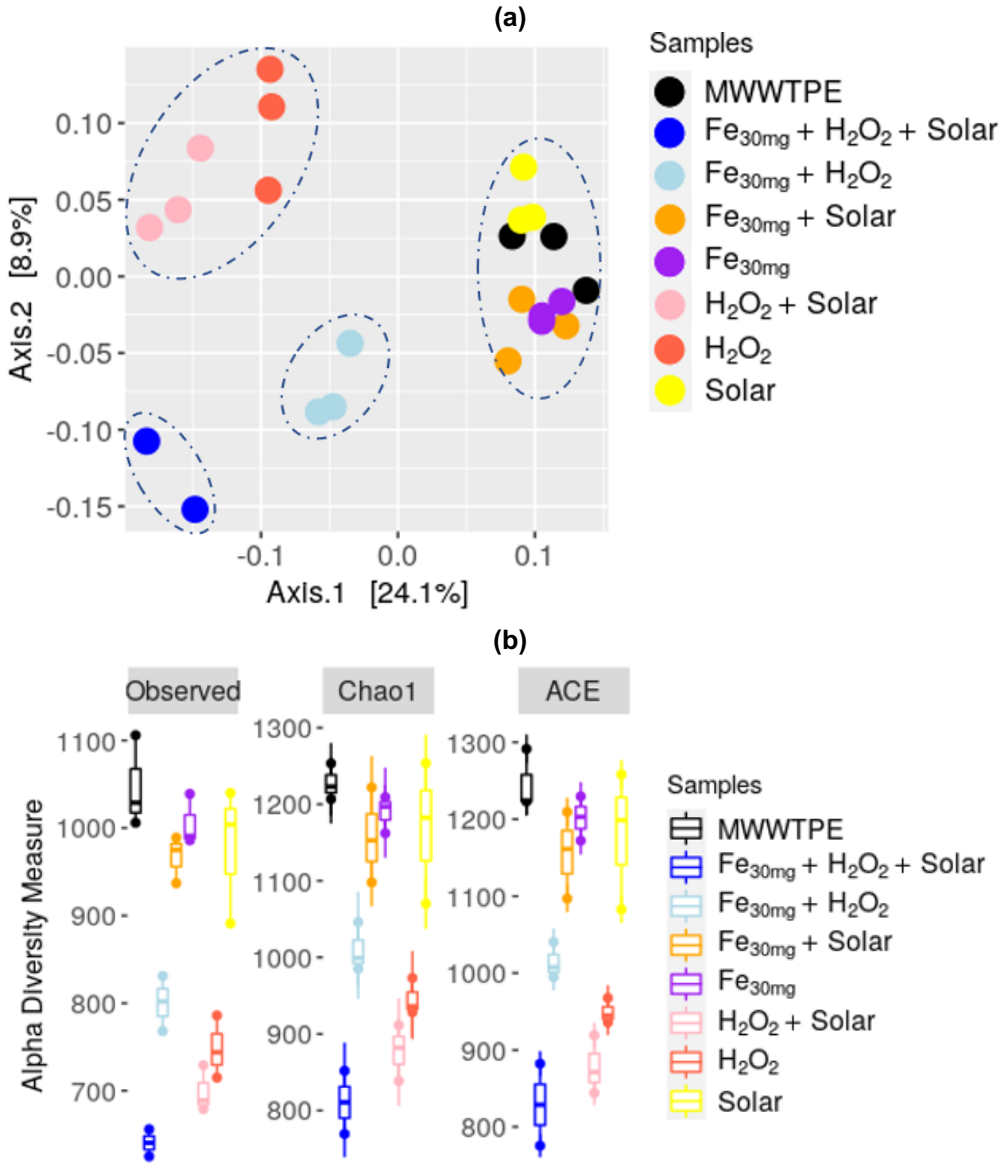

These results were confirmed by culture-based analysis of total heterotrophic bacteria and ARB. As shown in Figure II.6, solar photo-Fenton treatment achieved nearly 70% removal of cultivable THB. The treatment was also efficient in eliminating ARBs (85%

removal). ARB removal was enhanced under solar photo-Fenton (~1 log removal for ARB resistance to all tested antibiotics) compared to Fenton control. The removal of ARBs was limited to ~0.5 log, except for trimethoprim-resistant bacteria (~1 log removal).

Figure II.6 - Log removal of total heterotrophic bacteria and ARB for solar photo-Fenton and controls (Fenton, H_2O_2+Solar, H_2O_2)

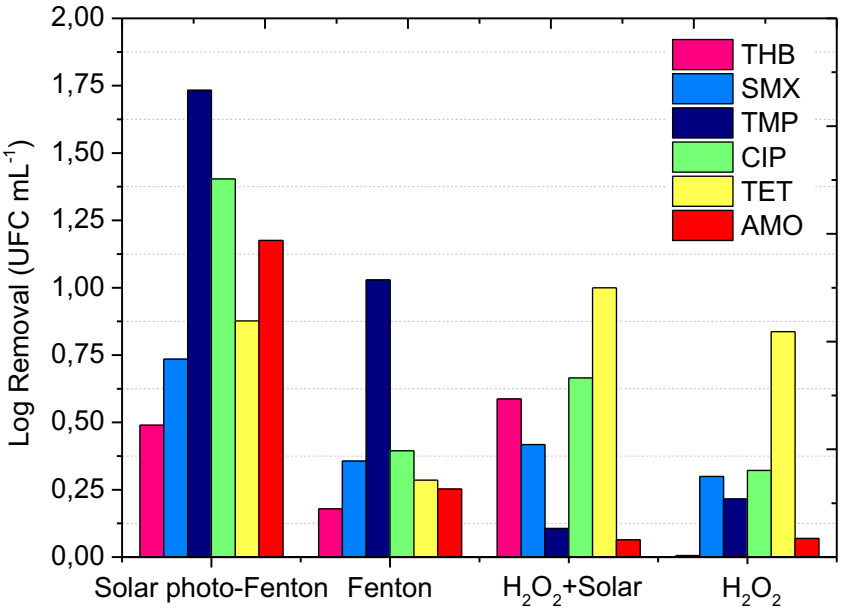

Enhanced effect of solar photo-Fenton compared with control Fenton is associated with an increase in H_2O_2 consumption (95%) compared with control Fenton (Figure II.7) (75%) due to the higher number of routes related to the formation of hydroxyl radical (Equations II.1-3), enhanced Fe^{2+} cycling and faster kinetics of $HO^{\bullet}$ formation under irradiation (MALATO *et al*., 2009). Different cell-damaging mechanisms are responsible for the effect of solar photo-Fenton upon bacteria in MWWTPE, such as (i) UVA alone increases cell permeability and promotes loss of Fe^{2+} from enzymes, thus launching an internal photo-Fenton process with the formation of reactive oxygen species (ROS) inside cells (GIANNAKIS, 2018a); (ii) secondary radicals formed by the exposition of natural organic matter and ions present in the matrix to UVA irradiation damage bacteria cell structure (ROMMOZZI *et al*., 2020); (iii) the UVB component of solar irradiation causes direct damage to DNA (FENG *et al*., 2020); (iv) external photo-Fenton reactions launched by the oxidative radicals formed in bulk due to the addition of iron salts and H_2O_2 to the system intensify outer cell damage (GIANNAKIS, 2018a);

and (v) transportation of H_2O_2 to the inner cell compartment via porins (FENG *et al*., 2020) enhances internal photo-Fenton reactions.

Figure II.7 - pH, hydrogen peroxide consumption, and dissolved iron concentration after solar photo-Fenton treatment and controls

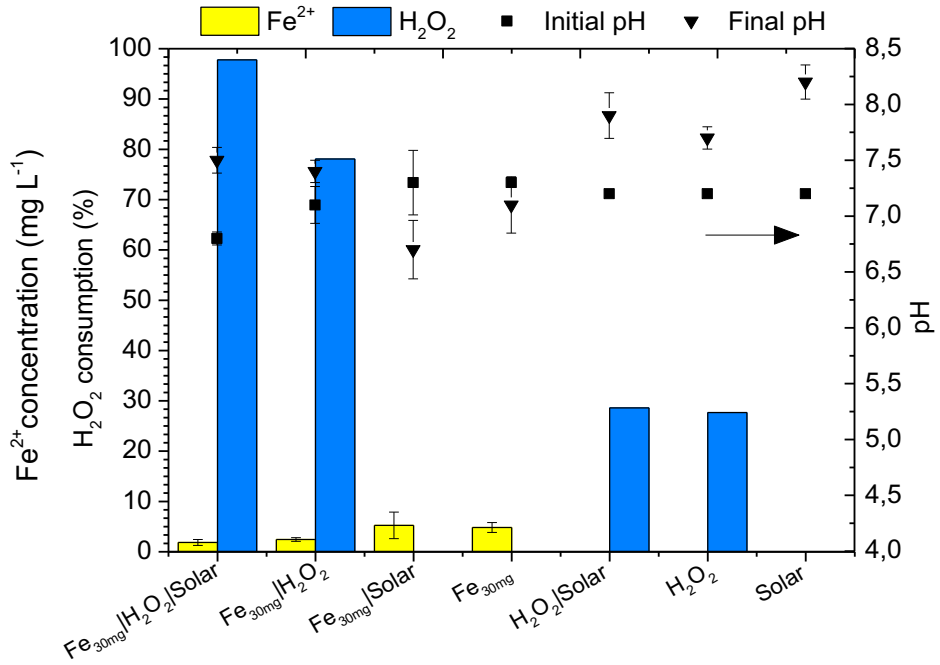

As shown in Figure II.7, pH ranged from 6.5 and 7.5 during solar photo-Fenton and control Fenton. The pH stability during photo-Fenton at neutral pH using the intermittent iron addition strategy was also observed by Starling *et al*. (2021a). Recent studies indicate that solar photo-Fenton efficiency is hindered at neutral pH due to iron precipitation (CARRA *et al*., 2013; CLARIZIA *et al*., 2017). However, the intermittent iron addition strategy mitigates this effect since dissolved iron is present in the system during the entire treatment. Iron precipitation occurs gradually, avoiding a turbidity peak usually associated with light scattering effects. Final Fe^{2+} concentration was under 5 mg L^{-1} after photo-Fenton and Fenton treatments, which is below discharge limits and presents no risks to aquatic environments (SILVA *et al*., 2018; STARLING *et al*., 2021a).

A cluster containing control samples (H_2O_2 + solar and H_2O_2) was formed on the upper left side (Figure II.5a). This is concurrent with results obtained in culture-based bacterial analyses of THB and ARB (Figure II.6). These controls were less efficient in the removal of ARBs (except for ARBs resistant to tetracycline - removal ~1 log)

compared to solar photo-Fenton treatment. Although H_2O_2+Solar control showed ~75% removal of THB (Figure II.6), the control containing only H_2O_2 did not show a significant percentage of THB removal, being efficient only in removing tetracycline-resistant ARBs. The effect of these controls upon microbial community and cultivable bacteria may be associated with H_2O_2 consumption (nearly 30%) (Figure II.7), which is related to the oxidation of matrix and bacteria cell components. H_2O_2 alone may disrupt the lipid bilayer of the bacteria cell membrane as it oxidizes lipids (SIDDIQUE; ARA; AFZAL, 2012). In addition, the transportation of H_2O_2 to the inner cell compartment and the release of Fe^{2+} from enzymes by the action of irradiation alone (FENG *et al*., 2020) promotes the internal photo-Fenton during the H_2O_2 + solar control (GIANNAKIS, 2018a), thus contributing to disinfection. Similar disinfection rates were observed for solar photo-Fenton at neutral pH and H_2O_2 + solar in previously published articles (GIANNAKIS, 2018a; MANIAKOVA *et al*., 2021; MICHAEL-KORDATOU; KARAOLIA; FATTA-KASSINOS, 2018; MICHAEL *et al*., 2020). However, although ARB regrowth was not evaluated in the present study, regrowth was observed after 48 h of storage only after H_2O_2 + Solar treatment elsewhere (MICHAEL *et al*., 2020).

The single cluster formed by MWWTPE and controls samples (Fe^{2+}; solar; Fe^{2+} + solar) (right center side) (Figure II.5a) shows that these controls had no significant effect upon the original bacterial community. This is confirmed in alpha diversity analysis (Figure II.5b), as no significant difference was detected between control samples and MWWTPE. Lack of impact upon MWWTPE microbial community diversity after solar irradiation alone is consistent with reports made in other studies (SERNA-GALVIS *et al*., 2019; VERBEL-OLARTE *et al*., 2021).

3.3 Effect of solar photo-Fenton on bacterial phyla

Solar photo-Fenton effectively removed most of the main phyla present in MWWTPE (Figure II.8a), achieving 86% removal of *Acidobacteria,* 80% removal of *Chlroflexi,* and around 79%, 76%, and 74% removal of *Actinobacteria*, *Bacteriodetes*, and *Firmicutes,* respectively. Unclassified taxa were reduced by 67%. These results are promising since priority ARB belong to *Proteobacteria* (*e.g. P. aeruginosa*, *A. baumannii*, *N. gonorrhea*, etc.), *Firmicutes* (*e.g. E. Faecium*, *S. pneumoniae*, *S. aureus*), and *Bacteroidetes* (*e.g. C. normanense*, *C. meningosepticum*) phyla (QUINTELA-BALUJA

et al., 2019; SU *et al*., 2017). Besides, bacteria from *Proteobacteria* and *Actinobacteria* phyla are major hosts of ARGs carried by Methicillin-Resistant *Staphylococcus aureus* [MRSA]-related (*mec*A, *qac*A, *qac*B, *nor*A) and Carbapenem-Resistant *Enterobacteriaceae* [CRE] (KPC, NDM, OXA-48) (YIN et al., 2019; ZHANG et al., 2021a, 2019a).

Figure II.8 - Phylogeny of bacterial communities (a); Abundance of *Proteobacteria* classes (b); and classes and genera *of Proteobacteria* in samples treated by solar photo-Fenton (c). Taxa with abundance below 1% and unclassified taxa were designated as NA

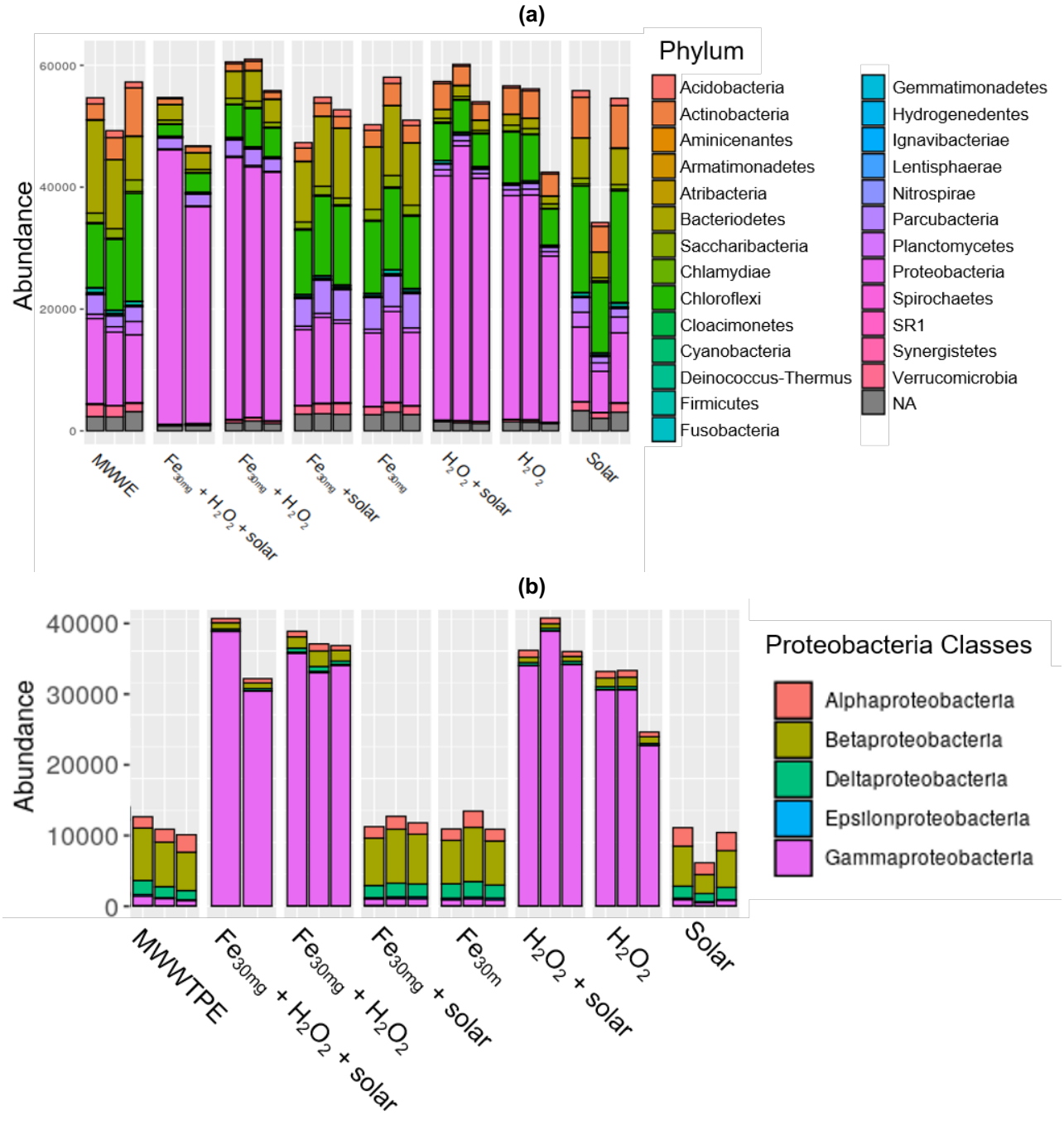

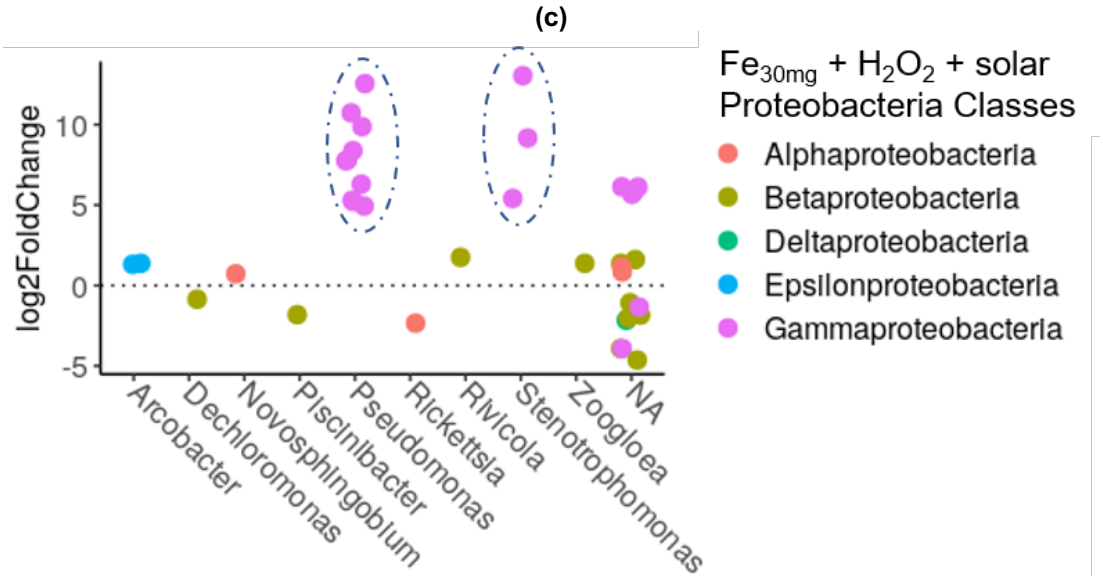

An almost four-fold enrichment was observed for *Proteobacteria* in all samples containing H_2O_2, thus indicating a positive selection of this group (Figure II.8a). *Proteobacteria* selection was also observed after ozonation of municipal wastewater (MOREIRA *et al*., 2021) and suggested higher resistance of this group to oxidative conditions. The bacterial community present in MWWTPE is sensitive to H_2O_2, which can function either as a disinfectant (APEL; HIRT, 2004) or as an oxygen source enhancing aerobic bacterial growth (HINCHEE; DOWNEY; AGGARWAL, 1991; ZAPPI *et al*., 2000). Treated samples presented five major classes within *Proteobacteria* phylum (Figure II.8b). Among these classes, the highest increase in solar photo-Fenton samples was observed for *Gammaproteobacteria,* mainly within genera *Pseudomonas* and *Stenotrophomonas* (Figure II.8c). Relative abundance of *Gammaproteobacteria* class also increased in the presence of H_2O_2 and after solar-driven AOPs elsewhere (MOREIRA *et al*., 2018; WANG *et al*., 2017a). Selection of *Pseudomonas* genera during solar photo-Fenton may be associated with their tolerance to H_2O_2 (BJARNSHOLT *et al*., 2005; MOREIRA *et al*., 2018) as they possess mechanisms to eliminate H_2O_2 present in the environment (MAGRO *et al*., 2019).

H_2O_2 scavenging mechanisms were associated with eight genes (KatA1, KatA2, KatMn, KatE, AhpCF, Gpx1, Gpx2, and Gpx3) in *Stenotrophomonas sp*. Among these genes, KatA2 played a critical role in survival in the presence of high H_2O_2concentrations (2.0 mM) (LI *et al*., 2020b). Solar photo-Fenton and control Fenton samples presented a 4-5 fold growth in the KatA2 and KatE genes, and AhpCF increased by 33%. Thus, suggesting a significant adaptive response to H_2O_2 stress.

Besides, *Pseudomonas* carries genes that encode efflux pumps, thus conferring resistance to both antibiotics and other disinfecting agents (PANG *et al*., 2019). *Pseudomonas* may also have benefited from the oxidation of organic components present MWWTPE via solar photo-Fenton as they have the ability to degrade carbonyl compounds as a feeding source (JOHNSON *et al*., 2011).

Critical priority of *Pseudomonas aeruginosa* (WHO, 2017) and *Stenotrophomonas maltophilia,* an emerging pathogen responsible for high morbidity and mortality (Gil-Gil *et al*., 2020), were both detected in MWWTPE samples (Figure II.2). Solar photo-Fenton reached total elimination of these species, while control Fenton eliminated almost 30% of *Stenotrophomonas maltophilia* and complete removal of *Pseudomonas aeruginosa* (data not shown). This confirms the potential of solar photo-Fenton to eliminate priority pathogens from MWWTPE, thus contributing to public health improvement.

3.4 Effect of solar photo-Fenton on priority pathogens

Six potential pathogens belonging to critical, high, and medium priority classes were detected in original MWWTPE samples (WHO, 2017) (Figure II.9). Solar photo-Fenton and Fenton completely removed high priority *Staphylococcus* and *Enterococcus* (Figure II.9). *Staphylococcus* infections carry high mortality levels when aggravated by antimicrobial resistance (GIULIERI *et al*., 2020), and *Enterococcus* is an opportunistic pathogen associated with increased mortality rates (LEAVIS; BONTEN; WILLEMS, 2006). In contrast, *Streptococcus sp.*, inserted in the same group, was not entirely removed by proposed treatments. Failure to eliminate this priority group may be associated with its ability to adapt membrane composition in hostile oxidative environments (PESAKHOV *et al*., 2007).

Regarding *Acinetobacter* genera, phylogenetic analysis of solar photo-Fenton samples revealed an absence of *A. baumannii*, a critical priority pathogen (WHO, 2017). *A. johnsonii* predominated in all samples. Despite rarely causing human infections, this organism may actively acquire exogenous DNA becoming an ARG reservoir (MONTAÑA *et al*., 2016). In the *Enterobacteriaceae* family, Fenton was not efficient at removing *Escherichia coli* or *Klebsiella pneumoniae* (*Enterobacteriaceae* family).

Nevertheless, solar photo-Fenton completely removed *Klebsiella pneumoniae* and achieved 30% removal of E. *Coli*. *Klebsiella pneumoniae* has a negatively charged outer capsule (PODSCHUN; ULLMANN, 1998) which may have complexed with iron, thus lowering Fenton efficiency in the absence of light. Elimination of *Klebsiella pneumoniae* from MWWTPE is critical to limit the spread of AMR as it is a major cause of hospital and community-acquired infections (MUNOZ-PRICE *et al*., 2013). The growth of *Pseudomonas* and *Stenotrophomonas* was associated with their tolerance to H_2O_2. Regarding species within the *Pseudomonas* family, *P. yamanorum* predominated in treated samples. Within *Stenotrophomonas*, *S. maltophilia,* a harmful β-lactam resistant pathogen (KUMAR *et al*., 2020), and S. *pavanii* ruled in MWWTPE sample, yet were entirely removed by solar photo-Fenton.

Figure II.9 - Phylogenetic tree showing the occurrence of WHO priority pathogens and selected genera. The blue symbol is the WHO logo, which represents each priority pathogen

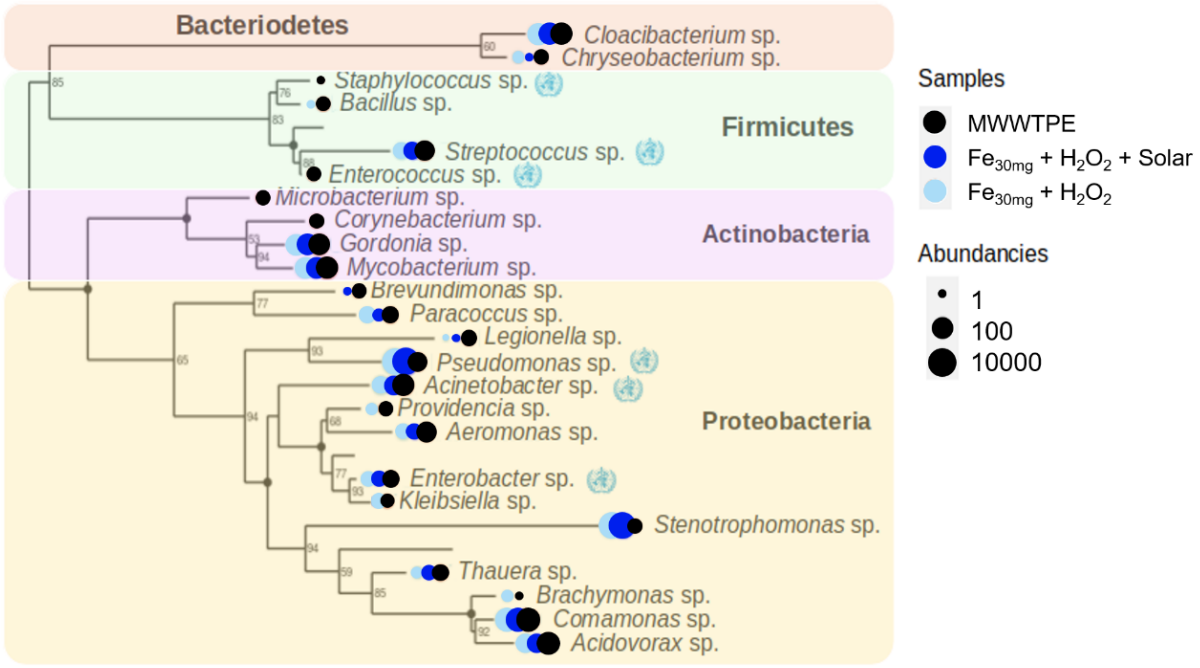

Regarding bacteria known as ARG vectors, solar photo-Fenton achieved a substantial reduction of intrinsically multi-drug resistant *Chryseobacterium*. This is relevant as this genera is known for its resistance to chlorination applied in conventional MWWTP (IZAGUIRRE-ANARIBA; SIVAPALAN, 2020). Solar photo-Fenton and Fenton achieved significant removal of *Legionella* and *Brevundimonas (Proteobacteria* cladon), commonly associated with nosocomial infections and considered pathogens of emerging concern in clinical locations (LI *et al*., 2018a; LYTLE *et al*., 2021; RYAN;

PEMBROKE, 2018). In contrast, *Gordonia sp.*, an opportunistic agent (BLASCHKE *et al.*, 2007), and *Mycobacterium sp.* (*Corynebacteriales*; *Actinobacteria*) were not removed after Fenton and solar photo-Fenton. Extensively TB drug-resistant and multidrug-resistant organism *Mycobacterium tuberculosis* (DUA *et al.*, 2018; KUMAR *et al.*, 2020) was not detected in any of the samples in this study (data not shown).

3.5 Effect of solar photo-Fenton on resistome profile: diversity and richness of ARGs

According to Figure II.10, ARGs which confer resistance to different classes of antibiotics are abundant in the MWWTPE used in this study. Most current studies associated with ARG removal via solar photo-Fenton investigate a limited ARGs list (*bla*$_{CTX}$, *bla*$_{TEM}$, *bla*$_{OXA}$, *sul*1, *sul*2, *emr*B, *tet*Q, *tet*X, and *tet*M) via qPCR (STARLING *et al.*, 2021b). This is the first study to use WGS to investigate ARG removal from MWWTPE. A greater ARGs diversity (69 variations within 19 major types) (Figure II.11) was detected, and their removal was analyzed in this study.

Figure II.10 - Relative occurrence of ARGs in MWWTPE, solar photo-Fenton, and Fenton samples

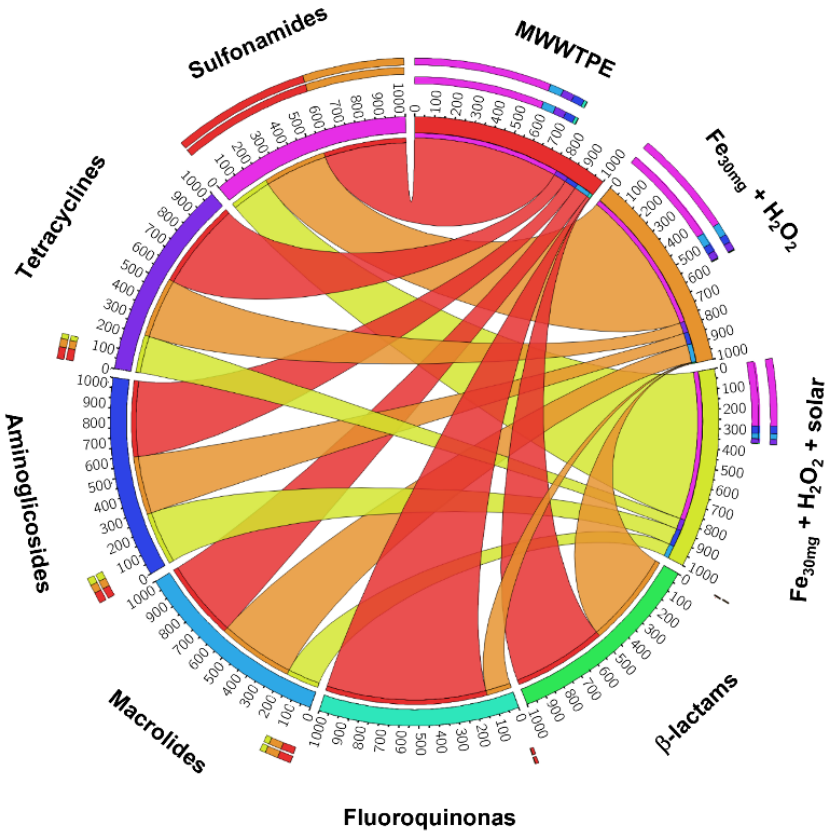

ARGs which confer resistance to broad-spectrum antibiotics, such as sulfonamides (*sul*1 and *sul*2), represented almost 74% of total ARGs present in MWWTPE, followed by ARGs associated to macrolides (mainly *erm*(F), *mph*(A), *mph*(E) and *msr*(E)) (~10%), tetracyclines (mainly *tet*A, *tet*B, *tet*O and *tet*W) (~9%) and aminoglycosides (mainly *aad*A, *aph*(3"), *aph*(6) and *str*A) (~6%). Overall, subtypes *tet*(X)_1, *tet*(X)_2, *mph*(E)_3 and *msr*(E)_4, and genes *sul*1 and *sul*2 (almost all subtypes) were the most abundant across MWWTPE samples (Figure II.11). According to Nguyen *et al*. (2021) and Raza *et al*. (2021), ARGs conferring resistance to sulfonamides and tetracyclines are frequently detected in MWWTPE regardless of predominant bacteria taxa, season, and location. Gene *sul*1 usually prevails in MWW worldwide due to high sequence conservation and transfer among different species (WEI *et al*., 2018).

Solar photo-Fenton removed nearly 60% of ARGs associated with sulfonamides (55%), macrolides (61%), and tetracyclines (61%), and wholly removed ARGs associated with β-lactams and fluoroquinolones. Regarding subtypes, the treatment removed 66% of *tet*(X)_1 and almost 60% of *tet*(X)_2, *mph*(E)_3, and *msr*(E)_4 (Figure II.11). Complete removal of ARGs associated with β-lactams is of remarkable relevance. Some of them are emerging threats to public health (*i.e.,* carbapenem-resistant *Enterobacteriaceae*-related genes: BKC, GES, IMP, OXA, etc.) (BUSH; JACOBY, 2010; LOGAN; WEINSTEIN, 2017). The effect of control Fenton upon ARGs was limited to 24% and 30% for ARGs associated with sulfonamides and tetracyclines, respectively, and no substantial decay of ARGs associated with macrolides (~3%) and fluoroquinolones (~7%) classes was detected after treatment.

Results obtained by the most recent works published on the application of solar photo-Fenton have shown the high efficiency of ARGs removal. Michael *et al*. (2019) reached complete removal of *sul*1, *qnr*S, *bla*OXA, *bla*CTX-M, and *tet*M, and 3 log units of *bla*TEM removal, and Fiorentino *et al*. (2019) removed sul1 genes to levels below the detection limits. While solar photo-Fenton successfully removed ARGs (CTX-M-1 and CTX-M-9), sunlight/H_2O_2 failed to remove these genes (GIANNAKIS, 2018a). These results agree with the high efficiency of ARG removal obtained in our study.

Figure II.11 - Heatmap of the distribution of ARGs as a percentage of reads per kilobase per million mapped reads (RPKM) in MWWTPE, solar photo-Fenton, and Fenton samples

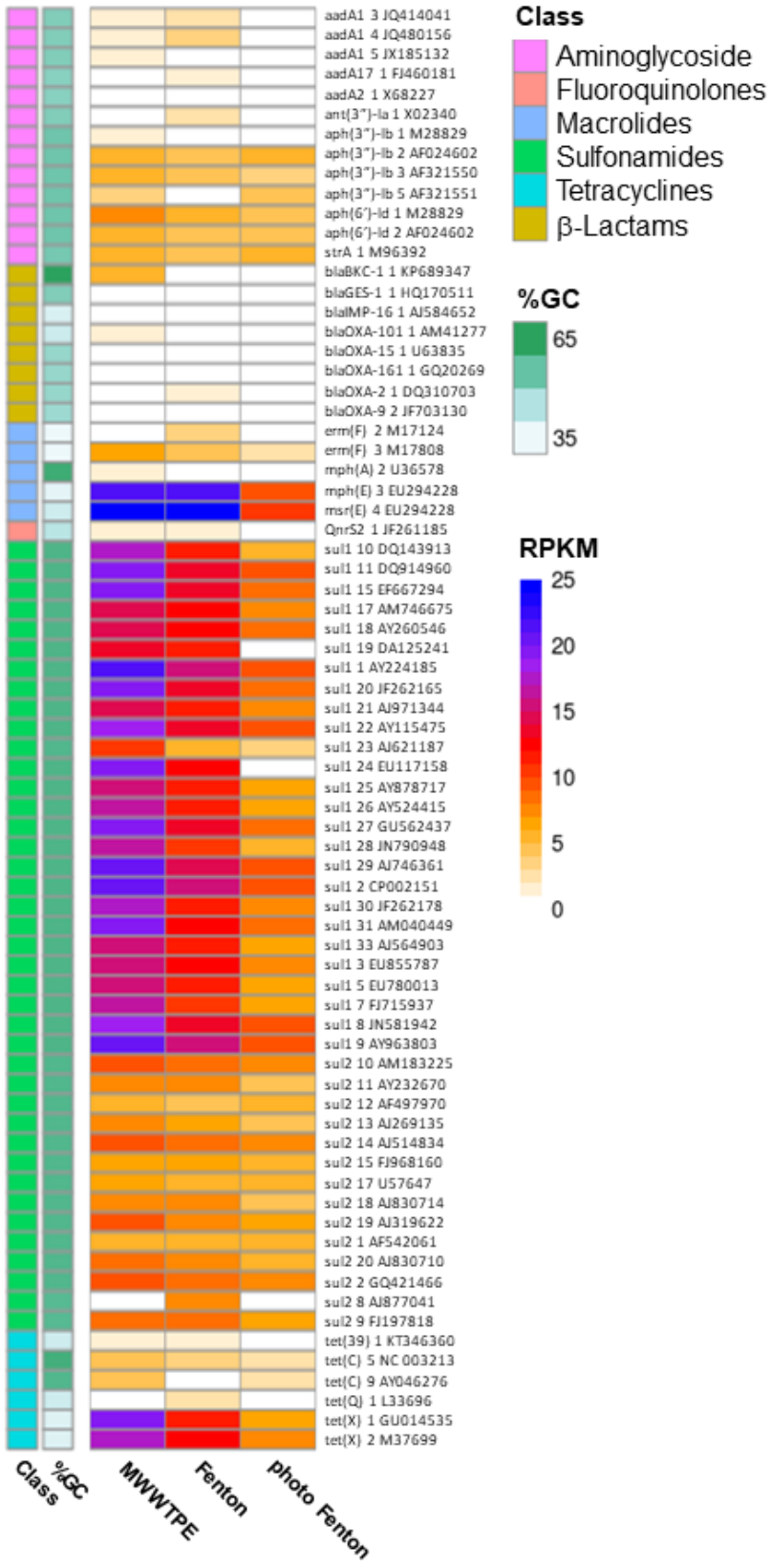

Limited removal of ARGs related to aminoglycosides via solar photo-Fenton (36% removal) and control Fenton (~26% removal) may be associated with the low GC content (~45%) of these genes (Figure II.11). Oxygen species usually react more readily with guanine bases in the DNA. Thus lower degradation rates are expected for genes presenting reduced GC content (REN *et al*., 2018; ZHANG *et al*., 2016). Removal rates above 50% were detected for *sul*1, *sul*2, and *tet*(C), and *mph*(A) and *bla*BKC were completely removed via solar photo-Fenton due to high GC content (~65%) associated with these ARGs. Despite having low GC content (~35%), *tet*(X)_1, *tet*(X)_2, *mph*(E)_3, and *msr*(E)_4 was significantly removed by solar photo-Fenton (>60%) as they were abundant in MWWTPE. After proposed oxidative treatment, the persistence of sulfonamide and tetracycline genes is associated with their high initial concentration in MWWTPE. Therefore, these ARGs may be potential indicators of ARG removal from MWWTPE.

3.6 Correlation between bacterial community and antimicrobial resistance genes

As co-existing patterns between ARGs and bacterial communities indicate potential hosts of AMR (JIA *et al*., 2020) and bacterial community is considered one of the main drivers of ARGs spread, specific relationships between bacterial hosts and ARG subtypes were investigated for MWWTPE used in this study before and after solar photo-Fenton treatment. Taxa of contigs carrying ARGs were predicted at their specific phyla and family levels, respectively (Figure II.12). As shown in Figure II.12, different ARG-taxa relations were observed before and after solar photo-Fenton and control Fenton treatments. For example, tetracycline and macrolide resistance genes were correlated with almost all families in MWWTPE, while sulfonamide, β-Lactam, and aminoglycoside resistance genes correlated mostly with *Proteobacteria (Pseudomonadaceae* and *Xanthommonadaceae)*.

Figure II.12 - Correlation between the absolute abundance of specific phyla and family levels carrying ARGs and the ARGs subtypes present in MWWTPE, Fenton, and solar photo-Fenton samples

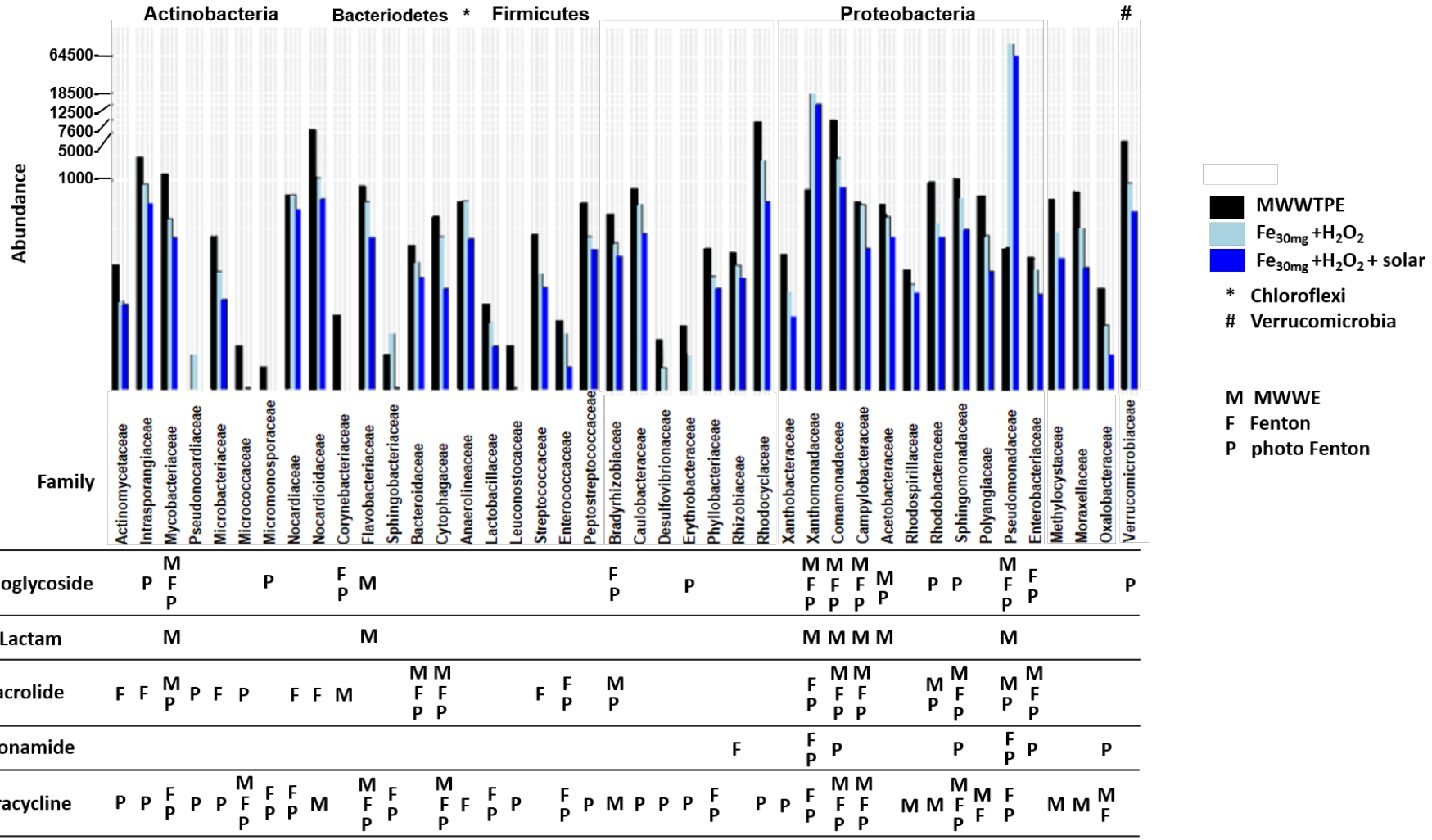

Although solar photo-Fenton treatment decreased the richness and diversity of the bacterial community in MWWTPE (Figure II.5a and b), significant enrichment in the abundance of *Proteobacteria* was observed after treatment (Figure II.8a). *Proteobacteria* have been reported to be potential hosts of genes that carry resistance to aminoglycosides (*i.e. str*A, *aph*, and *aad*A) and tetracyclines (*i.e. tet*Q, *tet*C, and *tet*X) (LUO *et al*., 2021b). Therefore, the increased abundance of this phylum contributed to the persistence of these ARGs after treatment (Figure II.11). Within *Proteobacteria*, *Pseudomonadaceae*, *Enterobacteriaceae*, *Campylobacteraceae*, *Comamonadaceae,* and *Xanthommonadaceae* also showed a strong correlation with ARGs related to sulfonamides and macrolides in MWWTPE samples. Increased abundance of *Pseudomonadaceae* and *Xanthommonadaceae* after treatment justifies the persistence of these ARGs after control Fenton and solar photo-Fenton.

The co-existence of ARGs associated with tetracycline, macrolides, and aminoglycosides (Figure II.12) was correlated with almost all families of bacteria present in MWWTPE. These ARGs persisted after treatment even after high removal rates (>60%) since they were abundant in the untreated sample (Figure II.11). Thus, relatively low removal of *aph*(3"), *aph*(6"), *str*A, *mph*(E), *msr*(E), and *tet*X might be due to their occurrence in a varied spectrum of hosts. Notably, families comprising multidrug-resistant bacteria, such as *Xanthommonadaceae, Campylobacteraceae, Sphingomonadaceae, Pseudomonadaceae*, and *Enterobacteriaceae*, were the leading carriers of beta-lactam resistance genes in MWWTPE samples (Figure II.12). Nevertheless, these ARGs were removed after the proposed treatment (Figure II.11), confirming the results shown in Figure II.12.

Results obtained here confirm the elimination of priority pathogens (Figure II.9) and ARGs (Figure II.10 and Figure II.11) via solar photo-Fenton, thus ensuring the combat of AMR spread via MWWTPE discharge by this process. Nonetheless, some groups known as co-hosts of ARGs were selected during treatment. This fact requires further investigation and points out the use of these groups as potential AMR indicators. The establishment of global and regional indicators of AMR is critical for the control of priority pathogens and has been currently under discussion by the scientific community (DI CESARE *et al*., 2020).

4 CONCLUSIONS

The evaluation of the effects of solar photo-Fenton upon bacterial communities, priority pathogens, and ARGs using metagenomic analyses presented in this study appear to be novel in the scientific literature. The lowest species richness and diversity were achieved via solar photo-Fenton (30 mg L^{-1} of Fe^{2+} and 50 mg L^{-1} of H_2O_2; 240 min) compared to controls as the intermittent iron addition strategy was effective for treatment conduction at neutral pH.

Solar photo-Fenton effectively removed the main phyla present in MWWTPE (86% removal of *Acidobacteria*, 80% of *Chlroflexi*, 79% of *Actinobacteria*, 76% of *Bacteriodetes*, and 74% of *Firmicutes*). Solar + H_2O_2 and H_2O_2 alone showed a lower impact upon the microbial community when compared to solar photo-Fenton. Enrichment of *Proteobacteria* after the application of the solar oxidative treatment should be further investigated as it indicates positive selective pressure and led to the persistence of ARGs carried by this group in treated samples.

Complete removal of high priority *Staphylococcus* and *Enterococcus*, critical priority *K. pneumoniae* and *P. aeruginosa,* and *S. maltophilia*, as well as substantial reduction of multi-drug resistant bacteria, were observed. The proposed treatment also reached nearly 60% removal of ARGs associated with sulfonamides, macrolides, and tetracyclines, as well as complete removal of those related to β-lactams and fluoroquinolones. These results confirm the potential of applying solar photo-Fenton as an additional treatment stage in MWWTP to control the spread of AMR in tropical countries.

CHAPTER III – Persulfate mediated solar photo-Fenton for MWWTP effluent quality improvement: impact on microbial community and removal of antimicrobial-resistant genes[3]

[3]This chapter was published according to the following reference: VILELA, Pâmela B.; STARLING, Maria Clara V. M.; MENDONÇA NETO, Rondon P.; SOUZA, Felipe A. R.; PIRES, Giovanna F. F.; AMORIM, Camila C. Solar photo-Fenton mediated by alternative oxidants for MWWTP effluent quality improvement: Impact on microbial community, priority pathogens and removal of antibiotic-resistant genes. Chemical Engineering Journal, v. 441, p. 136060, 2022. DOI: 10.1016/j.cej.2022.136060.

1 INTRODUCTION

Antimicrobials are crucial for the survival and maintenance of life quality and are considered the cornerstone of global public health (GOVINDARAJ VAITHINATHAN; VANITHA, 2018; HERNANDO-AMADO *et al*., 2019). Although antimicrobial resistance (AMR) occurs naturally and randomly, overexploitation of antimicrobials accelerates this process and plays a vital role in the selection of resistant microorganisms (BERENDONK *et al*., 2015; LUPO; COYNE; BERENDONK, 2012; YADAV; KAPLEY, 2021; ZHANG *et al*., 2019b). AMR allows for bacteria survival in the presence of antimicrobials, impairing the efficacy of these drugs on the fight against infections and posing public health challenges (AMARASIRI; SANO; SUZUKI, 2020; HERNANDO-AMADO *et al*., 2019; YADAV; KAPLEY, 2021). The rapid spread of multi- and pan-resistant bacteria which cause infections that cannot be treated by existing antimicrobials is especially alarming. This issue is not restricted to clinical environments as environmental compartments (*i.e*. animals, soil, water/wastewater) also contribute to AMR origin and spread. Hence, AMR is considered a One Health problem (BERENDONK *et al*., 2015; GIL-GIL *et al*., 2019; HERNANDO-AMADO *et al*., 2019; KAMENSHCHIKOVA *et al*., 2021; LÉGER *et al*., 2021; MEDINA; LEGIDO-QUIGLEY; HSU, 2020) and was recognized as one of the most threatening issues to public health by the World Health Organization (WHO) (2019 Antibacterial Agents, 2019; HERNANDO-AMADO *et al*., 2019; LAXMINARAYAN *et al*., 2020).

Biological reactors present in most Municipal Wastewater Treatment Plants (MWWTP) provide a perfect environment for the replication of antimicrobial-resistant bacteria (ARB) and antimicrobial resistance genes (ARGs) which persist in the treated effluent (FIORENTINO *et al*., 2019a; MOREIRA *et al*., 2018; STANTON *et al*., 2020). In addition, conventional disinfection technologies (*e.g.*, chlorination, UV processes, and ozonation) may be ineffective to eliminate these contaminants from the effluent. For instance, chlorine was ineffective for ARB removal and increased intra and extracellular concentrations of ARGs in the effluent (GUO; YUAN; YANG, 2015; HOU *et al*., 2019; JIN *et al*., 2020; LIU *et al*., 2018; WANG *et al*., 2020a). While UV disinfection significantly inactivated some resistant strains, the treatment was selective and increased the abundance of specific ARB. Furthermore, irradiation dosage applied during treatment did not guarantee the inactivation of ARGs (GUO; YUAN; YANG,

2013, 2015; WANG; CHEN, 2020; ZHANG *et al*., 2020a). Besides, ozonation resulted in ARB regrowth and enrichment of ARGs in the effluent (IAKOVIDES *et al*., 2019; SOUSA *et al*., 2017). Thus, it is critical to explore post-treatment wastewater strategies to eliminate these contaminants from MWWTP effluent (MWWTPE) and avoid their discharge into recipient water bodies.

Solar photo-Fenton constitutes an up-and-coming method for the complementary treatment of MWWTPE and stands out as an environmentally sustainable treatment that effectively removes ARB and ARGs (CLARA *et al*., 2021; GIANNAKIS *et al*., 2018a; IOANNOU-TTOFA *et al*., 2019a; POLO-LÓPEZ; SÁNCHEZ PÉREZ, 2021; VILELA *et al*., 2021a, 2021b). The reaction between ferrous iron (Fe^{2+}) and hydrogen peroxide (H_2O_2) (Equation III.1 and III.2) generates highly reactive and non-selective hydroxyl radicals (HO•, E_0 = 1.8–2.7 V) during the photo-Fenton process (GIANNAKIS *et al*., 2016b; MIRALLES-CUEVAS *et al*., 2017; RODRÍGUEZ-CHUECA *et al*., 2019a). Additionally, sunlight enhances Fe^{2+} cycling (LUEDER *et al*., 2020), and iron species formed in the system generate an extra route to produce oxidative radicals Equation III.3 (GIANNAKIS *et al*., 2016b).

$$Fe^{2+} + H_2O_2 \rightarrow Fe^{3+} + HO\bullet + OH^- \quad \text{(III.1)}$$

$$Fe^{3+} + H_2O_2 \rightarrow Fe^{2+} + HO_2\bullet + H^+ \quad \text{(III.2)}$$

$$Fe(OH)^{2+} + h\nu(540\text{-}580\ nm) \rightarrow Fe^{2+} + HO\bullet \quad \text{(III.3)}$$

Despite high reactivity of hydroxyl radical and promising results obtained via solar photo-Fenton using H_2O_2 as an oxidant for the removal of ARB and ARGs (DE LA OBRA JIMÉNEZ *et al*., 2019; FIORENTINO *et al*., 2019a; GIANNAKIS *et al*., 2018b, 2018a; IOANNOU-TTOFA *et al*., 2019a; POLO-LÓPEZ; SÁNCHEZ PÉREZ, 2021), AOPs based on sulfate radical ($SO_4\bullet^-$, E_0 = 2.5 − 3.1 V) have recently attracted significant attention due to longer half-life time (30–40 μs for sulfate radicals *vs*. 20 ns for hydroxyl radicals) and higher selectivity of $SO_4\bullet^-$ compared to HO• (OH; DONG; LIM, 2016; ZHOU *et al*., 2020). In the persulfate (PS) mediated photo-Fenton process (solar/Fe^{2+}/$S_2O_8^{-2}$), Fe^{2+} catalyses the disruption of the O-O bonds of persulfate anions ($S_2O_8^{-2}$) producing $SO_4\bullet^-$ radicals (Equation III.4) (KOLTHOFF; MEDALIA; RAAEN, 1951).

$$S_2O_8^{2-} + Fe^{2+} \rightarrow SO_4^{\bullet -} + Fe^{3+} + SO_4^{2-} \quad \text{(III.4)}$$

Despite the known efficiency of sulfate radicals on bacterial cell and DNA damage, very few studies have evaluated the efficiency of these radicals on the removal of ARB and ARGs in real MWWTPE (CLARA *et al*., 2021; GAO *et al*., 2020; QIU *et al*., 2020; ZHOU *et al*., 2020), and mechanisms associated with disinfection via sulfate radical-based AOPs are still unclear (XIAO *et al*., 2019). In addition, simultaneous application of both oxidants in a combined oxidant system (solar/Fe^{2+}/H_2O_2+$S_2O_8^{2-}$) has not yet been explored for the control of ARB and ARGs inherent to MWWTPE.

Hence, this study aimed to (i) investigate the effect of the persulfate mediated solar photo-Fenton process (solar/Fe^{2+}/$S_2O_8^{-2}$) upon microbiome diversity and (ii) ARGs; (iii) to compare the efficiency of PS mediated solar photo-Fenton with the combined oxidant system (solar/Fe^{2+}/H_2O_2+$S_2O_8^{2-}$) in the control of ARB and ARGs; and (iv) to evaluate the co-occurrence of ARGs and priority genera before and after proposed treatments.

2 MATERIAL AND METHODS

2.1 MWWTPE sampling

MWWTPE samples were obtained in the output of a secondary settling tank from a conventional activated sludge system pertaining to a MWWTP located in Belo Horizonte, in the southeast of Brazil, which receives wastewater from 1.5 million inhabitants (290 m^3 d^{-1}), including hospitals, industries, etc. Temperature, pH, Conductivity, Turbidity, Chemical Oxygen Demand (COD), Total Solids (TS), Total Fixed Solids (FS), Volatile Solids (VS), and Alkalinity were analyzed as according to APHA (APHA, 2013), as shown in Table III.1. Samples were filtered in 0.45 µm PVDF filter prior to Dissolved Organic Carbon (DOC), Dissolved Inorganic Carbon (DIC), and Total Nitrogen (TN) analysis by a Shimadzu TOC-VCN Analyzer. This filter was chosen as it does not cause sample contamination by exogenous organic matter (ABDEL-MOATI, 1990).

Table III.1 - Physicochemical characterization of MWWTPE

Parameter		MWWTPE		Reference
COD	mgO_2 L^{-1}	74	55	APHA 5220 D
pH	-	7.4	7.1	APHA 4500-H^+
Temp.	°C	24.0	24.0	APHA 2550
DOC	mg L^{-1}	12.81	10.33	
DIC	mg L^{-1}	12.61	16.89	
TN	mg L^{-1}	35.1	26.8	
Turbidity	NTU	22.7	24.3	APHA 2130 B
TS	mg L^{-1}	302	267	APHA 2540 B
VS	mg L^{-1}	132	120	APHA 2540 E
FS	mg L^{-1}	162	146	APHA 2540 E
Alkalinity	$mgCaCO_3$ L^{-1}	157	95	APHA 2320 B
Conductivity	µS	386	306	APHA 2510

2.2 Solar photo-Fenton mediated by alternative oxidants treatments

Solar photo-Fenton treatments of MWWTPE were conducted in a solar simulator chamber (SUNTEST CPS+, ATLAS) containing a Xenon lamp protected by a daylight filter, which emits light in the UV-Vis region (300-800 nm), thus simulating the solar spectrum. The irradiance was set at 268 W m^{-2} (330 to 800 nm) which is equivalent to 30 W m^{-2} (UV-A: 300-400 nm) correspond to annual average irradiance in Belo Horizonte/MG, Brazil) at 35°C. Experiments were performed in a glass reactor (400 mL) for 240 min under continuous magnetic stirring. Two adaptations to the solar photo-Fenton process were tested in this study:

(i) H_2O_2 was replaced by PS (282.27 mg L^{-1} of $S_2O_8^{2-}$) in a PS mediated solar photo-Fenton system (solar/Fe^{2+}/$S_2O_8^{-2}$);

(ii) The combination of H_2O_2 and PS (25 mg L^{-1} of H_2O_2 and 141.135 mg L^{-1} of $S_2O_8^{2-}$) as oxidants was tested in the solar/Fe^{2+}/ H_2O_2+$S_2O_8^{-2}$ system.

The molar concentration of $S_2O_8^{-2}$ (1.5 mM) used in the solar/Fe^{2+}/$S_2O_8^{2-}$ system was equivalent to the molar concentration of H_2O_2 applied elsewhere (VILELA *et al*., 2021b, 2021a). An equivalent molar concentration was also applied in the combined oxidant system (0.75 mM H_2O_2 + 0.75 mM PS = 1.5 mM of oxidant). Reactions were performed at initial neutral pH using intermittent iron additions (ferrous sulfate solution). Initial iron concentration (time = 0 min) was equivalent to 15 mg L^{-1}. Sequential iron additions (5 mg L^{-1}) occurred at 5, 10 and 15 min until a final total concentration of 30 mg L^{-1} of Fe^{2+} was reached as according to previous works (VILELA *et al*., 2021b, 2021a). This strategy was adopted to ensure the presence of dissolved iron throughout reactions. The persulfate and iron solutions were freshly prepared before being used to minimize variations in concentration caused by self-decomposition.

Control experiments consisted of PS mediated Fenton (Fe^{2+}/$S_2O_8^{2-}$), Solar/$S_2O_8^{2-}$, $S_2O_8^{2-}$ only, control Fenton in the presence of both oxidants (Fe^{2+}/$S_2O_8^{2-}$+H_2O_2), Solar/ H_2O_2+$S_2O_8^{2-}$, H_2O_2+$S_2O_8^{2-}$, Solar/Fe^{2+}, Fe^{2+} alone, and solar irradiation alone. Samples withdrawn during reactions enabled the quantification of residual $S_2O_8^{2-}$ (LIANG *et al*., 2008) and residual H_2O_2 (NOGUEIRA; OLIVEIRA; PATERLINI, 2005). Fe^{2+} concentrations were measured during reactions according to ISO 6332 spectrophotometric method (1,10-phenanthroline method, 510 nm) (JENKINS, 1982; VILELA *et al*., 2018). Samples obtained after 240 min of treatment were submitted to DNA extraction (FastDNA® Spin Kit for Soil) for ARB and ARG analysis. Catalase enzyme (460 mg L^{-1} in 0.04M phosphate buffer) or ascorbic acid solutions were added to samples prior to these analyses for consumption of residual H_2O_2 (POOLE, 2004) and residual $S_2O_8^{2-}$ (OLMEZ-HANCI; ARSLAN-ALATON; DURSUN, 2014), respectively.

2.3 DNA extraction and quality control

Total DNA extraction was performed using FastDNA® Spin Kit for Soil (MP Biomedicals) following the manufacturer's protocol. DNA concentration (average of 211 ng μL^{-1}) and purity (260nm/280nm ratio) were measured by a NanoDrop UV–Vis spectrophotometer (Thermo Fisher Scientific), and its structural integrity was determined by 0.8% agarose gel electrophoresis. Average purity ratio of DNA of all samples obtained in this study was 1.9, a satisfactory value as according to Manchester (1996).

2.4 Library Preparation and Sequencing

Extracted DNA was shipped to Macrogen for library preparation and sequencing. Paired-end fragment libraries with a length of 450nt from the V3-V4 hypervariable region of the 16S rRNA gene using the primers 338F ACTCCTACGGGAGGCAGCA and 806R GGACTACHVGGGTWTCTAAT. 300nt reads of each end were sequenced from fragments using the Illumina MiSeq platform. Besides, entire genomic DNA libraries were produced and sequenced by Illumina HiSeq in 150nt paired ends reads for WGS.

2.5 Bioinformatics analysis

2.5.1 Taxonomic Assignment

Sample pre-processing was carried out using the previously published method (VILELA *et al*., 2021b). Pre-processed data were used as input in R 3.6.3 (https://www.r-project.org/), Phyloseq (MCMURDIE; HOLMES, 2013), and vegan packages (OKSANEN *et al*., 2019). Diversity degrees were accessed by beta-diversity (PCoA) using the Bray-Curtis dissimilarity index. Alpha-diversity analyses were used for estimating the number of species with the indexes “Observed,” “Chao1,” and “Ace” (KIM *et al*., 2017). Alpha-diversity richness significances were checked by t-test analysis at a 90 percent confidence interval. Diversity and richness were calculated using rarified and non-rarefied versions of bacterial counts (ROWE; WINN, 2018). Non-rarefied counts were used for further analysis to avoid false positives and data loss (MCMURDIE; HOLMES, 2014). DESeq2 R packages were used to compare the

abundance of classes present in MWWTPE and treated samples (LOVE; HUBER; ANDERS, 2014).

2.5.2 Identification of ARGs

Sequenced reads were checked for quality (FastQC) (WINGETT; ANDREWS, 2018) and filtered by trimming primer adapters and low-quality sequences (Q<30) using Trimmomatic (BOLGER; LOHSE; USADEL, 2014). The resulting reads were then subjected to ARGs-OAP v2.0 (YIN *et al*., 2018) for quantifying ARGs. The abundance of ARGs was calculated and expressed as the number of copies of ARGs per cell. A heatmap with ARGs abundance was plotted according to antimicrobial classes using R package pheatmap (https://cran.r-project.org/web/packages/pheatmap/index.html). The analysis of genes that confer resistance to H_2O_2 (*katA1*, *katA2*, *katMn*, *katE*, *ahpCF*, *gpx1*, *gpx2*, and *gpx3*) was carried out using the previously published method (VILELA *et al*., 2021b). Inhouse perl and R scripts were used to parse data. Abundancies lower than $1e^{-05}$ were excluded, and results were parsed into Gephi software (BASTIAN; HEYMANN; JACOMY, 2009) to plot network graphs correlating the co-occurrence (JU *et al*., 2016) of WHO priority list of pathogens and ARG subtypes.

3 RESULTS AND DISCUSSION

3.1 Effect of alternative oxidants mediated solar photo-Fenton systems upon microbial community

The effect of solar photo-Fenton treatments mediated by alternative oxidants (solar/Fe^{2+}/$S_2O_8^{2-}$ and solar/Fe^{2+}/H_2O_2+$S_2O_8^{2-}$) upon MWWTPE microbial community diversity was analyzed by evaluating alpha and beta-diversity (Figure III.1). MWWTPE original samples did not cluster with samples obtained after treatments (Figure III.1a), thus indicating that bacteria taxonomic structures differ in MWWTPE and treated samples and confirming the impact of applied treatments on the microbiome. Alpha-diversity analysis indicated the excellent performance of solar/Fe^{2+}/$S_2O_8^{2-}$ as the number of Operational Taxonomic Units (OTUs) in samples treated by this process ($\bar{x}$ = 436 OTUs) was significantly lower (p-value = 0.07087) compared to MWWTPE ($\bar{x}$ = 871 OTUs) (Figure III.1b). These results confirm the disinfection potential of oxidative radicals produced in persulfate mediated solar photo-Fenton (*i.e.* $SO_4^{\bullet-}$ and HO•), which is a driving force to reduce bacterial diversity (GAO *et al*., 2020; QIU *et al*., 2020).

Figure III.1 - Beta diversity obtained by principal coordinates (PCoA) analysis (a) and alpha diversity metrics obtained by non-parametric richness estimator (Chao 1 and ACE) (b) of microbial communities identified in MWWTPE, treated samples, and controls

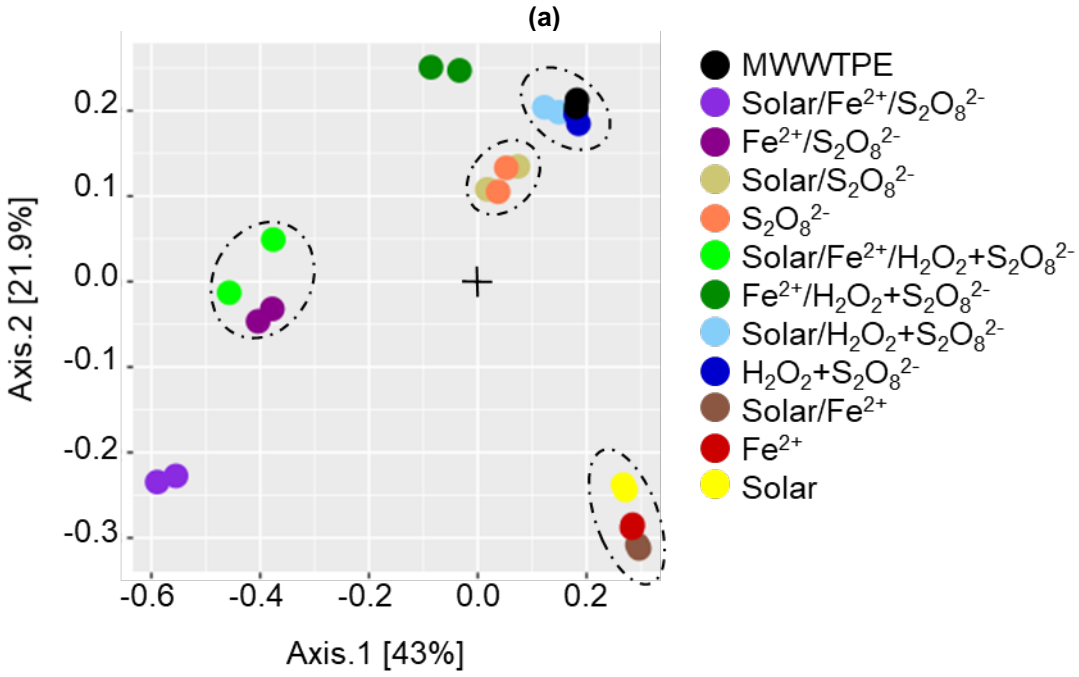

(b)

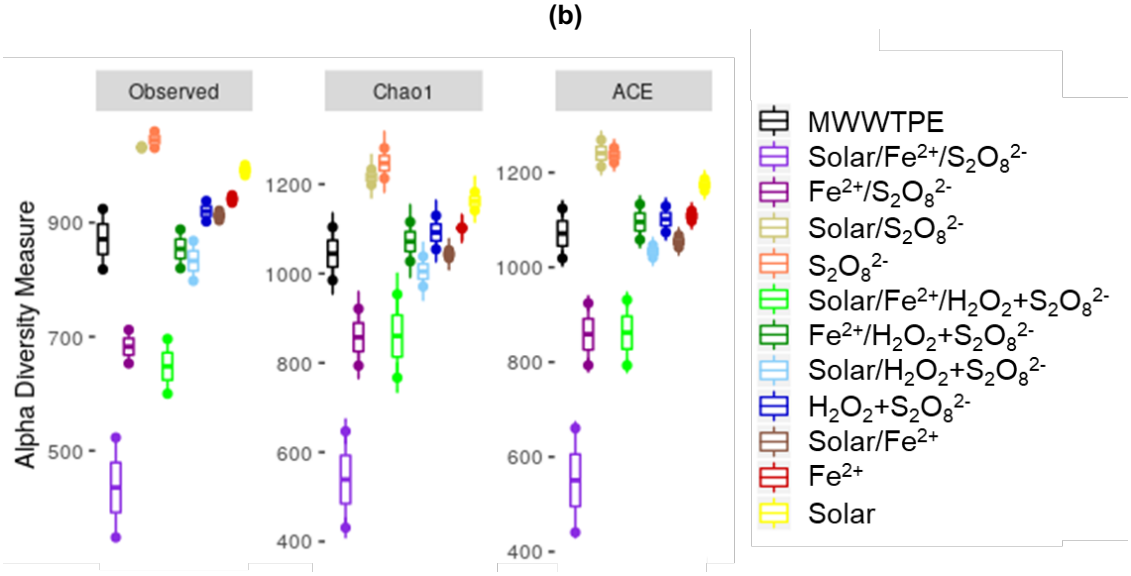

In solar/$Fe^{2+}/S_2O_8^{-2}$, persulfate activation by Fe^{2+} generates $SO_4^{\bullet -}$ (Equation III.4) leading to persulfate consumption in the system as shown in Figure III.2. Further transformation of sulfate radicals into hydroxyl radicals may also occur through Equation III.5 (WANG; WANG, 2018). Besides, at neutral pH (pH > 7), sulfate radical reaction with hydroxide anion may lead to the production of hydroxyl radical, as shown in Equation III.6 (ANIPSITAKIS; DIONYSIOU, 2004; WANG; WANG, 2018). Both oxidative radicals have disinfection potential as they cause damage to cell constituents (CANDEIAS; STEENKEN, 2000; DAVIES, 1987; KUMAR; POTTIBOYINA; SEVILLA, 2011; MARNETT, 2002), thus contributing to the effects on alpha and beta diversity shown in Figure III.1.

$$SO_4^{\bullet -} + H_2O \rightarrow SO_4^{2-} + HO^{\bullet} + H^+ \quad \text{(III.5)}$$

$$SO_4^{\bullet -} + OH^- \rightarrow SO_4^{2-} + HO^{\bullet} \quad \text{(III.6)}$$

Another main route for the formation of sulfate radicals occurs by photo-activation of persulfate as UV light irradiation breaks the peroxo band (O-O) to generate $SO_4^{\bullet -}$ (Equation III.7) (WANG; WANG, 2018; ZHANG *et al.*, 2019c). Even though most of the studies only focused on persulfate activation by UV light ($\lambda < 387$ nm), which corresponds to less than 5% of the solar spectrum (CHEN; MA; ZHAO, 2010), activation of persulfate by visible light ($\lambda \geq 420$ nm) showed excellent inactivation towards pathogenic bacteria elsewhere (WANG *et al.*, 2019b). Photo-activation of persulfate resulted in higher consumption of this oxidant in irradiated systems

(solar/Fe^{2+}/$S_2O_8^{-2}$ and solar/$S_2O_8^{-2}$) when compared to respective dark systems (Fe^{2+}/$S_2O_8^{-2}$ and $S_2O_8^{-2}$) (Figure III.2).

Figure III.2 - $S_2O_8^{2-}$ consumption and Fe^{2+} concentration during persulfate mediated solar photo-Fenton treatment (solar/Fe^{2+}/$S_2O_8^{2-}$) and controls (Fe^{2+}/$S_2O_8^{2-}$; solar/$S_2O_8^{2-}$; $S_2O_8^{2-}$)

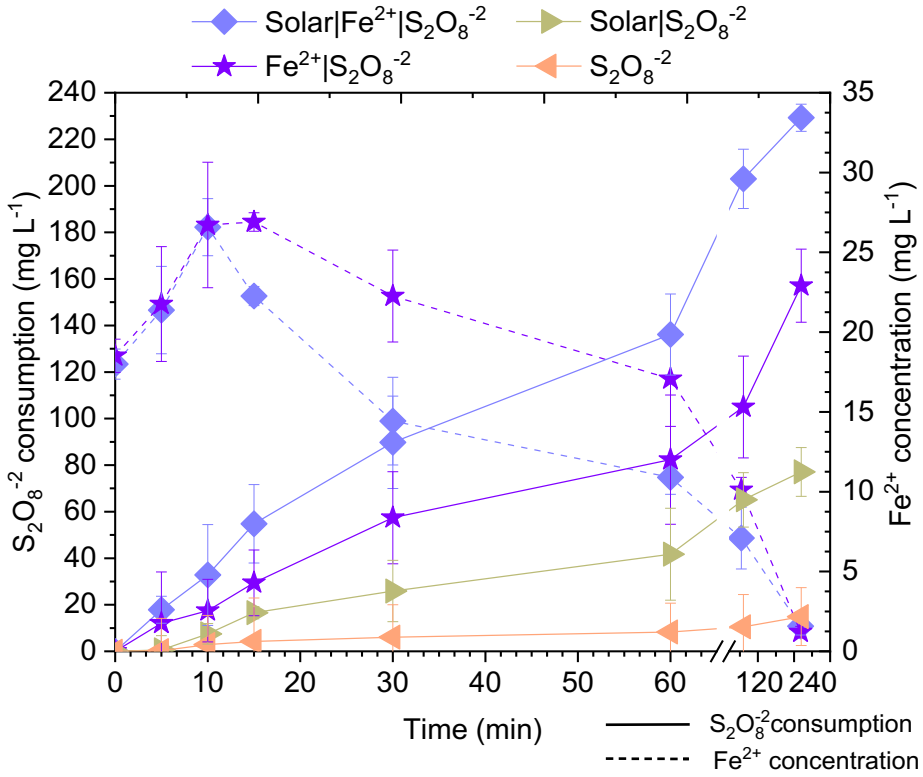

For instance, PS consumption during solar/Fe^{2+}/$S_2O_8^{-2}$ was equivalent to 81.2% (22.28 kJ L^{-1}) compared to 55.7% for Fe^{2+}/$S_2O_8^{-2}$ (Figure III.2). Enhanced Fe^{2+} cycling under irradiation (Equation III.3) may also have contributed to increased oxidant consumption. Higher PS consumption is directly related to increased generation of oxidative radicals ($SO_4^{\bullet -}$ and HO•) (Equations III.4 to III.7) which have known disinfection potential (CANDEIAS; STEENKEN, 2000; DAVIES, 1987; KUMAR; POTTIBOYINA; SEVILLA, 2011; MARNETT, 2002), thus justifying the greater effect upon microbial community observed for the irradiated system (Figure III.1).

$$SO_3^- - O - O - SO_3^- + h\nu \rightarrow 2SO_4^{\bullet -} \qquad \text{(III.7)}$$

Although acidic pH is optimum for the operation of Fenton systems, intermittent iron additions applied in this study ensured Fe^{2+} availability throughout treatment (from <5

mg L^{-1} up to 25 mg L^{-1}), enabling continuous PS consumption at neutral pH (7.1 – 7.9 range) (Figure III.2). The intermittent iron addition strategy effectively overcame pH limitations elsewhere (CARRA *et al*., 2013, 2014; CLARIZIA *et al*., 2017; DÍAZ-ANGULO *et al*., 2021; STARLING *et al*., 2021). The use of this strategy is also advantageous considering that excess Fe^{2+} may scavenge sulfate radicals (Equation III.8) (SONG *et al*., 2019; WANG; WANG, 2018) limiting disinfection potential. Besides, neutral pH enables the co-existence of oxidative radicals by conversion of sulfate to hydroxyl radicals in the presence of OH^- (Equation III.6) (GUAN *et al*., 2011).

$$SO_4^{\bullet -} + Fe^{2+} \rightarrow Fe^{3+} + SO_4^{2-} \quad \text{(III.8)}$$

The combined oxidant system (solar/Fe^{2+}/H_2O_2+$S_2O_8^{2-}$) also reduced the number of OTUs when compared to original MWWTPE sample (648 *versus* 871 OTUs – Figure III.1b). However, there was no significant difference in alpha diversity between MWWTPE and solar/Fe^{2+}/H_2O_2+$S_2O_8^{2-}$ (p-value > 0.1), so being less efficient than solar/Fe^{2+}/$S_2O_8^{2-}$. The combined oxidant system also did not show a significant difference (p-value > 0.1) when compared to by Fe^{2+}/$S_2O_8^{2-}$ (683 OTUs). This result was not expected as various reactions occur simultaneously in the combined oxidant system leading to the formation of distinct oxidative radicals, such as: (i) H_2O_2 activation by Fe^{2+} (Equation III.1) forming hydroxyl radicals; (ii) PS activation by Fe^{2+} forming sulfate radicals (Equation III.4), (iii) photo-activation of PS (Equation III.7) forming sulfate radicals, and (iv) PS activation by H_2O_2 producing sulfate radicals (Equation III.9) (HILLES *et al*., 2015).

$$S_2O_8^{2-} + H_2O_2 \rightarrow SO_4^{\bullet -} + HO_2^{\bullet} + HSO_4^- \quad \text{(III.9)}$$

Despite the higher number of routes leading to PS consumption in the combined oxidant system (141.135 mg L^{-1} of PS and 25 mg L^{-1} of H_2O_2), PS consumption within 5 and 10 min of reaction in this system (21 mg L-1 and 26 mg L^{-1}, respectively) (Figure III.3a) were similar to consumption in the persulfate mediated solar photo-Fenton (18 mg L^{-1} and 33 mg L^{-1}, respectively) (282.27 mg L^{-1} of PS) (Figure III.2).

Figure III.3 - $S_2O_8^{2-}$ and H_2O_2 consumption in the combined oxidant system (solar/Fe^{2+}/H_2O_2+$S_2O_8^{2-}$) and controls (Fe^{2+}/H_2O_2+$S_2O_8^{2-}$; solar/H_2O_2+$S_2O_8^{2-}$; H_2O_2+$S_2O_8^{2-}$) (a), Fe^{2+} concentration in solar/Fe^{2+}/H_2O_2+$S_2O_8^{2-}$ and Fe^{2+}/H_2O_2+ $S_2O_8^{2-}$ treatments (b)

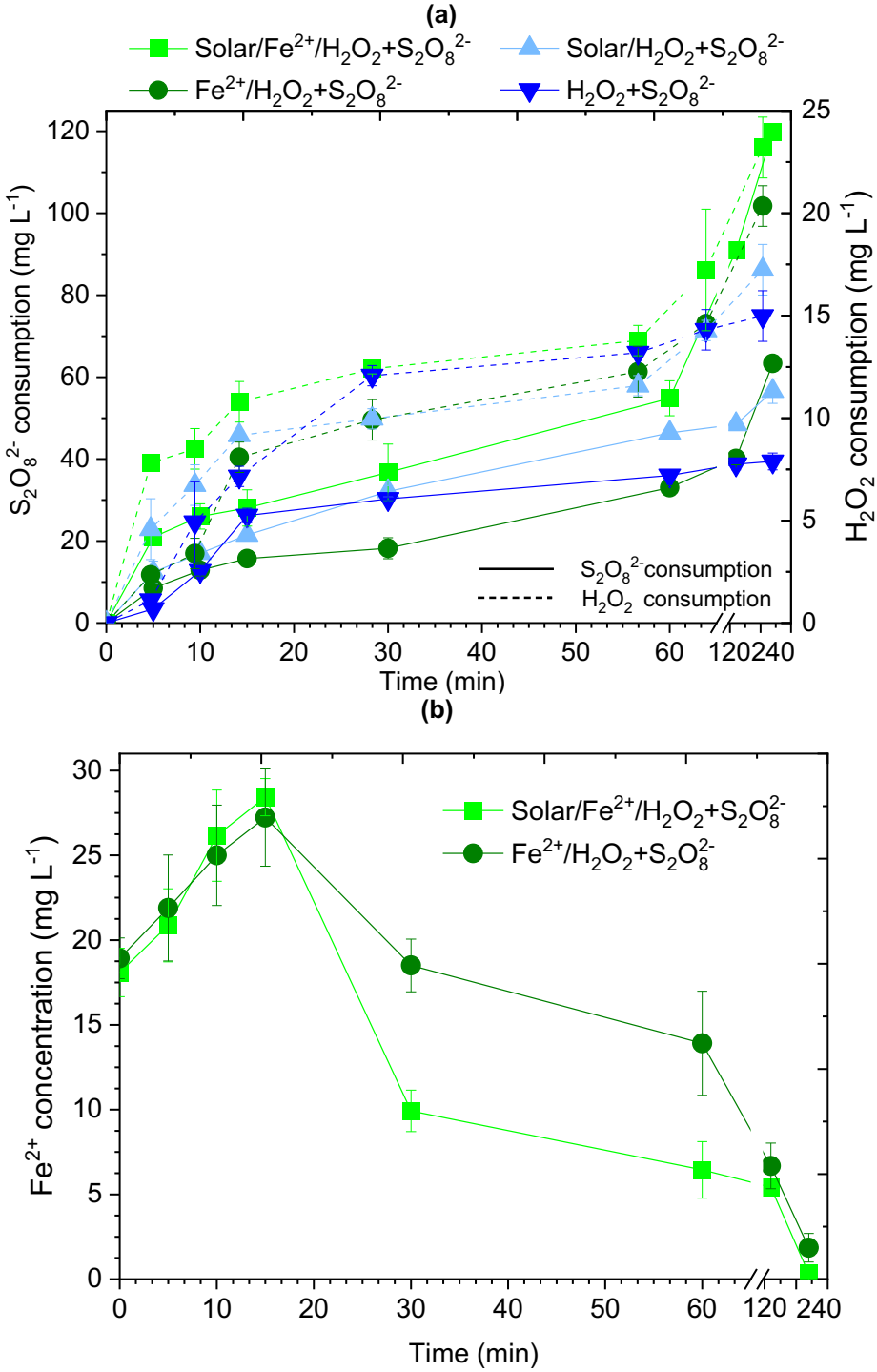

However, consumption of H_2O_2 in the combined oxidant system within 5 min of reaction (31 mg L^{-1}) (Figure III.2) was significantly higher than the consumption (10 mg L^{-1}) reported in a previous work in which 50 mg L^{-1} of H_2O_2 were used for solar photo-Fenton using the same iron addition strategy and effluent used in the present study

(VILELA *et al*., 2021b). Higher consumption of H_2O_2 in the combined oxidant system (up to 3x greater than in the H_2O_2 single system) persisted until up to 30 min of reaction. Enhanced H_2O_2 consumption in the presence of both oxidants is probably associated with: (i) the extra route of H_2O_2 consumption by reaction with PS (Equation III.9) as proven by persulfate consumption in the system containing H_2O_2 and persulfate only (Figure III.3), and (ii) pH decay from 6.7 to 3.0 during treatment (data not shown) since acidic conditions contribute to the predominance of dissolved Fe^{2+} in the system, thus increasing H_2O_2 activation by Fe^{2+}. Acidification occurs due to Fe^{2+} cycling to Fe^{3+}, which releases H^+ (Equation III.2). In contrast, pH increased from 6.7 to 7.9 in solar/H_2O_2+$S_2O_8^{2-}$ and H_2O_2+$S_2O_8^{2-}$.

Additionally, as H_2O_2 reaction with Fe^{2+} (k = 40 – 80 M^{-1} s^{-1}) is faster than the reaction between Fe^{2+} and PS (k = 30 M^{-1} s^{-1}) (LUO *et al*., 2021a), there is competition between H_2O_2 and PS for Fe^{2+} species, resulting in lower availability of Fe^{2+} during the combined oxidant treatment. While Fe^{2+} concentration reaches levels below 10 mg L^{-1} within 30 min of reaction in the combined oxidants system (Figure III.3b), it remains between 10 and 15 mg L^{-1} until 60 min of reaction (Figure III.2) in the PS mediated solar photo-Fenton. Considering that sulfate radical shows a longer lifespan (OH; DONG; LIM, 2016; ZHOU *et al*., 2020), it provides for the maintenance of hostile conditions for a longer period compared to hydroxyl radical. So, the system using only PS as an oxidant showed higher impact upon microbial community than solar photo-Fenton system mediated by both oxidants.

Regarding the combined oxidant system, the presence of PS slows down the loss of HO• due to H_2O_2 decomposition as observed in the study performed by Yan *et al*. (2013). Thus, the addition of PS to the traditional solar photo-Fenton system (H_2O_2 only) enhances the concentration of reactive radicals in the system increasing oxidation efficiency. However, excess PS may also work as a $SO_4^{\bullet -}$ scavenger, as shown in Equation III.10 and III.11 (HUIE; CLIFTON, 1989; QIAN *et al*., 2015). Considering results obtained for microbial community diversity after treatments, the use of equivalent molar concentrations of H_2O_2 and $S_2O_8^{2-}$ (1:1) possibly led to an excess of PS in the combined system. Alternative H_2O_2:$S_2O_8^{2-}$ ratios may overcome

this limitation and enhance the effect of the combined oxidant photo-Fenton system upon microbial community and improve ARB and ARGs removals.

$$SO_4^{\bullet -} + S_2O_8^{2-} \rightarrow SO_4^{2-} + S_2O_8^{\bullet -} \quad \text{(III.10)}$$

$$SO_4^{\bullet -} + SO_4^{\bullet -} \rightarrow S_2O_8^{2-} \quad \text{(III.11)}$$

3.2 Impact of solar photo-Fenton mediated by alternative oxidants upon bacterial phyla

Figure III.4 presents a summary of the phylogeny of bacterial community present in MWWTPE and samples submitted to persulfate-mediated solar photo-Fenton (Solar/Fe^{2+}/$S_2O_8^{2-}$), the combined oxidant system (Solar/Fe^{2+}/H_2O_2+$S_2O_8^{2-}$), and controls. *Actinobacteria*, *Proteobacteria,* and *Bacteroidetes* were the main phyla in MWWTPE samples (28.2 ± 2.2%, 25.6 ± 1.7%, and 23.5 ± 2.8% of total sequences, respectively). Phyla *Chloroflexi* (8.8 ± 1.3%) and *Firmicutes* (1.9 ± 0.2%) were also present in the effluent sample.

Figure III.4 - Barplots representing the composition of microbial community at phylum level for MWWTPE and samples obtained after PS-mediated solar photo-Fenton (Solar/Fe^{2+}/$S_2O_8^{2-}$), combined oxidant system (Solar/Fe^{2+}/H_2O_2+$S_2O_8^{2-}$) and controls (Fe^{2+}/$S_2O_8^{2-}$; Solar/$S_2O_8^{2-}$; $S_2O_8^{2-}$; Fe^{2+}/H_2O_2+$S_2O_8^{2-}$; Solar/H_2O_2+$S_2O_8^{2-}$; H_2O_2+$S_2O_8^{2-}$, Solar/Fe^{2+}; Fe^{2+}; Solar). Taxa with abundance below 1% and unclassified taxa were designated as NA

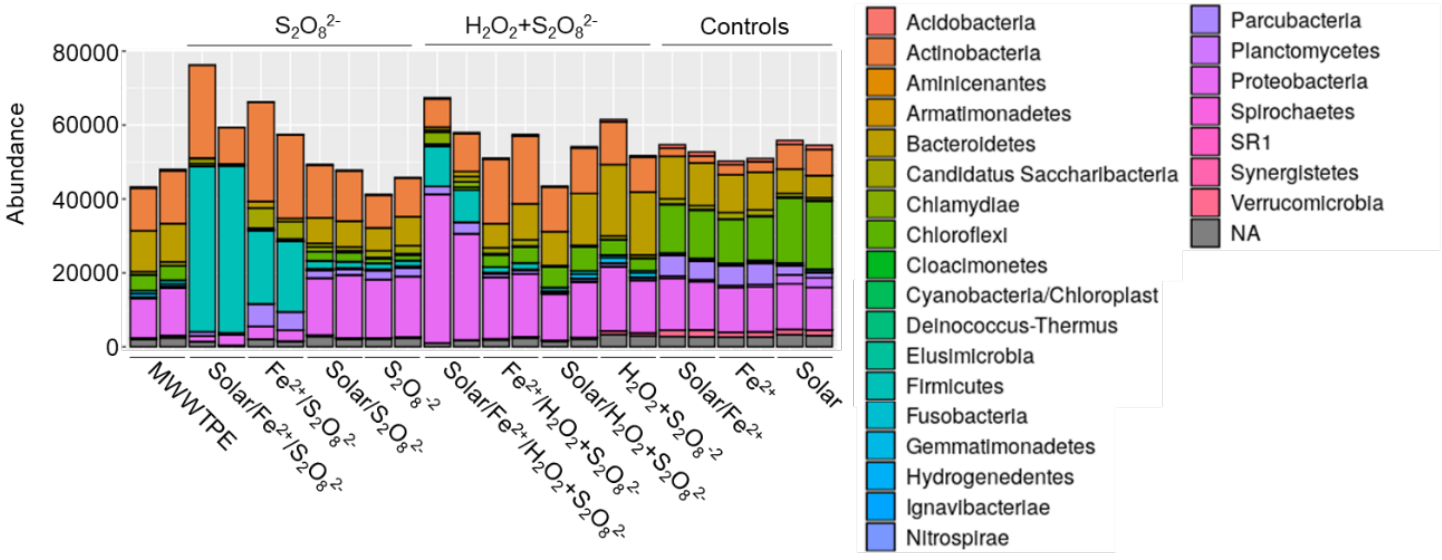

These results agree with other studies that reveal *Proteobacteria* and *Bacteroidetes* as the dominant microbial populations in effluents from activated sludge systems. Other main phyla include *Actinobacteria*, *Firmicutes*, and *Chloroflexi* (GUO *et al*., 2017; XIA *et al*., 2018; XIE *et al*., 2021; YANG *et al*., 2011). A recent study performed with

MWWTPE sampled in the same MWWTP as in this study showed that *Proteobacteria* was the dominant phylum, followed by *Actinobacteria* or *Bacteroidetes*, for which occurrence varied seasonally. Phyla *Chloroflexi*, *Firmicutes*, and *Acidobacteria* were also present in samples (VILELA *et al*., 2021b).

Solar/Fe^{2+}/$S_2O_8^{2-}$ achieved 88% removal of *Proteobacteria*, 99% reduction of *Bacteriodetes,* and complete removal of *Chloroflexi*. This effect reflects the disinfecting properties of $SO_4^{\bullet-}$ formed via persulfate activation by Fe^{2+}, and UV-Vis irradiation as discussed in section 3.1. Besides, hydroxyl radicals formed in the Solar/Fe^{2+}/$S_2O_8^{2-}$ at neutral pH conditions (Equation III.6) may also have contributed to the elimination of these phyla. Although mechanisms associated with the oxidation of biological molecules (*i.e*. microbial cells, DNA, etc.) by HO• radical have been widely discussed (CANDEIAS; STEENKEN, 2000; DAVIES, 1987; KUMAR; POTTIBOYINA; SEVILLA, 2011; MARNETT, 2002; SIMÕES *et al*., 2016; XIAO *et al*., 2019; YIN; XU; PORTER, 2011), pathways of oxidation of biomolecules by $SO_4^{\bullet-}$ are still unclear. Rodríguez-Chueca *et al*. (2017) suggested that $SO_4^{\bullet-}$ induced oxidative lipid peroxidation in the cell membrane, resulting in permeability loss and metabolic disturbance, finally leading to cell inactivation (RODRÍGUEZ-CHUECA *et al*., 2017). Prompt oxidation of cell components in the presence of sulfate radical obtained in other publications (BIANCO *et al*., 2017; MA *et al*., 2019; MICHAEL-KORDATOU *et al*., 2015; OH *et al*., 2014; QIU *et al*., 2020; RODRÍGUEZ-CHUECA *et al*., 2017, 2019b; SUN; TYREE; HUANG, 2016; WANG *et al*., 2019b; WORDOFA; WALKER; LIU, 2017; XIAO *et al*., 2019; ZHOU *et al*., 2020) aligns with high effect upon main phyla present in MWWTPE observed in the present study.

The impact of PS mediated solar photo-Fenton upon *Proteobacteria* is promissing since most priority pathogenic ARB listed by the WHO (GOVINDARAJ VAITHINATHAN; VANITHA, 2018) belong to this phylum (*e.g. H. pylori, P. aeruginosa*, *A. baumannii*, etc.), and some of the main pathogens associated with the spread of AMR belong to *Bacteroidetes* (*e.g. B. fragilis, C. normanense*, *C. meningosepticum*) (NGUYEN *et al*., 2021). Considering that solar photo-Fenton treatment carried out in the presence of H_2O_2 promoted an enrichment of *Proteobacteria* (VILELA *et al*.,

2021b), these results support the use of persulfate as an alternative oxidant for MWWTPE treatment.

On the other hand, solar/Fe^{2+}/$S_2O_8^{2-}$ did not achieve satisfactory abatement of the phylum *Actinobacteria* (~12%) and showed positive selection for representatives of *Firmicutes* (> 35-fold enrichment) (Figure III.4). *Firmicutes* abundance in MWWTPE was less than 2% ($\bar{x}$ = 783 OTU), yet it increased significantly to 67% ($\bar{x}$ = 27741 OTU) after PS-mediated solar photo-Fenton treatment, and to 32% ($\bar{x}$ = 12950 OTU) after PS-mediated Fenton control. Application of persulfate for wastewater treatment (GAO *et al*., 2020; QIU *et al*., 2020) and treatment of contaminated soil by *in situ* chemical oxidation (ISCO) (GOU *et al*., 2020; SONG *et al*., 2019) also led to selection of this phylum. *Firmicutes* are mainly represented by gram-positive bacteria which present a thicker and denser (20–80 nm) membrane layer compared to gram-negative bacteria (10-15 nm) (*e.g. Bacteriodetes* and *Chlroflexi)*. Hence, this group might be more resistant to oxidation by radicals generated in PS-mediated systems (CHEN *et al*., 2021). Besides that, capacity of bacteria belonging to *Firmicutes* to adapt to hostile environmental conditions (FILIPPIDOU *et al*., 2016) may have contributed to their increase even after exposure to extreme conditions in PS mediated solar photo-Fenton treatment.

Selection of the *Firmicutes* phylum is of great environmental concern as it comprises several genera which hold outstanding public-health relevance, such as *Staphylococcus*, *Streptococcus*, and *Enterococcus* (2019 Antibacterial Agents, 2019; HAVENGA *et al*., 2019). Among major classes of *Firmicutes*, the enrichment was observed almost exclusively for the *Clostridia* class (Figure III.5a). *Clostridia* is a highly polyphyletic class of *Firmicutes*, including *Clostridium difficile,* listed as an urgent priority group of AMR by the Centers for Disease Control and Prevention in the United States (LANZA *et al*., 2015). Besides these groups, *Firmicutes* enrichment was mainly observed for genus associated with human and animal gut microbiota such as *Eubacterium*, *Blautia*, *Coprococcus*, *Intestinibacter*, *Faecalibacterium,* and *Ruminococcus* (data not shown). Future studies must investigate selection mechanisms and alternatives to avoid the increase of this phylum after exposure to PS. Notwithstanding, solar/Fe^{2+}/$S_2O_8^{2-}$ treatment managed to eliminate some relevant

species pertaining to the *Bacilli* class identified in MWWTPE, such as *Streptococcus pneumoniae*, *Streptococcus pyogenes* (erythromycin resistance), and *Streptococcus agalactiae* (clindamycin resistance) (data not shown).

Figure III.5 - Abundance of different classes of *Firmicutes* (a) and *Proteobacteria* (b) in MWWTPE and samples obtained from persulfate-mediated (Solar/Fe^{2+}/$S_2O_8^{2-}$) and controls (Fe^{2+}/$S_2O_8^{2-}$; Solar/$S_2O_8^{2-}$; $S_2O_8^{2-}$), and combined oxidants system (Solar/Fe^{2+}/H_2O_2+$S_2O_8^{2-}$) and controls (Fe^{2+}/H_2O_2+$S_2O_8^{2-}$; Solar/H_2O_2+$S_2O_8^{2-}$; H_2O_2+$S_2O_8^{2-}$) experiments. Taxa with abundance below 1% and unclassified taxa were designated as NA

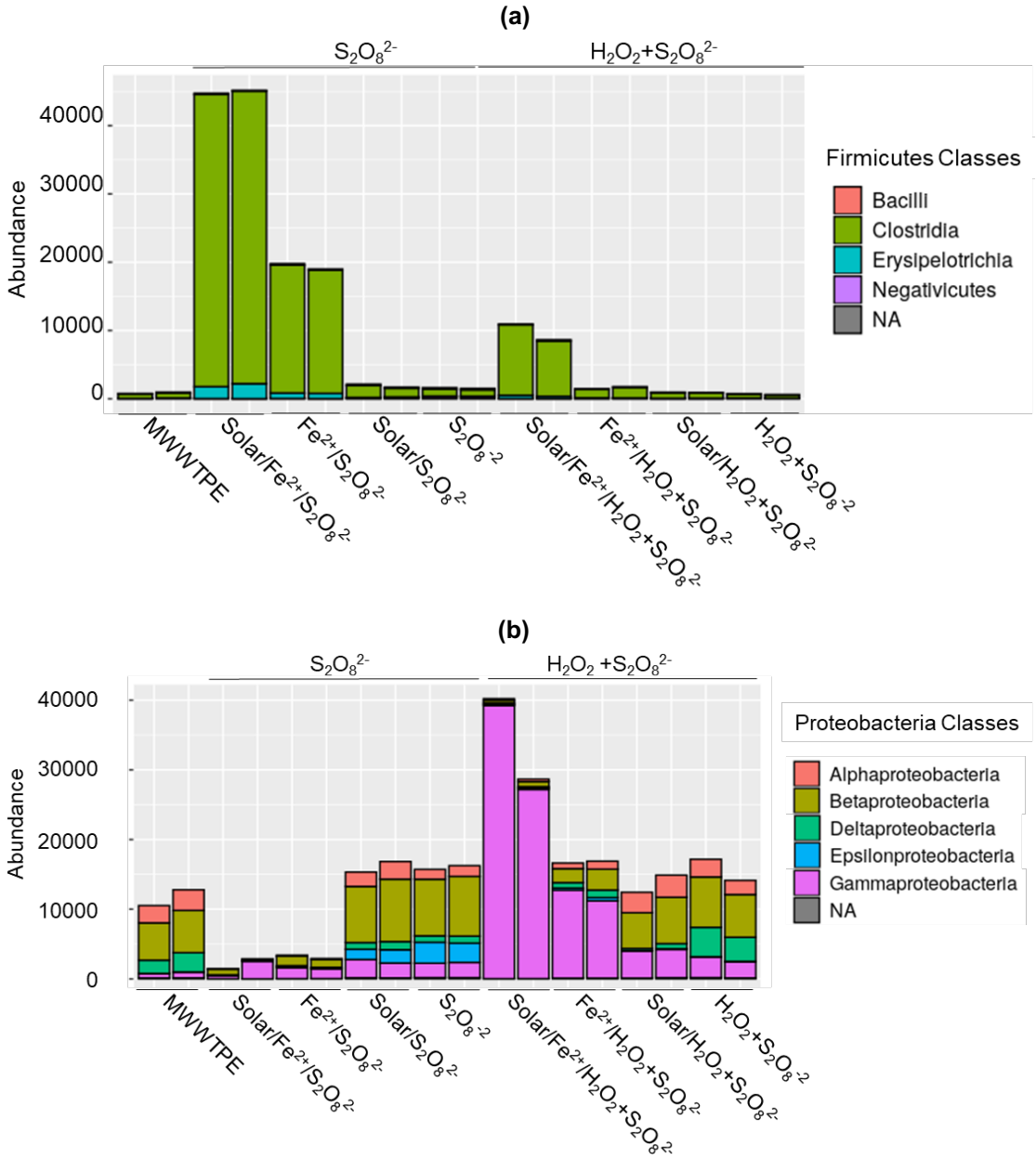

Meanwhile, the combined oxidant system (solar/Fe^{2+}/H_2O_2+$S_2O_8^{2-}$) achieved 88% removal of *Chloroflexi* and 92% removal of *Bacteroidetes.* Abatement of *Actinobacteria*

was below 50%. Similar to observations made for solar/Fe^{2+}/$S_2O_8^{2-}$, this treatment had a positive selection of phyla *Firmicutes* (> 8-fold) (Figure III.4). Besides, an enrichment of Proteobacteria (> 2-fold) was also observed in samples submitted to solar photo-Fenton applied in the presence of both oxidants (Figure III.4). This result confirms positive selective pressure of *Proteobacteria* in the presence of H_2O_2, as observed elsewhere (VILELA *et al*., 2021b). This effect is probably associated with inherent mechanisms of resistance to H_2O_2 held by *Proteobacteria,* such as scavenging mechanisms to eliminate H_2O_2 present in the environment (MAGRO *et al*., 2019) and a significant adaptive response to H_2O_2 stress (LI *et al*., 2020b). Besides that, H_2O_2 can function either as a disinfectant (APEL; HIRT, 2004) or as an oxygen source enhancing aerobic bacterial growth (HINCHEE; DOWNEY; AGGARWAL, 1991; ZAPPI *et al*., 2000). Enrichment of *Firmicutes* and *Proteobacteria* observed after the combined oxidant system indicates environmental risks associated with the use of this process, as these phyla comprise primary critical priority pathogens of public-health relevance (*e.g. Acinetobacter baumannii, Pseudomonas aeruginosa*, and *Enterobacteriaceae*) (GOVINDARAJ VAITHINATHAN; VANITHA, 2018; HAVENGA *et al*., 2019; NEILL, 2014). Hence, it is critical to investigate selection mechanisms and alternatives to avoid the selection of this group.

Among all five classes of *Proteobacteria*, the most significant enrichment was observed for *Gammaproteobacteria* class (Figure III.5b) which comprises species that are increasingly associated with severe nosocomial infections worldwide (BARTLETT, 2004; BONOMO; SZABO, 2006; GIL-GIL; MARTÍNEZ; BLANCO, 2020) (in example: *Acinetobacter baumannii and Pseudomonas aeruginosa*) as well as those from the *Enterobacteriaceae* family (*Klebsiella pneumoniae, Escherichia coli, Enterobacter spp.,* and *Proteus spp.*). All these species were identified in MWWTPE and presented association to carbapenem resistant genes (data not shown). *Pseudomonas aeruginosa* and *Stenotrophomonas sp.* related to a tetracycline-resistant gene were also detected in MWWTPE samples (data not shown). Despite complete removal of these species via solar photo-Fenton using only H_2O_2 as oxidant (VILELA *et al*., 2021b), the combined oxidants system favored their enrichment (> 2-fold). Interestingly, PS-mediated solar photo-Fenton did not achieve an effective removal of these species either.

The increase of *Pseudomonas* and *Stenotrophomonas* observed after treatment by the combined oxidant solar photo-Fenton (data not shown) corroborates with observations made after the treatment by solar photo-Fenton using only H_2O_2 as an oxidant (VILELA *et al*., 2021b). This selection may be associated with high tolerances of these groups to H_2O_2 (BJARNSHOLT *et al*., 2005; MOREIRA *et al*., 2018). The abundance of genes associated to H_2O_2 elimination mechanisms (*katA1*, *katA2*, *katMn*, *katE*, *ahpCF*, *Gpx1*, *Gpx2*, and *Gpx3)* which play a critical role for survival in the presence of high H_2O_2 concentrations (BJARNSHOLT *et al*., 2005; LI *et al*., 2020b; MAGRO *et al*., 2019) were analyzed in MWWTPE samples before and after treatment (Figure III.6). *katA2*, *katE*, *ahpC*, *Gpx1*, *Gpx2*, and *Gpx3* genes were identified in all samples (Figure III.6) and considerable enrichments were observed for *katA2* (from 2246 to 4000 *reads*) and *katE* (from 2083 to 3953 *reads*) after $Fe^{2+}/H_2O_2+S_2O_8^{2-}$ treatment. Furthermore, a discrete enrichment was observed for the *Gpx3* gene (from 2740 to 3270 *reads*) (Figure III.6). Although these genes are only related to tolerance and/or resistance to H_2O_2, *ahpC* and *Gpx2* genes also showed slight increase after treatments involving only $S_2O_8^{2-}$ as an oxidant. Thus, suggesting that these genes are more related to the survival of microorganisms under hostile conditions in general rather than strictly to the presence of H_2O_2.

Figure III.6 - Abundance of genes related to mechanisms to eliminate H_2O_2 in MWWTPE and samples obtained from persulfate-mediated and binary system experiments

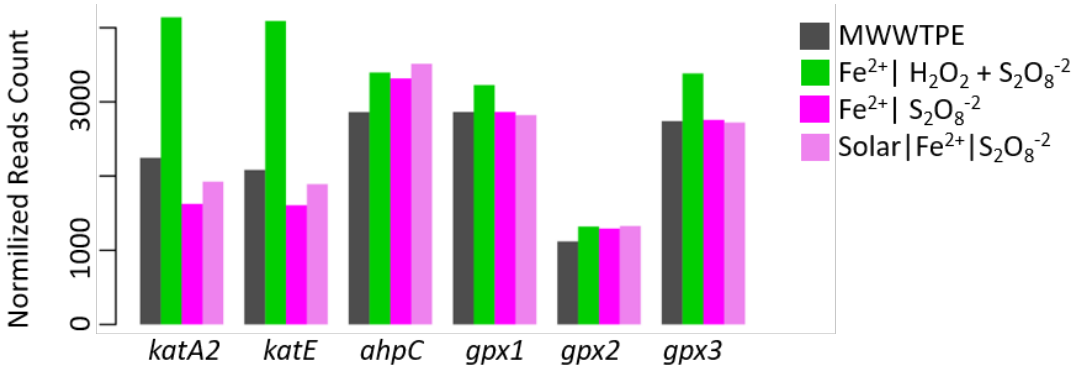

3.3 Effect of treatments on resistome profile: diversity and richness of ARGs

ARGs which confer resistance to different classes of antimicrobial are abundant in MWWTPE samples. In a previous study, the ResFinder ARG database *(ZANKARI et al*., 2012) enabled the detection of 69 variations of ARGs within 19 major types. In order to improve ARG annotation, the database used in this study combined ARBD

(LIU; POP, 2009) and CARD (JIA *et al*., 2017) with a hybrid UBLAST and BLASTX algorithm (YIN *et al*., 2018). This method enabled the detection of 971 variations of ARGs encompassing 63 major types and ten antibiotic classes (Figure III.7a and b).

Figure III.7 - Heatmap of the distribution of ARGs (a), and abundance of ARGs major subtypes (b) in MWWTPE, PS-mediated solar photo-Fenton (Solar/Fe^{2+}/$S_2O_8^{2-}$), PS-mediated control Fenton (Fe^{2+}/$S_2O_8^{2-}$), and Combined oxidants control Fenton (Fe^{2+}/H_2O_2+$S_2O_8^{2-}$) system

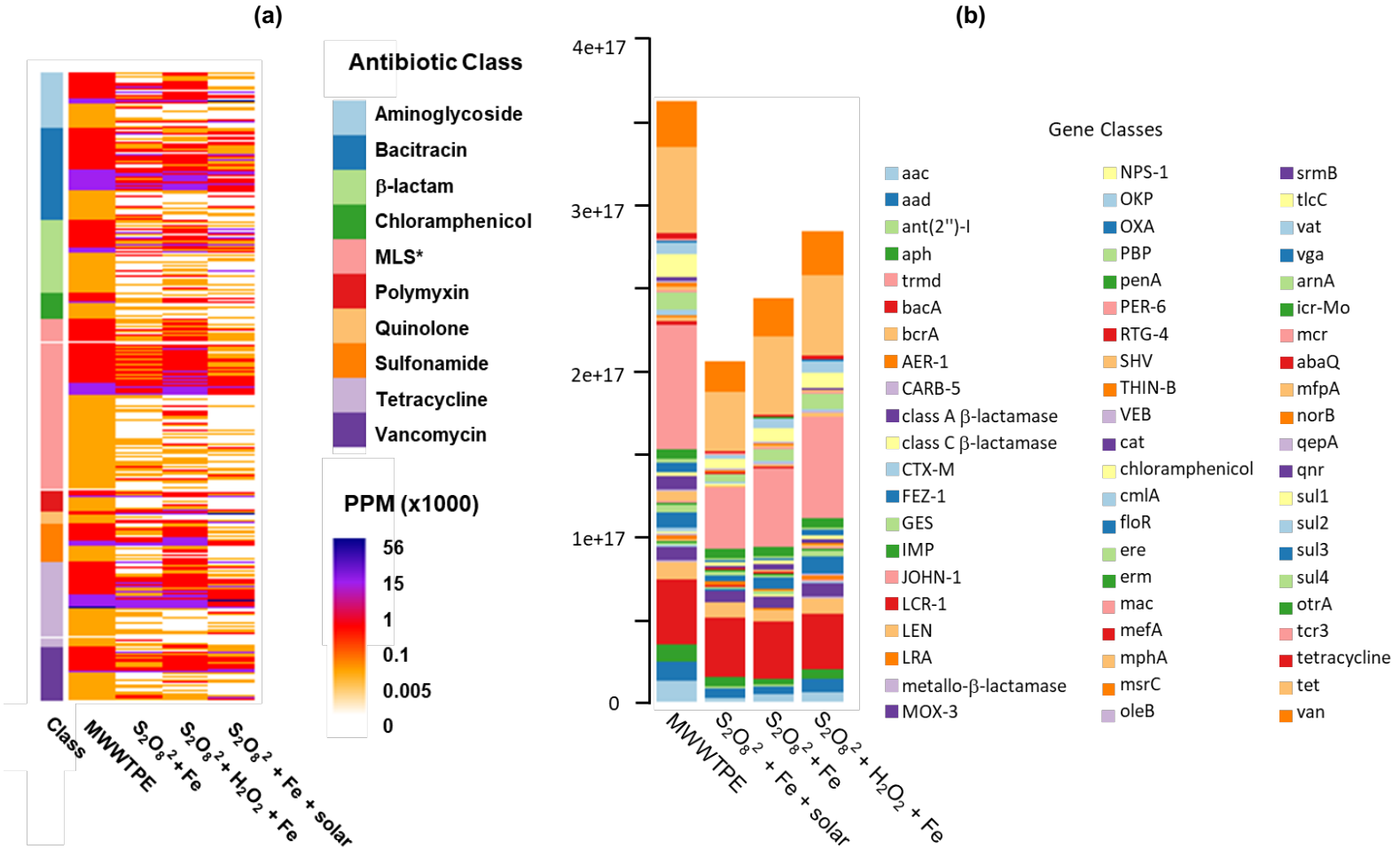

*MLS – Macrolide, Lincosamide, and Streptogramin; CLO – Chloramphenicol; TET – Tetracycline.

As shown in Figure III.7a, ARGs which confer resistance to macrolide-lincosamide-streptogramin (MLS) group (such as *ere*, *erm*, *mac*, *mef*, *mph*, *msr*, etc.) represented 26% of total ARGs present in MWWTPE, followed by 14% for ARGs associated with resistance to bacitracin (*bacA* and *bcrA*), 13% with tetracycline (*otrA*, *tcr3*, and subtypes of *tet*), 12% with β-lactams (mainly subtypes of *blaOXA*, *blaCTX*, *blaSHV*), and 10% associated with aminoglycosides (mainly *aac*, *aad*, *ant*, and *aph* subtypes). ARGs which confer resistance to vancomycin (only *van* subtypes, 8%), sulfonamides (mainly *sul1* and *sul2*, 6%), chloramphenicol (especially *cat*, *cmlA*, and *floR* subtypes, 5%), polymyxin (*arnA* and *mcr* subtypes, 3%) and quinolones (*aba*, *mfpA*, *norB*, *qepA*, and *qnr* subtypes, 2%) were also present in MWWTPE. Previous studies have also reported that ARGs conferring resistance to broad-spectrum antibiotics, mostly sulfonamides, macrolides, and tetracyclines, are frequently detected in MWWTPE due to high conservation and sequence transfer associated with these genes *(NGUYEN et al*., 2021; RAZA *et al*., 2021; WEI *et al*., 2018). Overall, most abundant genes present in MWWTPE were *macB* (7.3E+16 ppm), *bacA* (3.9E+16 ppm), *sul1* (1.4E+16 ppm), *vanR* (1.2E+16 ppm), *aadA* (1.1E+16 ppm), *bcrA* (1.0E+16 ppm), *arnA* (9.6E+15 ppm), *tetA* (8.4E+15 ppm), and *sul2* (6.6E+15 ppm).

Results show that solar/Fe^{2+}/$S_2O_8^{-2}$ (Figure III.7) removed 44% of total ARGs. In contrast, PS-mediated control Fenton and combined oxidant system controls (dark) achieved ~35% and 23% removals, respectively. Interestingly, whole-genome sequencing of the sample obtained after solar/Fe^{2+}/H_2O_2+$S_2O_8^{2-}$ could not be performed due to extensive DNA fragmentation (failure to pass Macrogen quality control) during this process. An electrophoresis gel is presented in Figure III.8 as a proof that solar/Fe^{2+}/H_2O_2+$S_2O_8^{-2}$ had a higher impact upon DNA integrity compared to other tested treatments. Direct and simultaneous exposure to H_2O_2 and PS can induce acute DNA damage (LEE; JEONG, 2007; WANG *et al*., 2017c). Extensive DNA degradation in the combined system probably occurred due to high DNA oxidative damage by SO_4•$^-$ and HO• radicals generated simultaneously in the combined solar/Fe^{2+}/H_2O_2+$S_2O_8^{2-}$ system (HENLE; LINN, 1997; ZHANG *et al*., 2020b).

Figure III.8 - High DNA mass ladder (Life Technologies) and DNA samples were loaded on 0.8% agarose gel

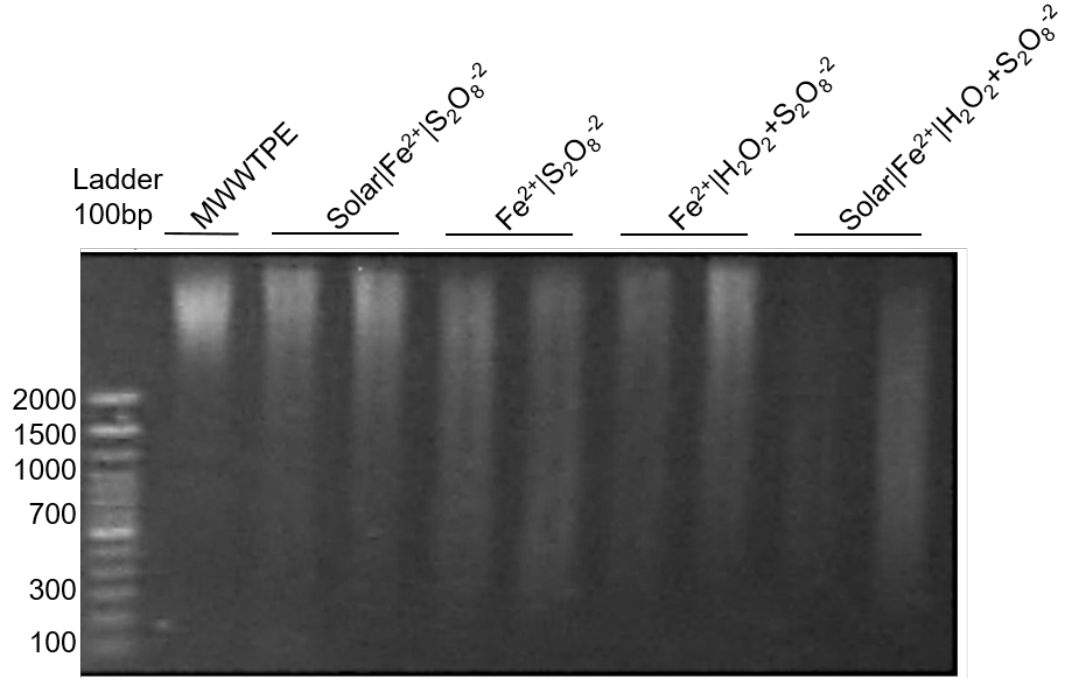

Solar/Fe^{2+}/$S_2O_8^{2-}$ achieved more than 50% removal of ARGs which confer resistance to broad-spectrum antibiotics, such as aminoglycoside, β-lactams, MLS, and sulfonamide. However, removals of ARGs resistant to tetracycline and vancomycin were limited to 37% and 34%, respectively. Regarding the removal of ARGs which confer resistance to antibiotics with a specific spectrum of action (*i.e.* bacitracin, chloramphenicol, polymyxin, and quinolone), Solar/Fe^{2+}/$S_2O_8^{2-}$ efficiency was greater than 60%, reaching more than 70% for genes that confer resistance to chloramphenicol. An exception was observed for ARGs conferring resistance to bacitracin, for which maximum removal was nearly ~10%. Regarding subtypes, the treatment achieved a high clearance for the most abundant genes originally present in MWWTPE (*macB*, *sul1*, *aadA*, *arnA*, *tetA*, and *sul2*, > 50%). As expected, removal of *bacA*, *bcrA*, and *vanR* was not high, following the clearance pattern found for this antibiotic class (10 and 34%, respectively).

Most current studies associated with ARG removal investigate the effectiveness of advanced treatment technologies for predetermined ARGs via qPCR, resulting in the assessment of a limited list of ARGs (mostly *blaCTX*, *blaTEM*, *blaOXA*, *sul1*, *sul2*, *emrB*, *tetQ*, *tetX*, and *tetM*) (CLARA *et al*., 2021). Besides, standard qPCR methods have limitations in the detection of emerging ARGs present in complex environmental

samples (*e.g.* wastewater samples). In contrast, the identification of ARGs via WGS is a highly sensitive technique that shows high specificity in detecting ARGs (LI; YAN, 2021). Still, it is not possible to compare results obtained via persulfate mediated solar photo-Fenton in this study with those observed in a previous publication which also used metagenomics to asses ARG removal after solar photo-Fenton (VILELA *et al*., 2021b) since databases used for ARG annotation differ. However, regardless of the method used to assess ARG removal from MWWTPE after oxidative processes, high removal efficiencies identified in this study are repeatedly reported (AHMED *et al*., 2020; FIORENTINO *et al*., 2019b; GIANNAKIS *et al*., 2018b; LI *et al*., 2021; MICHAEL *et al*., 2020; OH *et al*., 2014; VILELA *et al*., 2021b; ZHOU *et al*., 2020). Thus, confirming the potential of applying solar photo-Fenton as an additional treatment stage in MWWTP to control the spread of AMR.

3.4 Analysis of WHO priority pathogens and co-occurrence with ARGs

Correlation-based network analysis is a powerful method to discern the co-occurrence patterns between ARG and the microbial community (JU *et al*., 2016). MWWTPE samples analyzed in this study contained 54 ARG subtypes with robust correlations ($\rho > 0.8$) with pathogens listed in the WHO priority list (Figure III.9). Samples obtained after solar/Fe^{2+}/$S_2O_8^{-2}$ showed correlation to only 37% of ARGs originally present in the MWWTPE (Figure III.9), while 50 and 68% correlation remained after Fe^{2+}/$S_2O_8^{2-}$ and Fe^{2+}/H_2O_2+$S_2O_8^{2-}$, respectively (data not shown). These results confirm the need to apply advanced treatments to remove priority pathogens that show strong co-occurrence with various ARG subtypes from MWWTPE, thus reducing public health issues associated with MWWTPE discharge in the environment.

Figure III.9 - Co-occurrence patterns and contributor network associations between ARG subtypes and WHO priority pathogens present in MWWTPE, persulfate-mediated solar photo-Fenton (Solar/$Fe^{2+}/S_2O_8^{2-}$), persulfate-mediated control Fenton ($Fe^{2+}/S_2O_8^{2-}$), and control Fenton with combined oxidants system ($Fe^{2+}/H_2O_2+S_2O_8^{2-}$) depicted by network analysis. A node stands for an ARG subtype or a species and a connection (*i.e.,* edge) represents a significant (P-value ≤ 0.01) and strong (Spearman's correlation coefficient ρ > 0.80) pairwise correlation. Nodes colors defined as according to ARG types and samples. The size of each node is proportional to the number of connections (*i.e.* degree).

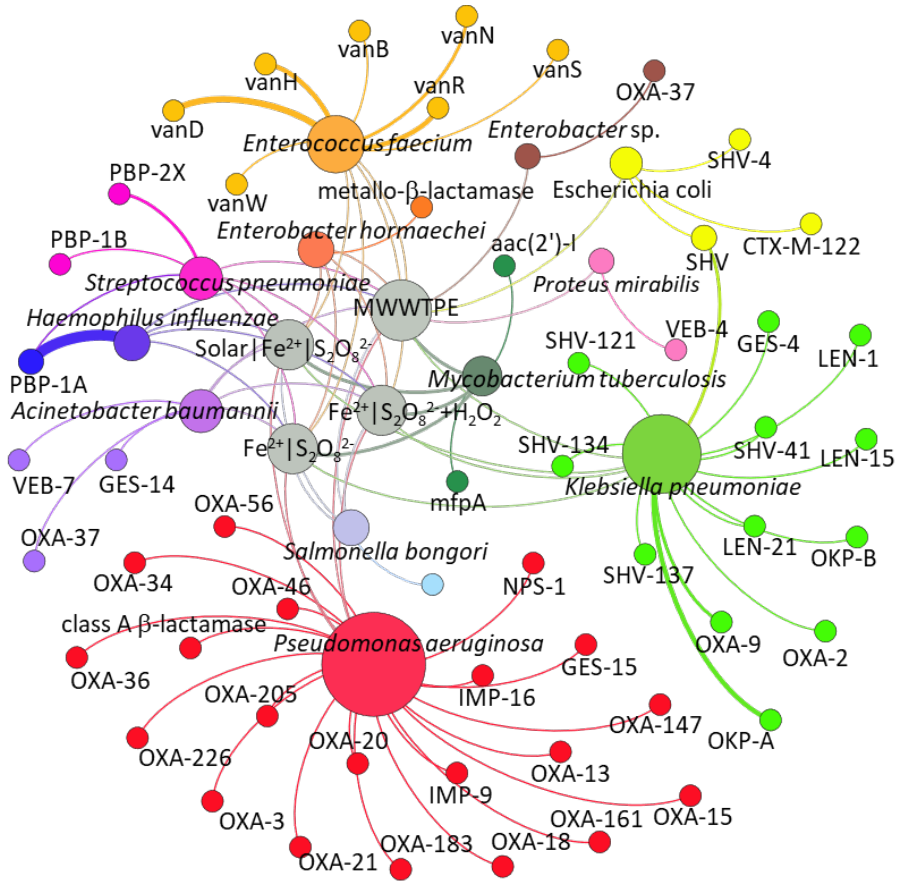

As shown in Figure III.9, critical priority *Pseudomonas aeruginosa* present in MWWTPE was significantly associated with 19 ARGs encoded as resistant to β-lactamic antibiotics (*blaGES-15, blaIMP-9, blaIMP-16, blaNPS-1, blaOXA-3, blaOXA-13, blaOXA-15, blaOXA-18, blaOXA-20, blaOXA-21, blaOXA-34, blaOXA-36, blaOXA-46, blaOXA-56, blaOXA-147, blaOXA-161, blaOXA-183, blaOXA-205, blaOXA-226*). Solar/$Fe^{2+}/S_2O_8^{-2}$ treatment reduced these associations to 7 ARGs (*blaGES-15, blaIMP-16, blaOXA-3, blaOXA-15, blaOXA-18, blaOXA-21, blaOXA-36*). β-lactam resistant genes were also strongly associated with *Klebsiella pneumoniae*, included in critical priority *Enterobacteriaceae* in both MWWTPE (*blaGES-4, blaLEN-1, blaLEN-15, blaLEN-21, blaOKP-A, blaOKP-B, blaOXA-2, blaOXA-9, blaSHV-41, blaSHV-121, blaSHV-134, blaSHV-137*) and samples submitted to PS mediated solar photo-Fenton (*blaLEN-21, blaOKP-B, blaOXA-2, blaOXA-9, blaSHV-41*). Moreover, critical priority

carbapenem-resistant *Acinetobacter baumannii* present in MWWTPE samples showed correlation with *blaOXA-37*, *blaVEB-7*, and *blaGES-14*. Correlation between *Acinetobacter baumannii* and *blaGES-14* subtype persisted even after solar/Fe^{2+}/$S_2O_8^{-2}$ (9.45E+14 ppm in MWWTPE *vs.* 4.78 E+14 after treatment). As this subtype possesses an extended spectrum of activity toward carbapenems (BONNIN *et al*., 2013), its prevalence presents a significant risk of transferring high-level resistance to carbapenems to the environment.

Regarding ARGs that confer resistance to vancomycin, *Enterococcus faecium* showed a strong relationship with subtypes *vanD, vanH* and *vanR* in MWWTPE (1.47E+15 ppm, 1.19E+15 ppm and 7.65E+14 ppm, respectively) and sample treated by solar/Fe^{2+}/$S_2O_8^{-2}$ (7.52E+14 ppm, 4.18E+14 ppm and 9.25E+14 ppm, respectively). A 9-fold increase in the occurrence of a *vanH* subtype (gene AAR37059) was observed after solar/Fe^{2+}/$S_2O_8^{-2}$ (8.92E+13 in MWWTPE ppm *vs.* 7.98 E+14 after treatment). *Haemophilus influenzae* and *Streptococcus pneumoniae* were identified as potential hosts of *blaPBP* subtypes (*1A*, *1B*, and *2X*). *Haemophilus influenzae* presented the most significant and strong pairwise correlation with blaPBP-1A (2.33E+15 ppm) in MWWTPE. However, only one subtype persisted (gene YP_001290033) after treatment by solar/Fe^{2+}/$S_2O_8^{-2}$.

Regarding medium priority *Streptococcus* pneumonia, solar/Fe^{2+}/$S_2O_8^{-2}$eliminated its correlation with the subtype *blaPBP-2X.* However, solar/Fe^{2+}/$S_2O_8^{-2}$ had no effect on *blaPBP-1A* subtype and promoted a 2-fold increase in *blaPBP-1B* subtype (1.71E+14 in MWWTPE ppm *vs.* 2.81E+14 after treatment). Besides, eight ARGs linked to resistance to β-lactams (*OKP*, *OXA*, *PBP*, *SHV*) and vancomycin (*vanD*, *vanH*, *vanN*, and *vanR*) showed co-occurrence with WHO priority pathogens before and after solar/Fe^{2+}/$S_2O_8^{-2}$ treatment. Thus, confirming the need to develop new drugs to treat infections related to these multi-resistant pathogens. In addition, *Mycobacterium tuberculosis*, the agent responsible for human tuberculosis, was present in MWWTPE and showed co-relation with two different ARGs: *aac(2')-I*, (aminoglycoside resistance) and *mfpA* (resistance to quinolones) in all samples. This co-occurrence was detected even after >98% removal of these ARGs via solar/Fe^{2+}/$S_2O_8^{-2}$.

4 CONCLUSIONS

This study confirms the effect of PS-mediated solar photo-Fenton upon bacterial communities, priority pathogens, and ARGs present in MWWTPE. These results generate critical data for a deep understanding of wastewater resistome and towards appropriate control of AMR associated to MWWTPE discharge. Besides, metagenomic analyses used in this study to assess treatment effectiveness for ARB and ARG removals appear to be novel in the scientific literature.

Lowest species richness and diversity, and removal of main phyla present in MWWTPE (88% removal of *Proteobacteria*, 99% of *Bacteroidetes,* and complete removal of *Chlroflexi*) after PS-mediated solar photo-Fenton confirmed treatment efficiency for disinfection. Still, it is critical to investigate the enrichment of *Firmicutes* observed after this treatment. Besides that, solar/Fe^{2+}/$S_2O_8^{-2}$ reached nearly 44% removal of total ARGs. In addition, the treatment achieved a high clearance for subtypes *macB*, *sul1*, *aadA*, *arnA*, *tetA*, and *sul2* (> 50%), the most abundant genes in the MWWTPE.

Co-occurrence patterns showed strong correlation between priority pathogens and various ARG subtypes in MWWTPE. Although solar/Fe^{2+}/$S_2O_8^{-2}$ eliminated 63% of these correlations, some critical correlations (in example: correlation between critical priority carbapenem-resistant *Acinetobacter baumannii* and GES-14 subtype) persisted even after PS-mediated solar photo-Fenton. This highlights the need to develop new technologies for the removal of these organisms from MWWTPE as some subtypes possess an extended activity spectrum towards carbapenems. Solar/Fe^{2+}/$S_2O_8^{-2}$ also provided a reduction of nearly 99% for *Mycobacterium tuberculosis*, thus eliminating a threat to public health.

On the other hand, the combined oxidant system (solar/Fe^{2+}/$S_2O_8^{2-}$+H_2O_2) showed no significant difference in alpha diversity in comparison with MWWTPE (p-value > 0.1), thus being less efficient than solar/Fe^{2+}/$S_2O_8^{2-}$. Furthermore, its effect on the main phyla was not expressive, and a positive selection was detected for Firmicutes (> 8-fold), and Proteobacteria (> 2-fold). This result was not expected as distinct reactions co-occur in this system and should lead to a higher number of reactive radicals ($SO_4^{\bullet -}$

and HO•). Therefore, different oxidant: oxidant ratios may improve the effectiveness of the combined oxidants system. Nevertheless, this treatment completely fragmented sample DNA hindering WGS analysis.

CHAPTER IV - Tackling antimicrobial resistance via secondary wastewater post-treatment using enhanced solar photo Fenton at pilot scale[4]

[4]Chapter under review for submission

1 INTRODUCTION

Antimicrobial resistance (AMR) is a naturally occurring process enhanced by anthropogenic activities involving overuse and misuse of antimicrobials (KARKMAN *et al*., 2018; KHAN *et al*., 2020). The presence of a highly diverse human-commensal, environmentally relevant and pathogenic bacterial communities, many of which harbour ARGs, combined with potential selective factors (namely, recalcitrant natural or synthetic compounds, including antimicrobial residues and metabolites, heavy metals and biocides) contributes to the occurrence of co-selection processes towards commonly applied biological wastewater treatment processes (*i.e.* conventional activated sludge - CAS). These conditions create an environment potentially conducive to facilitate the development and proliferation of novel resistant strains through mechanisms like horizontal gene transfer (HGT) and other critical pathways of AMR spread (ALEKSHUN; LEVY, 2007; ANDERSSON; HUGHES, 2014; CHOW; GHALY; GILLINGS, 2021; EMAMALIPOUR *et al*., 2020; HERNANDO-AMADO *et al*., 2019; LARSSON; FLACH, 2022; LI *et al*., 2022; MANAIA *et al*., 2018; MICHAEL-KORDATOU; KARAOLIA; FATTA-KASSINOS, 2018; RIZZO *et al*., 2020; WELLINGTON *et al*., 2013). Thus, it has become increasingly evident that MWWTP plays a critical role in the emergence, persistence, and proliferation of ARB and ARGs. Indeed, final MWWTP effluent (MWWTPE) has the potential to disseminate AMR in the environment, posing risk to human health and a long-term threat to environmental ecosystems (HILLER *et al*., 2019b; MANAIA *et al*., 2018; MIŁOBEDZKA *et al*., 2022; NGUYEN *et al*., 2021; OSIŃSKA *et al*., 2020; RAZA *et al*., 2022; RIZZO *et al*., 2013, 2020; WANG *et al*., 2020b).

Conventional activated sludge (CAS) is amongst the main treatment technologies applied in MWWTP located in urbanized areas in Brazil and worldwide (RODRIGUES-SILVA; MARIA; AMORIM, 2022). The investigation of antimicrobial resistance profile in full-scale CAS plants indicates a limited capacity to reduce antimicrobial resistance to negligible levels, hence secondary effluent may represent a discharge of up to 10^{12} ARB/day or 10^{18} ARGs/day (MANAIA *et al*., 2016, 2018; RIZZO *et al*., 2020; VAZ-MOREIRA; NUNES; MANAIA, 2014). For instance, ARB removal via CAS treatment in a MWWTP in southeastern Brazil was limited to 1.1 logs unit (CFU mL^{-1}) with high prevalence of ampicillin, sulfadiazine, and amoxicillin-resistant bacteria. Besides,

63.6 % of the ARB isolates from CAS effluent expressed multi-drug resistance (MDR) phenotype (MACHADO *et al*., 2023) and ARGs removals were limited to 0.2-0.5 log, with highest removal rates below 1-2 log units (LEROY-FREITAS *et al*., 2022). These results reinforce the need for the application of a post-treatment stage to mitigate the release of ARB (*e.g.* MDR), and ARGs into the environment (HILLER *et al*., 2019a; KIRCHNER *et al*., 2020; MANAIA *et al*., 2016, 2018; MIŁOBEDZKA *et al*., 2022; RIZZO *et al*., 2020; WANG *et al*., 2020b).

In general, conventional disinfection technologies, namely chlorination, ozonation and high energy demand processes (*e.g*. UV processes), may be ineffective to eliminate ARB and ARGs from MWWTPE and promote the formation of hazardous byproducts (DIAS *et al*., 2022; GUO; YUAN; YANG, 2015; HOU *et al*., 2019; IAKOVIDES *et al*., 2019; JIN *et al*., 2020; LEROY-FREITAS *et al*., 2022; SOUSA *et al*., 2017; WANG *et al*., 2021a). The stressful conditions imposed by the operating conditions of these disinfection processes are responsible for damaging vital components (*i.e*. membranes, enzymes and DNA). However, it has been demonstrated that bacterial populations have the capability to survive these treatment processes by activating defense and repair mechanisms, thereby enabling the recovery of ARB and ARGs, ultimately promoting the persistence of a residual microbial community with increased resistance (DI CESARE *et al*., 2016; MANAIA *et al*., 2018; MICHAEL-KORDATOU; KARAOLIA; FATTA-KASSINOS, 2018; RIZZO *et al*., 2020). In contrast, the application of other disinfection technologies, such as photo-Fenton, has gained attention as a cost-effective method for disinfection in which oxidative radicals damage cell membranes and DNA thus promoting ARB and ARGs removals (GUO *et al*., 2020; LI *et al*., 2021; MICHAEL-KORDATOU; KARAOLIA; FATTA-KASSINOS, 2018; RIZZO, 2022; RIZZO *et al*., 2020). In addition, as sunlight may be used as an irradiation source during photo-Fenton, this technology becomes a promising sustainable alternative for post-treatment of MWWTPE in areas with high solar irradiance, such as tropical countries (Starling *et al*., 2021b). Bench-scale solar photo-Fenton has been proved effective for decreasing the resistome load in MWWTPE (VILELA *et al*., 2021a, 2021b).

Despite recent knowledge on the efficiency of solar photo-Fenton (solar/Fe^{2+}/H_2O_2) against ARB and ARG (GIANNAKIS *et al*., 2016a; MICHAEL-KORDATOU;

KARAOLIA; FATTA-KASSINOS, 2018; MIKLOS *et al*., 2018; RIZZO, 2022; RIZZO *et al*., 2019, 2020), innovative studies have investigated means for further improvement of this process by using alternative oxidants. In this direction, persulfate ($S_2O_8^{-2}$) has been proposed as a possible alternative (solar/Fe^{2+}/$S_2O_8^{-2}$) (Ike *et al*., 2018; Lee *et al*., 2020; Starling *et al*., 2021a; Vilela *et al*., 2022; Wacławek *et al*., 2017) or as a complimentary oxidant to hydrogen peroxide (H_2O_2) in a combined system (H_2O_2 + $S_2O_8^{-2}$) (Bararpour *et al*., 2018; Chu *et al*., 2011; Epold *et al*., 2015; Epold and Dulova, 2015; Kaur *et al*., 2020; Monteagudo *et al*., 2015; Qiu *et al*., 2022; Vilela *et al*., 2022; Wu *et al*., 2023). These alternatives rely on the fact that sulfate radical ($SO_4^{\bullet-}$) has a higher redox potential (2.5 − 3.1 V *vs.* 1.8–2.7 V) in addition to longer half-life time (30–40 μs *vs*. 20 ns) and higher selectivity compared to hydroxyl radical (HO•) (OH; DONG; LIM, 2016; ZHOU *et al*., 2020). Furthermore, sulfate radical may yield hydroxyl radical generation at neutral pH (ANIPSITAKIS; DIONYSIOU, 2004; WANG; WANG, 2018), and this is desirable for post-treatment of secondary effluent since the simultaneous action of oxidative radicals enhances disinfection as both have great potential to cause damage to cell constituents (CANDEIAS; STEENKEN, 2000; DAVIES, 1987; KUMAR; POTTIBOYINA; SEVILLA, 2011; MARNETT, 2002). The combination of these two oxidants (H_2O_2+$S_2O_8^{-2}$) might also be interesting considering that H_2O_2 may act as an additional activator of $S_2O_8^{-2}$ (HILLES *et al*., 2015), resulting in alternative routes for radical formation as shown in Eq. 1 (CRIMI; TAYLOR, 2007; MONTEAGUDO *et al*., 2015).

$$S_2O_8^{2-} + H_2O_2 \rightarrow 2SO_4^{\bullet-} + 2HO^{\bullet} \qquad \text{(IV.1)}$$

Monteagudo *et al*. (2015) demonstrated that oxidation using $S_2O_8^{-2}$ simultaneously activated by Fe^{2+}/H_2O_2 is a potential alternative for treatment of wastewater containing emerging contaminants (*i.c.* carbamazepine), due to elevated synergistic effect. Besides, MWWTPE treatment in the presence of both oxidants removed high-priority pathogens and intrinsically multi-drug resistance bacteria (Vilela *et al*., 2022). Despite successful results, treatment scale-up is currently one of the main challenges associated with the application of this process. Among solar reactors, the Compound Parabolic Collector (CPC) is a consolidated solution for the application of solar oxidative treatments. CPC design features enable the concentration of 100% of

incident sunlight (diffuse and direct irradiation), thus accelerating reactions. Besides, CPC modular design increases treatment capacity (volume) (GIANNAKIS *et al*., 2016b; MALATO *et al*., 2009; NAHIM-GRANADOS *et al*., 2020). However, as far as the authors know, there are no previous publications exploring simultaneous use of $S_2O_8^{-2}/H_2O_2$ in solar photo-Fenton at CPC reactor for ARB and ARGs removal from MWWTP secondary effluents.

In this context, the main goal of this work is to test and compare the efficiency of three solar photo-Fenton systems: (i) solar photo-Fenton (solar/Fe^{2+}/H_2O_2), (ii) PS mediated solar photo-Fenton (solar/$Fe^{2+}/S_2O_8^{-2}$), and (iii) the combined treatment (solar/Fe^{2+}/H_2O_2+$S_2O_8^{-2}$), as post-treatment of MWWTPE according to their removal of ARB and ARGs at pilot scale in a CPC reactor at circumneutral pH.

2 MATERIAL AND METHODS

2.1 Sampling

WWTPE was sampled in the output of a secondary settling tank from a CAS system in a MWWTP located in Belo Horizonte-MG (Brazil), which receives wastewater from 1.5 million inhabitants (290 m^3 d^{-1}), including hospitals and industries. MWWTPE physicochemical characterization (Table IV.1) was performed as according to APHA (2017).

Table IV.1 - Physicochemical and microbiological characterization of Municipal Wastewater Treatment Plants effluent (MWWTPE) sampled in the output of a secondary settling tank from a conventional activated sludge (CAS) system in a MWWTP located in Belo Horizonte (Brazil)

Parameter	Unit	MWWTPE sample			Reference
		09/07	16/07	23/07	
Temperature	°C	26	24	22.4	APHA 2550
pH	-	7.2	7.2	6.9	APHA 4500 B
ORP	mV	235.3	227.3	304.3	APHA 2580
OD	mg L^{-1}	5.72	5.85	5.01	APHA 4500 G
Conductivity	µS cm^{-1}	555	556	604	APHA 2510
Turbidity	NTU	33.4	34.7	37.5	APHA 2130 B
Alkalinity	mg$CaCO_3$ L^{-1}	208	211	143	APHA 2320 B
COD	mgO_2 L^{-1}	143	150	275	APHA 5220 D
TS	mg L^{-1}	328	332	363	APHA 2540 B
TDS	mg L^{-1}	253	260	280	
TSS	mg L^{-1}	75	78	83	
Total Coliforms	MPN 100mL^{-1}	1.41×10^6	1.12×10^6	1.99×10^6	APHA 9223B
Escherichia coli	MPN 100mL^{-1}	1.21×10^5	8.99×10^4	9.96×10^4	
THB	CFU mL^{-1}	8.70×10^3	7.35×10^3	3.60×10^4	APHA 9215
ARB	CFU mL^{-1}	1.74×10^3	8.19×10^2	3.80×10^3	

ORP = redox potential; OD = Dissolved oxygen; COD = Chemical Oxygen Demand; TS = Total Solids; TDS = Total Dissolved Solids; TSS = Total Suspended Solids; THB = Total Heterotrophic Bacteria; ARB = Antimicrobial-resistant bacteria.

2.2 Experimental set-up

Solar photo-Fenton treatment of MWWTPE was conducted in batch in a Compound Parabolic Concentrator (CPC) pilot scale reactor designed according to Malato et al. (2009). The CPC reactor contained six borosilicate tubes (Schott-Duran type 3.3) totaling 2.1 m^2 of irradiated area, and three recirculation tanks with a maximum volume of 50 L. The reactor was segregated into three independent systems (two tubes each; 15 L of total volume) to allow for the application of all three treatment conditions simultaneously (under the same natural solar irradiation): solar/Fe^{2+}/H_2O_2, solar/Fe^{2+}/$S_2O_8^{-2}$, and solar/Fe^{2+}/ H_2O_2+$S_2O_8^{-2}$. Reactor inclination corresponded to

the latitude of Belo Horizonte/MG, Brazil (20º), thus enabling the concentration of total incident irradiation (direct and diffuse). A global radiometer (Kipp and Zonnen CMP10) connected to a data logger (METEON) was coupled to the CPC, so that incident irradiation (W m^{-2}) was measured during treatment (every 5 min). Accumulated UV radiation (Q_{UV}) is quantified (kJ L^{-1}), according to Equation IV.2 (MALATO et al., 2009).

$$Q_{UV,n} = Q_{UV,n-1} + \Delta t_n \overline{UV}_{G,n} \frac{A_r}{V_t} \quad \text{(IV.2)}$$

where $Q_{UV,n}$ is the total accumulated UV radiation (kJ L^{-1}), Δt_n represents the time interval (s), $UV_{G,n}$ is the average radiation (W m^{-2}), A_r is the irradiated area (0.7 m^2; two collectors), and V_t is the volume of treated wastewater (15 L).

2.3 Experimental conditions

Proposed treatments (solar/Fe^{2+}/H_2O_2, solar/Fe^{2+}/$S_2O_8^{-2}$, and solar/Fe^{2+}/ H_2O_2+$S_2O_8^{-2}$) were carried out in July (winter) and performed with MWWTPE collected on three consecutive days. Reactions were performed simultaneously between 11 am and 3 pm (240 min of reaction) with average accumulated radiation of 10.46 KJ L^{-1} (σ = 0.99 KJ L^{-1}, n = 6 days), so that incident natural solar irradiation would be the same for all tested conditions (Table IV.2). Technical replicates were also performed using the same effluent on two consecutive days. pH and temperature were constantly monitored during treatment.

Table IV.2 – Concentration of oxidants (H_2O_2 and/or $S_2O_8^{2-}$) and iron (Fe^{2+}) applied in solar photo-Fenton treatments tested in this study including times corresponding to intermittent additions of iron

AOP	Oxidant	Fe^{2+}
Solar photo-Fenton (solar/Fe^{2+}/H_2O_2)	50 mg L^{-1} H_2O_2	Time 0 → 15 mg L^{-1} Time 5 → 5 mg L^{-1} Time 10 → 5 mg L^{-1} Time 15 → 5 mg L^{-1} Total → 30 mg L^{-1} of Fe^{2+} (0.5 mM)
PS mediated solar photo-Fenton (solar/Fe^{2+}/$S_2O_8^{-2}$)	282.27 mg L^{-1} $S_2O_8^{2-}$	
Combined oxidant system (solar/Fe^{2+}/ H_2O_2+$S_2O_8^{-2}$)	25 mg L^{-1} H_2O_2 + 141.135 mg L^{-1} $S_2O_8^{2-}$	

H_2O_2 and $S_2O_8^{-2}$ concentrations (1.5 mM of each individually or 0.75 mM each simultaneously) used in treatments were previously defined in works performed in bench scale (VILELA *et al*., 2021b, 2022a). Reactions were performed at initial neutral pH using intermittent iron additions (ferrous sulfate solution: 25 g L^{-1}). This strategy

was adopted according to previous works (VILELA *et al*., 2021b, 2022a). The persulfate and iron solutions were freshly prepared before being used to minimize variations in concentration caused by self-decomposition.

Samples were withdrawn during treatments for quantification of residual $S_2O_8^{2-}$ (LIANG *et al*., 2008) and H_2O_2 (NOGUEIRA; OLIVEIRA; PATERLINI, 2005). For samples taken for the analyses of iron ions (Fe^{2+} and Fe^{3+}) (APHA, 2017; ISO, 1988) and microbiological parameters (Total Coliforms, *Escherichia coli*, Total Heterotrophic Bacteria, ARB and ARG), residual H_2O_2 and/or $S_2O_8^{2-}$ were removed by adding catalase enzyme (460 mg L^{-1} in phosphate buffer; 0.1:1.9, v/v) (POOLE, 2004) or ascorbic acid (0.1:1, v/v) (OLMEZ-HANCI; ARSLAN-ALATON; DURSUN, 2014), respectively. Samples were filtered through 0.45 µm PVDF filter prior to the quantification of iron ions. pH was re-adjusted to neutral values prior to microbiological analysis when necessary.

Total coliforms and *E. coli* were used as biological indicators of wastewater treatment efficiency. These parameters were measured by QuantiTray technique with Colilert media (IDEXX/APHA 9223B) following the manufacturer's instruction. The abundance and prevalence of viable and culturable resistant microorganisms (*i.e.* ARB) was achieved by the spread plate method followed by microbial identification using Matrix-assisted laser desorption ionization-time of flight (MALDI-TOF) (section 2.4). ARG analyses were conducted by Real-Time Polymerase Chain Reaction (qPCR) after sample preparation for molecular biology analyses.

2.4 Culture-based analysis for enumeration and identification of ARB

Colony-forming units (CFUs) of total heterotrophic bacteria (THB) and ARB were measured with a standard plate dilution technique on plate count agar (PCA, KASVI) alone and supplemented with the target antibiotics (Table IV.3), respectively. These drugs were chosen as they correspond to different classes of antimicrobial agents that are strongly associated with AMR in MWWTPE (VILELA *et al*., 2021b, 2022a). For ARB culture, the working concentrations of each antibiotic (Table IV.3) in supplemented media were higher than the minimum inhibitory concentrations for resistant bacteria according to Clinical and Laboratory Standards Institute (CLSI)

guidelines (CLSI, 2020). Plating was carried out by sowing on surface 100 µl-aliquots of effluents and its 10^{-1} and 10^{-2} dilutions, in triplicates. Culture plates were incubated under aerobiosis, at 37 ± 1°C for 48 h before CFUs enumeration.

The frequency of ARB occurrence in samples was calculated by dividing its mean count by THB count. This yielded the concentration of ARB expressed as colony forming units per milliliter (CFU mL^{-1}). The frequencies of ARB resistant among the MWWTPE was estimated according to Equation IV.3. Removal and the log removal (Log Removal Value – LRV) of ARB was calculated using Equation IV.4 and Equation IV.5, respectively.

$$\text{Frequencies of ARB} = \frac{\text{CFU mL}^{-1} \text{ in medium with antibiotic}}{\text{CFU mL}^{-1} \text{ in medium without antibiotic}} \quad \text{(IV.3)}$$

$$\text{ARB removal} = C_t/C_0 \quad \text{(IV.4)}$$

$$\text{Log removal} = \text{Log}_{10}C_t/C_0 \quad \text{(IV.5)}$$

Where C_0 is the ARB concentration in MWWTPE, and C_t is the ARB concentration after treatment at time t. Data analysis graphing was conducted by OriginPro 2022 software.

Table IV.3 – Antimicrobial agents added to agar medium in the spread plate method for the analyses of cultivable ARB in samples collected before, during and after proposed treatments via solar photo-Fenton

Class		Target antibiotic	Concentration in the agar medium
β-lactams	1st generation cephalosporin	Cefalexin (LEX)	1 mg L^{-1}
	Aminopenicillin	Amoxicillin (AMX)	32 mg L^{-1}
Fluoroquinolones	-	Ciprofloxacin (CIP)	4 mg L^{-1}
Macrolides	-	Azithromycin (AZM)	1000 mg L^{-1}
Sulfonamides	-	Co-trimoxazole (SXT)	350 mg L^{-1}

2.4.1 Isolation and identification of ARB and THB

After cultivation of THB and ARB, and CFU enumeration, colonies showing different morphotypes according to visual inspection were selected from each plate. For plates with more than one morphotype, three colonies of each were subculture. For plates with only one morphotype, three colonies were replicated. Strains were stored in saline solution supplemented with glycerin (20%) at -20°C.

For microbial identification, strains were replicated in brain-heart infusion (BHI) broth and incubated at 37 ± 1°C for up to 24 h for subsequent culture in PCA medium (37 ±

1°C for 24 h). Strains that grew after subculturing were collected with a swab and immediately placed into Stuart medium for transportation at room temperature to a partner laboratory. Samples were then cultured on Chromagar Orientation (Difco) at 35 ± 2°C up to 18-24 hours, under aerobiosis. Matrix-assisted laser desorption ionization-time of flight (MALDI-TOF) (Microflex LT, Bruker Daltonics, Bremen, Germany) and the Biotyper software (version 4.1) were used to obtain the mass spectra and identify isolates, following the manufacturer's instructions. For secure identification up to the genus and probable species levels, threshold score values were defined as 2.000 to 2.299 and > 2.300, respectively.

2.5 Quantification of ARGs

2.5.1 Sample pretreatment and DNA extraction

Samples (0.5 L) were concentrated by filtered through a 0.22 µm mixed cellulose esters (MCE) membrane. Total DNA extraction was performed using FastDNA® Spin Kit for Soil (MP Biomedicals) according to the protocol of the manufacturer. DNA concentration and purity were measured by a NanoDrop UV–Vis spectrophotometer (Thermo Fisher Scientific). Structural integrity was determined by 1% agarose gel electrophoresis.

2.5.2 Primer design

The selection of primers used for ARG quantification was based on ARGs previously detected in samples form the same MWWTPE via Whole Genome Sequencing analysis (VILELA *et al*., 2021b). The detected ARGs included those conferring resistance to aminoglycosides (*aadA*1, *aph*(6) and *str*A), β-lactams (*bla*GES and *bla*IMP-16), fluoroquinolones (*qnr*S2), macrolides (*mph*(E), *msr*(E) and *erm*(F)), sulphonamides (*sul*1 and *sul*2), and tetracycline (*tet*C, *tet*39 and *tet*X). ARG copies was quantified using SYBR-Green based qPCR. Primers' sequences are listed in Table IV.4. Reference sequences for selected target genes were assembled using the Antibiotic Resistance Gene-ANNOTation (GUPTA et al., 2014). Primer sets were designed for individual gene targets using the RDP EcoFunPrimer design tool (https://github.com/rdpstaff/EcoFunPrimer).

Table IV.4 - Primers and conditions used for PCR and ARG quantification in MWWTPE and samples collected during and after proposed treatments via solar photo-Fenton

Target ARG	Primer	Sequence (5'-3')	Annealing Temperature (°C)	Amplicon Size (bp)
*aad*A1	aadA1-FW aadA1-RV	CAGGTATCTTCGAGCCAGCC GCGGGACAACGTAAGCACTA	60	221
*aph*6	aph(6)-FW aph(6)-RV	GGCTGGCTGGTGATAGATCC GCGTTGCTCCTCTTCTCCAT	60	237
bla$_{GES}$	blaGES-FW blaGES-RV	TGAGAAGCTAGAGCGCGAAA AGCCACAGTACGTGCCATAG	60	475
bla$_{IMP}$	blaIMP-16-FW blaIMP-16-RV	ACGTAGTGGTTTGGTTGCCT CCTTTAACAGCCTGCTCCCA	60	220
*erm*F	erm(F) -FW erm(F) -RV	CCACCGCCAACTGTCAAATC TTTCAGGGACAACTTCCAGCA	60	274
mph(E)	mph(E) -FW mph(E) -RV	AGCGATTGATTTTGCTGGGC CCCAACTGAGCTTTTGCTCC	60	210
msr(E)	msr(E) -FW msr(E) -RV	ATGCTGGGCGTGATGTTTTG ACTTGTTGGGAAAATGCGGC	60	313
*qnr*S2	qnrS2-FW qnrS2-RW	TTTCGACGTGCTAACTTGCG TTTGCTCGGGAAAAGTTGGC	60	212
*str*A	strA-FW strA-RV	TACCGGACGAGGACAAGAGT CCCAGTTCTCTTCGGCGTTA	60	246
*sul*1	sul1-FW sul1-RV	CACCGAGACCAATAGCGGAA AGGCTGGTGGTTATGCACTC	60	267
*sul*2	sul2-FW sul2-RV	ACATTGCGGCGTTCTTTGAC ATGAAGTCAGCTCCACCTGC	60	292
*tet*C	tetC-FW tetC-RV	GGAGTCGCATAAGGGAGAGC GACCAGTGACGAAGGCTTGA	60	260
*tet*X	tetX-FW tetX-RV	ATGGAAACCGGCTAATGGCA GGTAATGGGCGCTTGCTTTT	60	286
*tet*39	tet39-FW tet39-RV	GCACCTATCCTTGGAGCGTT AAAGCAGCAGCAAAGAACGG	60	326

*FW = Forward primer, RV = Reverse primer.

2.5.3 Detection and quantification of ARGs

Conventional PCR assays were conducted for the detection of target ARGs in MWWTPE samples prior and after proposed treatments using a Thermal Cycler (ThermoFisher Scientific) for PCR amplification. PCR products were analyzed using electrophoresis on a 1.0% agarose gel in TAE buffer. qPCR analyses were performed on a Light Cycler 480 Real-Time PCR System (ThermoFisher Scientific) for all targets described in Table IV.4, except for *qnr*S2 that was not detected in samples after conventional PCR. For relative quantification of ARGs copy number in samples, a standard curve was built using MWWTPE as a calibrator. Relative concentration of ARGs was normalized by the 16S rRNA-encoding gene used as an internal control. Reaction mixture consisted of: 1µL of extracted DNA (concentration 10 ng μL^{-1}), 5µL of SYBR Premix Ex Taq (Promega, EUA), 1.0 µL of the respective forward and reverse primers, 0.1 µL of dye, and 2.9µL of DNA-free water (Sigma-Aldrich). The qPCR

regime is a two-step cycle (95 °C for denature and 60 °C for primer annealing and elongation). Melting curves were obtained to confirm the amplification specificity. Samples and negative control (NTC) were analyzed in duplicates, while standard curve reactions were analyzed in triplicates.

2.6 Statistical analysis

Statistical analysis was performed using OriginPro 2022 software. One-Way analysis of variation (ANOVA), t-test, and significance test were performed at a significant 99.9% confidence level ($p < 0.01$). The FDR method adjusted the P-value to reduce false-positive results (BENJAMINI; HOCHBERG, 1995).

3 RESULTS

3.1 Bacteria enumeration and diversity

Regarding biological indicators of wastewater treatment efficiency, THB counts ranged from 7.4 x 10^3 to 3.6 × 10^4 CFU mL^{-1}, Total Coliforms from 1.1 to 2.60 × 10^6 MPN $100mL^{-1}$, and *E. coli* from 8.2 x 10^4 to 1.3 × 10^5 MPN $100mL^{-1}$. All solar photo-Fenton treatments reached >99% removal of biological indicators (Figure IV.1).

Figure IV.1 - Decay of Total Coliform (a) and *E. coli* (b), in MWWTPE solar photo-Fenton treatments: solar/Fe^{2+}/H_2O_2 (Fe^{2+} = 0.5 mM; H_2O_2 = 1.5 mM), Solar/Fe^{2+}/$S_2O_8^{2-}$ (Fe^{2+} = 0.5 mM; $S_2O_8^{2-}$ = 1.5 mM), and solar/Fe^{2+}/H_2O_2+$S_2O_8^{2-}$ (Fe^{2+} = 0.5 mM; H_2O_2 = 0.75 mM + $S_2O_8^{2-}$ = 0.75mM) conducted at initial neutral pH in CPC reactor as according to accumulated irradiation (30 minutes = 1.46 KJ L^-; 1 hour = 2.99 KJ L^{-1}; 2 hours = 6.04 KJ L^{-1}; 3 hours = 8.51 KJ L^{-1}); 4 hours = 10.41 KJ L^{-1})

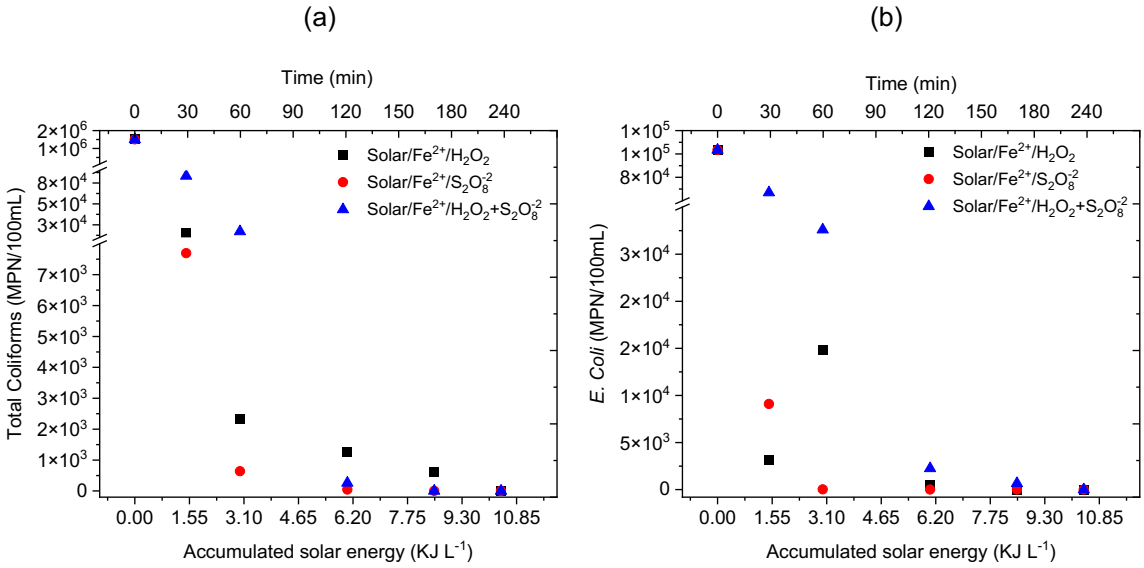

For Total Coliforms, solar/Fe^{2+}/$S_2O_8^{2-}$ achieved 4.5 log removal within 6.04 KJ L^{-1} (120 min) *vs.* 3.8 log removal for the combined treatment, within 8.51 KJ L^{-1} (180 min) there was no more Total Coliforms growth for both treatments. While solar/Fe^{2+}/H_2O_2 reached 3.4 log removal within 8.51 KJ L^{-1} (180 min), and no grow within 10.41 KJ L^{-1} (240 min). Concerning *E. coli* removal, solar/Fe^{2+}/$S_2O_8^{2-}$ reached 3.6 log removal within 2.99 KJ L^{-1} (60 min), while the other treatments required 8.51 KJ L^{-1} (180 min) to achieved 4.0 and 2.2 log removal for solar/Fe^{2+}/H_2O_2 and solar/Fe^{2+}/H_2O_2+$S_2O_8^{2-}$, respectively. For TBH removal, solar photo-Fenton treatments performed as follows: solar/Fe^{2+}/H_2O_2 (1.5 log removal, 97% removal efficiency) < solar/Fe^{2+}/$S_2O_8^{2-}$ (2.3 log

removal, 99% removal efficiency) < solar/Fe^{2+}/H_2O_2+$S_2O_8^{2-}$ (2.8 log removal, >99% removal) within 10.41 KJ L^{-1} (240 min) (data not shown).

ARB counts in MWWTPE ranged from 2.2 x 10^1 to 1.6 × 10^4 CFU mL^{-1}. The following calculated ARB frequencies were detected considering all THB colonies cultivated from MWWTPE: 33±5% of ARB resistant to LEX > 26±7% to AMZ > 16±1% to AMX > 4±2% to CIP > 3±1% to SXT. Concerning ARB removal, solar photo-Fenton treatments were efficient for the removal of most of cultivable ARB (Figure IV.2). Solar/Fe^{2+}/$S_2O_8^{2-}$ achieved removal efficiencies greater than 90% after 2.99 KJ L^{-1} (60 min) for almost all ARB targeted (Figure IV.2), with average of 2.8 log removal, though SXT-resistant bacteria showed the highest resistance to this treatment (average 1.7 log removal).

Figure IV.2 - Removal of ARB (C/C_0) resistant to antibiotics: cefalexin (LEX), amoxicillin (AMX), ciprofloxacin (CIP), azithromycin (AZM), and co-trimoxazole (SXT), during solar/Fe^{2+}/H_2O_2 (a), solar/Fe^{2+}/$S_2O_8^{2-}$(b), and solar/Fe^{2+}/H_2O_2+$S_2O_8^{2-}$(c) as according to accumulated irradiation (30 minutes = 1.46 KJ L^{-1}; 1 hour = 2.99 KJ L^{-1}; 2 hours = 6.04 KJ L^{-1}; 3 hours = 8.51 KJ L^{-1}; 4 hours = 10.41 KJ L^{-1})

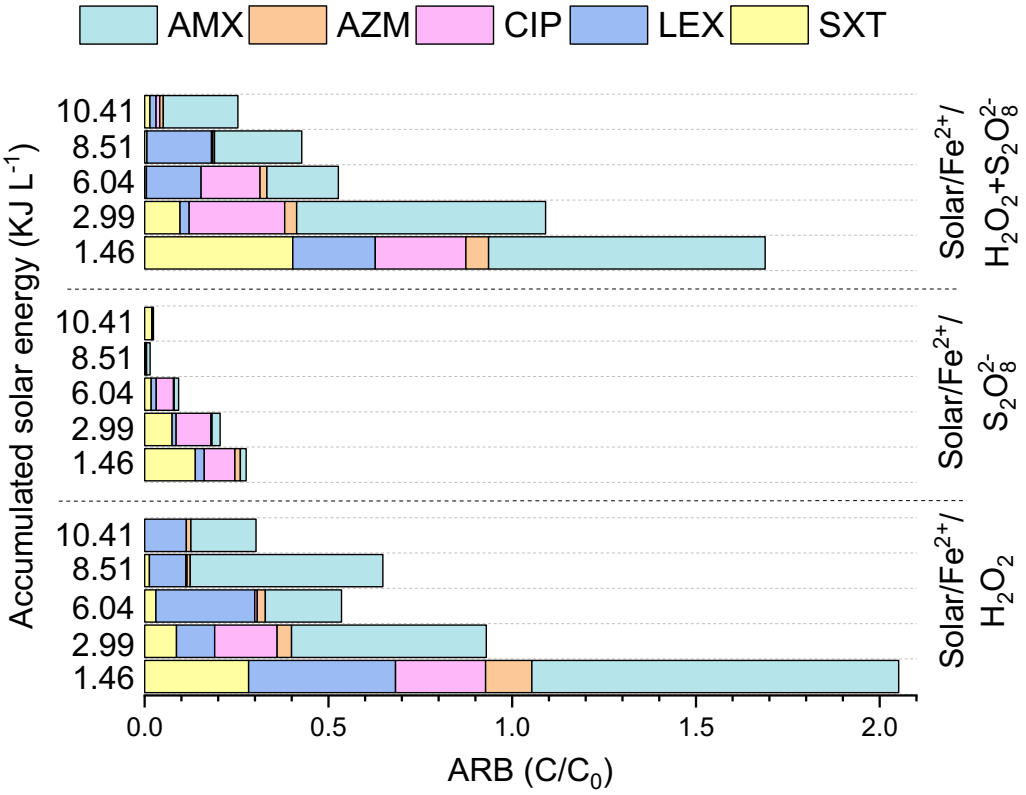

Solar/Fe^{2+}/H_2O_2 and solar/Fe^{2+}/H_2O_2+$S_2O_8^{2-}$ showed similar behavior, with an average of 1.6 log removal. However, solar/Fe^{2+}/H_2O_2 did not show great removal of AMX (0.4

average log removal) and LEX-resistant ARB (0.8 average log removal), but averages log removals were greater than 2.0 for SXT, CIP and AZM-resistant ARB. Solar/Fe^{2+}/H_2O_2+$S_2O_8^{2-}$ did not show great removal of AMX-resistant ARB (average 0.5 log removal), but 1.6 log removal considering the average removal for all ARB. Interestingly, these treatments achieved this same removal efficiency for an accumulated radiation of 6.04 KJ L^{-1} (120 min). Despite that, increased counts of LEX-resistant ARB were observed after this treatment.

3.2 Bacteria identification

A total of 51 strains showing different morphologies were observed and isolated from colonies cultivated from MWWTPE and treated samples. Thirteen of these strains could be securely identified up to the genus level with indication of most probable species. For five of these strains a MALDI-TOF score value > 2.3 was obtained, thus indicating high certainty of probable species identification (Table IV.5). Thus, several species of proteobacteria were identified in MWWTPE, such as *Klebsiella pneumoniae*, *Stenotrophomonas maltophila*, and *Serratia marcescens*. Within the *Firmicutes* phylum, representants of *Bacillus* spp. were identified, in addition to WHO priority *Enterococcus faecium*. However, most isolates were recovered from selective pressures due to antimicrobials against which they are intrinsically resistant, except for *Bacillus* ssp., *Enterobacter* ssp., *E. coli, K. pneumoniae, Raoultella ornithinolytica, S. marcescens*, and *S. maltophilia* (EUCAST, 2023). This is a significant result since these species have been commonly associated with multidrug resistance *(SENG et al*., 2016; WANG *et al*., 2021b).

Data regarding identified strains recovered from raw effluent and after treatments are shown in Table IV.5. Most strains recovered were gram-negative bacilli. Except for *Aeromonas caviae* and *Pseudomonas putida* strains, bacterial species recovered in selected pressures employed suggested the presence of acquired resistance determinants. Noteworthy, *E. coli* isolates were recovered from cultures supplemented with all antibiotics used, while *K. pneumoniae, E. faecium, S. marcescens,* and *S. maltophilia* grew under CIP and STX selective pressure. In addition, *K. pneumoniae* were recovered from cultures supplemented with LEX (BrCAST, 2023). Despite having expected resistance phenotype to most antibiotics from the macrolide class due to low

permeability of these antibiotics through their membrane, some *Enterobacteriaceae* are susceptible to azithromycin as this antibiotic is more permeable (FANNER; LI; HANCOCK, 1992; GOMES *et al*., 2017). For instance, *Enterobacter* ssp. and *E. coli* isolated from MWWTPE, and samples treated by solar photo-Fenton (solar/Fe^{2+}/H_2O_2) were recovered from cultures supplemented with AZM.

Despite the effective removal of most ARB by proposed treatments, the persistence of some particular strains, even after 10.41 KJ L^{-1} accumulated irradiation (240 min) of treatment is concerning. For instance, after solar/Fe^{2+}/H_2O_2 gram-negative strains identified as *K. pneumoniae, S. marcescens* and *S. maltophilia*, and gram-positive *E. faecium* grew under some selective pressures but the same was not observed in MWWTPE. The same was observed for *K. pneumoniae* and *E. faecium* after solar/Fe^{2+}/$S_2O_8^{2-}$, and after solar/Fe^{2+}/ H_2O_2+$S_2O_8^{2-}$, with the addition of the *Bacillus subtilis* strain.

Table IV.5 - Identification of acquired resistance phenotype to amoxicillin (AMX), azithromycin (AZM), cefalexin (LEX), ciprofloxacin (CIP) in MWWTPE and samples taken within 30 minutes (1.46 KJ L^{-1}), 1 hour (2.99 KJ L^{-1}), 2 hours (6.04 KJ L^{-1}), 3 hours (8.51 KJ L^{-1}), and 4 hours (10.41 KJ L^{-1}) of solar/Fe^{2+}/H_2O_2, solar/Fe^{2+}/$S_2O_8^{2-}$, and solar/Fe^{2+}/H_2O_2+$S_2O_8^{2-}$ treatments. Color intensity[a] indicates the number of antibiotics tested to which ARB showed resistance. "X" indicates growth of strains with intrinsic resistance to target antibiotics

Treatment	Accumulated solar energy (KJ L^{-1})	*Aeromonas caviae*[b]	*Bacillus cereus*[b]	*Bacillus subtilis*[b]	*Enterobacter ssp.*[b]	*Enterococcus faecium*[c]	*Escherichia coli*[c]	*Klebsiella pneumoniae*[c]	*Pseudomonas putida*[b]	*Raoultella ornithinolytica*[b]	*Serratia marcescens*[c]	*Stenotrophomonas maltophilia*[c]
MWWTPE	0.00	X	X	X	X	X	AMX | AZM LEX | CIP	X	X	LEX	X	X
Solar/ Fe^{2+}/H_2O_2	1.46		CIP	CIP	CIP	X	AMX | AZM LEX | CIP	LEX | CIP	X		SXT	CIP
	2.99		X	X	CIP	X	AZM	LEX | CIP | SXT	X		SXT	CIP | SXT
	6.04		X	X	CIP	SXT	LEX | CIP	X	X	X	X	CIP | SXT
	8.51		CIP	X	AZM	SXT	AZM | SXT	X	X	X	X	CIP | SXT
	10.41		X	X		SXT		CIP | SXT	X		SXT	CIP | SXT
Solar/ Fe^{2+}/$S_2O_8^{2-}$	1.46		X	X	X	CIP | SXT		LEX | CIP | SXT	X		CIP | SXT	X
	2.99		X	X	X	X		LEX | CIP	X		CIP | SXT	CIP SXT
	6.04		X	X		SXT		LEX | CIP | SXT	X		CIP | SXT	X
	8.51					X		LEX | SXT	X		SXT	
	10.41					SXT		SXT			X	
Solar/Fe^{2+}/ H_2O_2+$S_2O_8^{2-}$	1.46		X	X	X	AMX		X	X	X	SXT	CIP
	2.99		CIP	X	X	CIP | SXT		LEX | CIP	X		CIP | SXT	SXT
	6.04		X			X		X		X		X
	8.51		X	X	X	X		CIP	X	LEX		X
	10.41		X	CIP	X	SXT		LEX	X	LEX		X

[a] 0 1 2 3 4 5

[b]Secure genus identification, probable species identification

[c]Highly probable species identification

3.3 Diversity and abundance of ARGs

The diversity of ARGs evaluated from the number of each target in MWWTPE was *erm*F (13%) > *sul*2 (12%) > *str*A (12%) > *bla*$_{IMP}$ (10%) > *mph*E (10%) > *sul*1 (8%) > *aph*6 (7%) > *msr*E (6%) > *tet*C (5%) > *tet*X (5%) > *tet*39 (4%) > *aad*A1 (4%) > *bla*$_{GES}$ (4%). Therefore, the MWWTPE presents a majority of genes encoding sulphonamide and macrolide resistance, with no significant difference between then relative abundance ($p < 0.01$). Genes encoding resistance to aminoglycoside, β-lactam and tetracycline were also representative in samples. Figure IV.3 shows relative abundance of all tested ARGs after solar photo-Fenton treatments.

Figure IV.3 - Heatmap of relative abundance of ARGs (%) in samples obtained after solar photo-Fenton (Solar/Fe^{2+}/H_2O_2), PS-mediated solar photo-Fenton (Solar/Fe^{2+}/$S_2O_8^{2-}$), and combined oxidant system (Solar/Fe^{2+}/H_2O_2+$S_2O_8^{2-}$) within 30 minutes (1.46 KJ L^{-1}), 1 hour (2.99 KJ L^{-1}), 2 hours (6.04 KJ L^{-1}), 3 hours (8.51 KJ L^{-1}), and 4 hours (10.41 KJ L^{-1}) considering ARG detection in MWWTPE

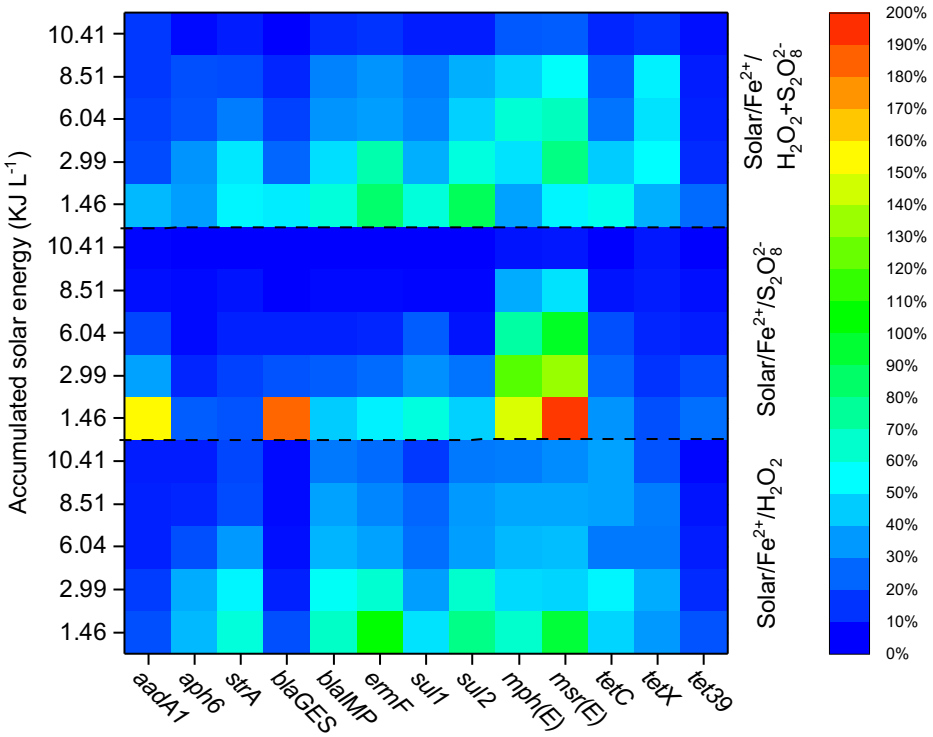

Among treatments employed, solar photo-Fenton decreased the copy number of most ARGs targeted. The Solar/Fe^{2+}/$S_2O_8^{2-}$ combination after 10.41 KJ L^{-1} decreased the load of twelve ARGs by 90%. Average log removal for all ARGs was equivalent to 1.1 for this treatment. However, enrichment of some ARGs (*i.e.* *aad*A1, *bla*GES, *erm*F, *mph*E, and *msr*E) was also observed (Figure IV.3). Solar/Fe^{2+}/H_2O_2 and

solar/Fe^{2+}/H_2O_2+$S_2O_8^{2-}$ treatments were not as effective for removing targeted ARGs, reaching an average log removal of 0.5 and 0.4, respectively. In addition, the enrichment of ARGs could also be observed for these approaches, especially in the beginning of treatment (1.46 to 2.99 KJ L^{-1}) (Figure IV.3).

Figure IV.4 shows the relative abundance of ARGs in MWWTPE and samples obtained after solar/Fe^{2+}/H_2O_2, solar/Fe^{2+}/$S_2O_8^{2-}$, and solar/Fe^{2+}/H_2O_2+$S_2O_8^{2-}$. Note that the difference in letters denotes significant difference between the respectively ARGs concentrations ($p < 0.01$) according to the Tukey test. The letters above represent the statistical analysis between the MWWTPE and the three treatments simultaneously. While the letters below represent the statistical analysis between the MWWTPE and each of the treatments separately

Figure IV.4 - Relative abundance of (a) *aad*A1, (b) *aph*6 and (c) *str*A, associated with streptomycin resistance (aminoglycoside); (d) *bla*$_{GES}$, associated with carbapenem resistance (β-lactam), and (e) *bla*$_{IMP}$, associated with β-lactam resistance; (f) *mph*E, (g) *msr*E and (h) *erm*F, macrolide resistance gene; (i) *sul*1 and (j) *sul*2, sulphonamide resistance gene; (k) *tet*C, (l) *tet*39 and (m) *tet*X, tetracycline resistance gene in MWWTPE and samples obtained after solar/Fe^{2+}/H_2O_2, solar/Fe^{2+}/$S_2O_8^{2-}$, and solar/Fe^{2+}/H_2O_2+$S_2O_8^{2-}$ within 30 minutes (1.46 KJ L^{-1}), 1 hour (2.99 KJ L^{-1}), 2 hours (6.04 KJ L^{-1}), 3 hours (8.51 KJ L^{-1}), and 4 hours (10.41 KJ L^{-1})

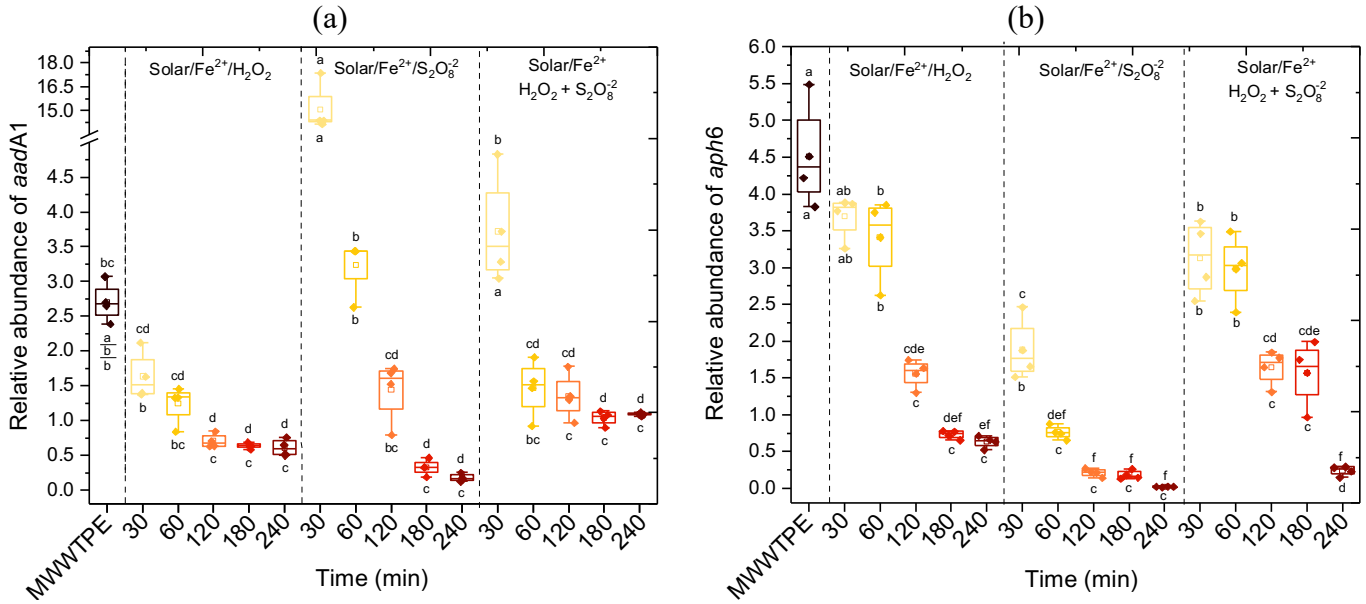

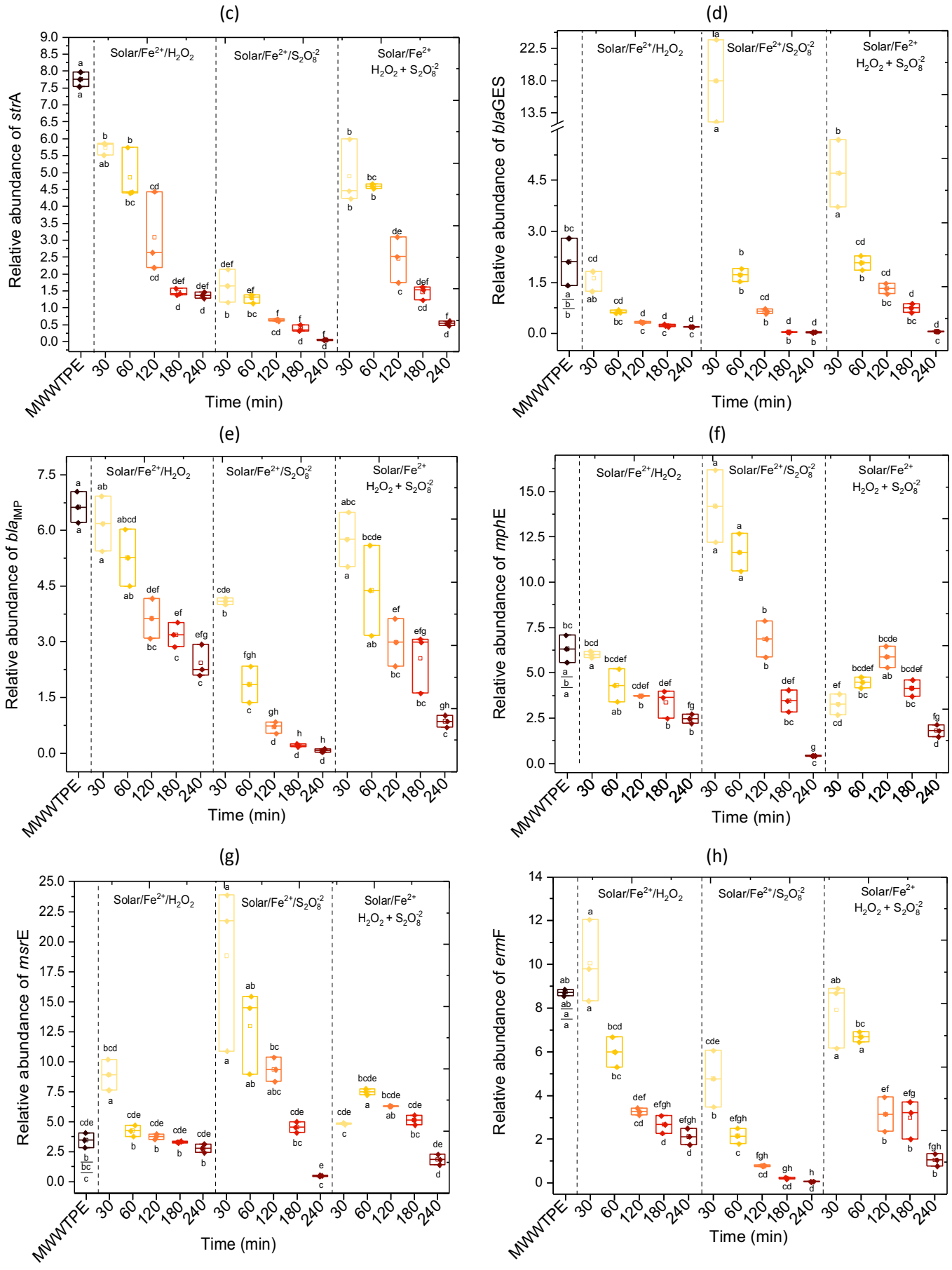
(c)
Relative abundance of strA
Solar/Fe2+/H2O2
Solar/Fe2+/S2O8-2
Solar/Fe2+ H2O2 + S2O8-2
MWWTPE
Time (min)
(d)
Relative abundance of blaGES
(e)
Relative abundance of blaIMP
(f)
Relative abundance of mphE
(g)
Relative abundance of msrE
(h)
Relative abundance of ermF

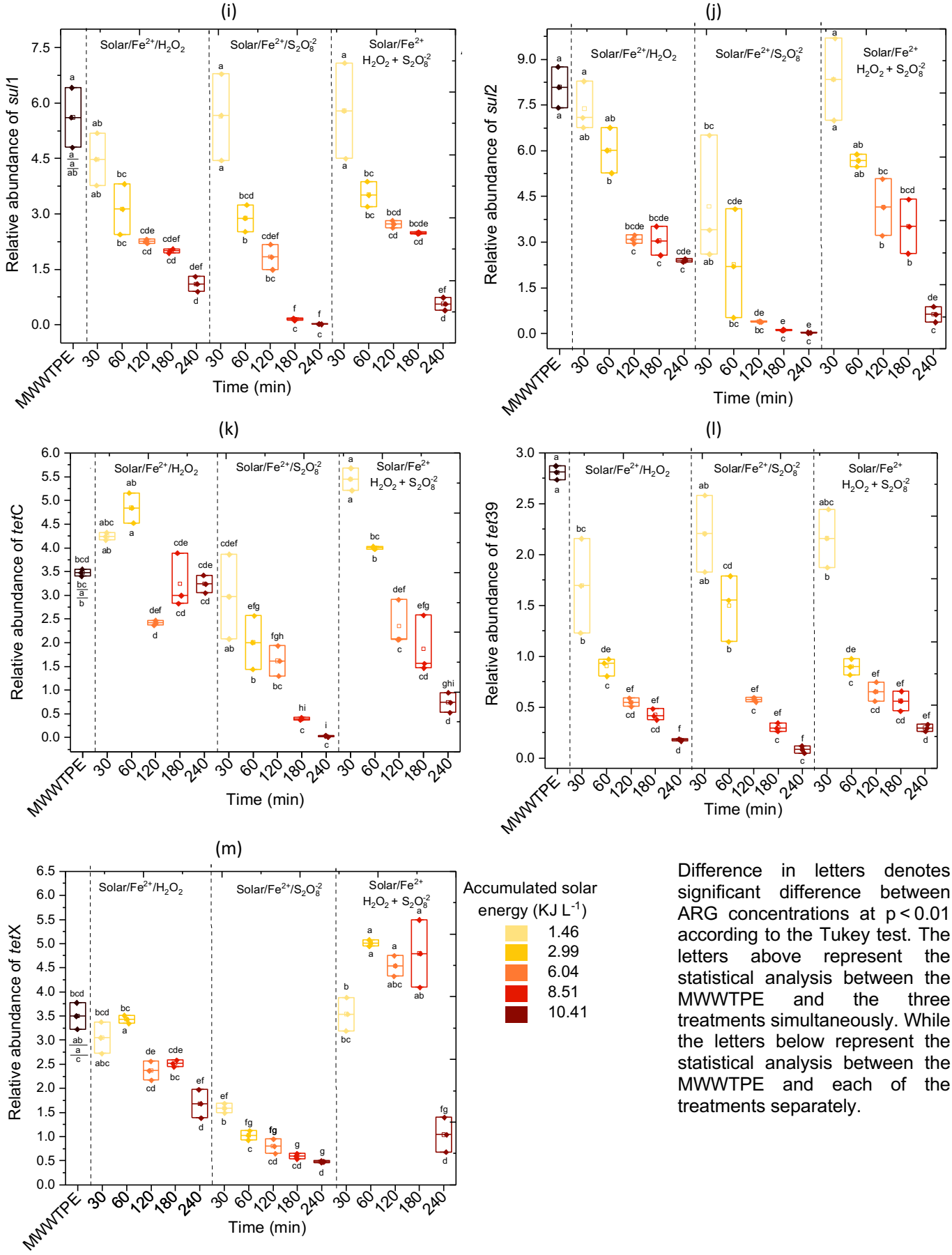

Difference in letters denotes significant difference between ARG concentrations at $p < 0.01$ according to the Tukey test. The letters above represent the statistical analysis between the MWWTPE and the three treatments simultaneously. While the letters below represent the statistical analysis between the MWWTPE and each of the treatments separately.

Substantial enrichments of the streptomycin resistance gene *aad*A1 (Figure IV.4a), the extended spectrum beta-lactamase-encoding gene *bla*$_{GES}$ (Figure IV.4d), and the macrolide resistance genes *msr*E and *mph*E (Figure IV.4c and Figure IV.4d) were observed mainly in Solar/Fe^{2+}/$S_2O_8^{-2}$. The same effect was observed for tetracycline resistance gene *tet*C (Figure IV.4f) during solar/Fe^{2+}/H_2O_2 and solar/Fe^{2+}/H_2O_2+$S_2O_8^{-2}$. For erythromycin resistance gene *erm*F and tetracycline resistance gene *tet*X, significant enrichments were only observed for the solar/Fe^{2+}/H_2O_2 (Figure IV.4e) and in the combined oxidant system (Figure IV.4g), respectively.

For most of the target ARGs, solar/Fe^{2+}/H_2O_2 achieved maximum removal within 2.99 KJ L^{-1} (2h) of treatment (*i.e. aad*A1, *aph*6, *bla*$_{GES}$, *mph*E, *sul*2) (Figure IV.4). A total treatment time of 4h was only required for the removal of *sul*1 and tetracycline conferring resistance ARGs (10.41 KJ L^{-1}) (Figure IV.4e). Regarding solar/Fe^{2+}/$S_2O_8^{2}$, genes that were more resistant to oxidative treatment were those that confer resistance to macrolides (*i.e. mphE*, *msrE*, *ermF)* (Figure IV.4c-e), and *tet*X (Figure IV.4g). On the other hand, solar/Fe^{2+}/H_2O_2+$S_2O_8^{-2}$ only obtained satisfactory removals in short reaction times for *aad*A1 (Figure IV.4a) and *erm*F (Figure IV.4e) (2.99 KJ L^{-1}; 2h of reaction). For the other target ARGs, an accumulated radiation of 10.41 KJ L^{-1} (240 min of reaction) was required.

4 DISCUSSION

Similarly, to most MWWTP operating in developing countries, the MWWTP investigated in this study operates only up to the secondary stage. Therefore, it is neither designed nor efficient for ARB and ARG removal and could potentially threaten the ecological balance and safety of rivers receiving treated MWWTPE. Concentrations of pathogen indicators (*i.e.* Total Coliform and *E. coli*) in MWWTPE analyzed in this study are similar to the concentrations detected elsewhere (10^4-10^6 CFU mL^{-1}) (VAZ-MOREIRA; NUNES; MANAIA, 2014). In contrast, THB concentration is below frequently detected values (10^4–10^7 CFU mL^{-1}) (MANAIA *et al*., 2016; VAZ-MOREIRA; NUNES; MANAIA, 2014), which implies the outstanding performance of the MWWTP regarding this parameter. Regarding cultivable ARB, MWWTPE showed a high frequency of bacteria resistant to β-lactams (AMX and LEX). However, most isolates were obtained from selective pressures created by antimicrobials to which they possess intrinsic resistance. In this case, only five strains isolated from MWWTPE showed growth under selective pressure that suggest acquired resistance mechanisms (Table IV.5). Of particular concern is the *E. coli* isolates recovered under selective pressure due to β-lactams (AMX and LEX), fluoroquinolone (CIP) and macrolide (AZM). Nevertheless, its removal through the applied treatments is a remarkable outcome.

Regarding ARGs, results are in agreement with previous studies performed with samples from the same MWWTP for which ARG absolute concentrations ranging from 3.6 to 6.1 log copies mL^{-1} were reported, with predominance of *sul*1 > bla_{TEM} > *tet*A > *erm*B > *qnr*B (LEROY-FREITAS *et al*., 2022). Even so, the predominance of macrolide resistance gene *erm*F in this study is concerning, since *erm* genes encode 23S rRNA methyltransferases which prevents macrolide, lincosamide and streptogramin B from interacting with its binding site. Therefore, *erm*-catalyzed methylation is associated with inducible macrolide–lincosamine–streptogramin B (MLS_B) resistance (DINOS, 2017; LUND *et al*., 2022). Nevertheless, post-treatment of MWWTPE is critical to promote the elimination of these ARB and ARGs prior to wastewater disposal in order to prevent the spread of these pathogens to the environment.

Post-treatment conditions proposed in this study corroborate with the potential of solar photo-Fenton to remove ARB and ARGs. Besides, treatments showed high efficiency against biological indicators which is in line with results reported by several authors who obtained successful inactivation of *E. coli* and Total coliforms by solar photo-Fenton in CPC reactors (AGULLÓ-BARCELÓ *et al*., 2013; BERRUTI *et al*., 2022; GIANNAKIS *et al*., 2016b). Data shows faster removal in treatments using only persulfate as an oxidant, probably due to the drop in pH (6.9 to 2.95 – Figure IV.5) observed throughout this reaction compared to stable pH at the near neutral range (5.9 to 7.15 - Figure IV.5) during other treatments. It was expected that this condition would lead to higher removal rates via solar/Fe^{2+}/H_2O_2+$S_2O_8^{2-}$, as the circumneutral pH favors the co-occurrence of $SO_4^{\bullet-}$ and HO• radicals in the presence of both oxidants as according to Equation IV.6 (WANG *et al*., 2017b; YIN *et al*., 2022).

$$SO_4^{\bullet-} + H_2O \rightarrow SO_4^{2-} + H^+ + HO^{\bullet} \qquad \text{(IV.6)}$$

Figure IV.5 - pH and temperature evolution during solar/Fe^{2+}/H_2O_2, solar/Fe^{2+}/$S_2O_8^{2-}$, and solar/Fe^{2+}/H_2O_2+$S_2O_8^{2-}$

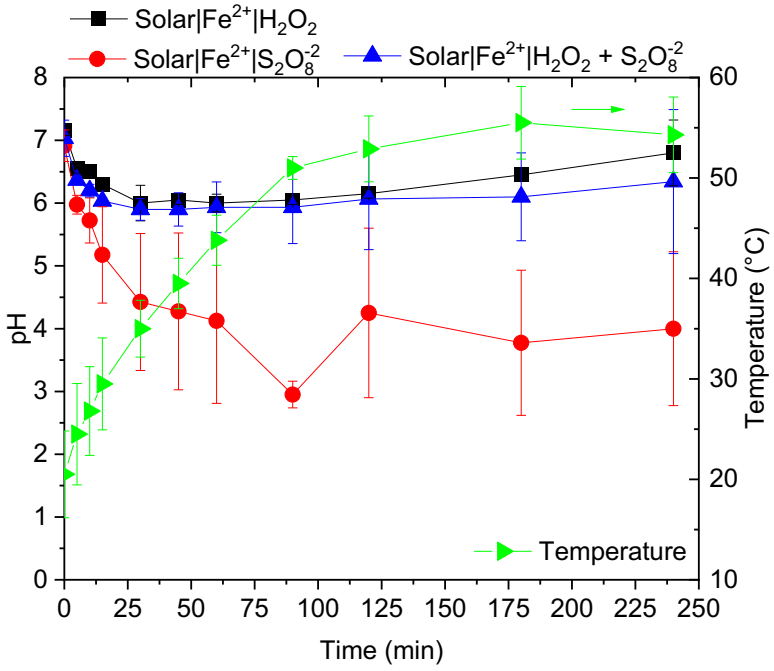

Furthermore, temperature probably contributed to disinfection in all photo-Fenton treatments as effluent temperature ranged from 20 to 57°C (Figure IV.5) during reactions as a consequence of the accumulation of total radiation (direct and diffuse) promoted by the CPC reactor. Considering that the majority of bacteria thrive within

the optimal temperature range between 35 and 40°C (Tortora *et al*., 2010), temperature effect upon disinfection was expected (BERNEY *et al*., 2006). Extensive experimental evidence has consistently shown the enhanced disinfection efficiency of elevated temperatures in solar-based wastewater disinfection processes due to the synergistic interplay between temperature and radiation (CASTRO-ALFÉREZ *et al*., 2017; GIANNAKIS *et al*., 2016a). Furthermore, temperature also affects Fe^{2+}/Fe^{3+}, H_2O_2 and $S_2O_8^{2-}$ availability and reactivity during solar photo-Fenton. For instance, reduction of ferric iron in the presence of H_2O_2 (Equation IV.7) can be favored by high temperature as show by Malato *et al*. (2009). Yet, H_2O_2 tends to be thermally decomposed into H_2O and O_2, and is subjected to a scavenging effect by temperatures above 30°C (YIP; LAM; HU, 2005).

$$H_2O_2 + Fe^{3+} \rightarrow Fe^{2+} + HO_2\bullet + H^+ \qquad \text{(IV.7)}$$

In contrast, higher temperatures have a positive influence in the performance of treatments that apply $S_2O_8^{2-}$ as this oxidant can be induced by thermal activation for temperatures > 40 °C leading to ROS production according to Equation IV.8 and Equation IV.9 (WANG *et al*., 2017b; YIN *et al*., 2022).

$$S_2O_8^{2-} \xrightarrow{heat} 2SO_4\bullet^- \qquad \text{(IV.8)}$$

$$HSO_5^- \xrightarrow{heat} SO_4\bullet^- + HO\bullet \qquad \text{(IV.9)}$$

The combination of these factors allowed for the acquisition of very interesting results for the three tested conditions. Regarding ARB, solar/$Fe^{2+}/S_2O_8^{2-}$ achieved > 99% removal of all growth in antibiotic-enriched PCA media including samples taken within a few minutes of treatment. For instance, this treatment achieved > than 85% removal within 1.46 KJ L^{-1} (30 minutes of reaction). This performance is associated with the level of oxidative stress and cell membrane damage induced by oxidative reactions conducted in the presence of $S_2O_8^{2-}$ as demonstrated by Vilela *et al*. (2022b). As previously shown and confirmed in this study, $S_2O_8^{2-}$ activation by Fe^{2+} and its photo-activation by visible light generates $SO_4\bullet^-$ leading to remarkable abatement of bacterial community (Vilela *et al*., 2022; Yang *et al*., 2019), in addition to disinfection (CANDEIAS; STEENKEN, 2000; DAVIES, 1987; KUMAR; POTTIBOYINA; SEVILLA, 2011; MARNETT, 2002). However, scale-up from bench scale (Vilela *et al*., 2022) to

pilot scale in a CPC reactor in real conditions showed different profiles of pH during treatment. A decay in the pH to 6.9 to 4.4 was observed for the treatment (1.46 KJ L^{-1}, 30 min) conducted in the CPC (Figure IV.5). Production of hydrogen ions according to Equation IV.10 and Equation IV.11 are known to occur in this system (ZHOU *et al*., 2023), thus justifying pH decay in the system.

$$S_2O_8^{2-} + Fe^{2+} \rightarrow SO_4^{\bullet-} + SO_4^{2-} + Fe^{3+} \quad \text{(IV.10)}$$
$$2S_2O_8^{2-} + 2H_2O \rightarrow 4\ SO_4^{2-} + 4H^+ + O_2 \quad \text{(IV.11)}$$

pH drop to acidic conditions probably enhanced ARB removal as almost all physiological reactions are pH dependent, and low pH leads to microbial inactivation (GIANNAKIS *et al*., 2016b). In addition, acid pH may result in protonation of DNA bases, which leads to major DNA structural damage (ZHOU *et al*., 2023), thus explaining high removal of ARGs in this system (Figure IV.3). Another interesting factor, which may also be associated to enhanced treatment performance is the temperature (Figure IV.5). While in the bench experiments, temperature remained stable at 35°C (Vilela *et al*., 2022), media temperature increased in the CPC reactor reaching temperatures in the order of 40 - 55 °C during treatment. All these factors taking place simultaneously in the system probably led to better performance of the solar/Fe^{2+}/$S_2O_8^{2-}$ treatment compared to solar/Fe^{2+}/H_2O_2 and solar/Fe^{2+}/H_2O_2+$S_2O_8^{2-}$. Nevertheless, as sulfate radical shows a longer lifespan (OH; DONG; LIM, 2016; ZHOU *et al*., 2020) providing for the maintenance of hostile conditions for a longer reaction time compared to hydroxyl radicals, some strains, such as *E. faecium, K. pneumoniae*, and *S. marcescens*, remained after 10.41 KJ L^{-1} of treatment.

Despite also counting with direct (bacteria cell damage by temperature) and indirect (radical activation) effects of temperature (Equation IV.5 and Equation IV.6), solar/Fe^{2+}/H_2O_2+$S_2O_8^{2-}$ treatment did not show high removal efficiency. Lower efficiency of this treatment may be associated to co-occurrence of various reactions and radicals in this system such as (i) HO• by H_2O_2/Fe^{2+}activation (Equation IV.12), (ii) HO• by $SO_4^{\bullet-}$ reaction in circumneutral pH (Equation IV.6), (iii) $SO_4^{\bullet-}$ by $S_2O_8^{2-}$/ Fe^{2+} activation (Equation IV.10), (iv) $SO_4^{\bullet-}$ by photo-activation (Equation IV.13), and (v) $SO_4^{\bullet-}$ and HO• by $S_2O_8^{2-}$activation by H_2O_2 (Equation IV.1) (Vilela *et al*., 2022).

$$Fe^{2+} + H_2O_2 \rightarrow Fe^{3+} + HO\bullet + OH^- \quad \text{(IV.12)}$$

$$SO_3^- - O - O - SO_3^- + h\nu \rightarrow 2SO_4\bullet^- \quad \text{(IV.13)}$$

As a consequence of competition between these routes, the consumption of $S_2O_8^{2-}$ was almost 4x lower in the combined treatment (Figure IV.6c) compared to solar/Fe^{2+}/$S_2O_8^{2-}$ (Figure IV.6b). In contrast, consumption of H_2O_2 in the combined treatment (Figure IV.6c), mainly in the initial times (up to 15 min), was higher than in the solar/Fe^{2+}/H_2O_2 treatment (Figure IV.6a). This result was also reported in a previous study for experiments conducted at bench scale (Vilela *et al*., 2022). This behavior is probably associated with the extra route of H_2O_2 consumption by reacting with $S_2O_8^{2-}$. Moreover, the combined solar photo-Fenton system is singular as the addition of $S_2O_8^{2-}$ decreases the rate of H_2O_2 decomposition leading to lower HO• loss (Vilela *et al*., 2022; Yan *et al*., 2013), consequently enhancing the concentration of reactive radicals in the system. This should have led to increased treatment efficiency which did not occur. This is probably related to an excess of H_2O_2 or $S_2O_8^{2-}$ in the system (Figure IV.6), which can result in ROS scavenging. For instance, excess $S_2O_8^{2-}$ may also work as a $SO_4\bullet^-$ scavenger, as shown in Equation IV.14 and Equation IV.15 (HUIE; CLIFTON, 1989; QIAN *et al*., 2015). Thus, decreasing ARB and ARGs removals. Besides that, no pH decay was observed at pilot scale, as also noted elsewhere (Vilela *et al*., 2022).

$$SO_4\bullet^- + S_2O_8^{2-} \rightarrow SO_4^{2-} + S_2O_8\bullet^- \quad \text{(IV.14)}$$

$$SO_4\bullet^- + SO_4\bullet^- \rightarrow S_2O_8^{2-} \quad \text{(IV.15)}$$

Figure IV.6 - Oxidant consumption and dissolved iron concentration evolution in (a) solar/Fe^{2+}/H_2O_2, (b) solar/Fe^{2+}/$S_2O_8^{2-}$, and (c) solar/Fe^{2+}/H_2O_2+$S_2O_8^{2-}$

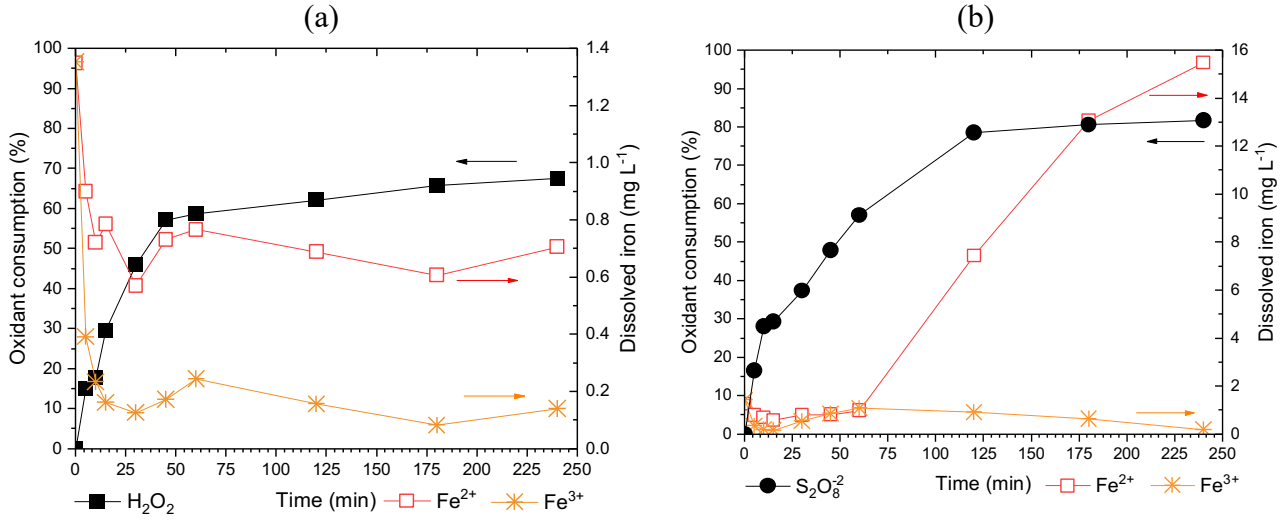

(c)

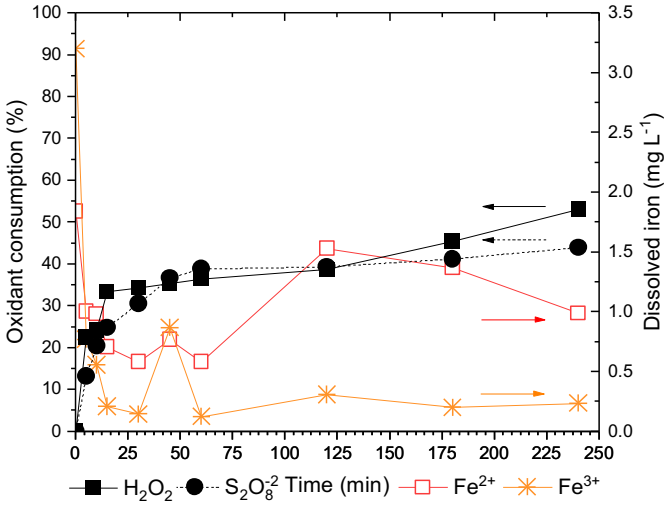

Results obtained by solar/Fe^{2+}/H_2O_2 were very similar to those obtained by solar/Fe^{2+}/H_2O_2+$S_2O_8^{2-}$. Regarding removal of ARB, none of these treatments were effective, with increased counts of bacteria resistant to β-lactam antibiotics AMX and LEX. MALDI-TOF analysis identified strains which persisted after these treatments (Table IV.5) revealing predominance of aerobic bacteria (*i.e. E. faecium, S. maltophilia, S. marcescens,* and *Pseudomonas* sp.). This indicates that, besides ruling as an oxidant, H_2O_2 also functions as an oxygen source, enhancing aerobic bacterial growth and selecting individuals with this metabolism (HINCHEE; DOWNEY; AGGARWAL, 1991; ZAPPI *et al*., 2000). A similar result was also reported for samples treated by solar photo-Fenton at bench scale and analyzed by whole genome sequencing (Vilela *et al*., 2022, 2021b). Likewise, all species identified from cultivated strains belong to *Proteobacteria* and *Firmicutes.* This finding was expected according to previous characterization of bacterial community diversity in samples from the same MWWTPE after solar photo-Fenton treatments applied in bench scale under similar operational conditions (Vilela *et al*., 2022, 2021b).

Concerning the identified strains, most belonged to the *Enterobacterales* order (*i.e. Enterobacter* spp., *E. coli*, *K. pneumoniae*, *S. marcescens*, and *Raoultella* spp.) and were susceptible to AMX, LEX, CIP and SXT (EUCAST, 2023). Yet some of the strains isolated from MWWTPE (*i.e. Bacillus* ssp., *Enterobacter* ssp., *E. faecium*, *E. coli*, *K. pneumoniae*, *S. marcescens*, *S. maltophilia,* and *Raoultella* spp.) under selective pressure by these antibiotics, thus possibly indicating acquired resistance (Table IV.5).

Bacterial populations have the potential to survive treatment processes by activating defense and repair mechanisms (MANAIA *et al*., 2016; MARANO; CYTRYN, 2018; MICHAEL-KORDATOU; KARAOLIA; FATTA-KASSINOS, 2018), which can be further stimulated by the intense metabolic activity induced by oxidative conditions during solar photo-Fenton treatments. Enhanced defense responses, including increased horizontal gene transfer (HGT) rates, could explain the release of intracellular ARGs from damaged bacterial cells and their subsequent spread to other bacteria. Therefore, results observed in this study may be attributed to the interplay between oxidative stress, defense mechanisms, and HGT in bacterial populations.

In contrast, the spread of ARGs may be stimulated under hostile conditions, such as those created by the oxidative environment generated during solar photo-Fenton treatments. As bacteria cell membrane is attacked by ROS, it loses integrity and releases cytoplasmic contents (*i.e.* ARGs), subsequently enhancing the spread of resistance genes within bacterial communities. As shown in Figure IV.3, ARGs removal showed a decreasing profile over time during proposed treatments. This behavior is clear for most target ARGs (Figure IV.3). However, an enrichment was observed for some ARGs, mainly in initial treatment times. This is shown in Figure IV.4 which presents relative abundance of target ARGs over time during the three proposed treatments.

In addition, ARGs can occur in both intracellular and extracellular forms, and either in genomic or plasmid form. In this work, intracellular ARGs were assessed by extracting DNA from cells after treatment, therefore extracellular ARGs were not separately quantified by the methodology applied in this study. However, it is reasonable to speculate that extracellular ARGs possibly interacted with matrix components, such as organic matter, or Fe^{3+}, forming complexes that could potentially be trapped during filtration performed prior to DNA extraction. Consequently, extracellular ARGs were possibly extracted along with intracellular ARGs and also quantified by qPCR. Thus, potentially explaining the enrichment of certain target ARGs.

Similar findings have also been reported by Zhang *et al*. (2021). As previously discussed, solar/Fe^{2+}/$S_2O_8^{2-}$ showed higher production of ROS which prevailed during treatment. This allowed for a higher inactivation of ARB, and consequently increase of

ARGs in this system throughout reaction. In contrast, hostile conditions were restricted to the beginning for the other two treatments, and this may have limited ARGs removal (as well as ARB inactivation). While it is not feasible to establish a direct correlation between the observed resistance phenotype and the prevalence of target ARGs after treatments, it is important to observe that ARGs related to sulfonamide resistance (*sul*1 and *sul*2) were initially detected at high relative abundance in samples (Figure IV.4). Additionally, the emergence of the SXT resistance phenotype in the identified strains, including *E. faecium*, *S. marcescens*, and *S. maltophilia*, warrants attention.

As this is the first study to present the removal of these target ARGs, it is not possible to compare treatment efficiency with other processes. However, in terms of total ARG removal, results reported in this study suggest that the solar photo-Fenton is a promising treatment technology, especially for tropical developing countries. Even so, proposed treatments still demonstrate a strong potential for ARB and ARG removals compared to conventional disinfection methods, such as chlorination, ozonation and UV irradiation, applied in MWWTP. For instance, Machado *et al*. (2023) observed a higher prevalence of ARB in the effluent from a MWWTP after UV disinfection of secondary wastewater. Similar results have also been observed for other processes (Guo *et al*., 2015; Sousa *et al*., 2017; Liu *et al*., 2018; Hou *et al*., 2019; Iakovides *et al*., 2019; Jin *et al*., 2020; Manna Wang *et al*., 2021; H. Wang *et a*l., 2020; Zhang *et al*., 2020).

Yet, some outcomes of this study which are associated to limitations related to the applied methodology should be further analyzed, such as: (i) understanding mechanisms leading to acquired resistance during proposed treatments; (ii) evaluating the removal of intracellular and extracellular ARGs and the effect of oxidative stress conditions on HGT. Furthermore, results achieved with solar/Fe^{2+}/H_2O_2+$S_2O_8^{2-}$ treatment were not as expressive as expected. As distinct reactions of radical production (SO_4•$^-$ and HO•) co-occur in this system, it should lead to higher treatment efficiency. However, low consumption of oxidants (H_2O_2 and $S_2O_8^{2-}$) demonstrated that oxidant concentrations used in this treatment may be in excess, which probably led to radical scavenging, not allowing for full action on the bacterial community and ARGs. Therefore, alternative H_2O_2:$S_2O_8^{2-}$ ratios may improve the effectiveness of the

combined system. Thereafter, considering particularities of each of the proposed treatments and results obtained in this study, photo-Fenton applied in a CPC reactor is a remarkable alternative for ARB removal of MWWTPE.

5 CONCLUSION

This study corroborates with the potential of solar photo-Fenton treatments for the removal of ARB and ARGs present in MWWTPE. Solar/Fe^{2+}/$S_2O_8^{2-}$ achieved the best results for both removal of ARBs and ARGs which might be associated to pH reduction during treatment. However, hostile conditions provided by this treatment led to favorable conditions for some priority bacterial strains (*e.g. E. faecium, K. pneumoniae*, *S. marcescens,* and *S. maltophilia*).

Lower efficiency of Arb and ARG removals were observed for solar/Fe^{2+}/H_2O_2 and solar/Fe^{2+}/ H_2O_2 +$S_2O_8^{2-}$, yet there was no pH decay, a great advantage for process scale-up. Nevertheless, these treatments were not as efficient to remove gram-positive bacteria (*e.g. Bacillus* sp. and *Enterococcus* sp.), which demonstrates the need for optimization of initial oxidant (H_2O_2), and Fe^{2+} concentrations throughout reaction.

Finally, results obtained in this study imply that the solar photo-Fenton system performed in a pilot scale CPC reactor is a promising alternative for post-treatment of wastewater considering both ARB inactivation and ARGs degradation, especially compared to conventional treatment alternatives. However, selection of some ARB and acquired resistance phenotypes were observed during proposed treatments. Thus, mechanisms of ROS actions upon ARB and ARGs must be further investigated in future studies.

CHAPTER V – Coaction of sulfate and hydroxyl radicals in enhanced solar photo-Fenton: Tackling antimicrobial resistance via secondary wastewater post-treatment[5]

[5]Chapter under review for submission

1 INTRODUCTION

Wastewater Treatment Plants (WWTPs) offer significant potential as valuable sources of water, energy, nutrients, organic matter, and other sustainable and accessible resources (KEHREIN *et al*., 2020; LAWSON *et al*., 2019; MAHMUD *et al*., 2021). In addition, WWTPs play an essential role in effectively addressing water scarcity by offering a viable option for water reuse for activities such as aquaculture, irrigation, recreation, industrial and urban uses (FERRO *et al*., 2015; MANNINA; GULHAN; NI, 2022; RIZZO *et al*., 2020). Proper management and implementation of wastewater reuse requires remarkable technological advances in wastewater treatment as it relies on the combination of physicochemical and biological treatments to reach reuse standards for each use (KHAN *et al*., 2022; MANAIA *et al*., 2018; MANIKANDAN *et al*., 2022; ROBBINS *et al*., 2022). However, the pervasive presence of emerging chemical and microbiological contaminants after conventional wastewater treatment that may lead to environmental and public health risks has raised substantial environmental concerns related to wastewater reuse (FATTA-KASSINOS; MERIC; NIKOLAOU, 2011; GWENZI; MUSIYIWA; MANGORI, 2020; KUMAR *et al*., 2022; PATEL *et al*., 2019; SAMBAZA; NAICKER, 2023).

Recent advances on analytical chemistry and toxicology directed concerns related to wastewater beyond organic contamination (*e.g.* solids, organic matter and nutrients) (DAUGHTON, 2004; RIZZO *et al*., 2019; SONUNE; GHATE, 2004; VON SPERLING, 2016). Contaminants of emerging concern (CECs) such as endocrine disruptors, illicit drugs, personal care products, pesticides, pharmaceuticals (*e.g.* antimicrobials), resistant microorganisms (*i.e.* antimicrobial - resistant bacteria - ARB which harbors antimicrobial resistance genes - ARG) have gained prominence as significant contributors to the issue (ALYGIZAKIS *et al*., 2020; BRACK *et al*., 2022; EBELE; ABOU-ELWAFA ABDALLAH; HARRAD, 2017; FATTA-KASSINOS *et al*., 2015; KRZEMINSKI *et al*., 2019; LADO RIBEIRO *et al*., 2019; WEAR *et al*., 2021). Conventional treatment processes are not specifically designed to effectively remove these contaminants from wastewater, resulting in their persistence in the environment (DANNER *et al*., 2019; DONG *et al*., 2016; TIWARI *et al*., 2017).

The occurrence of antibiotics in environmental compartments, primarily attributed to the discharge of effluents from WWTP, is of particular concern (HERNANDO *et al*., 2006; MICHAEL *et al*., 2013; RIZZO *et al*., 2013). Environmental contamination by antibiotics, even in very low concentrations, represents an important path for the dissemination of antimicrobial resistance (AMR) (LE-MINH *et al*., 2010; MORIN-CRINI *et al*., 2022; RIZZO *et al*., 2013; SAMREEN *et al*., 2021; VIKESLAND *et al*., 2019a). As the occurrence and spread of AMR is one of the biggest threats to global public health (COLLIGNON; MCEWEN, 2019; HAVENGA *et al*., 2019; HILLER *et al*., 2019a; MANAIA *et al*., 2020b), it is critical to address this issue on the perspective of wastewater treatment to control this source of environmental contamination.

As an alternative to conventional strategies, advanced oxidation processes (AOPs) are effective methods to degrade recalcitrant compounds (GANIYU; SABLE; GAMAL EL-DIN, 2022; GIANNAKIS *et al*., 2016a; RAHIM POURAN; ABDUL AZIZ; WAN DAUD, 2015). AOPSs are based on the generation of highly reactive free radicals such as hydroxyl radicals (radical HO•, E_0 = 2.8 V) or sulfate radicals ($SO_4^{\bullet -}$, E_0 = 2.6 V) (LADO RIBEIRO *et al*., 2019; RIZZO, 2011; RIZZO *et al*., 2020). Despite successful results achieved through several AOPs, including Fenton, photo-Fenton, ozonation, UV/H_2O_2, UV/Cl_2, as potential alternatives for post-treatment in WWTP to enhance the removal of CECs and disinfection (including ARBs), significant issues and gaps in the mechanistic actions of these processes towards ARB and ARG remain unraveled (LADO RIBEIRO *et al*., 2019; MORIN-CRINI *et al*., 2022; RIZZO, 2022; RIZZO *et al*., 2019). For instance, regrowth of ARB and enrichment of ARGs were observed after ozonation (IAKOVIDES *et al*., 2019; SOUSA *et al*., 2017). Chlorination and UV process, show low performance towards ARBs (GUO; YUAN; YANG, 2015; WANG *et al*., 2021a; ZHANG *et al*., 2020a). UV/H_2O_2 is a well-established process for CECs degradation and bacteria inactivation. However, its effect on AMR, particularly concerning ARG removal, was ineffective under realistic conditions for WWTP (RIZZO, 2022; WANG; CHEN, 2022). In addition, ozonation and UV-based process have been associated with the selection of ARGs and ARBs, potentially increasing the risk of AMR transfer into the environment (MICHAEL-KORDATOU; KARAOLIA; FATTA-KASSINOS, 2018).

Nevertheless, photo-Fenton oxidation has undergone extensive investigation as a promising alternative for the removal of CECs, inactivation of microorganisms, and ARGs (GIANNAKIS *et al*., 2016a; MICHAEL-KORDATOU; KARAOLIA; FATTA-KASSINOS, 2018; RIZZO, 2022; RIZZO *et al*., 2020; WANG; CHEN, 2022). Significant improvements of photo-Fenton over the years have enhanced its oxidation capacity and degradation efficiency towards these contaminants. For instance, harnessing solar radiation as a light source enables the catalytic effect under longer wavelengths. This sustainable approach offers a promising alternative, especially in regions with abundant solar irradiance (*i.e.* tropical countries such as Brazil) (CLARA *et al*., 2021; RIZZO, 2022; RIZZO *et al*., 2019, 2020).

H_2O_2 has been recently reported to enhance $S_2O_8^{2-}$ activation by heterogeneous catalysts (BARARPOUR *et al*., 2018; LI *et al*., 2017; XU *et al*., 2019a, 2019b). However, the potential of using both oxidants/radicals simultaneously in homogeneous catalysts is rarely investigated (EPOLD; DULOVA, 2015; EPOLD; TRAPIDO; DULOVA, 2015; KAUR; KATTEL; DULOVA, 2020; KHATAEE *et al*., 2016; QIU *et al*., 2022; WU *et al*., 2023). When practiced, it is carried out under unrealistic conditions (*e.g.* water solutions or simulated wastewater, longer reaction times or micro lab scale).

Considering that solar photo-Fenton efficiency is influenced by the complex interplay between matrix constituents (LADO RIBEIRO *et al*., 2019), this study aimed investigate and compare (i) the efficiency of enhanced solar photo-Fenton (solar/Fe^{2+}/H_2O_2+$S_2O_8^{2-}$), (ii) the effect of oxidants ratio (m:m), and (iii) the role which the reactive species ($SO_4^{\bullet-}$ and HO•) on the removal of antibiotics (namely, sulfamethoxazole, sulfadiazine, and trimethoprim) and ARB in a secondary WWTP effluent (WWTPE). To the best of our knowledge, this particular area of research has not been previously explored or studied elsewhere.

2 MATERIAL AND METHODS

2.1 Sampling

MWWTPE was sampled in the output of a secondary settling tank from a Conventional Activated Sludge (CAS) system in a MWWTP located in Belo Horizonte (Brazil), which receives wastewater from 1.5 million inhabitants (290 m^3 d^{-1}), including hospitals and industries. WWTPE was collected on two different days and physicochemical characterization (Table V.1) was performed as according to APHA (2017).

Table V.1 - Physicochemical characterization of Municipal Wastewater Treatment Plants effluent (MWWTPE) sampled in the output of a secondary settling tank from a conventional activated sludge (CAS) system in a MWWTP located in Belo Horizonte (Brazil)

Parameter[1]	Unit	MWWTPE[2]	Reference
Temp.	°C	19.2 ± 2.8	APHA 2550
pH	-	7.6 ± 0.2	APHA 4500 B
ORP	mV	72.7 ± 0.3	APHA 2580
OD	mg L^{-1}	6.4 ± 2.8	APHA 4500 G
Conductivity	µS cm^{-1}	527.6 ± 58.6	APHA 2510
Turbidity	NTU	17.1 ± 5.9	APHA 2130 B
Total alkalinity	mg$CaCO_3$ L^{-1}	164.0 ± 1.0	APHA 2320 B
Hardness	mg L^{-1}	67.0 ± 1.0	APHA 2340
COD	mgO_2 L^{-1}	77.0 ± 8.0	APHA 5220 D
TDS	mg L^{-1}	385.0 ± 18.0	APHA 2540 B
TSS	mg L^{-1}	10.0 ± 2.0	

[1]ORP = redox potential; OD = Dissolved oxygen; COD = Chemical Oxygen Demand; TS = Total Solids; TDS = Total Dissolved Solids; TSS = Total Suspended Solids. [2]Average values; n=2

2.2 Experimental set-up

Enhanced solar photo-Fenton treatment of MWWTPE was conducted in a solar simulator chamber (SUNTEST CPS+, ATLAS) containing a Xenon lamp protected by a daylight filter, which emits light in the UV-Vis region (300-800 nm), thus simulating the solar spectrum. The irradiance was set at 268 W m^{-2} (330 to 800 nm) which is equivalent to 30 W m^{-2} (UV-A: 300-400 nm) corresponding to the annual average irradiance in Belo Horizonte/MG. Accumulated irradiation (Q_{UV}, KJ L^{-1}) was determined as according to Equation V.1 (MALATO *et al*., 2009).

$$Q_{UV,n} = Q_{UV,n-1} + \Delta t_n \overline{UV}_{G,n} \frac{A_r}{V_t} \quad \text{(V.1)}$$

where A_r is the irradiated area (m^2), and V_t is the reactor volume (L), Δt_n represents the time interval (s), $UV_{G,n}$ is the average incident irradiation (W m^{-2}).

Experiments (Table V.2) were performed at circumneutral pH in a glass container (0.12 m x 0.12 m; 0.10 m of height; volume 1000 mL) with opaque black walls for 60 min under continuous stirring. The temperature, pH and accumulated radiation were monitored throughout reactions. Reactions were performed simultaneously in technical duplicates. Three different oxidant:oxidant ratios were tested in this study. Experiments were also performed in the presence of sulfate and hydroxyl radical scavengers.

Table V.2 – Concentration of oxidants (H_2O_2 and/or $S_2O_8^{2-}$), iron (Fe^{2+}) and radical scavenging (tert-butyl alcohol – t-BuOH or methanol - MetOH) applied in enhanced solar photo-Fenton treatment tested in this study including times corresponding to intermittent additions of iron

AOP	Tests	H_2O_2: $S_2O_8^{2-}$ ratios	Oxidant	Radical scavenging	Fe^{2+}
Enhanced solar photo-Fenton (solar/Fe^{2+}/ H_2O_2+$S_2O_8^{-2}$)	1	1:1	0.75 mM H_2O_2 + 0.75 mM $S_2O_8^{2-}$	10mM t-BuOH	$t_0 \rightarrow$ 15 mg L^{-1}
	2	1:1	0.75 mM H_2O_2 + 0.75 mM $S_2O_8^{2-}$		
	3	1:1	0.75 mM H_2O_2 + 0.75 mM $S_2O_8^{2-}$	100mM MetOH	$t_{5, 10, 15\ min} \rightarrow$ 5 mg L^1 Total $\rightarrow$ 30 mg L^{-1} (0.5 mM)
	4	1.5:1	0.75 mM H_2O_2 + 0.5 mM $S_2O_8^{2-}$		
	5	1:10	0.075 mM H_2O_2 + 0.75 mM $S_2O_8^{2-}$		

Reactions were performed at circumneutral pH using intermittent iron additions (ferrous sulfate solution) strategy. This strategy was adopted according to previous works (VILELA *et al*., 2021b, 2022a), as well as H_2O_2 and $S_2O_8^{-2}$ concentrations for 1:1 molar ratio (25 mg L^{-1} H_2O_2 + 141.1 mg L^{-1} $S_2O_8^{2-}$). The concentrations of the two alcohols: tert-butyl alcohol – t-BuOH and methanol – MetOH, used to ensure the total radical scavenging, was adopted according to López-Vinent *et al*. (2022). The effect of oxidant concentration was examined by varying initial oxidant concentrations according to Chu, Wang and Leung (2011). Persulfate and iron solutions were freshly prepared before use to minimize variations in concentration caused by self-decomposition.

2.3 Physicochemical analyses

Samples were withdrawn during treatments for quantification of $S_2O_8^{2-}$ (LIANG *et al*., 2008) and H_2O_2 (limit of quantification, LOQ = 0.5 mg L^{-1}) (NOGUEIRA; OLIVEIRA; PATERLINI, 2005). Samples were filtered through 0.45 µm PVDF filter prior to iron ions analyzes.

2.4 Microbiological analyses

Samples were withdrawn and residual H_2O_2 and $S_2O_8^{2-}$ was removed by adding catalase enzyme (460 mg L^{-1} in phosphate buffer; 0.1:1.9, v/v) (POOLE, 2004) and ascorbic acid (0.1:1, v/v) (OLMEZ-HANCI; ARSLAN-ALATON; DURSUN, 2014), respectively. If necessary, pH was re-adjusted to neutral values, prior to microbiological analyzes.

Total coliforms and *E. coli* were selected as biological indicators of wastewater treatment efficiency pathogen indicators and measured by QuantiTray technique with Colilert media (IDEXX/APHA 9223B) following manufacturer instruction. The abundance and prevalence of resistant microorganisms (*i.e*. ARB) that are viable and culturable was achieved by spread plate method. Samples were also prepared for further molecular biology analyses by filtering 30 mL of samples through a 0.22 µm mixed cellulose esters (MCE) membrane, samples were filtered in duplicates. Membranes were stored in sterile tubes at -20°C for further analysis.

2.4.1 Culture-based analysis for enumeration and identification of ARB

Colony-forming units (CFUs) of total heterotrophic bacteria (THB) and ARB were measured with a standard plate dilution technique on plate count agar (PCA, KASVI) alone and supplemented with co-trimoxazole (SXT, 350 mg L^{-1}), a combination of trimethoprim and sulphamethoxazole antibiotics, respectively. The working concentrations of SXT in supplemented media was higher than the minimum inhibitory concentrations for resistant bacteria according to Clinical and Laboratory Standards Institute (CLSI) guidelines (CLSI, 2020). Plating was carried out by sowing treated and untreated samples on agar surface, directly, and after dilutions (10^0 and 10^{-1}). Each sample was incubated at 37 ± 1°C for 48 h before the enumeration of CFUs. The frequency of ARB was calculated by dividing ARB mean count by the THB. This yielded the concentration of ARB expressed as colony forming units per milliliter (CFU mL^{-1}). Removal and log removal of ARB was calculated using Equation V.2 and Equation V.3, respectively.

$$\text{ARB removal} = C_t/C_0 \quad \text{(V.2)}$$

$$\text{Log removal} = \text{Log}_{10}C_t/C_0 \quad \text{(V.3)}$$

Where C_0 is ARB concentration in MWWTPE, and C_t is the ARB concentration after treatment at time t. All plates were done in triplicates, and the average count was used for data interpretation.

2.4.2 Isolation and identification of ARB and THB

For THB and ARB plating, colonies with different morphotypes were selected from each plate by visual inspection after CFU enumeration. On plates with more than one morphotype, five colonies of each morphotype were selected. On plates with only one morphotype, only five colonies were selected. Each selected strain was isolated in saline solution with glycerin (20%) and stored at -20°C. Subsequently, isolated strains were replicated in brain-heart infusion (BHI) broth and incubated at 37 ± 1°C up to 24 h for subsequent culture in PCA medium (37 ± 1°C for 24 h). Strains that grew after subculturing were identified by matrix-assisted laser desorption ionization-time of flight (MALDI-TOF) Microflex LT (Bruker Daltonik).

A single colony of each bacterial strain was added to the steel target plate. For each strain, 1 µl of 70% formic acid and 1 µl of MALDI-TOF MS matrix solution containing α-cyano-4-hydroxycinnamic acid (HCCA) (Bruker Daltonik) were applied to the spot and allowed to air-dry. Spectra were acquired using the FlexControl MicroFlex LT mass spectrometer (Bruker Daltonik) equipped with a 60-Hz nitrogen laser. A total of 240 laser shots were fired in spiral movements to collect 40 shot steps for each strain spot. The mass range detection parameters were set from 1,960 to 20,137 m/z, with Ion source 1 voltage at 19.99 kV, Ion source 2 voltage at 18.24 kV, and a lens voltage of 6.0 kV for data acquisition. A calibration was performed using a bacterial test standard (*E. coli* DH5 alpha; Bruker Daltonik) prior to measurements Identification score criteria applied as threshold in this study were those recommended by the manufacturer: (i) score ≥ 2.300 indicates a secure species-level identification; (ii) score ≥2.000 and <2.299 indicates a secure genus and probable species-level identification.

2.4.3 Antimicrobial susceptibility test

For strains with score ≥2.000, antibiotic susceptibility tests were performed using the Kirby-Bauer disc diffusion (CLSI, 2020). All the isolates were inoculated in Mueller-Hinton agar and incubated at 37°C for 24 h. Each isolate was resuspended in saline

solution (0.9 % NaCl) and turbidity was adjusted based on McFarland scale (pattern 0.5). Inoculation was performed on Mueller-Hinton agar and a set of antibiotic discs (SENSIDISC DME®) was distributed over the agar surface. The selection of antibiotics for testing (Table V.3) was based on the EUCAST Expected Resistant Phenotypes v. 1.2 guideline (EUCAST, 2023) and clinical study published by Brazilian medical centers regarding the treatment of strains identified through MALDI-TOF. Plates were incubated in a bacteriological incubator at 37°C for 24 h and inhibition halos were read in the sequence.

Table V.3 – Strains group identified through MALDI-TOF; Strains expected resistance based on the EUCAST Expected Resistant Phenotypes v. 1.2 guideline; Selected antibiotics for the antibiotic susceptibility tests

Group	Expected resistance	Tested Antibiotics
Enterobacterales (*i.e. Klebsiella* spp., *Leclercia* spp., *Raoultella* spp., *Citrobacter* spp., *Enterobacter* spp.)	Benzylpenicillin, glycopeptides, lipoglycopeptides, fusidic acid, macrolides (with some exceptions - Azithromycin and erythromycin), lincosamides, streptogramins, rifampicin, and oxazolidinones	Amikacin (AMK, 30µg), Amoxillin-Clavulanic Acid (AMC, 30µg), Ampicillin-Sulbactam (SAM, 20µg), Azitromycin (AZM, 15µg), Ceftazidime (CAZ, 30µg), Cephalexin (LEX, 30µg), Ciprofloxacin (CIP, 5µg), Ertapenem (ETP, 10µg), Erythromycin (ERY, 15µg), Gentamicin (GEN, 10µg), Imipenem (IPM, 10µg), Meropenem (MEM, 10µg), Nalidixic Acid (NAL, 30µg), Streptomycin (STR, 10µg), Tetracyclin (TET, 30µg), and Sulfazotrim (SXT, 25µg)
Non-fermentative gram-negative bacteria (*i.e. Acinetobacter* spp.)	Benzylpenicillin, first- and second generation cephalosporins, glycopeptides, lipoglycopeptides, fusidic acid, macrolides, lincosamides, streptogramins, rifampicin and oxazolidinones	Amikacin (AMK, 30µg), Ciprofloxacin (CIP, 5µg), Gentamicin (GEN, 10µg), Imipenem (IPM, 10µg), Levofloxacin (LVX, 5µg), Meropenem (MEM, 10µg), and Sulfazotrim (SXT, 25µg)
Gram-positive bacteria (*i.e. Bacillus* spp.)	Aztreonam, temocillin, polymyxin B/colistin and nalidixic acid	Erythromycin (ERY, 15µg), Gentamicin (GEN, 10µg), Tetracyclin (TET, 30µg), Vancomycin (VAN) and Sulfazotrim (SXT, 25µg)

The interpretation of results followed the M100 guideline by CLSI (2023) which classifies strains as susceptible, intermediate, or resistant. Susceptibility profile was performed with 74 strains. Tested antibiotics were related to nine classes: aminoglycosides (AMK, GEN, and STR), β-lactams: carbapenems (ETP, IPM, and MEM), cephalosporins (CAZ and LEX), and penicillinics (β-lactamase inhibitors - AMC and SAM), fluoroquinolones and quinolones (CIP, LVX and NAL), macrolides (AZM and ERY), sulfonamides and trimethoprim: folate inhibitors (SXT), Vancomycin (VAN) and tetracyclines (TET). Strains resistant to 3 or more classes of antibiotics were

considered Multi-Drug Resistant (MDR) and Pan-Drug Resistant (PDR) bacteria were those resistant to all tested antibiotics.

2.5 Data processing and statistical analysis

Data analysis and graphing, and statistical analysis were performed using OriginPro 2022 software. One-Way analysis of variation (ANOVA), t-test, and significance test were performed at a significance level of 99.9% ($p < 0.01$). The FDR method adjusted the P-value to reduce false-positive results (BENJAMINI; HOCHBERG, 1995). Iron speciation diagrams as a function of pH were performed in MINEQL+ (Version 5.0) using Fe equilibrium constants.

3 RESULTS AND DISCUSSION

3.1 Enhanced solar photo-Fenton: Baseline operating conditions

The activation of persulfate anion ($S_2O_8^{-2}$) with the components used in solar photo-Fenton (*i.e.* solar radiation, Fe^{2+}, and H_2O_2) was examined. In the enhanced solar photo-Fenton various reactions occur simultaneously leading to the formation of distinct oxidative radicals, such as:

(i) HO• by H_2O_2/Fe^{2+}activation (Equation V.4)

$$Fe^{2+} + H_2O_2 \rightarrow Fe^{3+} + HO\bullet + OH^- \quad (V.4)$$

(ii) $SO_4\bullet^-$ by $S_2O_8^{2-}$ activation by Fe^{2+} (Equation V.5)

$$S_2O_8^{2-} + Fe^{2+} \rightarrow SO_4\bullet^- + SO_4^{2-} + Fe^{3+} \quad (V.5)$$

Nonetheless, the generated radical may react with a target pollutant or with Fe^{2+} as shown in Equation V.6

$$Fe^{2+} + SO_4\bullet^- \rightarrow Fe^{3+} + SO_4^{2-} \quad (V.6)$$

(iii) $SO_4\bullet^-$ by photo-activation Equation V.7

$$SO_3^- - O - O - SO_3^- + h\nu_{(254nm)} \rightarrow 2SO_4\bullet^- \quad (V.7)$$

(iv) $SO_4\bullet^-$ and HO• via $S_2O_8^{2-}$activation by H_2O_2 (Equation V.8)

$$S_2O_8^{2-} + H_2O_2 \rightarrow 2SO_4\bullet^- + 2HO\bullet \quad (V.8)$$

Initially, 1:1 molar ratio of H_2O_2 and $S_2O_8^{-2}$ was used. This experimental condition led to 57% consumption of H_2O_2 ($H_2O_{2initial}$ = 25 mg L^{-1}, H_2O_{2final} = 11 mg L^{-1}) and 52% consumption of $S_2O_8^{-2}$ ($S_2O_8^{-2}{}_{initial}$ = 141.1 mg L^{-1}, $S_2O_8^{-2}{}_{final}$ = 67.2 mg L^{-1}) (Figure V.1). This result was also reported in the previously published work (Vilela *et al*., 2022b). In addition, the strategy of intermittent additions of iron was successful, as it allowed the reaction to occur at circumneutral pH with continuous presence of soluble and reactive Fe^{2+} throughout treatment (Figure V.2), and consequent formation of radicals by Equation V.4 and Equation V.5.

Figure V.1 - Response variables measured during solar/Fe^{2+}/H_2O_2+$S_2O_8^{2-}$ at circumneutral pH using intermittent iron additions (15 mg L^{-1} followed by 5 mg L^{-1} at 5, 10 and 15 min + 25 mg L^{-1} or 0.75mM of H_2O_2 + 141.1 mg L^{-1} or 0.75mM of $S_2O_8^{2-}$)

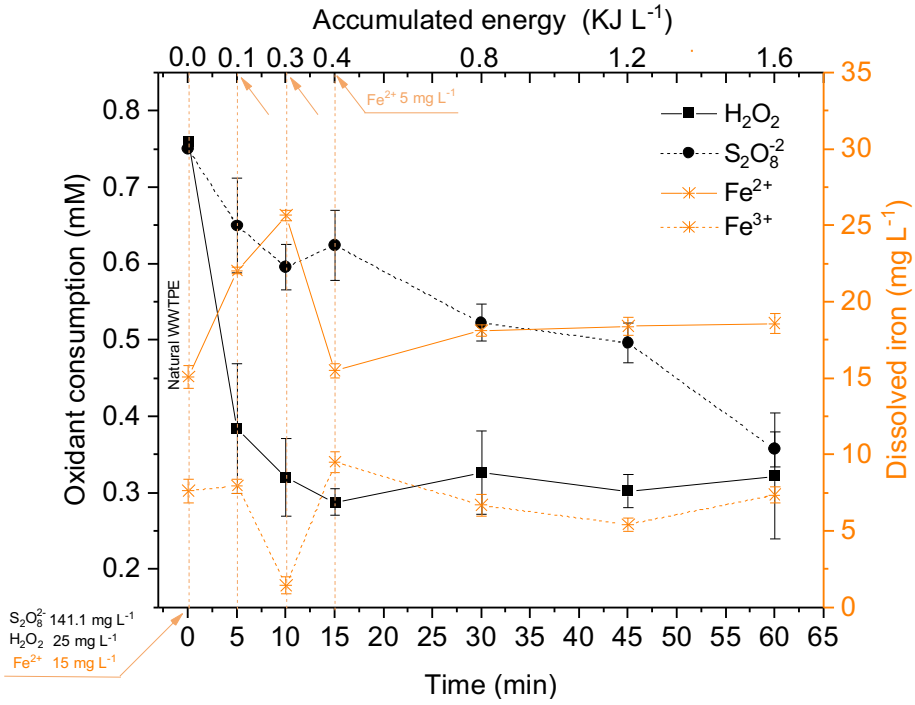

Figure V.2 - pH and temperature evolution during solar/Fe^{2+}/H_2O_2+$S_2O_8^{2-}$ at circumneutral pH using intermittent iron additions (15 mg L^{-1} followed by 5 mg L^{-1} at 5, 10 and 15 min with 25 mg L^{-1} or 0.75mM of H_2O_2 and 141.1 mg L^{-1} or 0.75mM of $S_2O_8^{2-}$)

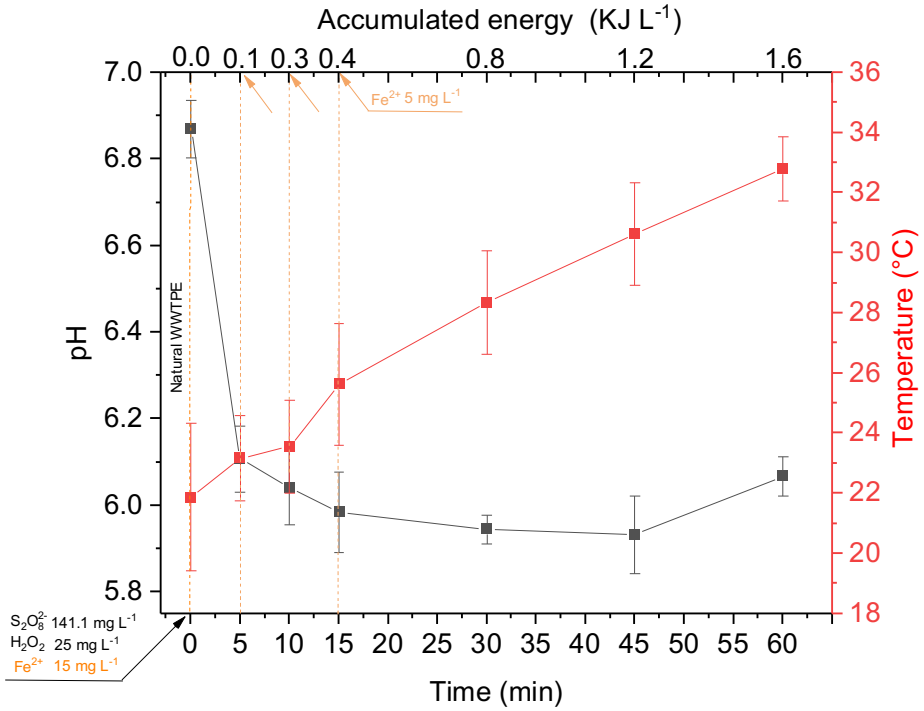

Furthermore, in addition to enhanced Fe^{2+} cycling (Equation V.9) in the traditional photo-Fenton system, there is an extra route for $HO^{\bullet}$ formation (Equation V.10) under UV-A irradiation via light adsorption by iron hydroxides formed in the system (TARR, 2003), as observed by Vilela *et al*. (2022, 2023). Moreover, a reaction between $S_2O_8^{-2}$ and Fe^{3+} (Equation V.11) is also reported to occur.

$$Fe^{3+} + H_2O_2 \rightarrow Fe^{2+} + HO_2^{\bullet} + H^+ \quad (V.9)$$

$$Fe(OH)^{2+} + h\nu_{(540\text{-}580\ nm)} \rightarrow Fe^{2+} + HO^{\bullet} \quad (V.10)$$

$$S_2O_8^{2-} + Fe^{3+} + ½\ O_2 \rightarrow SO_4^{\bullet -} + SO_4^{2-} + FeO^{2+} \quad (V.11)$$

Therefore, the combination of these oxidants is likely to enhance the efficiency of treatment, since Fe^{3+} activation of $S_2O_8^{2-}$ may improve the degradation process. In addition, this activation limits $SO_4^{\bullet -}$ scavenging via Equation V.5. Low solubility of Fe^{3+} is one of the main challenges related to the $Fe^{3+}/S_2O_8^{2-}$ process. However, results shown in Figure V.1 demonstrate that even in the absence of organic or inorganic complexation (*e.g* EDDS), Fe^{3+} was available in the system. Another factor that may have interfered with the availability of Fe^{2+} is related to temperature increase (Figure V.2). Despite not reaching considerable values for the thermal activation of $S_2O_8^{2-}$ (T > 40°C), the reduction of Fe^{3+} in the presence of H_2O_2 (Equation V.9) may be favored by high temperatures. Yet, H_2O_2 tends to be thermally decomposed into H_2O and O_2, and is subject to a scavenging effect by temperatures above 30°C (YIP; LAM; HU, 2005). However, this effect is not observed in the results obtained, since even after 40 min (30°C < T < 33°C) we still have a considerable residual H_2O_2. Finally, despite the possible occurrence of a significant drop in pH associated to the occurrence of the $H_2O/S_2O_8^{2-}$ reaction (Equation V.12), as previously observed by Vilela *et al*. (2022), no significant change was observed ($p > 0.01$) after the initial decrease within 5 min of reaction (pH = 6.11 ± 0.08) (Figure V.2).

$$2S_2O_8^{2-} + 2H_2O \rightarrow 4\ SO_4^{2-} + 4H^+ + O_2 \quad (V.12)$$

3.1 Effect of $S_2O_8^{2-}$ and H_2O_2 ratios: Synergy of sulfate and hydroxyl radicals

Regardless of the synergistic effect observed using $S_2O_8^{2-}$ with H_2O_2 in addition to Fe^{2+} and solar irradiation in previous studies, a possible mechanism of radical scavenging through the excessive concentration of persulfate was also indicated. In this way, the evaluated variables still demonstrate a high concentration of Fe^{2+} available for reaction with greater availability of Fe^{2+} compared to Fe^{3+} (Figure V.3).

Figure V.3 - Response variables measured during solar/Fe^{2+}/H_2O_2+$S_2O_8^{2-}$ at circumneutral pH using intermittent iron additions (15 mg L^{-1} followed by 5 mg L^{-1} at 5, 10 and 15 min) with 1:1 H_2O_2:$S_2O_8^{2-}$ (0.75mM of H_2O_2 and 0.5mM of $S_2O_8^{2-}$) (a), and 1.5:1 H_2O_2:$S_2O_8^{2-}$ (0.075mM of H_2O_2 and 0.75mM of $S_2O_8^{2-}$ (b)

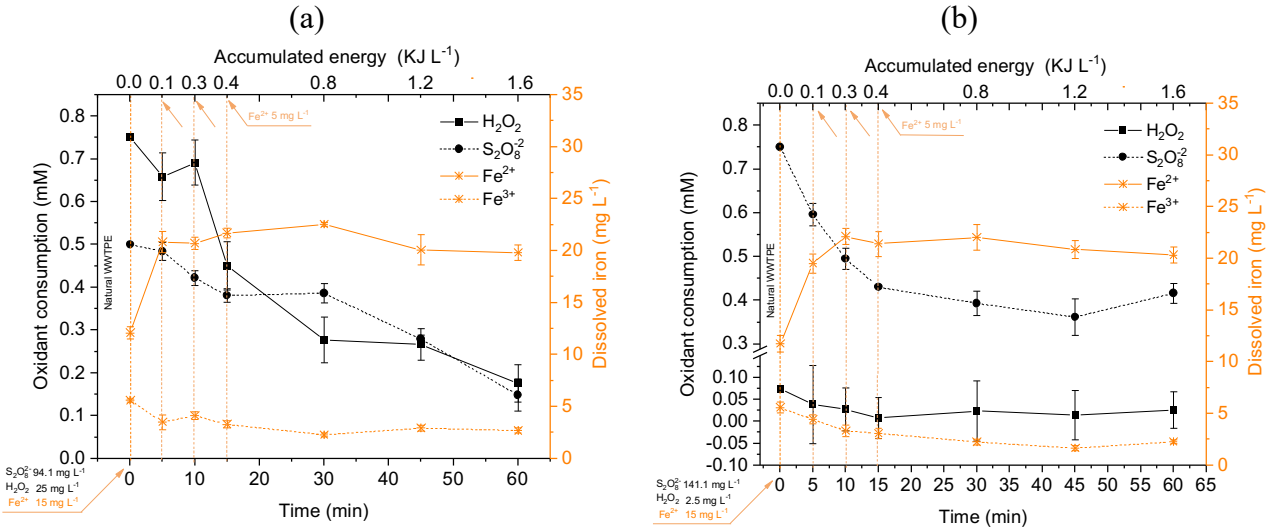

Regarding the consumption of oxidants, the reaction with 1:1 and 1.5:1 molar ratio of H_2O_2:$S_2O_8^{2-}$ obtained the highest consumption of oxidants, with consumption of 77% of H_2O_2 and 70% of $S_2O_8^{2-}$. While the reaction with 1:10 H_2O_2:$S_2O_8^{2-}$ molar ratio, despite almost complete consumption of H_2O_2 (> 98%), consumed only 52% of the $S_2O_8^{2-}$. Furthermore, no significant variations were observed in temperature or pH in the three evaluated conditions (Figure V.4).

3.1.1 Removal of biological indicators: Occurrence and identification of ARB

Regarding biological indicators, THB counts ranged from 1.7 x 10^4 to 1.9 × 10^3 CFU mL^{-1}, Total Coliforms from 2.40 to 2.60 × 10^5 MPN $100mL^{-1}$, and *E. coli* from 8.2 x 10^4 to 7.94 × 10^5 MPN $100mL^{-1}$ in MWWTPE. All tested enhanced solar photo-Fenton

conditions reached >90% removal of biological indicators (Table V.4). ARB counts in MWWTPE ranged from 4.6 x 10^2 to 4.0 × 10^1 CFU mL^{-1}.

Figure V.4 - pH and temperature evolution during solar/Fe^{2+}/H_2O_2+$S_2O_8^{2-}$ at circumneutral pH using intermittent iron additions (15 mg L^{-1} followed by 5 mg L^{-1} at 5, 10 and 15 min) with 0.75mM (25 mg L^{-1}) of H_2O_2 and 0.5mM (94.1 mg L^{-1}) of $S_2O_8^{2-}$ and 0.075mM (2.5 mg L^{-1}) of H_2O_2 and 0.75mM (141.1 mg L^{-1}) of $S_2O_8^{2-}$

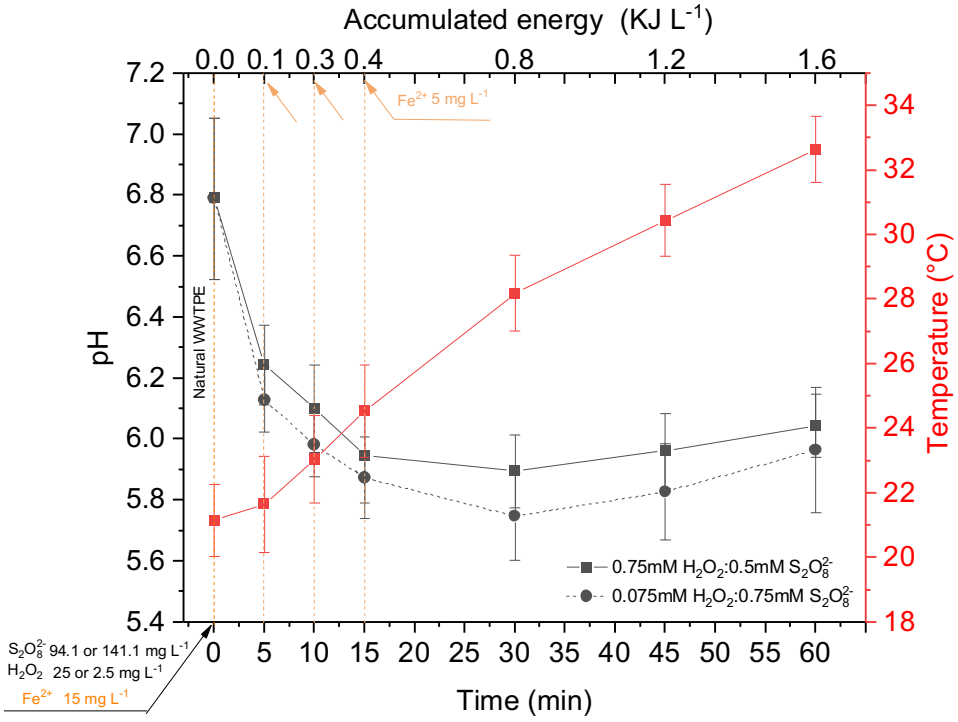

Concerning ARB removal, the reaction with the 1:10 H_2O_2:$S_2O_8^{2-}$ molar ratio was not efficient, achieving a log of removal of 0.3 (55%). The other tested conditions showed log removals >1.6. This result demonstrates the importance of H_2O_2 as a disinfectant.

Table V.4 - Counts of THB and ARBs (CFU mL^{-1}) in MWWTPE and after enhanced solar photo-Fenton treatments

	THB	ARB
Sample	CFU mL^{-1}	
MWWTPE	9.23 10^3	2.53 10^2
1:1	9.05 10^1	7.00 10^0
1.5:1	1.45 10^2	5.00 10^0
1:10	9.85 10^2	1.14 10^2

THB: total heterotrophic bacteria; ARB: Antimicrobial Resistance Bacteria; MWWTPE: Municipal Wastewater Treatment Plant.

A total of 42 strains were isolated from MWWTPE and treated samples. Only proteobacteria species were identified in MWWTPE, such as *Klebsiella pneumoniae*, *Klebsiella variicola, Acinetobacter parvus*, *Raoultella ornithinolytica*, *Leclercia adecarboxylata* and *Escherichia coli*. These results changed after treatments, as for 1:1 molar ratio of oxidants (0.75:0.75 mM H_2O_2:$S_2O_8^{2-}$), a predominance of bacteria from the *Firmicutes* phylum, consisting of *Bacillus* spp. were identified, in addition to a *Raoultella ornithinolytica*, and an *Escherichia coli* strain. The same was observed with the highest molar ratio 1.5:1 molar ratio of oxidants (0.75:0.5 mM H_2O_2:$S_2O_8^{2-}$). However, a higher frequency of *E. coli* strains and *Klebsiella pneumoniae* were also identified after this treatment. Although, after the condition with 1:10 molar ratio (0.075:0.5 mM H_2O_2:$S_2O_8^{2-}$), only proteobacteria species were identified, with a predominance of *Klebsiella pneumoniae* strains.

ARB regrowth was also observed in all these samples after incubation following 24 and 48 hours of treatment. Regrowth results followed the same pattern observed previously, except for that observed in the condition of 1:10 molar ratio, since only *Bacillus* ssp. was isolated and identified. In order to investigate the multi-resistance of the isolates antibiotic susceptibility tests were performed for strains with score ≥2.000 (Table V.5).

3.1.1.1 ARB resistance profiles

Table V.5 shows the phenotype of the isolated ARB. A total of 42 strains were identified in MWWTPE and treatment samples, with 43% of them classified as gram (+) (*i.e. Bacillus* spp.). The gram (-) strains identified, were divided into two groups. Only one non-fermentative gram-negative strain (*Acinetobacter parvus*) as isolated from MWWTPE. The others 55% strains are *Enterobacterales* (*i.e. Klebsiella* ssp., *Raoultella* ssp., *Escherichia coli*, *Enterobacter* ssp., and *Leclercia* ssp.), which were isolated from MWWTPE and after treatments. Interestingly, most isolates recovered from MWWTPE was from selective pressures due to antimicrobials (SXT), some isolated ARBs are from condition with 1:10 molar ratio (0.075:0.5 mM H_2O_2:$S_2O_8^{2-}$). The MWWTPE isolates were all identified as *E. coli*, and all showed a multi-drug resistant (MDR) (β-lactams – penicillinics, macrolides, aminoglycosides, fluoroquinolones and quinolones, tetracyclines, and folate inhibitors).

Table V.5 - Antibiotic resistance profile of Enterobacterales (a), Non-fermentative gram-negative bacteria (b), and Gram-positive bacteria (c) isolates in MWWTPE and samples taken within 60 minutes (1.6 KJ L^{-1}), and after 24/48h of solar/Fe^{2+}/H_2O_2+$S_2O_8^{2-}$ treatment with molar oxidant ratio of 1:1, 1.5:1 and 1:10. "X" indicates strains with intrinsic resistance to target antibiotics. Color intensity[c] indicates the resistance profile

(a)

			Species	Antibiotic Resistance Phenotype															
				β-lactams							Macrolides		Aminoglycosides			Fluoroquinolones and Quinolones		Tetracyclines	Folate inhibitors
				Carbapenems			Cephalosporins		Penicillinics										
				ETP	IPM	MEM	LEX	CAZ	SAM	AMC	ERY	AZM	STR	AMK	GEN	CIP	NAL	TET	SUT
MWWTPE		THB	*Klebsiella variicola*[a]																
			Klebsiella variicola[a]																
			Raoultella ornithinolytica[b]																
			Escherichia coli[b]																
			Klebsiella pneumoniae[a]								X	X	X					X	
		ARB	*Escherichia coli*[b]																
			Escherichia coli[b]																
			Escherichia coli[b]																
			Escherichia coli[b]																
			Escherichia coli[b]																
Oxidant ratio (H_2O_2:$S_2O_8^{2-}$)	1:1	THB	*Escherichia coli*[b]																
		ARB	*Raoultella ornithinolytica*[b]																
	1.5:1	THB	*Klebsiella pneumoniae*[a]								X	X	X					X	
			Escherichia coli[a]																
			Escherichia coli[b]																
	1:10	THB	*Klebsiella pneumoniae*[b]								X	X	X					X	
			Escherichia coli[b]																
			Enterobacter cloacae[b]																
			Escherichia coli[b]																
		ARB	*Klebsiella variicola*[b]																
			Raoultella ornithinolytica[b]																
			Klebsiella pneumoniae[a]								X	X	X					X	
			Leclercia adecarboxylata[b]																

(b)

		Species	Antibiotic Resistance Phenotype						
			β-lactams		Aminoglycosides		Fluoroquinolones and Quinolones		Folate inhibitors
			Carbapenems						
			IPM	MEM	AMI	GEN	CIP	LVX	SUT
MWWTPE	THB	*Acinetobacter parvus*[c]							

(c)

Oxidant ratio (H_2O_2:$S_2O_8^{2-}$)				Species	Antibiotic Resistance Phenotype			
					Macrolides	Aminoglycosides	Tetracyclines	Glicopeptídeos
					ERY	GEN	TET	VAN
1:1	THB	60'	*Bacillus cereus*[a]		25	8		
			Bacillus mojavensis[a]		30	35		
			Bacillus cereus[a]					
			Bacillus subtilis[a]					
			Bacillus pumilus[a]					
		24h	*Bacillus cereus*[a]		15	20		
			Bacillus cereus[a]		15	20		
		48h	*Bacillus cereus*[a]		30	20		
1.5:1		60'	*Bacillus subtilis*[a]		17	20		
			Bacillus cereus[a]		20	20		
		24h	*Bacillus cereus*[a]		22			
			Bacillus cereus[a]		25	22		
		48h	*Bacillus cereus*[a]		20	15		
			Bacillus subtilis[a]		25	20		
1:10		24h	*Bacillus cereus*[a]		25	22		
			Bacillus subtilis[a]		25	21		
		48h	*Bacillus cereus*[a]		25	15		
			Bacillus subtilis[a]		20	15		

[a] Secure genus identification, probable species identification (2.000 < Score < 2.299)

[b] Highly probable species identification Score > 2.300)

[c] Resistant Intermediary Susceptible Resistant Parental and Susceptible Oral Intermediary Parental and Susceptible Oral

From the strains isolated after the treatment conditions:

(i) Condition with 1:1 molar ratio (0.75:0.75 mM H_2O_2:$S_2O_8^{2-}$)

The two identified gram (-) strains (*Raoultella* ssp. and *Escherichia coli*) showed MDR phenotype. As well as the higher frequency of gram (-) strains. Regrowth of gram (+) strains was also observed after 24h and after 48h, with a probable MDR phenotype;

(ii) Condition with 1.5:1 molar ratio (0.75:0.5 mM H_2O_2:$S_2O_8^{2-}$)

Two different species was isolated (*Klebsiella* ssp. And *Escherichia coli*), with MDR *Escherichia coli*, and the *Klebsiella* ssp. presented acquired resistance to fluoroquinolones and quinolones (CIP and NAL). The gram (+) strains grow after treatments and in the regrowth at 24 and 48h. However, only 24h isolated strains showed a MDR phenotype;

(iii) Condition with 1:10 molar ratio (0.075:0.75 mM H_2O_2:$S_2O_8^{2-}$)

This condition shows the most of isolated strains, both THB and ARBs. Interestingly, they are also the strains that present MDR phenotype. Although only gram (-) was observed after this condition, after a period of 24 and 48 hours, gram (+) regrowth occurred, and those isolated within 48 hours showed a MDR profile as well.

3.2 Qualitative investigation of the free radicals mechanism involved in the Solar/Fe^{2+}/H_2O_2+$S_2O_8^{-2}$

During the enhanced solar photo-Fenton, sulfate ($SO_4^{\bullet-}$) and hydroxyl (HO•) radicals could be the main oxidizing species formed (Equation V.4 and V.5). To explain the probable contributions of these radicals in this system, the experiments were also carried out in the presence of appropriate quenchers of HO• and $SO_4^{\bullet-}$.

Tert-butyl alcohol (t-BuOH) reacts 1000-fold faster with HO• radicals (k = (3.8–7.6) × 10^8 M^{-1} s^{-1}) (Equation V.13) than with $SO_4^{\bullet-}$ radicals (k = (4.0–9.1) × 10^5 M^{-1} s^{-1}) (Equation V.14). Methanol reacts approximately 80-fold faster with hydroxyl radicals (Equation V.15) than with sulfate radicals (Equation V.16) (k = 9.7 × 10^8 M^{-1} s^{-1} and k

= 1.1 × 10^7 M^{-1} s^{-1}, respectively). Thus, excess tert-butyl alcohol act as a HO• scavenging radicals, and excess methanol act as a $SO_4^{\bullet-}$ scavenging radicals.

$$HO^{\bullet} + CH_3OH \rightarrow H_2O + CH_2OH \quad (V.13)$$
$$SO_4^{\bullet-} + CH_3OH \rightarrow SO_4^{2-} + {}^{\bullet}CH_2OH + H^+ \quad (V.14)$$
$$HO^{\bullet} + (CH_3)_3COH \rightarrow {}^{\bullet}CH_2(CH_3)_2COH + H_2O \quad (V.15)$$
$$SO_4^{\bullet-} + (CH_3)_3COH \rightarrow H^+ + SO_4^{2-} + {}^{\bullet}CH_2(CH_3)_2COH \quad (V.16)$$

Despite the use of quenchers, the evaluated variables still demonstrate a high concentration of Fe^{2+} available for reaction with greater availability of Fe^{2+} compared to Fe^{3+} (Figure V.5). Thus, the excess of Fe^{2+} ions may reduce or may improve the available sulfate and hydroxyl radical contents. Regarding the consumption of oxidants, the reaction with t-BuOH obtained a consumption of oxidants of 61% of H_2O_2 and 55% of $S_2O_8^{2-}$. While the reaction with MetOH consumed only 56% of H_2O_2 and 39% of the $S_2O_8^{2-}$.

Figure V.5 - Response variables measured during solar/Fe^{2+}/H_2O_2+$S_2O_8^{2-}$ at circumneutral pH using intermittent iron additions (15 mg L^{-1} followed by 5 mg L^{-1} at 5, 10 and 15 min) with 0.75mM (25 mg L^{-1}) of H_2O_2 and 0.75mM (141.1 mg L^{-1}) of $S_2O_8^{2-}$) and 10mM tert-butyl alcohol (t-BuOH) (a), and 100 methanol (MetOH) (b)

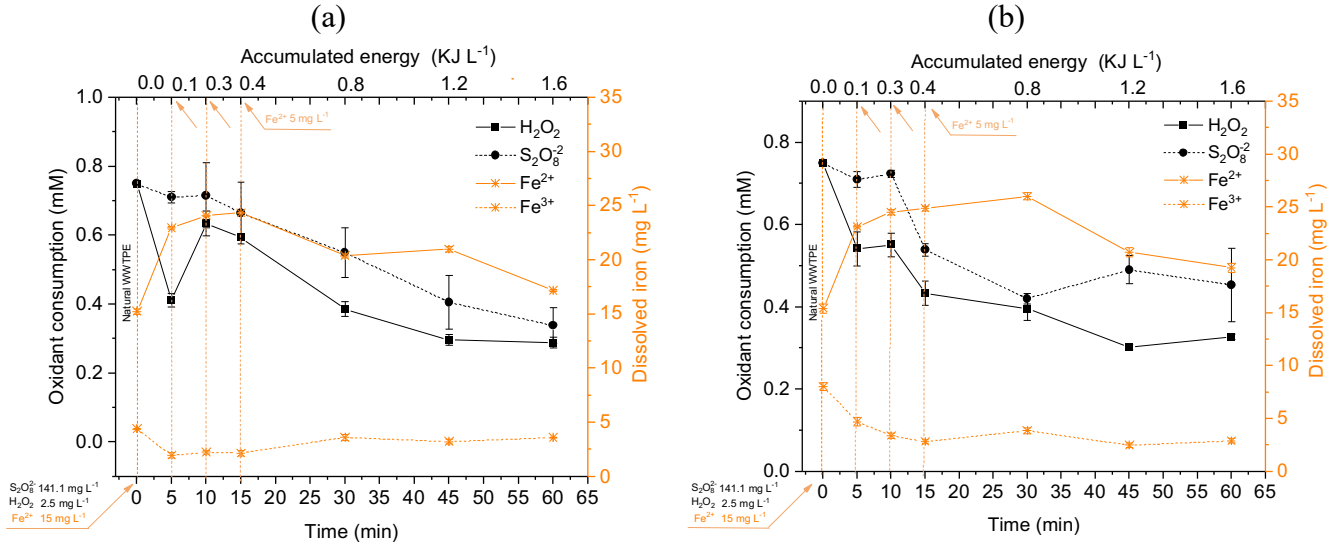

Furthermore, no significant variations were observed in temperature or pH in the evaluated conditions (Figure V.6). The investigation of this phenomenon should be hereafter studied, possibly using lower concentrations of oxidants.

Figure V.6 - pH and temperature evolution during solar/Fe^{2+}/H_2O_2+$S_2O_8^{2-}$ at circumneutral pH using intermittent iron additions (15 mg L^{-1} followed by 5 mg L^{-1} at 5, 10 and 15 min) with 0.75mM (25 mg L^{-1}) of H_2O_2 and 0.75mM (141.1 mg L^{-1}) of $S_2O_8^{2-}$) and 10mM tert-butyl alcohol (t-BuOH) or 100 methanol (MetOH)

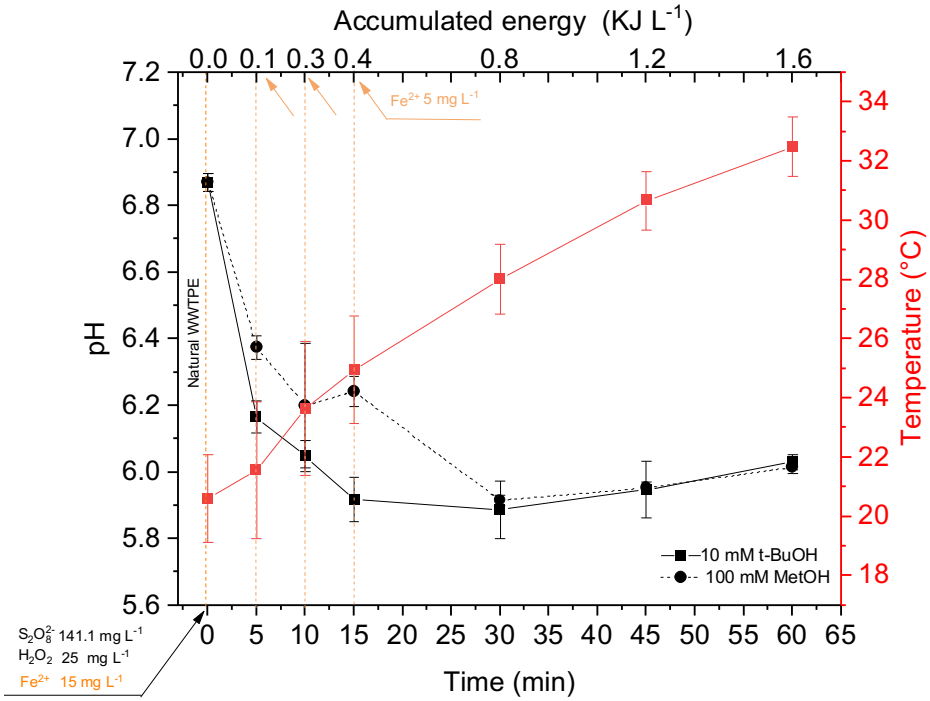

Related to ARB removal, generally, the rate of degradation in the absence of scavengers is remarkably higher than in their presence, because HO• and $SO_4^{\bullet-}$ were both involved in the degradation reaction. Interestingly, while the treatment without the use of appropriate quenchers obtained a moderate removal of ARBs, the addition of t-BuOH and MetOH resulted in a removal higher than 99%. A possible explanation for the result obtained is that the high formation of radicals during enhanced solar photo-Fenton causes it to less removal efficiency by scavenging mechanisms of the radicals themselves. For instance, excess $S_2O_8^{2-}$ may also work as a $SO_4^{\bullet-}$ scavenger, as shown in Equation V.17 and Equation V.18 (HUIE; CLIFTON, 1989; QIAN *et al.*, 2015). While during the use of these quenchers, the scavenging of only one of the radicals allows the enhanced action of the other.

$$SO_4^{\bullet-} + S_2O_8^{2-} \rightarrow SO_4^{2-} + S_2O_8^{\bullet-} \quad \text{(V.17)}$$

$$SO_4^{\bullet-} + SO_4^{\bullet-} \rightarrow S_2O_8^{2-} \quad \text{(V.18)}$$

For instance, sulfate radicals were the main oxidant species when t-BuOH was added (inhibited HO•). In contrast, both radicals were inhibited when using methanol. Therefore, it is likely that excess sulfate radicals are harming the reaction.

Furthermore, other possible reasons are: (i) no excess of scavengers was used, (ii) other formed radicals have a more effective action in the degradation process. For instance, oxidative intermediate species, such as superoxide (O_2•) (Equation V.19) could be attributed to the degradation in the presence of quenchers.

$$Fe^{2+} + O_2 \rightarrow Fe^{3+} + O_2\bullet \qquad (V.19)$$

Another possible explanation considers that the concentration used for t-BuOH and/or MetOH can have toxic effects on microbial communities, since microorganisms may be sensitive to the presence of these chemicals, and their use in the experimental conditions influenced the observed microbial responses.

3.2.1 ARB resistance profiles

A total of 23 strains were isolated from samples treatment using quenchers. Species identified, such as *Klebsiella pneumoniae*, *Enterobacter asburiae* and *Escherichia coli* were a minority, while gram (+) (*Bacillus* ssp.) strains predominated in these samples. In order to investigate the multi-resistance of the isolates antibiotic susceptibility tests were performed for strains with score ≥2.000 (Table V.6). From the strains isolated after the conditions:

(i) Condition with 10mM t-BuOH

The identified gram (+) strains are more frequente than gram (-) strains, but both are related with a probable MDR phenotype;

(i) Condition with 100 mM MetOH

The majority identify strains are related with a problable MDR phenotype.

Table V.6 - Antibiotic resistance profile of Enterobacterales (a) and Gram-positive bacteria (b) isolates in samples taken within 30 minutes (0.8 KJ L^{-1}) and 60 minutes (1.6 KJ L^{-1}) of solar/Fe^{2+}/H_2O_2+$S_2O_8^{2-}$ treatment with 10mM tert-butyl alcohol (t-BuOH) or 100 methanol (MetOH). "X" indicates strains with intrinsic resistance to target antibiotics. Color intensity[c] indicates the resistance profile

(a)

Quencher				Species	Antibiotic Resistance Phenotype															
					β-lactams							Macrolides		Aminoglycosides			Fluoroquinolones and Quinolones		Tetracyclines	Folate inhibitors
					Carbapenems			Cephalosporins		Penicillinics										
					ETP	IPM	MEM	LEX	CAZ	SAM	AMC	ERY	AZM	STR	AMK	GEN	CIP	NAL	TET	SUT
	t-BuOH	30 min	THB	*Escherichia coli*[a]																
				Klebsiella pneumoniae[b]				X				X					X	X		X
		60 min		*Escherichia coli*[b]				X				X		X	X		X			
				Enterobacter asburiae[a]	X	X	X	X	X	X	X	X	X	X	X	X	X	X	X	X	X
			ARB	*Escherichia coli*[b]		X		X			X	X		X			X	X		
	MetOH	30 min	THB	*Escherichia coli*[b]				X				X	X							
				Enterobacter kobei[a]	X	X	X	X	X	X	X	X	X	X	X	X	X	X	X	X	X
		60 min		*Escherichia coli*[b]				X	X	X	X	X	X		X					
				Escherichia coli[b]	X	X	X	X	X	X	X	X	X	X		X	X	X	X	X	X
			ARB	*Klebsiella pneumoniae*[a]				X				X								X

(b)

Quencher				Species	Antibiotic Resistance Phenotype			
					Macrolides	Aminoglycosides	Tetracyclines	Glicopeptídeos
					ERY	GEN	TET	VAN
	t-BuOH	THB	30 min	*Bacillus cereus*[a]		22		
				Bacillus mojavensis[a]	X	X	X	X
				Bacillus mojavensis[a]	X	X	20	
				Bacillus cereus[a]	X	20	X	X
				Bacillus mojavensis[a]	X	20	20	X
				Bacillus licheniformis[a]	X	X	X	X
	MetOH	THB	30 min	*Bacillus cereus*[a]	X	X	X	X
			60 min	*Bacillus megaterium*[b]	X	X	X	
				Bacillus vallismortis[a]	X	23	X	X
				Bacillus cereus[a]	X	15	X	X
				Bacillus subtilis[a]	X	17	23	X

[a] Secure genus identification, probable species identification (2.000 < Score < 2.299)

[b] Highly probable species identification Score > 2.300)

[c] Resistant; Intermediary; Susceptible; Resistant Parental and Susceptible Oral; Intermediary Parental and Susceptible Oral

4 CONCLUSION

This study investigated the efficiency and mechanisms of enhanced solar photo-Fenton for the removal of ARBs from WWTPE. Through an examination of the interplay between matrix constituents and the influence of oxidant ratios on the photo-Fenton process, the results demonstrated that enhanced solar photo-Fenton is a potential alternative for post-treatment MWWTP.

The addition of $S_2O_8^{2-}$ to the solar/Fe^{2+}/H_2O_2 system showed a synergistic effect, but also indicated a potential radical scavenging mechanism due to excessive persulfate concentration. The study highlighted the importance of the H_2O_2: $S_2O_8^{2-}$ molar ratio for improving oxidant consumption. Additionally, the removal of biological indicators (*i.e.* THB, Total Coliforms, and *E. coli*) exhibited substantial removal (>90%) under all enhanced solar photo-Fenton conditions. However, ARB counts varied, with the 1:10 H_2O_2:$S_2O_8^{2-}$ molar ratio showing lower efficiency, emphasizing the significance of H_2O_2 as a disinfectant.

Furthermore, microbial analysis revealed shifts in bacterial composition after treatment, with the Firmicutes phylum dominating in certain conditions. The occurrence of ARB regrowth was observed, particularly in the 1:10 molar ratio condition, emphasizing the need for comprehensive antimicrobial strategies. Notably, the study identified 42 strains in WWTPE and treated samples, with gram-positive *Bacillus* spp. prevailing. The majority of gram-negative strains belonged to *Enterobacterales*, including multi-drug resistant *E. coli* isolates recovered under selective antimicrobial pressures.

The investigation into the role of sulfate ($SO_4^{\bullet -}$) and hydroxyl (HO•) radicals during enhanced solar photo-Fenton demonstrated their significant contribution to degradation. Quenching experiments further confirmed the involvement of both radicals in the degradation process. However, the experimental conditions showed a greater potential for removing ARBs in the presence of these chelators, possibly due to (i) no excess of scavengers, (ii) other formed radicals, and/or (iii) toxic effects of t-BuOH and MetOH on microbial communities. However, the conditions were not

sufficient to ensure a comprehensive understanding of the mechanisms of action of the radicals, warranting the need for further experiments.

Nevertheless, this pioneering research provides valuable insights into the complex dynamics of enhanced solar photo-Fenton for wastewater treatment, shedding light on its effectiveness in mitigating AMR spread. The findings underscore the importance of optimizing oxidant ratios and understanding radical scavenging mechanisms to enhance the overall efficiency of the treatment process.

GENERAL CONCLUSIONS AND FUTURE PERSPECTIVES

Until the present moment, it is reasonable to consider that the general objective of this thesis: “To evaluate the efficiency of solar photo-Fenton using hydrogen peroxide (H_2O_2) and sodium persulfate ($S_2O_8^{-2}$) as oxidants as well as the combination of both in the removal of ARB and ARGs inherent to MWWTPE and treatment impact upon microbiome and resistome profile” is achievable. Regarding the specific objectives, the main results achieved are:

- Objective 1: To investigate the elimination and inactivation of free-cell DNA (plasmids) in MWWTPE via solar photo-Fenton;

Experiments proposed to fulfill this first specific objective were fully completed. Results indicated the potential of solar photo-Fenton to improve wastewater quality and reduce the spread of AMR in the environment by hampering the discharge of cell-free DNA onto the environment.

Publication: VILELA, Pâmela B.; MARTINS, Alessandra S.; STARLING, Maria Clara V. M.; DE SOUZA, Felipe A. R.; PIRES, Giovana F. F.; AGUILAR, Ananda P.; PINTO, Maria Eduarda A.; MENDES, Tiago A. O.; AMORIM, Camila C. Solar photon-Fenton process eliminates free plasmid DNA harboring antimicrobial resistance genes from wastewater. Journal of Environmental Management, v. 285, October 2020. DOI: 10.1016/j.jenvman.2021.112204.

- Objective 2: To Investigate the effects of solar photo-Fenton upon priority pathogens, bacterial community and resistome profile present in MWWTPE;

Experiments conducted to achieve this specific objective generated the first study that investigates the effect of solar photo-Fenton on ARB and ARGs in MWWTPE by WGS. As a result, solar photo-Fenton effectively removed the main phyla and ARGs and achieved the removal of some high-priority pathogens and intrinsically multi-drug ARB. Nevertheless, results showed enrichment of *Proteobacteria* after solar photo-Fenton and controls with H_2O_2. Further investigation is warranted to fully explore and understand the implications of the findings presented in Chapters 2 and 5, as they may not yet provide a complete answer to the underlying question.

Publication: VILELA, Pâmela B.; MENDONÇA NETO, Rondon P.; STARLING, Maria Clara V. M.; DA S. MARTINS, Alessandra; PIRES, Giovanna F. F.; SOUZA, Felipe A. R.; AMORIM, Camila C. Metagenomic analysis of MWWTP effluent treated via solar photo-Fenton at neutral pH: Effects upon microbial community, priority pathogens, and antibiotic resistance genes. Science of The Total Environment, v. 801, p. 149599, 2021. DOI: 10.1016/j.scitotenv.2021.149599.

Future publication: VILELA, Pâmela B. et al. *Coaction of sulfate and hydroxyl radicals in enhanced solar photo-Fenton: Tackling antimicrobial resistance via secondary wastewater post-treatment.*

- Objective 3: To investigate the impact of enhanced solar photo-Fenton upon microbiome diversity, priority pathogens and resistome profile present in MWWTPE;

The experiments designed to achieve this specific objective have been successfully completed, revealing compelling evidence of the substantial potential of enhanced solar photo-Fenton. However, just as the use of H_2O_2 led to enrichment of *Proteobacteria*, the use of $S_2O_8^{-2}$ led to enrichment of *Firmicutes*. Further investigation is warranted to fully explore and understand the implications of the findings presented in Chapters 3 and 5, as they may not yet provide a complete answer to the underlying question.

Publication: VILELA, Pâmela B.; STARLING, Maria Clara V. M.; MENDONÇA NETO, Rondon P.; SOUZA, Felipe A. R.; PIRES, Giovanna F. F.; AMORIM, Camila C. Solar photo-Fenton mediated by alternative oxidants for MWWTP effluent quality improvement: Impact on microbial community, priority pathogens and removal of antibiotic-resistant genes. Chemical Engineering Journal, v. 441, p. 136060, 2022. DOI: 10.1016/j.cej.2022.136060.

Future publication: VILELA, Pâmela B. et al. *Coaction of sulfate and hydroxyl radicals in enhanced solar photo-Fenton: Tackling antimicrobial resistance via secondary wastewater post-treatment.*

- Objective 4: To compare the efficiency of solar photo-Fenton and enhanced solar photo-Fenton by (i) persulfate and (ii) binary oxidants system (H_2O_2 + $S_2O_8^{-2}$) in tackling antimicrobial resistance by removal of ARB and ARGs on bench scale;

The comparison of solar photo-Fenton treatments with the use of alternative oxidants have been successfully completed with approaches that appear to be novel in the scientific literature. The results obtained allowed to analyze the particularities of the three alternatives to the conventional photo-Fenton. Yet, the system using the combination of H_2O_2 and $S_2O_8^{-2}$ as oxidants was less efficient than the treatment using only one oxidant (H_2O_2 or $S_2O_8^{-2}$). This outcome was not expected considering the multitude of pathways available for radical formation. Therefore, a comprehensive investigation was undertaken to elucidate the mechanisms underlying the synergistic action of these oxidants. However, further investigation is warranted to gain a deeper understanding of this issue, as the achieved results (Chapter 5) were deemed insufficient.

Future publication: VILELA, Pâmela B. et al. *Coaction of sulfate and hydroxyl radicals in enhanced solar photo-Fenton: Tackling antimicrobial resistance via secondary wastewater post-treatment.*

- Objective 5: To compare the efficiency of solar photo-Fenton and enhanced solar photo-Fenton by (i) persulfate and (ii) binary oxidants system (H_2O_2 + $S_2O_8^{-2}$) in tackling antimicrobial resistance by removal of ARB and ARGs on pilot scale;

The successful completion of the comparison of solar photo-Fenton treatments in a pilot-scale CPC reactor provides compelling evidence for the potential of this approach for tackling antimicrobial resistance via secondary wastewater post-treatment. The results indicate that the solar photo-Fenton system implemented in the CPC reactor holds promise for wastewater disinfection, as it demonstrates efficient degradation and inactivation of ARB and ARGs. However, due to technical limitations, the specific role and mechanism of ROS in binary oxidants system (H_2O_2 + $S_2O_8^{-2}$) could not be fully determined in Chapter 4 and 5, necessitating further investigation.

Future publication: VILELA, Pâmela B. et al. *Tackling antimicrobial resistance via secondary wastewater post-treatment using enhanced solar photo Fenton at pilot scale.*

Future publication: VILELA, Pâmela B. et al. *Coaction of sulfate and hydroxyl radicals in enhanced solar photo-Fenton: Tackling antimicrobial resistance via secondary wastewater post-treatment.*

REFERENCES

2019 Antibacterial Agents. [s.l: s.n.].

ABDEL-MOATI, A. R. Adsorption of dissolved organic carbon (DOC) on glass fibre filters during particulate organic carbon (POC) determination. **Water Research**, *[S. l.]*, v. 24, n. 6, p. 763–764, 1990. DOI: 10.1016/0043-1354(90)90033-3.

ABDELRAHEEM, Wael H. M.; NADAGOUDA, Mallikarjuna N.; DIONYSIOU, Dionysios D. Solar light-assisted remediation of domestic wastewater by NB-TiO2 nanoparticles for potable reuse. **Applied Catalysis B: Environmental**, *[S. l.]*, v. 269, n. January, p. 118807, 2020. DOI: 10.1016/j.apcatb.2020.118807. Disponível em: https://doi.org/10.1016/j.apcatb.2020.118807.

ADEGOKE, Anthony A.; STENSTRÖM, Thor A.; OKOH, Anthony I. Stenotrophomonas maltophilia as an emerging ubiquitous pathogen: Looking beyond contemporary antibiotic therapy. **Frontiers in Microbiology**, *[S. l.]*, v. 8, n. NOV, p. 1–18, 2017. DOI: 10.3389/fmicb.2017.02276.

ADELEYE, Adeyemi S.; XUE, Jie; ZHAO, Yixin; TAYLOR, Alicia A.; ZENOBIO, Jenny E.; SUN, Yian; HAN, Ziwei; SALAWU, Omobayo A.; ZHU, Yurong. Abundance, fate, and effects of pharmaceuticals and personal care products in aquatic environments. **Journal of Hazardous Materials**, *[S. l.]*, v. 424, n. PB, p. 127284, 2022. DOI: 10.1016/j.jhazmat.2021.127284. Disponível em: https://doi.org/10.1016/j.jhazmat.2021.127284.

AGULLÓ-BARCELÓ, M.; POLO-LÓPEZ, M. I.; LUCENA, F.; JOFRE, J.; FERNÁNDEZ-IBÁÑEZ, P. Solar Advanced Oxidation Processes as disinfection tertiary treatments for real wastewater: Implications for water reclamation. **Applied Catalysis B: Environmental**, *[S. l.]*, v. 136–137, p. 341–350, 2013. DOI: 10.1016/j.apcatb.2013.01.069.

AHMED, Yunus; LU, Ji; YUAN, Zhiguo; BOND, Philip L.; GUO, Jianhua. Efficient inactivation of antibiotic resistant bacteria and antibiotic resistance genes by photo-Fenton process under visible LED light and neutral pH. **Water Research**, *[S. l.]*, v. 179, 2020. DOI: 10.1016/j.watres.2020.115878.

ALBANESE, Davide; FONTANA, Paolo; DE FILIPPO, Carlotta; CAVALIERI, Duccio; DONATI, Claudio. MICCA: A complete and accurate software for taxonomic profiling of metagenomic data. **Scientific Reports**, *[S. l.]*, v. 5, p. 1–7, 2015. DOI: 10.1038/srep09743.

ALEKSHUN, Michael N.; LEVY, Stuart B. Molecular Mechanisms of Antibacterial Multidrug Resistance. **Cell**, *[S. l.]*, v. 128, n. 6, p. 1037–1050, 2007. DOI: 10.1016/j.cell.2007.03.004.

ALYGIZAKIS, Nikiforos A. et al. Evaluation of chemical and biological contaminants of emerging concern in treated wastewater intended for agricultural reuse. **Environment International**, *[S. l.]*, v. 138, n. November 2019, p. 105597, 2020. DOI: 10.1016/j.envint.2020.105597. Disponível em: https://doi.org/10.1016/j.envint.2020.105597.

AMANOLLAHI, Hawzhin; MOUSSAVI, Gholamreza; GIANNAKIS, Stefanos. Enhanced vacuum UV-based process (VUV/H2O2/PMS) for the effective removal of

ammonia from water: Engineering configuration and mechanistic considerations. **Journal of Hazardous Materials**, *[S. l.]*, v. 402, n. August 2020, p. 123789, 2021. DOI: 10.1016/j.jhazmat.2020.123789. Disponível em: https://doi.org/10.1016/j.jhazmat.2020.123789.

AMARASIRI, Mohan; SANO, Daisuke; SUZUKI, Satoru. Understanding human health risks caused by antibiotic resistant bacteria (ARB) and antibiotic resistance genes (ARG) in water environments: Current knowledge and questions to be answered. **Critical Reviews in Environmental Science and Technology**, *[S. l.]*, v. 50, n. 19, p. 2016–2059, 2020. DOI: 10.1080/10643389.2019.1692611. Disponível em: https://doi.org/10.1080/10643389.2019.1692611.

AMINOV, Rustam I.; MACKIE, Roderick I. Evolution and ecology of antibiotic resistance genes. *[S. l.]*, v. 271, n. 2, p. 147–161, 2007. DOI: 10.1111/j.1574-6968.2007.00757.x.

ANDERSSON, Dan I.; HUGHES, Diarmaid. Microbiological effects of sublethal levels of antibiotics. **Nature Reviews Microbiology**, *[S. l.]*, v. 12, n. 7, p. 465–478, 2014. DOI: 10.1038/nrmicro3270.

ANIPSITAKIS, George P.; DIONYSIOU, Dionysios D. Radical generation by the interaction of transition metals with common oxidants. **Environmental Science and Technology**, *[S. l.]*, v. 38, n. 13, p. 3705–3712, 2004. DOI: 10.1021/es035121o.

ANTONELLI, Alberto; D'ANDREA, Marco Maria; VAGGELLI, Guendalina; DOCQUIER, Jean Denis; ROSSOLINI, Gian Maria. OXA-372, a novel carbapenem-hydrolysing class D β-lactamase from a Citrobacter freundii isolated from a hospital wastewater plant. **Journal of Antimicrobial Chemotherapy**, *[S. l.]*, v. 70, n. 10, p. 2749–2756, 2015. DOI: 10.1093/jac/dkv181.

APEL, Klaus; HIRT, Heribert. Reactive oxygen species: Metabolism, oxidative stress, and signal transduction. **Annual Review of Plant Biology**, *[S. l.]*, v. 55, p. 373–399, 2004. DOI: 10.1146/annurev.arplant.55.031903.141701.

ARSLAN-ALATON, Idil; KARATAS, Ayten; PEHLIVAN, Öznur; KOBA UCUN, Olga; ÖLMEZ-HANCI, Tugba. Effect of UV-A-assisted iron-based and UV-C-driven oxidation processes on organic matter and antibiotic resistance removal in tertiary treated urban wastewater. **Catalysis Today**, *[S. l.]*, 2020. DOI: 10.1016/j.cattod.2020.02.037.

AUTA, Asa; HADI, Muhammad Abdul; OGA, Enoche; ADEWUYI, Emmanuel O.; ABDU-AGUYE, Samirah N.; ADELOYE, Davies; STRICKLAND-HODGE, Barry; MORGAN, Daniel J. Global access to antibiotics without prescription in community pharmacies: A systematic review and meta-analysis. **Journal of Infection**, *[S. l.]*, v. 78, n. 1, p. 8–18, 2019. DOI: 10.1016/j.jinf.2018.07.001. Disponível em: https://doi.org/10.1016/j.jinf.2018.07.001.

BAEKKESKOV, Erik; RUBIN, Olivier; MUNKHOLM, Louise; ZAMAN, Wesal. Antimicrobial Resistance as a Global Health Crisis. **Oxford Research Encyclopedia of Politics**, *[S. l.]*, v. 2050, n. July, p. 1–23, 2020. DOI: 10.1093/acrefore/9780190228637.013.1626.

BAKER-AUSTIN, Craig; WRIGHT, Meredith S.; STEPANAUSKAS, Ramunas; MCARTHUR, J. V. Co-selection of antibiotic and metal resistance. **Trends in Microbiology**, *[S. l.]*, v. 14, n. 4, p. 176–182, 2006. DOI: 10.1016/j.tim.2006.02.006.

BAQUERO, Fernando; MARTÍNEZ, José Luis; CANTÓN, Rafael. Antibiotics and antibiotic resistance in water environments. *[S. l.]*, v. 19, n. 3, p. 260–265, 2008. DOI: 10.1016/j.copbio.2008.05.006.

BARANCHESHME, Fateme; MUNIR, Mariya. Strategies to combat antibiotic resistance in the wastewater treatment plants. **Frontiers in Microbiology**, *[S. l.]*, v. 8, n. JAN, 2018. DOI: 10.3389/fmicb.2017.02603.

BARARPOUR, S. Toufigh; FEYLIZADEH, Mohammad Reza; DELPARISH, Amin; QANBARZADEH, Mojtaba; RAEISZADEH, Milad; FEILIZADEH, Mehrzad. Investigation of 2-nitrophenol solar degradation in the simultaneous presence of K2S2O8 and H2O2: Using experimental design and artificial neural network. **Journal of Cleaner Production**, *[S. l.]*, v. 176, p. 1154–1162, 2018. DOI: 10.1016/j.jclepro.2017.11.191.

BARTLETT, John G. Nosocomial bloodstream infections in US hospitals: Analysis of 24,179 cases from a prospective nationwide surveillance study. **Infectious Diseases in Clinical Practice**, *[S. l.]*, v. 12, n. 6, p. 376, 2004. DOI: 10.1097/01.idc.0000144912.27311.19.

BASSETTI, Matteo; POULAKOU, Garyphallia; RUPPE, Etienne; BOUZA, Emilio; VAN HAL, Sebastian J.; BRINK, Adrian. Antimicrobial resistance in the next 30 years, humankind, bugs and drugs: a visionary approach. **Intensive Care Medicine**, *[S. l.]*, v. 43, n. 10, p. 1464–1475, 2017. DOI: 10.1007/s00134-017-4878-x.

BASTIAN, Mathieu; HEYMANN, Sebastien; JACOMY, M. Gephi: An open source software for exploring and manipulating networks. BT - International AAAI Conference on Weblogs and Social. **International AAAI Conference on Weblogs and Social Media**, *[S. l.]*, p. 361–362, 2009.

BENJAMINI, Yoav; HOCHBERG, Yosef. Controlling the False Discovery Rate: A Practical and Powerful Approach to Multiple Testing. **Journal of the Royal Statistical Society: Series B (Methodological)**, *[S. l.]*, v. 57, n. 1, p. 289–300, 1995. DOI: 10.1111/j.2517-6161.1995.tb02031.x.

BERENDONK, Thomas U. et al. Tackling antibiotic resistance: The environmental framework. **Nature Reviews Microbiology**, *[S. l.]*, v. 13, n. 5, p. 310–317, 2015. DOI: 10.1038/nrmicro3439.

BERNEY, M.; WEILENMANN, H. U.; SIMONETTI, A.; EGLI, T. Efficacy of solar disinfection of Escherichia coli, Shigella flexneri, Salmonella Typhimurium and Vibrio cholerae. **Journal of Applied Microbiology**, *[S. l.]*, v. 101, n. 4, p. 828–836, 2006. DOI: 10.1111/j.1365-2672.2006.02983.x.

BERRUTI, Ilaria; NAHIM-GRANADOS, Samira; ABELEDO-LAMEIRO, María Jesús; OLLER, Isabel; POLO-LÓPEZ, María Inmaculada. Recent advances in solar photochemical processes for water and wastewater disinfection. **Chemical Engineering Journal Advances**, *[S. l.]*, v. 10, n. January, 2022. DOI: 10.1016/j.ceja.2022.100248.

BIANCO, A.; POLO−LÓPEZ, M. I.; FERNÁNDEZ−IBÁÑEZ, P.; BRIGANTE, M.; MAILHOT, G. Disinfection of water inoculated with Enterococcus faecalis using solar/Fe(III)EDDS-H2O2 or S2O82− process. **Water Research**, *[S. l.]*, v. 118, p. 249–260, 2017. DOI: 10.1016/j.watres.2017.03.061.

BJARNSHOLT, Thomas et al. Pseudomonas aeruginosa tolerance to tobramycin, hydrogen peroxide and polymorphonuclear leukocytes is quorum-sensing dependent. **Microbiology**, *[S. l.]*, v. 151, n. 2, p. 373–383, 2005. DOI: 10.1099/mic.0.27463-0.

BLASCHKE, Anne J.; BENDER, Jeffrey; BYINGTON, Carrie L.; KORGENSKI, Kent; DALY, Judy; PETTI, Cathy A.; PAVIA, Andrew T.; AMPOFO, Krow. Gordonia species: Emerging pathogens in pediatric patients that are identified by 16S ribosomal RNA gene sequencing. **Clinical Infectious Diseases**, *[S. l.]*, v. 45, n. 4, p. 483–486, 2007. DOI: 10.1086/520018.

BOLGER, Anthony M.; LOHSE, Marc; USADEL, Bjoern. Trimmomatic: A flexible trimmer for Illumina sequence data. **Bioinformatics**, *[S. l.]*, v. 30, n. 15, p. 2114–2120, 2014. DOI: 10.1093/bioinformatics/btu170.

BONDARCZUK, Kinga; PIOTROWSKA-SEGET, Zofia. Microbial diversity and antibiotic resistance in a final effluent-receiving lake. **Science of the Total Environment**, *[S. l.]*, v. 650, p. 2951–2961, 2019. DOI: 10.1016/j.scitotenv.2018.10.050.

BONNIN, Rémy A.; ROTIMI, Vincent O.; AL HUBAIL, Mona; GASIOROWSKI, Elise; AL SWEIH, Noura; NORDMANN, Patrice; POIRELA, Laurent. Wide dissemination of GES-type carbapenemases in Acinetobacter baumannii isolates in Kuwait. **Antimicrobial Agents and Chemotherapy**, *[S. l.]*, v. 57, n. 1, p. 183–188, 2013. DOI: 10.1128/AAC.01384-12.

BONOMO, Robert A.; SZABO, Dora. Mechanisms of multidrug resistance in Acinetobacter species and Pseudomonas aeruginosa. **Clinical Infectious Diseases**, *[S. l.]*, v. 43, n. SUPPL. 2, p. 49–56, 2006. DOI: 10.1086/504477.

BORTOLAIA, Valeria et al. ResFinder 4.0 for predictions of phenotypes from genotypes. **Journal of Antimicrobial Chemotherapy**, *[S. l.]*, v. 75, n. 12, p. 3491–3500, 2020. DOI: 10.1093/jac/dkaa345.

BRACK, Werner et al. One planet: one health. A call to support the initiative on a global science–policy body on chemicals and waste. **Environmental Sciences Europe**, *[S. l.]*, v. 34, n. 1, 2022. DOI: 10.1186/s12302-022-00602-6. Disponível em: https://doi.org/10.1186/s12302-022-00602-6.

BRCAST. Brazilian Committee on Antimicrobial Susceptibility Testing - Tabelas de pontos de corte para interpretação de CIMs e diâmetros de halos. *[S. l.]*, p. 1–65, 2019. Disponível em: http://brcast.org.br/.

BUCKNER, Michelle M. C.; CIUSA, Maria Laura; PIDDOCK, Laura J. V. Strategies to combat antimicrobial resistance: Anti-plasmid and plasmid curing. **FEMS Microbiology Reviews**, *[S. l.]*, v. 42, n. 6, p. 781–804, 2018. DOI: 10.1093/femsre/fuy031.

BUSH, Karen; JACOBY, George A. Updated functional classification of β-lactamases. **Antimicrobial Agents and Chemotherapy**, *[S. l.]*, v. 54, n. 3, p. 969–976, 2010. DOI: 10.1128/AAC.01009-09.

CACACE, Damiano et al. Antibiotic resistance genes in treated wastewater and in the receiving water bodies: A pan-European survey of urban settings. **Water Research**, *[S. l.]*, v. 162, p. 320–330, 2019. DOI: 10.1016/j.watres.2019.06.039. Disponível em: https://doi.org/10.1016/j.watres.2019.06.039.

CAMACHO, Christiam; COULOURIS, George; AVAGYAN, Vahram; MA, Ning; PAPADOPOULOS, Jason; BEALER, Kevin; MADDEN, Thomas L. BLAST+: Architecture and applications. **BMC Bioinformatics**, *[S. l.]*, v. 10, p. 1–9, 2009. DOI: 10.1186/1471-2105-10-421.

CANDEIAS, Luis P.; STEENKEN, Steen. Reaction of HO· with Guanine derivatives in aqueous solution: Formation of two different redox-active OH-adduct radicals and their unimolecular transformation reactions. Properties of G(-H)·. **Chemistry - A European Journal**, *[S. l.]*, v. 6, n. 3, p. 475–484, 2000. DOI: 10.1002/(SICI)1521-3765(20000204)6:3<475::AID-CHEM475>3.0.CO;2-E.

CANTÓN, Rafael; RUIZ-GARBAJOSA, Patricia. Co-resistance: An opportunity for the bacteria and resistance genes. **Current Opinion in Pharmacology**, *[S. l.]*, v. 11, n. 5, p. 477–485, 2011. DOI: 10.1016/j.coph.2011.07.007.

CARRA, I.; CASAS LÓPEZ, J. L.; SANTOS-JUANES, L.; MALATO, S.; SÁNCHEZ PÉREZ, J. A. Iron dosage as a strategy to operate the photo-Fenton process at initial neutral pH. **Chemical Engineering Journal**, *[S. l.]*, v. 224, n. 1, p. 67–74, 2013. DOI: 10.1016/j.cej.2012.09.065. Disponível em: http://dx.doi.org/10.1016/j.cej.2012.09.065.

CARRA, I.; MALATO, S.; JIMÉNEZ, M.; MALDONADO, M. I.; SÁNCHEZ PÉREZ, J. A. Microcontaminant removal by solar photo-Fenton at natural pH run with sequential and continuous iron additions. **Chemical Engineering Journal**, *[S. l.]*, v. 235, p. 132–140, 2014. DOI: 10.1016/j.cej.2013.09.029. Disponível em: http://dx.doi.org/10.1016/j.cej.2013.09.029.

CASTRO-ALFÉREZ, María; POLO-LÓPEZ, María Inmaculada; MARUGÁN, Javier; FERNÁNDEZ-IBÁÑEZ, Pilar. Mechanistic modeling of UV and mild-heat synergistic effect on solar water disinfection. **Chemical Engineering Journal**, *[S. l.]*, v. 316, p. 111–120, 2017. DOI: 10.1016/j.cej.2017.01.026.

CHAN, Weng Tat; VERMA, Chandra S.; LANE, David P.; GAN, Samuel Ken En. A comparison and optimization of methods and factors affecting the transformation of Escherichia coli. **Bioscience Reports**, *[S. l.]*, v. 33, n. 6, 2013. DOI: 10.1042/BSR20130098.

CHEN, Chuncheng; MA, Wanhong; ZHAO, Jincai. Semiconductor-mediated photodegradation of pollutants under visible-light irradiation. **Chemical Society Reviews**, *[S. l.]*, v. 39, n. 11, p. 4206–4219, 2010. DOI: 10.1039/b921692h.

CHEN, Yi Di; DUAN, Xiaoguang; ZHOU, Xu; WANG, Rupeng; WANG, Shaobin; REN, Nan qi; HO, Shih Hsin. Advanced oxidation processes for water disinfection: Features, mechanisms and prospects. **Chemical Engineering Journal**, *[S. l.]*, v. 409, n. August 2020, p. 128207, 2021. DOI: 10.1016/j.cej.2020.128207. Disponível em: https://doi.org/10.1016/j.cej.2020.128207.

CHENG, Xiaoxiao; XU, Jiannong; SMITH, Geoffrey; ZHANG, Yanyan. Metagenomic insights into dissemination of antibiotic resistance across bacterial genera in wastewater treatment. **Chemosphere**, *[S. l.]*, v. 271, p. 129563, 2021. DOI: 10.1016/j.chemosphere.2021.129563. Disponível em: https://doi.org/10.1016/j.chemosphere.2021.129563.

CHOW, Louise K. M.; GHALY, Timothy M.; GILLINGS, Michael R. A survey of sub-inhibitory concentrations of antibiotics in the environment. **Journal of Environmental**

Sciences (China), *[S. l.]*, v. 99, p. 21–27, 2021. DOI: 10.1016/j.jes.2020.05.030. Disponível em: https://doi.org/10.1016/j.jes.2020.05.030.

CHU, W.; WANG, Y. R.; LEUNG, H. F. Synergy of sulfate and hydroxyl radicals in UV/S2O82-/H2O2 oxidation of iodinated X-ray contrast medium iopromide. **Chemical Engineering Journal**, *[S. l.]*, v. 178, p. 154–160, 2011. DOI: 10.1016/j.cej.2011.10.033. Disponível em: http://dx.doi.org/10.1016/j.cej.2011.10.033.

CLARA, Maria; STARLING, V. M.; MENDONÇA, Rondon P. De; PIRES, Giovanna F. F.; BECCALLI, Pâmela; AMORIM, Camila C. Science of the Total Environment Combat of antimicrobial resistance in municipal wastewater treatment plant ef fl uent via solar advanced oxidation processes : Achievements and perspectives. **Science of the Total Environment**, *[S. l.]*, v. 786, p. 147448, 2021. DOI: 10.1016/j.scitotenv.2021.147448. Disponível em: https://doi.org/10.1016/j.scitotenv.2021.147448.

CLARIZIA, L.; RUSSO, D.; DI SOMMA, I.; MAROTTA, R.; ANDREOZZI, R. Homogeneous photo-Fenton processes at near neutral pH: A review. **Applied Catalysis B: Environmental**, *[S. l.]*, v. 209, p. 358–371, 2017. DOI: 10.1016/j.apcatb.2017.03.011. Disponível em: http://dx.doi.org/10.1016/j.apcatb.2017.03.011.

COLE, James R. et al. Ribosomal Database Project: Data and tools for high throughput rRNA analysis. **Nucleic Acids Research**, *[S. l.]*, v. 42, n. D1, p. 633–642, 2014. DOI: 10.1093/nar/gkt1244.

COLLIGNON, Peter J.; MCEWEN, Scott A. One health-its importance in helping to better control antimicrobial resistance. **Tropical Medicine and Infectious Disease**, *[S. l.]*, v. 4, n. 1, 2019. DOI: 10.3390/tropicalmed4010022.

COSTA, Elizangela P.; ROCCAMANTE, Melina; AMORIM, Camila C.; OLLER, Isabel; SÁNCHEZ PÉREZ, José A.; MALATO, Sixto. New trend on open solar photoreactors to treat micropollutants by photo-Fenton at circumneutral pH: Increasing optical pathway. **Chemical Engineering Journal**, *[S. l.]*, v. 385, n. September 2019, p. 123982, 2020. DOI: 10.1016/j.cej.2019.123982. Disponível em: https://doi.org/10.1016/j.cej.2019.123982.

COSTA, Elizangela P.; ROCCAMANTE, Melina; PLAZA-BOLAÑOS, Patricia; OLLER, Isabel; AGÜERA, Ana; AMORIM, Camila C.; MALATO, Sixto. Aluminized surface to improve solar light absorption in open reactors: Application for micropollutants removal in effluents from municipal wastewater treatment plants. **Science of the Total Environment**, *[S. l.]*, v. 755, p. 142624, 2021. DOI: 10.1016/j.scitotenv.2020.142624. Disponível em: https://doi.org/10.1016/j.scitotenv.2020.142624.

COSTA, Elizângela Pinheiro; STARLING, Maria Clara Vieira Martins; AMORIM, Camila C. Simultaneous removal of emerging contaminants and disinfection for municipal wastewater treatment plant effluent quality improvement: a systemic analysis of the literature. **Environmental Science and Pollution Research**, *[S. l.]*, v. 28, n. 19, p. 24092–24111, 2021. DOI: 10.1007/s11356-021-12363-5.

CRIMI, Michelle L.; TAYLOR, Jesse. Experimental evaluation of catalyzed hydrogen peroxide and sodium persulfate for destruction of BTEX contaminants. **Soil and Sediment Contamination**, *[S. l.]*, v. 16, n. 1, p. 29–45, 2007. DOI: 10.1080/15320380601077792.

DA CUNHA, Camila Cristina Rodrigues Ferreira; FREITAS, Mylena Gomes; DA SILVA RODRIGUES, Daniel Aparecido; DE BARROS, André Luis Correa; RIBEIRO, Marcelo Carlos; SANSON, Ananda Lima; AFONSO, Robson José de Cássia Franco. Low-temperature partitioning extraction followed by liquid chromatography tandem mass spectrometry determination of multiclass antibiotics in solid and soluble wastewater fractions. **Journal of Chromatography A**, *[S. l.]*, v. 1650, p. 462256, 2021. DOI: 10.1016/j.chroma.2021.462256. Disponível em: https://doi.org/10.1016/j.chroma.2021.462256.

DA SILVA, Romário Justino; MACIEL, Bruna Gomes; MEDINA-LLAMAS, Juan Carlos; CHÁVEZ-GUAJARDO, Alicia Elizabeth; ALCARAZ-ESPINOZA, José Jarib; PINTO DE MELO, Celso. Extraction of plasmid DNA by use of a magnetic maghemite-polyaniline nanocomposite. **Analytical Biochemistry**, *[S. l.]*, v. 575, n. November 2018, p. 27–35, 2019. DOI: 10.1016/j.ab.2019.03.013. Disponível em: https://doi.org/10.1016/j.ab.2019.03.013.

DANNER, Marie Claire; ROBERTSON, Anne; BEHRENDS, Volker; REISS, Julia. Antibiotic pollution in surface fresh waters: Occurrence and effects. **Science of the Total Environment**, *[S. l.]*, v. 664, p. 793–804, 2019. DOI: 10.1016/j.scitotenv.2019.01.406. Disponível em: https://doi.org/10.1016/j.scitotenv.2019.01.406.

DAUGHTON, Christian G. Non-regulated water contaminants: Emerging research. **Environmental Impact Assessment Review**, *[S. l.]*, v. 24, n. 7–8, p. 711–732, 2004. DOI: 10.1016/j.eiar.2004.06.003.

DAVIES, J. Origins and evolution of antibiotic resistance. **Microbiología (Madrid, Spain)**, *[S. l.]*, v. 12, n. 1, p. 9–16, 1996. DOI: 10.1128/mmbr.00016-10.

DAVIES, K. J. Protein damage and degradation by oxygen radicals. I. general aspects. **Journal of Biological Chemistry**, *[S. l.]*, v. 262, n. 20, p. 9895–9901, 1987. DOI: 10.1016/s0021-9258(18)48018-0. Disponível em: http://dx.doi.org/10.1016/S0021-9258(18)48018-0.

DE CELIS, Miguel; BELDA, Ignacio; ORTIZ-ÁLVAREZ, Rüdiger; ARREGUI, Lucía; MARQUINA, Domingo; SERRANO, Susana; SANTOS, Antonio. Tuning up microbiome analysis to monitor WWTPs' biological reactors functioning. **Scientific Reports**, *[S. l.]*, v. 10, n. 1, p. 1–9, 2020. DOI: 10.1038/s41598-020-61092-1.

DE LA OBRA JIMÉNEZ, I.; LÓPEZ, J. L. Casa.; IBÁÑEZ, G. Rivas; GARCÍA, B. Esteban; PÉREZ, J. A. Sánche. Kinetic assessment of antibiotic resistant bacteria inactivation by solar photo-Fenton in batch and continuous flow mode for wastewater reuse. **Water Research**, *[S. l.]*, v. 159, p. 184–191, 2019. DOI: 10.1016/j.watres.2019.04.059.

DE PAIVA, Lílian Cardoso; DINIZ, Raphael Hermano Santos; VIDIGAL, Pedro Marcus Pereira; MENDES, Tiago Antônio de Oliveira; SANTANA, Mateus Ferreira; CERDÁN, María Esperanza; GONZÁLEZ-SISO, María Isabel; SILVEIRA, Wendel Batista Da. Genomic analysis and lactose transporter expression in Kluyveromyces marxianus CCT 7735. **Fungal Biology**, *[S. l.]*, v. 123, n. 9, p. 687–697, 2019. DOI: 10.1016/j.funbio.2019.06.004.

DEVI, Parmila; DAS, Umashankar; DALAI, Ajay K. In-situ chemical oxidation: Principle and applications of peroxide and persulfate treatments in wastewater systems.

Science of the Total Environment, *[S. l.]*, v. 571, p. 643–657, 2016. DOI: 10.1016/j.scitotenv.2016.07.032. Disponível em: http://dx.doi.org/10.1016/j.scitotenv.2016.07.032.

DI CESARE, Andrea; CORNO, Gianluca; MANAIA, Célia M.; RIZZO, Luigi. Impact of disinfection processes on bacterial community in urban wastewater: Should we rethink microbial assessment methods? **Journal of Environmental Chemical Engineering**, *[S. l.]*, v. 8, n. 5, 2020. DOI: 10.1016/j.jece.2020.104393.

DI CESARE, Andrea; FONTANETO, Diego; DOPPELBAUER, Julia; CORNO, Gianluca. Fitness and Recovery of Bacterial Communities and Antibiotic Resistance Genes in Urban Wastewaters Exposed to Classical Disinfection Treatments. **Environmental Science and Technology**, *[S. l.]*, v. 50, n. 18, p. 10153–10161, 2016. DOI: 10.1021/acs.est.6b02268.

DIAS, Marcela França; LEROY-FREITAS, Deborah; MACHADO, Elayne Cristina; DA SILVA SANTOS, Leticia; LEAL, Cintia Dutra; DA ROCHA FERNANDES, Gabriel; DE ARAÚJO, Juliana Calábria. Effects of activated sludge and UV disinfection processes on the bacterial community and antibiotic resistance profile in a municipal wastewater treatment plant. **Environmental Science and Pollution Research**, *[S. l.]*, v. 29, n. 24, p. 36088–36099, 2022. DOI: 10.1007/s11356-022-18749-3. Disponível em: https://doi.org/10.1007/s11356-022-18749-3.

DÍAZ-ANGULO, Jennyfer; COTILLAS, Salvador; GOMES, Ana I.; MIRANDA, Sandra M.; MUESES, Miguel; MACHUCA-MARTÍNEZ, Fiderman; RODRIGO, Manuel A.; BOAVENTURA, Rui A. R.; VILAR, Vítor J. P. A tube-in-tube membrane microreactor for tertiary treatment of urban wastewaters by photo-Fenton at neutral pH: A proof of concept. **Chemosphere**, *[S. l.]*, v. 263, p. 128049, 2021. DOI: 10.1016/j.chemosphere.2020.128049. Disponível em: https://doi.org/10.1016/j.chemosphere.2020.128049.

DINOS, George P. The macrolide antibiotic renaissance. **British Journal of Pharmacology**, *[S. l.]*, v. 174, n. 18, p. 2967–2983, 2017. DOI: 10.1111/bph.13936.

DONG, Huiyu; YUAN, Xiangjuan; WANG, Weidong; QIANG, Zhimin. Occurrence and removal of antibiotics in ecological and conventional wastewater treatment processes: A field study. **Journal of Environmental Management**, *[S. l.]*, v. 178, p. 11–19, 2016. DOI: 10.1016/j.jenvman.2016.04.037. Disponível em: http://dx.doi.org/10.1016/j.jenvman.2016.04.037.

DONG, Peiyan; WANG, Hui; FANG, Tingting; WANG, Yun; YE, Quanhui. Assessment of extracellular antibiotic resistance genes (eARGs) in typical environmental samples and the transforming ability of eARG. **Environment International**, *[S. l.]*, v. 125, n. January, p. 90–96, 2019. DOI: 10.1016/j.envint.2019.01.050. Disponível em: https://doi.org/10.1016/j.envint.2019.01.050.

DOS SANTOS, Alexsandro Jhones; BRILLAS, Enric; CABOT, Pere L.; SIRÉS, Ignasi. Simultaneous persulfate activation by electrogenerated H2O2 and anodic oxidation at a boron-doped diamond anode for the treatment of dye solutions. **Science of the Total Environment**, *[S. l.]*, v. 747, p. 141541, 2020. DOI: 10.1016/j.scitotenv.2020.141541. Disponível em: https://doi.org/10.1016/j.scitotenv.2020.141541.

DUA, Kamal et al. Multi-drug resistant Mycobacterium tuberculosis & oxidative stress complexity: Emerging need for novel drug delivery approaches. **Biomedicine and**

Pharmacotherapy, *[S. l.]*, v. 107, n. June, p. 1218–1229, 2018. DOI: 10.1016/j.biopha.2018.08.101.

EBELE, Anekwe Jennifer; ABOU-ELWAFA ABDALLAH, Mohamed; HARRAD, Stuart. Pharmaceuticals and personal care products (PPCPs) in the freshwater aquatic environment. **Emerging Contaminants**, *[S. l.]*, v. 3, n. 1, p. 1–16, 2017. DOI: 10.1016/j.emcon.2016.12.004. Disponível em: http://dx.doi.org/10.1016/j.emcon.2016.12.004.

ECKERT, Ester M. et al. Every fifth published metagenome is not available to science. **PLoS Biology**, *[S. l.]*, v. 18, n. 4, p. 1–7, 2020. DOI: 10.1371/journal.pbio.3000698.

EMAMALIPOUR, Melissa et al. Horizontal Gene Transfer: From Evolutionary Flexibility to Disease Progression. **Frontiers in Cell and Developmental Biology**, *[S. l.]*, v. 8, n. May, 2020. DOI: 10.3389/fcell.2020.00229.

EPOLD, Irina; DULOVA, Niina. Oxidative degradation of levofloxacin in aqueous solution by S2O82-/Fe2+, S2O82-/H2O2 and S2O82-/OH- processes: A comparative study. **Journal of Environmental Chemical Engineering**, *[S. l.]*, v. 3, n. 2, p. 1207–1214, 2015. DOI: 10.1016/j.jece.2015.04.019. Disponível em: http://dx.doi.org/10.1016/j.jece.2015.04.019.

EPOLD, Irina; TRAPIDO, Marina; DULOVA, Niina. Degradation of levofloxacin in aqueous solutions by Fenton, ferrous ion-activated persulfate and combined Fenton/persulfate systems. **Chemical Engineering Journal**, *[S. l.]*, v. 279, p. 452–462, 2015. DOI: 10.1016/j.cej.2015.05.054. Disponível em: http://dx.doi.org/10.1016/j.cej.2015.05.054.

EUCAST. Definitions of “Expected Phenotypes” Expected Phenotypes. *[S. l.]*, n. October 2021, p. 5–8, 2022.

FANNER, Susan; LI, Zusheng; HANCOCK, Robert E. W. Coti To the Dibasic Macroh ’ De Azithromycin. *[S. l.]*, p. 27–33, 1992.

FATTA-KASSINOS, Despo et al. COST Action ES1403: New and Emerging challenges and opportunities in wastewater REUSe (NEREUS). **Environmental Science and Pollution Research**, *[S. l.]*, v. 22, n. 9, p. 7183–7186, 2015. DOI: 10.1007/s11356-015-4278-0.

FATTA-KASSINOS, Despo; MERIC, Sureyya; NIKOLAOU, Anastasia. Pharmaceutical residues in environmental waters and wastewater: Current state of knowledge and future research. **Analytical and Bioanalytical Chemistry**, *[S. l.]*, v. 399, n. 1, p. 251–275, 2011. DOI: 10.1007/s00216-010-4300-9.

FENG, Ling; PEILLEX-DELPHE, Céline; LÜ, Changwei; WANG, Da; GIANNAKIS, Stefanos; PULGARIN, Cesar. Employing bacterial mutations for the elucidation of photo-Fenton disinfection: Focus on the intracellular and extracellular inactivation mechanisms induced by UVA and H2O2. **Water Research**, *[S. l.]*, v. 182, 2020. DOI: 10.1016/j.watres.2020.116049.

FERNANDES, Telma; VAZ-MOREIRA, Ivone; MANAIA, Célia M. Neighbor urban wastewater treatment plants display distinct profiles of bacterial community and antibiotic resistance genes. **Environmental Science and Pollution Research**, *[S. l.]*, v. 26, n. 11, p. 11269–11278, 2019. DOI: 10.1007/s11356-019-04546-y.

FERRO, Giovanna; FIORENTINO, Antonino; ALFEREZ, María Castro; POLO-LÓPEZ,

M. Inmaculada; RIZZO, Luigi; FERNÁNDEZ-IBÁÑEZ, Pilar. Urban wastewater disinfection for agricultural reuse: effect of solar driven AOPs in the inactivation of a multidrug resistant E. coli strain. **Applied Catalysis B: Environmental**, *[S. l.]*, v. 178, p. 65–73, 2015. DOI: 10.1016/j.apcatb.2014.10.043.

FERRO, Giovanna; GUARINO, Francesco; CASTIGLIONE, Stefano; RIZZO, Luigi. Antibiotic resistance spread potential in urban wastewater effluents disinfected by UV/H2O2 process. **Science of the Total Environment**, *[S. l.]*, v. 560–561, p. 29–35, 2016. DOI: 10.1016/j.scitotenv.2016.04.047. Disponível em: http://dx.doi.org/10.1016/j.scitotenv.2016.04.047.

FILIPPIDOU, Sevasti; WUNDERLIN, Tina; JUNIER, Thomas; JEANNERET, Nicole; DORADOR, Cristina; MOLINA, Veronica; JOHNSON, David R.; JUNIER, Pilar. A combination of extreme environmental conditions favor the prevalence of endospore-forming firmicutes. **Frontiers in Microbiology**, *[S. l.]*, v. 7, n. NOV, p. 1–11, 2016. DOI: 10.3389/fmicb.2016.01707.

FIORENTINO, Antonino; ESTEBAN, Belén; GARRIDO-CARDENAS, José Antonio; KOWALSKA, Katarzyna; RIZZO, Luigi; AGUERA, Ana; PÉREZ, José Antonio Sánchez. Effect of solar photo-Fenton process in raceway pond reactors at neutral pH on antibiotic resistance determinants in secondary treated urban wastewater. **Journal of Hazardous Materials**, *[S. l.]*, v. 378, n. April, p. 120737, 2019. a. DOI: 10.1016/j.jhazmat.2019.06.014. Disponível em: https://doi.org/10.1016/j.jhazmat.2019.06.014.

FIORENTINO, Antonino; ESTEBAN, Belén; GARRIDO-CARDENAS, José Antonio; KOWALSKA, Katarzyna; RIZZO, Luigi; AGUERA, Ana; PÉREZ, José Antonio Sánchez. Effect of solar photo-Fenton process in raceway pond reactors at neutral pH on antibiotic resistance determinants in secondary treated urban wastewater. **Journal of Hazardous Materials**, *[S. l.]*, v. 378, n. April, p. 120737, 2019. b. DOI: 10.1016/j.jhazmat.2019.06.014. Disponível em: https://doi.org/10.1016/j.jhazmat.2019.06.014.

FIORENTINO, Antonino; FERRO, Giovanna; ALFEREZ, María Castro; POLO-LÓPEZ, Maria Inmaculada; FERNÁNDEZ-IBAÑEZ, Pilar; RIZZO, Luigi. Inactivation and regrowth of multidrug resistant bacteria in urban wastewater after disinfection by solar-driven and chlorination processes. **Journal of Photochemistry and Photobiology B: Biology**, *[S. l.]*, v. 148, p. 43–50, 2015. DOI: 10.1016/j.jphotobiol.2015.03.029. Disponível em: http://dx.doi.org/10.1016/j.jphotobiol.2015.03.029.

GANIYU, Soliu Oladejo; SABLE, Shailesh; GAMAL EL-DIN, Mohamed. Advanced oxidation processes for the degradation of dissolved organics in produced water: A review of process performance, degradation kinetics and pathway. **Chemical Engineering Journal**, *[S. l.]*, v. 429, n. June 2021, p. 132492, 2022. DOI: 10.1016/j.cej.2021.132492. Disponível em: https://doi.org/10.1016/j.cej.2021.132492.

GAO, Jing Feng; DUAN, Wan Jun; ZHANG, Wen Zhi; WU, Zhi Long. Effects of persulfate treatment on antibiotic resistance genes abundance and the bacterial community in secondary effluent. **Chemical Engineering Journal**, *[S. l.]*, v. 382, n. May 2019, p. 121860, 2020. DOI: 10.1016/j.cej.2019.05.221. Disponível em: https://doi.org/10.1016/j.cej.2019.05.221.

GARNER, Emily et al. Next generation sequencing approaches to evaluate water and

wastewater quality. **Water Research**, *[S. l.]*, v. 194, p. 116907, 2021. DOI: 10.1016/j.watres.2021.116907. Disponível em: https://doi.org/10.1016/j.watres.2021.116907.

GIANNAKIS, Stefanos. Analogies and differences among bacterial and viral disinfection by the photo-Fenton process at neutral pH: a mini review. **Environmental Science and Pollution Research**, *[S. l.]*, v. 25, n. 28, p. 27676–27692, 2018. a. DOI: 10.1007/s11356-017-0926-x.

GIANNAKIS, Stefanos. Analogies and differences among bacterial and viral disinfection by the photo-Fenton process at neutral pH: a mini review. **Environmental Science and Pollution Research**, *[S. l.]*, v. 25, n. 28, p. 27676–27692, 2018. b. DOI: 10.1007/s11356-017-0926-x.

GIANNAKIS, Stefanos; LE, Truong Thien Melvin; ENTENZA, Jose Manuel; PULGARIN, Cesar. Solar photo-Fenton disinfection of 11 antibiotic-resistant bacteria (ARB) and elimination of representative AR genes. Evidence that antibiotic resistance does not imply resistance to oxidative treatment. **Water Research**, *[S. l.]*, v. 143, p. 334–345, 2018. a. DOI: 10.1016/j.watres.2018.06.062. Disponível em: https://doi.org/10.1016/j.watres.2018.06.062.

GIANNAKIS, Stefanos; LÓPEZ, María Inmaculada Polo; SPUHLER, Dorothee; PÉREZ, José Antonio Sánchez; IBÁÑEZ, Pilar Fernández; PULGARIN, César. Solar disinfection is an augmentable, in situ-generated photo-Fenton reaction-Part 2: A review of the applications for drinking water and wastewater disinfection. **Applied Catalysis B: Environmental**, *[S. l.]*, v. 198, p. 431–446, 2016. a. DOI: 10.1016/j.apcatb.2016.06.007.

GIANNAKIS, Stefanos; POLO LÓPEZ, María Inmaculada; SPUHLER, Dorothee; SÁNCHEZ PÉREZ, Jose Antonio; FERNÁNDEZ IBÁÑEZ, Pilar; PULGARIN, César. Solar disinfection is an augmentable, in situ-generated photo-Fenton reaction—Part 1: A review of the mechanisms and the fundamental aspects of the process. **Applied Catalysis B: Environmental**, *[S. l.]*, v. 199, p. 199–223, 2016. b. DOI: 10.1016/j.apcatb.2016.06.009.

GIANNAKIS, Stefanos; WATTS, Samuel; RTIMI, Sami; PULGARIN, Cesar. Solar light and the photo-Fenton process against antibiotic resistant bacteria in wastewater: A kinetic study with a Streptomycin-resistant strain. **Catalysis Today**, *[S. l.]*, v. 313, n. October 2017, p. 86–93, 2018. b. DOI: 10.1016/j.cattod.2017.10.033. Disponível em: https://doi.org/10.1016/j.cattod.2017.10.033.

GIL-GIL, Teresa; LABORDA, Pablo; SANZ-GARCÍA, Fernando; HERNANDO-AMADO, Sara; BLANCO, Paula; MARTÍNEZ, José Luis. Antimicrobial resistance: A multifaceted problem with multipronged solutions. **MicrobiologyOpen**, *[S. l.]*, v. 8, n. 11, p. 1–4, 2019. DOI: 10.1002/mbo3.945.

GIL-GIL, Teresa; MARTÍNEZ, José Luis; BLANCO, Paula. Mechanisms of antimicrobial resistance in Stenotrophomonas maltophilia: a review of current knowledge. **Expert Review of Anti-Infective Therapy**, *[S. l.]*, v. 18, n. 4, p. 335–347, 2020. DOI: 10.1080/14787210.2020.1730178. Disponível em: https://doi.org/10.1080/14787210.2020.1730178.

GIULIERI, Stefano G. et al. Comprehensive genomic investigation of adaptive mutations driving the low-level oxacillin resistance phenotype in staphylococcus

aureus. **mBio**, *[S. l.]*, v. 11, n. 6, p. 1–18, 2020. DOI: 10.1128/mBio.02882-20.

GOKCEZADE, Joseph; SIENSKI, Grzegorz; DUCHEK, Peter. Efficient CRISPR/Cas9 plasmids for rapid and versatile genome editing in Drosophila. **G3: Genes, Genomes, Genetics**, *[S. l.]*, v. 4, n. 11, p. 2279–2282, 2014. DOI: 10.1534/g3.114.014126.

GOMES, Cláudia; MARTÍNEZ-PUCHOL, Sandra; PALMA, Noemí; HORNA, Gertrudis; RUIZ-ROLDÁN, Lidia; PONS, Maria J.; RUIZ, Joaquim. Macrolide resistance mechanisms in Enterobacteriaceae: Focus on azithromycin. **Critical Reviews in Microbiology**, *[S. l.]*, v. 43, n. 1, p. 1–30, 2017. DOI: 10.3109/1040841X.2015.1136261. Disponível em: http://dx.doi.org/10.3109/1040841X.2015.1136261.

GOOD, I. J. The Population Frequencies of Species and the Estimation of Population Parameters. **Biometrika**, *[S. l.]*, v. 40, n. 3/4, p. 237, 1953. DOI: 10.2307/2333344.

GOU, Yaling; ZHAO, Qianyun; YANG, Sucai; WANG, Hongqi; QIAO, Pengwei; SONG, Yun; CHENG, Yanjun; LI, Peizhong. Removal of polycyclic aromatic hydrocarbons (PAHs) and the response of indigenous bacteria in highly contaminated aged soil after persulfate oxidation. **Ecotoxicology and Environmental Safety**, *[S. l.]*, v. 190, n. September 2019, p. 110092, 2020. DOI: 10.1016/j.ecoenv.2019.110092. Disponível em: https://doi.org/10.1016/j.ecoenv.2019.110092.

GOVINDARAJ VAITHINATHAN, Asokan; VANITHA, A. WHO global priority pathogens list on antibiotic resistance: an urgent need for action to integrate One Health data. **Perspectives in Public Health**, *[S. l.]*, v. 138, n. 2, p. 87–88, 2018. DOI: 10.1177/1757913917743881.

GUAN, Ying Hong; MA, Jun; LI, Xu Chun; FANG, Jing Yun; CHEN, Li Wei. Influence of pH on the formation of sulfate and hydroxyl radicals in the UV/Peroxymonosulfate system. **Environmental Science and Technology**, *[S. l.]*, v. 45, n. 21, p. 9308–9314, 2011. DOI: 10.1021/es2017363.

GUO, Jianhua; NI, Bing Jie; HAN, Xiaoyu; CHEN, Xueming; BOND, Philip; PENG, Yongzhen; YUAN, Zhiguo. Unraveling microbial structure and diversity of activated sludge in a full-scale simultaneous nitrogen and phosphorus removal plant using metagenomic sequencing. **Enzyme and Microbial Technology**, *[S. l.]*, v. 102, n. March, p. 16–25, 2017. DOI: 10.1016/j.enzmictec.2017.03.009. Disponível em: http://dx.doi.org/10.1016/j.enzmictec.2017.03.009.

GUO, Jianhua; WANG, Yue; AHMED, Yunus; JIN, Min; LI, Jie. Control Strategies to Combat Dissemination of Antibiotic Resistance in Urban Water Systems. **Handbook of Environmental Chemistry**, *[S. l.]*, v. 91, p. 147–187, 2020. DOI: 10.1007/698_2020_474.

GUO, Mei Ting; YUAN, Qing Bin; YANG, Jian. Microbial selectivity of UV treatment on antibiotic-resistant heterotrophic bacteria in secondary effluents of a municipal wastewater treatment plant. **Water Research**, *[S. l.]*, v. 47, n. 16, p. 6388–6394, 2013. DOI: 10.1016/j.watres.2013.08.012. Disponível em: http://dx.doi.org/10.1016/j.watres.2013.08.012.

GUO, Mei Ting; YUAN, Qing Bin; YANG, Jian. Distinguishing effects of ultraviolet exposure and chlorination on the horizontal transfer of antibiotic resistance genes in municipal wastewater. **Environmental Science and Technology**, *[S. l.]*, v. 49, n. 9,

p. 5771–5778, 2015. DOI: 10.1021/acs.est.5b00644.

GUPTA, Sushim Kumar; PADMANABHAN, Babu Roshan; DIENE, Seydina M.; LOPEZ-ROJAS, Rafael; KEMPF, Marie; LANDRAUD, Luce; ROLAIN, Jean Marc. ARG-annot, a new bioinformatic tool to discover antibiotic resistance genes in bacterial genomes. **Antimicrobial Agents and Chemotherapy**, *[S. l.]*, v. 58, n. 1, p. 212–220, 2014. DOI: 10.1128/AAC.01310-13.

GWENZI, Willis; MUSIYIWA, Kumbirai; MANGORI, Lynda. Sources, behaviour and health risks of antimicrobial resistance genes in wastewaters: A hotspot reservoir. **Journal of Environmental Chemical Engineering**, *[S. l.]*, v. 8, n. 1, p. 102220, 2020. DOI: 10.1016/j.jece.2018.02.028. Disponível em: https://doi.org/10.1016/j.jece.2018.02.028.

HAO, Mingju; HE, Yuzhang; ZHANG, Haifang; LIAO, Xiao Ping; LIU, Ya Hong; SUN, Jian; DU, Hong; KREISWIRTH, Barry N.; CHEN, Liang. CRISPR-Cas9-mediated carbapenemase gene and plasmid curing in carbapenem-resistant enterobacteriaceae. **Antimicrobial Agents and Chemotherapy**, *[S. l.]*, v. 64, n. 9, 2020. DOI: 10.1128/AAC.00843-20.

HAQUE, Mainul; SARTELLI, Massimo; MCKIMM, Judy; ABU BAKAR, Muhamad. Infection and Drug Resistance Dovepress Health care-associated infections-an overview. **Infection and Drug Resistance**, *[S. l.]*, v. 11, n. 1, p. 2321–2333, 2018. Disponível em: http://dx.doi.org/10.2147/IDR.S177247.

HAVENGA, Benjamin; NDLOVU, Thando; CLEMENTS, Tanya; REYNEKE, Brandon; WASO, Monique; KHAN, Wesaal. Exploring the antimicrobial resistance profiles of WHO critical priority list bacterial strains. **BMC Microbiology**, *[S. l.]*, v. 19, n. 1, p. 1–16, 2019. DOI: 10.1186/s12866-019-1687-0.

HENDRIKSEN, Rene S. et al. Global monitoring of antimicrobial resistance based on metagenomics analyses of urban sewage. **Nature Communications**, *[S. l.]*, v. 10, n. 1, 2019. DOI: 10.1038/s41467-019-08853-3.

HENLE, E. S.; LINN, S. Formation, prevention, and repair of DNA damage by iron/hydrogen peroxide. **Journal of Biological Chemistry**, *[S. l.]*, v. 272, n. 31, p. 19095–19098, 1997. DOI: 10.1074/jbc.272.31.19095.

HENRIQUES NORMARK, B.; NORMARK, S. Evolution and spread of antibiotic resistance. **Journal of Internal Medicine**, *[S. l.]*, v. 252, n. 2, p. 91–106, 2002. DOI: 10.1046/j.1365-2796.2002.01026.x.

HERNANDO-AMADO, Sara; COQUE, Teresa M.; BAQUERO, Fernando; MARTÍNEZ, José L. Defining and combating antibiotic resistance from One Health and Global Health perspectives. **Nature Microbiology**, *[S. l.]*, v. 4, n. 9, p. 1432–1442, 2019. DOI: 10.1038/s41564-019-0503-9. Disponível em: http://dx.doi.org/10.1038/s41564-019-0503-9.

HERNANDO, M. D.; MEZCUA, M.; FERNÁNDEZ-ALBA, A. R.; BARCELÓ, D. Environmental risk assessment of pharmaceutical residues in wastewater effluents, surface waters and sediments. **Talanta**, *[S. l.]*, v. 69, n. 2 SPEC. ISS., p. 334–342, 2006. DOI: 10.1016/j.talanta.2005.09.037.

HILLER, C. X.; HÜBNER, U.; FAJNOROVA, S.; SCHWARTZ, T.; DREWES, J. E. Antibiotic microbial resistance (AMR) removal efficiencies by conventional and

advanced wastewater treatment processes: A review. **Science of the Total Environment**, *[S. l.]*, v. 685, p. 596–608, 2019. a. DOI: 10.1016/j.scitotenv.2019.05.315. Disponível em: https://doi.org/10.1016/j.scitotenv.2019.05.315.

HILLER, C. X.; HÜBNER, U.; FAJNOROVA, S.; SCHWARTZ, T.; DREWES, J. E. Antibiotic microbial resistance (AMR) removal efficiencies by conventional and advanced wastewater treatment processes: A review. **Science of the Total Environment**, *[S. l.]*, v. 685, p. 596–608, 2019. b. DOI: 10.1016/j.scitotenv.2019.05.315. Disponível em: https://doi.org/10.1016/j.scitotenv.2019.05.315.

HILLES, Ahmed H.; ABU AMR, Salem S.; HUSSEIN, Rim A.; ARAFA, Anwar I.; EL-SEBAIE, Olfat D. Effect of persulfate and persulfate/H2O2 on biodegradability of an anaerobic stabilized landfill leachate. **Waste Management**, *[S. l.]*, v. 44, p. 172–177, 2015. DOI: 10.1016/j.wasman.2015.07.046. Disponível em: http://dx.doi.org/10.1016/j.wasman.2015.07.046.

HINCHEE, Robert E.; DOWNEY, Douglas C.; AGGARWAL, Pradeep K. Use of hydrogen peroxide as an oxygen source for in situ biodegradation. Part I. Field studies. **Journal of Hazardous Materials**, *[S. l.]*, v. 27, n. 3, p. 287–299, 1991. DOI: 10.1016/0304-3894(91)80055-S.

HOFER, Ursula. Stop that plasmid. **Nature Reviews Microbiology**, *[S. l.]*, v. 19, p. 41579, 2020. DOI: 10.1038/s41579-020-0349-4. Disponível em: http://dx.doi.org/10.1038/s41579-020-0349-4.

HOLMES, Alison H.; MOORE, Luke S. P.; SUNDSFJORD, Arnfinn; STEINBAKK, Martin; REGMI, Sadie; KARKEY, Abhilasha; GUERIN, Philippe J.; PIDDOCK, Laura J. V. Understanding the mechanisms and drivers of antimicrobial resistance. **The Lancet**, *[S. l.]*, v. 387, n. 10014, p. 176–187, 2016. DOI: 10.1016/S0140-6736(15)00473-0.

HOU, Ai ming et al. Chlorine injury enhances antibiotic resistance in Pseudomonas aeruginosa through over expression of drug efflux pumps. **Water Research**, *[S. l.]*, v. 156, p. 366–371, 2019. DOI: 10.1016/j.watres.2019.03.035. Disponível em: https://doi.org/10.1016/j.watres.2019.03.035.

HOU, Kunjie; PI, Zhoujie; YAO, Fubing; WU, Bo; HE, Li; LI, Xiaoming; WANG, Dongbo; DONG, Haoran; YANG, Qi. A critical review on the mechanisms of persulfate activation by iron-based materials: Clarifying some ambiguity and controversies. **Chemical Engineering Journal**, *[S. l.]*, v. 407, n. June 2020, 2021. DOI: 10.1016/j.cej.2020.127078.

HUIE, Robert E.; CLIFTON, Carol L. Rate constants for hydrogen abstraction reactions of the sulfate radical, SO4−. Alkanes and ethers. **International Journal of Chemical Kinetics**, *[S. l.]*, v. 21, n. 8, p. 611–619, 1989. DOI: 10.1002/kin.550210802.

IAKOVIDES, I. C. et al. Continuous ozonation of urban wastewater: Removal of antibiotics, antibiotic-resistant Escherichia coli and antibiotic resistance genes and phytotoxicity. **Water Research**, *[S. l.]*, v. 159, p. 333–347, 2019. DOI: 10.1016/j.watres.2019.05.025. Disponível em: https://doi.org/10.1016/j.watres.2019.05.025.

IKE, Ikechukwu A.; LINDEN, Karl G.; ORBELL, John D.; DUKE, Mikel. Critical review of the science and sustainability of persulphate advanced oxidation processes. **Chemical Engineering Journal**, *[S. l.]*, v. 338, n. October 2017, p. 651–669, 2018. DOI: 10.1016/j.cej.2018.01.034. Disponível em: https://doi.org/10.1016/j.cej.2018.01.034.

IOANNOU-TTOFA, Lida; RAJ, Saurav; PRAKASH, Halan; FATTA-KASSINOS, Despo. Solar photo-Fenton oxidation for the removal of ampicillin, total cultivable and resistant E. coli and ecotoxicity from secondary-treated wastewater effluents. **Chemical Engineering Journal**, *[S. l.]*, v. 355, n. May 2018, p. 91–102, 2019. a. DOI: 10.1016/j.cej.2018.08.057. Disponível em: https://doi.org/10.1016/j.cej.2018.08.057.

IOANNOU-TTOFA, Lida; RAJ, Saurav; PRAKASH, Halan; FATTA-KASSINOS, Despo. Solar photo-Fenton oxidation for the removal of ampicillin, total cultivable and resistant E. coli and ecotoxicity from secondary-treated wastewater effluents. **Chemical Engineering Journal**, *[S. l.]*, v. 355, n. August 2018, p. 91–102, 2019. b. DOI: 10.1016/j.cej.2018.08.057. Disponível em: https://doi.org/10.1016/j.cej.2018.08.057.

ISHII, Satoshi. Quantification of antibiotic resistance genes for environmental monitoring: Current methods and future directions. **Current Opinion in Environmental Science and Health**, *[S. l.]*, v. 16, p. 47–53, 2020. DOI: 10.1016/j.coesh.2020.02.004. Disponível em: https://doi.org/10.1016/j.coesh.2020.02.004.

IZAGUIRRE-ANARIBA, Dora E.; SIVAPALAN, Vel. Chryseobacterium indologenes, an Emerging Bacteria: A Case Report and Review of Literature. **Cureus**, *[S. l.]*, v. 12, n. 1, p. 1–7, 2020. DOI: 10.7759/cureus.6720.

JENKINS, S. H. Standard Methods for the Examination of Water and Wastewater. **Water Research**, *[S. l.]*, v. 16, n. 10, p. 1495–1496, 1982. DOI: 10.1016/0043-1354(82)90249-4.

JIA, Baofeng et al. CARD 2017: Expansion and model-centric curation of the comprehensive antibiotic resistance database. **Nucleic Acids Research**, *[S. l.]*, v. 45, n. D1, p. D566–D573, 2017. DOI: 10.1093/nar/gkw1004.

JIA, Shuyu; BIAN, Kaiqin; SHI, Peng; YE, Lin; LIU, Chang Hong. Metagenomic profiling of antibiotic resistance genes and their associations with bacterial community during multiple disinfection regimes in a full-scale drinking water treatment plant. **Water Research**, *[S. l.]*, v. 176, p. 115721, 2020. DOI: 10.1016/j.watres.2020.115721. Disponível em: https://doi.org/10.1016/j.watres.2020.115721.

JIANG, Qi; FENG, Mingbao; YE, Chengsong; YU, Xin. Effects and relevant mechanisms of non-antibiotic factors on the horizontal transfer of antibiotic resistance genes in water environments: A review. **Science of The Total Environment**, *[S. l.]*, v. 806, p. 150568, 2022. DOI: 10.1016/J.SCITOTENV.2021.150568.

JIANG, Xiawei; CUI, Xinjie; XU, Hao; LIU, Wenhong; TAO, Fangfang; SHAO, Tiejuan; PAN, Xiaoping; ZHENG, Beiwen. Whole genome sequencing of extended-spectrum beta-lactamase (ESBL)-producing escherichia coli isolated from a wastewater treatment plant in China. **Frontiers in Microbiology**, *[S. l.]*, v. 10, n. AUG, 2019. DOI: 10.3389/fmicb.2019.01797.

JIN, Min et al. Chlorine disinfection promotes the exchange of antibiotic resistance genes across bacterial genera by natural transformation. **ISME Journal**, *[S. l.]*, v. 14, n. 7, p. 1847–1856, 2020. DOI: 10.1038/s41396-020-0656-9. Disponível em: http://dx.doi.org/10.1038/s41396-020-0656-9.

JOHNSON, Richard J.; SMITH, Ben E.; SUTTON, Paul A.; MCGENITY, Terry J.; ROWLAND, Steven J.; WHITBY, Corinne. Microbial biodegradation of aromatic alkanoic naphthenic acids is affected by the degree of alkyl side chain branching. **ISME Journal**, *[S. l.]*, v. 5, n. 3, p. 486–496, 2011. DOI: 10.1038/ismej.2010.146.

JU, Feng; LI, Bing; MA, Liping; WANG, Yubo; HUANG, Danping; ZHANG, Tong. Antibiotic resistance genes and human bacterial pathogens: Co-occurrence, removal, and enrichment in municipal sewage sludge digesters. **Water Research**, *[S. l.]*, v. 91, p. 1–10, 2016. DOI: 10.1016/j.watres.2015.11.071. Disponível em: http://dx.doi.org/10.1016/j.watres.2015.11.071.

KAHLMETER, Gunnar. Defining antibiotic resistance-towards international harmonization. **Upsala Journal of Medical Sciences**, *[S. l.]*, v. 119, n. 2, p. 78–86, 2014. DOI: 10.3109/03009734.2014.901446.

KAMENSHCHIKOVA, A.; WOLFFS, P. F. G.; HOEBE, C. J. P. A.; HORSTMAN, K. Anthropocentric framings of One Health: an analysis of international antimicrobial resistance policy documents. **Critical Public Health**, *[S. l.]*, v. 31, n. 3, p. 306–315, 2021. DOI: 10.1080/09581596.2019.1684442. Disponível em: https://doi.org/10.1080/09581596.2019.1684442.

KARAOLIA, P.; MICHAEL-KORDATOU, I.; HAPESHI, E.; ALEXANDER, J.; SCHWARTZ, T.; FATTA-KASSINOS, D. Investigation of the potential of a Membrane BioReactor followed by solar Fenton oxidation to remove antibiotic-related microcontaminants. **Chemical Engineering Journal**, *[S. l.]*, v. 310, p. 491–502, 2017. DOI: 10.1016/j.cej.2016.04.113. Disponível em: http://dx.doi.org/10.1016/j.cej.2016.04.113.

KARAOLIA, Popi et al. Removal of antibiotics, antibiotic-resistant bacteria and their associated genes by graphene-based TiO2 composite photocatalysts under solar radiation in urban wastewaters. **Applied Catalysis B: Environmental**, *[S. l.]*, v. 224, n. November 2017, p. 810–824, 2018. DOI: 10.1016/j.apcatb.2017.11.020.

KARAOLIA, Popi; MICHAEL, Irene; GARCÍA-FERNÁNDEZ, Irene; AGÜERA, Ana; MALATO, Sixto; FERNÁNDEZ-IBÁÑEZ, Pilar; FATTA-KASSINOS, Despo. Reduction of clarithromycin and sulfamethoxazole-resistant Enterococcus by pilot-scale solar-driven Fenton oxidation. **Science of The Total Environment**, *[S. l.]*, v. 468–469, p. 19–27, 2014. DOI: 10.1016/J.SCITOTENV.2013.08.027.

KARKMAN, Antti; DO, Thi Thuy; WALSH, Fiona; VIRTA, Marko P. J. Antibiotic-Resistance Genes in Waste Water. **Trends in Microbiology**, *[S. l.]*, v. 26, n. 3, p. 220–228, 2018. DOI: 10.1016/j.tim.2017.09.005.

KAUR, Balpreet; KATTEL, Eneliis; DULOVA, Niina. Insights into nonylphenol degradation by UV-activated persulfate and persulfate/hydrogen peroxide systems in aqueous matrices: a comparative study. **Environmental Science and Pollution Research**, *[S. l.]*, v. 27, n. 18, p. 22499–22510, 2020. DOI: 10.1007/s11356-020-08886-y.

KAVITHA, V.; PALANIVELU, K. The role of ferrous ion in Fenton and photo-Fenton processes for the degradation of phenol. **Chemosphere**, *[S. l.]*, v. 55, n. 9, p. 1235–1243, 2004. DOI: 10.1016/j.chemosphere.2003.12.022.

KEHREIN, Philipp; VAN LOOSDRECHT, Mark; OSSEWEIJER, Patricia; GARFÍ, Marianna; DEWULF, Jo; POSADA, John. A critical review of resource recovery from municipal wastewater treatment plants-market supply potentials, technologies and bottlenecks. **Environmental Science: Water Research and Technology**, *[S. l.]*, v. 6, n. 4, p. 877–910, 2020. DOI: 10.1039/c9ew00905a.

KHAN, Nadeem A. et al. Occurrence, sources and conventional treatment techniques for various antibiotics present in hospital wastewaters: A critical review. **TrAC - Trends in Analytical Chemistry**, *[S. l.]*, v. 129, 2020. DOI: 10.1016/j.trac.2020.115921.

KHAN, Sanaullah; SOHAIL, M.; HAN, Changseok; KHAN, Javed Ali; KHAN, Hasan M.; DIONYSIOU, Dionysios D. Degradation of highly chlorinated pesticide, lindane, in water using UV/persulfate: kinetics and mechanism, toxicity evaluation, and synergism by H2O2. **Journal of Hazardous Materials**, *[S. l.]*, v. 402, n. January 2020, p. 123558, 2021. DOI: 10.1016/j.jhazmat.2020.123558. Disponível em: https://doi.org/10.1016/j.jhazmat.2020.123558.

KHAN, Syed Abdul Rehman; PONCE, Pablo; YU, Zhang; GOLPÎRA, Hêriş; MATHEW, Manoj. Environmental technology and wastewater treatment: Strategies to achieve environmental sustainability. **Chemosphere**, *[S. l.]*, v. 286, n. July 2021, 2022. DOI: 10.1016/j.chemosphere.2021.131532.

KHATAEE, Alireza; ALEBOYEH, Hamid; SHEYDAEI, Mohsen; ALEBOYEH, Azam. Comprehensive monitoring of the performance of homogenous and heterogeneous UV/H2O2/S2O82-/Fe2+ processes in mineralization of Acid Red 73. **Research on Chemical Intermediates**, *[S. l.]*, v. 42, n. 2, p. 571–580, 2016. DOI: 10.1007/s11164-015-2042-1. Disponível em: http://dx.doi.org/10.1007/s11164-015-2042-1.

KIM, Bo Ra; SHIN, Jiwon; GUEVARRA, Robin B.; LEE, Jun Hyung; KIM, Doo Wan; SEOL, Kuk Hwan; LEE, Ju Hoon; KIM, Hyeun Bum; ISAACSON, Richard E. Deciphering diversity indices for a better understanding of microbial communities. **Journal of Microbiology and Biotechnology**, *[S. l.]*, v. 27, n. 12, p. 2089–2093, 2017. DOI: 10.4014/jmb.1709.09027.

KIRCHNER, K.; BRÜCKNER, I.; KLAER, K.; HAMMERS-WIRTZ, M.; PINNEKAMP, J.; ROSENBAUM, M. A. Microbial Counts and Antibiotic Resistances during Conventional Wastewater Treatment and Wastewater Ozonation. **Ozone: Science and Engineering**, *[S. l.]*, v. 42, n. 2, p. 108–119, 2020. DOI: 10.1080/01919512.2019.1645641. Disponível em: https://doi.org/10.1080/01919512.2019.1645641.

KLAMERTH, N.; MALATO, S.; AGÜERA, A.; FERNÁNDEZ-ALBA, A. Photo-Fenton and modified photo-Fenton at neutral pH for the treatment of emerging contaminants in wastewater treatment plant effluents: A comparison. **Water Research**, *[S. l.]*, v. 47, n. 2, p. 833–840, 2013. DOI: 10.1016/j.watres.2012.11.008.

KOLTHOFF, I. M.; MEDALIA, A. I.; RAAEN, Helen Parks. The Reaction between Ferrous Iron and Peroxides. IV. Reaction with Potassium Persulfate. **Journal of the American Chemical Society**, *[S. l.]*, v. 73, n. 4, p. 1733–1739, 1951. DOI: 10.1021/ja01148a089.

KRZEMINSKI, Pawel et al. Performance of secondary wastewater treatment methods for the removal of contaminants of emerging concern implicated in crop uptake and antibiotic resistance spread: A review. **Science of the Total Environment**, *[S. l.]*, v. 648, p. 1052–1081, 2019. DOI: 10.1016/j.scitotenv.2018.08.130. Disponível em: https://doi.org/10.1016/j.scitotenv.2018.08.130.

KRZYWINSKI, Martin; SCHEIN, Jacqueline; BIROL, Inanç; CONNORS, Joseph; GASCOYNE, Randy; HORSMAN, Doug; JONES, Steven J.; MARRA, Marco A. Circos: An information aesthetic for comparative genomics. **Genome Research**, *[S. l.]*, v. 19, n. 9, p. 1639–1645, 2009. DOI: 10.1101/gr.092759.109.

KUMAR, Anil; POTTIBOYINA, Venkata; SEVILLA, Michael D. Hydroxyl radical (OH•) reaction with guanine in an aqueous environment: A DFT study. **Journal of Physical Chemistry B**, *[S. l.]*, v. 115, n. 50, p. 15129–15137, 2011. DOI: 10.1021/jp208841q.

KUMAR, Rohitashw; QURESHI, Mahrukh; VISHWAKARMA, Dinesh Kumar; AL-ANSARI, Nadhir; KURIQI, Alban; ELBELTAGI, Ahmed; SARASWAT, Anuj. A review on emerging water contaminants and the application of sustainable removal technologies. **Case Studies in Chemical and Environmental Engineering**, *[S. l.]*, v. 6, n. March, p. 100219, 2022. DOI: 10.1016/j.cscee.2022.100219. Disponível em: https://doi.org/10.1016/j.cscee.2022.100219.

KUMAR, Sanjeet; BANSAL, Kanika; PATIL, Prashant P.; KAUR, Amandeep; KAUR, Satinder; JASWAL, Vivek; GAUTAM, Vikas; PATIL, Prabhu B. Genomic insights into evolution of extensive drug resistance in Stenotrophomonas maltophilia complex. **Genomics**, *[S. l.]*, v. 112, n. 6, p. 4171–4178, 2020. DOI: 10.1016/j.ygeno.2020.06.049. Disponível em: https://doi.org/10.1016/j.ygeno.2020.06.049.

KÜMMERER, Klaus. Antibiotics in the aquatic environment - A review - Part II. *[S. l.]*, v. 75, n. 4, p. 435–441, 2009. a. DOI: 10.1016/j.chemosphere.2008.12.006. Disponível em: http://dx.doi.org/10.1016/j.chemosphere.2008.12.006.

KÜMMERER, Klaus. The presence of pharmaceuticals in the environment due to human use - present knowledge and future challenges. **Journal of Environmental Management**, *[S. l.]*, v. 90, n. 8, p. 2354–2366, 2009. b. DOI: 10.1016/j.jenvman.2009.01.023.

LADO RIBEIRO, Ana R.; MOREIRA, Nuno F. F.; LI PUMA, Gianluca; SILVA, Adrián M. T. Impact of water matrix on the removal of micropollutants by advanced oxidation technologies. **Chemical Engineering Journal**, *[S. l.]*, v. 363, n. October 2018, p. 155–173, 2019. DOI: 10.1016/j.cej.2019.01.080. Disponível em: https://doi.org/10.1016/j.cej.2019.01.080.

LANZA, Val Fernández; TEDIM, Ana P.; MARTÍNEZ, José Luís; BAQUERO, Fernando; COQUE, Teresa M. The Plasmidome of Firmicutes: Impact on the Emergence and the Spread of Resistance to Antimicrobials. **Plasmids: Biology and Impact in Biotechnology and Discovery**, *[S. l.]*, p. 379–419, 2015. DOI: 10.1128/9781555818982.ch21.

LARSSON, D. G. Joaki. et al. Critical knowledge gaps and research needs related to the environmental dimensions of antibiotic resistance. **Environment International**, *[S. l.]*, v. 117, n. May, p. 132–138, 2018. DOI: 10.1016/j.envint.2018.04.041.

LARSSON, D. G. Joaki.; FLACH, Carl Fredrik. Antibiotic resistance in the environment. **Nature Reviews Microbiology**, *[S. l.]*, v. 20, n. 5, p. 257–269, 2022. DOI: 10.1038/s41579-021-00649-x.

LAWSON, Christopher E. et al. Common principles and best practices for engineering microbiomes. **Nature Reviews Microbiology**, *[S. l.]*, v. 17, n. 12, p. 725–741, 2019. DOI: 10.1038/s41579-019-0255-9. Disponível em: http://dx.doi.org/10.1038/s41579-019-0255-9.

LAXMINARAYAN, Ramanan et al. The Lancet Infectious Diseases Commission on antimicrobial resistance: 6 years later. **The Lancet Infectious Diseases**, *[S. l.]*, v. 20, n. 4, p. e51–e60, 2020. DOI: 10.1016/S1473-3099(20)30003-7. Disponível em: http://dx.doi.org/10.1016/S1473-3099(20)30003-7.

LE-MINH, N.; KHAN, S. J.; DREWES, J. E.; STUETZ, R. M. Fate of antibiotics during municipal water recycling treatment processes. **Water Research**, *[S. l.]*, v. 44, n. 15, p. 4295–4323, 2010. DOI: 10.1016/j.watres.2010.06.020. Disponível em: http://dx.doi.org/10.1016/j.watres.2010.06.020.

LEAVIS, Helen L.; BONTEN, Marc JM; WILLEMS, Rob JL. Identification of high-risk enterococcal clonal complexes: global dispersion and antibiotic resistance. **Current Opinion in Microbiology**, *[S. l.]*, v. 9, n. 5, p. 454–460, 2006. DOI: 10.1016/j.mib.2006.07.001.

LEE, Jaesang; VON GUNTEN, Urs; KIM, Jae Hong. Persulfate-Based Advanced Oxidation: Critical Assessment of Opportunities and Roadblocks. **Environmental Science and Technology**, *[S. l.]*, v. 54, n. 6, p. 3064–3081, 2020. DOI: 10.1021/acs.est.9b07082.

LEE, Jangwoo; JEON, Jong Hun; SHIN, Jingyeong; JANG, Hyun Min; KIM, Sungpyo; SONG, Myoung Seok; KIM, Young Mo. Quantitative and qualitative changes in antibiotic resistance genes after passing through treatment processes in municipal wastewater treatment plants. **Science of the Total Environment**, *[S. l.]*, v. 605–606, p. 906–914, 2017. DOI: 10.1016/j.scitotenv.2017.06.250. Disponível em: http://dx.doi.org/10.1016/j.scitotenv.2017.06.250.

LEE, Kyung Jin; JEONG, Hye Gwang. Protective effects of kahweol and cafestol against hydrogen peroxide-induced oxidative stress and DNA damage. **Toxicology Letters**, *[S. l.]*, v. 173, n. 2, p. 80–87, 2007. DOI: 10.1016/j.toxlet.2007.06.008.

LEE, Yunho; CHOI, Yegyun; HE, Huan; DODD, Michael C. Degradation kinetics of antibiotic resistance gene meca of methicillin-resistant staphylococcus aureus (mrsa) during water disinfection with chlorine, ozone, and ultraviolet light. **Environmental Science and Technology**, *[S. l.]*, v. 55, n. 4, p. 2541–2552, 2021. DOI: 10.1021/acs.est.0c05274.

LÉGER, Anaïs et al. AMR-Intervene: A social-ecological framework to capture the diversity of actions to tackle antimicrobial resistance from a One Health perspective. **Journal of Antimicrobial Chemotherapy**, *[S. l.]*, v. 76, n. 1, p. 1–21, 2021. DOI: 10.1093/JAC/DKAA394.

LEKUNBERRI, Itziar; VILLAGRASA, Marta; BALCÁZAR, José Luis; BORREGO, Carles M. Contribution of bacteriophage and plasmid DNA to the mobilization of antibiotic resistance genes in a river receiving treated wastewater discharges. **Science**

of the Total Environment, *[S. l.]*, v. 601–602, p. 206–209, 2017. DOI: 10.1016/j.scitotenv.2017.05.174. Disponível em: http://dx.doi.org/10.1016/j.scitotenv.2017.05.174.

LEROY-FREITAS, D.; MACHADO, E. C.; TORRES-FRANCO, A. F.; DIAS, M. F.; LEAL, C. D.; ARAÚJO, J. C. Exploring the microbiome, antibiotic resistance genes, mobile genetic element, and potential resistant pathogens in municipal wastewater treatment plants in Brazil. **Science of the Total Environment**, *[S. l.]*, v. 842, n. April, 2022. DOI: 10.1016/j.scitotenv.2022.156773.

LI, Bing; ZHANG, Tong; XU, Zhaoyi; FANG, Herbert Han Ping. Rapid analysis of 21 antibiotics of multiple classes in municipal wastewater using ultra performance liquid chromatography-tandem mass spectrometry. **Analytica Chimica Acta**, *[S. l.]*, v. 645, n. 1–2, p. 64–72, 2009. DOI: 10.1016/j.aca.2009.04.042.

LI, Bo; YAN, Tao. Next generation sequencing reveals limitation of qPCR methods in quantifying emerging antibiotic resistance genes (ARGs) in the environment. **Applied Microbiology and Biotechnology**, *[S. l.]*, v. 105, n. 7, p. 2925–2936, 2021. DOI: 10.1007/s00253-021-11202-4.

LI, Huan; LI, Shang; TANG, Wei; YANG, Yang; ZHAO, Jianfu; XIA, Siqing; ZHANG, Weixian; WANG, Hong. Influence of secondary water supply systems on microbial community structure and opportunistic pathogen gene markers. **Water Research**, *[S. l.]*, v. 136, p. 160–168, 2018. a. DOI: 10.1016/j.watres.2018.02.031. Disponível em: https://doi.org/10.1016/j.watres.2018.02.031.

LI, Jianan; CHENG, Weixiao; XU, Like; JIAO, Yanan; BAIG, Shams Ali; CHEN, Hong. Occurrence and removal of antibiotics and the corresponding resistance genes in wastewater treatment plants: effluents' influence to downstream water environment. **Environmental Science and Pollution Research**, *[S. l.]*, v. 23, n. 7, p. 6826–6835, 2016. DOI: 10.1007/s11356-015-5916-2.

LI, Li Guan; HUANG, Qi; YIN, Xiaole; ZHANG, Tong. Source tracking of antibiotic resistance genes in the environment — Challenges, progress, and prospects. **Water Research**, *[S. l.]*, v. 185, p. 116127, 2020. a. DOI: 10.1016/j.watres.2020.116127. Disponível em: https://doi.org/10.1016/j.watres.2020.116127.

LI, Li Hua; SHIH, Yung Luen; HUANG, Jing Yun; WU, Chao Jung; HUANG, Yi Wei; HUANG, Hsin Hui; TSAI, Yu Chieh; YANG, Tsuey Ching. Protection from hydrogen peroxide stress relies mainly on AhpCF and KatA2 in Stenotrophomonas maltophilia. **Journal of Biomedical Science**, *[S. l.]*, v. 27, n. 1, p. 1–9, 2020. b. DOI: 10.1186/s12929-020-00631-4.

LI, Liguan; DECHESNE, Arnaud; HE, Zhiming; MADSEN, Jonas Stenløkke; NESME, Joseph; SØRENSEN, Søren J.; SMETS, Barth F. Estimating the Transfer Range of Plasmids Encoding Antimicrobial Resistance in a Wastewater Treatment Plant Microbial Community. **Environmental Science and Technology Letters**, *[S. l.]*, v. 5, n. 5, p. 260–265, 2018. b. DOI: 10.1021/acs.estlett.8b00105.

LI, Liguan; DECHESNE, Arnaud; MADSEN, Jonas Stenløkke; NESME, Joseph; SØRENSEN, Søren J.; SMETS, Barth F. Plasmids persist in a microbial community by providing fitness benefit to multiple phylotypes. **ISME Journal**, *[S. l.]*, 2020. c. DOI: 10.1038/s41396-020-0596-4.

LI, Meng; YANG, Xiaofang; WANG, Dong Sheng; YUAN, Jin. Enhanced oxidation of erythromycin by persulfate activated iron powder–H2O2 system: Role of the surface Fe species and synergistic effect of hydroxyl and sulfate radicals. **Chemical Engineering Journal**, *[S. l.]*, v. 317, p. 103–111, 2017. DOI: 10.1016/j.cej.2016.12.126. Disponível em: http://dx.doi.org/10.1016/j.cej.2016.12.126.

LI, Shengnan; ONDON, Brim Stevy; HO, Shih Hsin; JIANG, Jiwei; LI, Fengxiang. Antibiotic resistant bacteria and genes in wastewater treatment plants: From occurrence to treatment strategies. **Science of the Total Environment**, *[S. l.]*, v. 838, n. March, p. 156544, 2022. DOI: 10.1016/j.scitotenv.2022.156544. Disponível em: https://doi.org/10.1016/j.scitotenv.2022.156544.

LI, Shengnan; ZHANG, Chaofan; LI, Fengxiang; HUA, Tao; ZHOU, Qixing; HO, Shih Hsin. Technologies towards antibiotic resistance genes (ARGs) removal from aquatic environment: A critical review. **Journal of Hazardous Materials**, *[S. l.]*, v. 411, n. August 2020, p. 125148, 2021. DOI: 10.1016/j.jhazmat.2021.125148. Disponível em: https://doi.org/10.1016/j.jhazmat.2021.125148.

LI, Zheng Hao; YUAN, Li; GAO, Shu Xian; WANG, Liang; SHENG, Guo Ping. Mitigated membrane fouling and enhanced removal of extracellular antibiotic resistance genes from wastewater effluent via an integrated pre-coagulation and microfiltration process. **Water Research**, *[S. l.]*, v. 159, p. 145–152, 2019. DOI: 10.1016/j.watres.2019.05.005. Disponível em: https://doi.org/10.1016/j.watres.2019.05.005.

LIANG, Chenju; HUANG, Chiu Fen; MOHANTY, Nihar; KURAKALVA, Rama Mohan. A rapid spectrophotometric determination of persulfate anion in ISCO. **Chemosphere**, *[S. l.]*, v. 73, n. 9, p. 1540–1543, 2008. DOI: 10.1016/j.chemosphere.2008.08.043. Disponível em: http://dx.doi.org/10.1016/j.chemosphere.2008.08.043.

LIU, Bo; POP, Mihai. ARDB - Antibiotic resistance genes database. **Nucleic Acids Research**, *[S. l.]*, v. 37, n. SUPPL. 1, p. 443–447, 2009. DOI: 10.1093/nar/gkn656.

LIU, Shan Shan et al. Chlorine disinfection increases both intracellular and extracellular antibiotic resistance genes in a full-scale wastewater treatment plant. **Water Research**, *[S. l.]*, v. 136, p. 131–136, 2018. DOI: 10.1016/j.watres.2018.02.036. Disponível em: https://doi.org/10.1016/j.watres.2018.02.036.

LIU, Zongbao; KLÜMPER, Uli; LIU, Yang; YANG, Yuchun; WEI, Qiaoyan; LIN, Jih Gaw; GU, Ji Dong; LI, Meng. Metagenomic and metatranscriptomic analyses reveal activity and hosts of antibiotic resistance genes in activated sludge. **Environment International**, *[S. l.]*, v. 129, n. April, p. 208–220, 2019. DOI: 10.1016/j.envint.2019.05.036. Disponível em: https://doi.org/10.1016/j.envint.2019.05.036.

LOGAN, Latania K.; WEINSTEIN, Robert A. The epidemiology of Carbapenem-resistant enterobacteriaceae: The impact and evolution of a global menace. **Journal of Infectious Diseases**, *[S. l.]*, v. 215, n. Suppl 1, p. S28–S36, 2017. DOI: 10.1093/infdis/jiw282.

LÓPEZ-VINENT, Núria; CRUZ-ALCALDE, Alberto; MOUSSAVI, Gholamreza; DEL CASTILLO GONZALEZ, Isabel; HERNANDEZ LEHMANN, Aurelio; GIMÉNEZ, Jaime; GIANNAKIS, Stefanos. Improving ferrate disinfection and decontamination performance at neutral pH by activating peroxymonosulfate under solar light. **Chemical Engineering Journal**, *[S. l.]*, v. 450, n. July, 2022. DOI:

10.1016/j.cej.2022.137904.

LOVE, Michael I.; HUBER, Wolfgang; ANDERS, Simon. Moderated estimation of fold change and dispersion for RNA-seq data with DESeq2. **Genome Biology**, *[S. l.]*, v. 15, n. 12, p. 1–21, 2014. DOI: 10.1186/s13059-014-0550-8.

LUEDER, Ulf; JØRGENSEN, Bo Barker; KAPPLER, Andreas; SCHMIDT, Caroline. Photochemistry of iron in aquatic environments. **Environmental Science: Processes and Impacts**, *[S. l.]*, v. 22, n. 1, p. 12–24, 2020. DOI: 10.1039/c9em00415g.

LUND, David; KIEFFER, Nicolas; PARRAS-MOLTÓ, Marcos; EBMEYER, Stefan; BERGLUND, Fanny; JOHNNING, Anna; JOAKIM LARSSON, D. G.; KRISTIANSSON, Erik. Large-scale characterization of the macrolide resistome reveals high diversity and several new pathogen-associated genes. **Microbial Genomics**, *[S. l.]*, v. 8, n. 1, 2022. DOI: 10.1099/mgen.0.000770.

LUO, Hongwei; ZENG, Yifeng; HE, Dongqin; PAN, Xiangliang. Application of iron-based materials in heterogeneous advanced oxidation processes for wastewater treatment: A review. **Chemical Engineering Journal**, *[S. l.]*, v. 407, n. May 2020, p. 127191, 2021. a. DOI: 10.1016/j.cej.2020.127191. Disponível em: https://doi.org/10.1016/j.cej.2020.127191.

LUO, Jingyang; HUANG, Wenxuan; ZHANG, Qin; WU, Yang; FANG, Fang; CAO, Jiashun; SU, Yinglong. Distinct effects of hypochlorite types on the reduction of antibiotic resistance genes during waste activated sludge fermentation: Insights of bacterial community, cellular activity, and genetic expression. **Journal of Hazardous Materials**, *[S. l.]*, v. 403, n. September 2020, p. 124010, 2021. b. DOI: 10.1016/j.jhazmat.2020.124010. Disponível em: https://doi.org/10.1016/j.jhazmat.2020.124010.

LUPO, Agnese; COYNE, Sébastien; BERENDONK, Thomas Ulrich. Origin and evolution of antibiotic resistance: The common mechanisms of emergence and spread in water bodies. *[S. l.]*, v. 3, n. JAN, p. 1–13, 2012. DOI: 10.3389/fmicb.2012.00018.

LYTLE, Darren A.; PFALLER, Stacy; MUHLEN, Christy; STRUEWING, Ian; TRIANTAFYLLIDOU, Simoni; WHITE, Colin; HAYES, Sam; KING, Dawn; LU, Jingrang. A comprehensive evaluation of monochloramine disinfection on water quality, Legionella and other important microorganisms in a hospital. **Water Research**, *[S. l.]*, v. 189, p. 116656, 2021. DOI: 10.1016/j.watres.2020.116656. Disponível em: https://doi.org/10.1016/j.watres.2020.116656.

MA, Hongkun; ZHANG, Lingling; HUANG, Xinmei; DING, Wei; JIN, Hui; LI, Zifu; CHENG, Shikun; ZHENG, Lei. A novel three-dimensional galvanic cell enhanced Fe2+/persulfate system: High efficiency, mechanism and damaging effect of antibiotic resistant E. coli and genes. **Chemical Engineering Journal**, *[S. l.]*, v. 362, n. September 2018, p. 667–678, 2019. DOI: 10.1016/j.cej.2019.01.042. Disponível em: https://doi.org/10.1016/j.cej.2019.01.042.

MA, Liping; LI, An Dong; YIN, Xiao Le; ZHANG, Tong. The Prevalence of Integrons as the Carrier of Antibiotic Resistance Genes in Natural and Man-Made Environments. **Environmental Science and Technology**, *[S. l.]*, v. 51, n. 10, p. 5721–5728, 2017. DOI: 10.1021/acs.est.6b05887.

MACHADO, Elayne Cristina; FREITAS, Deborah Leroy; LEAL, Cintia Dutra; DE

OLIVEIRA, Amanda Teodoro; ZERBINI, Adriana; CHERNICHARO, Carlos Augusto; DE ARAÚJO, Juliana Calábria. Antibiotic resistance profile of wastewater treatment plants in Brazil reveals different patterns of resistance and multi resistant bacteria in final effluents. **Science of the Total Environment**, *[S. l.]*, v. 857, n. May 2022, 2023. DOI: 10.1016/j.scitotenv.2022.159376.

MACHADO, Elayne Cristina; LEAL, Cíntia Dutra; COELHO, Bruna Lopes; CHERNICHARO, Carlos Augusto de Lemos; ARAÚJO, Juliana Calábria De. Detecção e quantificação de bactérias resistentes aos antibióticos ampicilina e cloranfenicol em estações de tratamento de esgoto doméstico. **Engenharia Sanitaria e Ambiental**, *[S. l.]*, v. 25, n. 6, p. 847–857, 2020. DOI: 10.1590/s1413-4152202020180001.

MAGRO, Massimiliano et al. H2O2 Tolerance in Pseudomonas Fluorescens: Synergy between Pyoverdine-Iron(III) Complex and a Blue Extracellular Product Revealed by a Nanotechnology-Based Electrochemical Approach. **ChemElectroChem**, *[S. l.]*, v. 77146, p. 1–6, 2019. DOI: 10.1002/celc.201900902.

MAHMUD, Roksana; MONI, Sheikh Moniruzzaman; HIGH, Karen; CARBAJALES-DALE, Michael. Integration of techno-economic analysis and life cycle assessment for sustainable process design – A review. **Journal of Cleaner Production**, *[S. l.]*, v. 317, n. June, 2021. DOI: 10.1016/j.jclepro.2021.128247.

MALATO, S.; FERNÁNDEZ-IBÁÑEZ, P.; MALDONADO, M. I.; BLANCO, J.; GERNJAK, W. Decontamination and disinfection of water by solar photocatalysis: Recent overview and trends. **Catalysis Today**, *[S. l.]*, v. 147, n. 1, p. 1–59, 2009. DOI: 10.1016/j.cattod.2009.06.018.

MANAIA, Célia M. et al. Antibiotic resistance in wastewater treatment plants: Tackling the black box. **Environment International**, *[S. l.]*, v. 115, n. December 2017, p. 312–324, 2018. DOI: 10.1016/j.envint.2018.03.044. Disponível em: https://doi.org/10.1016/j.envint.2018.03.044.

MANAIA, Celia M.; DONNER, Erica; VAZ-MOREIRA, Ivone; HONG, Peiying. **Antibiotic resistance in the environment: A worldwide overview**. [s.l: s.n.].

MANAIA, Célia M.; GRAHAM, David; TOPP, Edward; MARTINEZ, José Luis; COLLIGNON, Peter; GAZE, William H. Antibiotic Resistance in the Environment: Expert Perspectives. **Handbook of Environmental Chemistry**, *[S. l.]*, v. 91, p. 1–18, 2020. b. DOI: 10.1007/698_2020_472.

MANAIA, Célia M.; MACEDO, Gonçalo; FATTA-KASSINOS, Despo; NUNES, Olga C. Antibiotic resistance in urban aquatic environments: can it be controlled? **Applied Microbiology and Biotechnology**, *[S. l.]*, v. 100, n. 4, p. 1543–1557, 2016. DOI: 10.1007/s00253-015-7202-0.

MANCHESTER, Keith L. Use of UV methods for measurement of protein and nucleic acid concentrations. **BioTechniques**, *[S. l.]*, v. 20, n. 6, p. 968–970, 1996. DOI: 10.2144/96206bm05.

MANIAKOVA, Gulnara; SALMERÓN, Irene; POLO-LÓPEZ, María Inmaculada; OLLER, Isabel; RIZZO, Luigi; MALATO, Sixto. Simultaneous removal of contaminants of emerging concern and pathogens from urban wastewater by homogeneous solar driven advanced oxidation processes. **Science of the Total Environment**, *[S. l.]*, v. 766, p. 144320, 2021. DOI: 10.1016/j.scitotenv.2020.144320. Disponível em:

https://doi.org/10.1016/j.scitotenv.2020.144320.

MANIKANDAN, Sivasubramanian; SUBBAIYA, Ramasamy; SARAVANAN, Muthupandian; PONRAJ, Mohanadoss; SELVAM, Masilamani; PUGAZHENDHI, Arivalagan. A critical review of advanced nanotechnology and hybrid membrane based water recycling, reuse, and wastewater treatment processes. **Chemosphere**, *[S. l.]*, v. 289, n. November 2021, p. 132867, 2022. DOI: 10.1016/j.chemosphere.2021.132867. Disponível em: https://doi.org/10.1016/j.chemosphere.2021.132867.

MANNINA, Giorgio; GULHAN, Hazal; NI, Bing Jie. Water reuse from wastewater treatment: The transition towards circular economy in the water sector. **Bioresource Technology**, *[S. l.]*, v. 363, n. July, p. 127951, 2022. DOI: 10.1016/j.biortech.2022.127951. Disponível em: https://doi.org/10.1016/j.biortech.2022.127951.

MARANO, Roberto B. M.; CYTRYN, Eddie. The Mobile Resistome in Wastewater Treatment Facilities and Downstream Environments - Introduction Horizontal Gene Transfer in Prokaryotes. **Antimicrobial Resistance in Wastewater Treatment Processes**, *[S. l.]*, p. 129–155, 2018. Disponível em: https://doi.org/10.1002/9781119192428.ch8.

MARNETT, Lawrence J. Oxy radicals, lipid peroxidation and DNA damage. **Toxicology**, *[S. l.]*, v. 181–182, p. 219–222, 2002. DOI: 10.1016/S0300-483X(02)00448-1.

MCMURDIE, Paul J.; HOLMES, Susan. Phyloseq: An R Package for Reproducible Interactive Analysis and Graphics of Microbiome Census Data. **PLoS ONE**, *[S. l.]*, v. 8, n. 4, 2013. DOI: 10.1371/journal.pone.0061217.

MCMURDIE, Paul J.; HOLMES, Susan. Waste Not, Want Not: Why Rarefying Microbiome Data Is Inadmissible. **PLoS Computational Biology**, *[S. l.]*, v. 10, n. 4, 2014. DOI: 10.1371/journal.pcbi.1003531.

MEDINA, Marie Jo; LEGIDO-QUIGLEY, Helena; HSU, Li Yang. Antimicrobial Resistance in One Health. **Advanced Sciences and Technologies for Security Applications**, *[S. l.]*, p. 209–229, 2020. DOI: 10.1007/978-3-030-23491-1_10.

MICHAEL-KORDATOU, I.; IACOVOU, M.; FRONTISTIS, Z.; HAPESHI, E.; DIONYSIOU, D. D.; FATTA-KASSINOS, D. Erythromycin oxidation and ERY-resistant Escherichia coli inactivation in urban wastewater by sulfate radical-based oxidation process under UV-C irradiation. **Water Research**, *[S. l.]*, v. 85, p. 346–358, 2015. DOI: 10.1016/j.watres.2015.08.050. Disponível em: http://dx.doi.org/10.1016/j.watres.2015.08.050.

MICHAEL-KORDATOU, I.; KARAOLIA, P.; FATTA-KASSINOS, D. The role of operating parameters and oxidative damage mechanisms of advanced chemical oxidation processes in the combat against antibiotic-resistant bacteria and resistance genes present in urban wastewater. **Water Research**, *[S. l.]*, v. 129, p. 208–230, 2018. DOI: 10.1016/j.watres.2017.10.007. Disponível em: https://doi.org/10.1016/j.watres.2017.10.007.

MICHAEL, I.; RIZZO, L.; MCARDELL, C. S.; MANAIA, C. M.; MERLIN, C.; SCHWARTZ, T.; DAGOT, C.; FATTA-KASSINOS, D. Urban wastewater treatment plants as hotspots for the release of antibiotics in the environment: A review. **Water**

Research, *[S. l.]*, v. 47, n. 3, p. 957–995, 2013. DOI: 10.1016/j.watres.2012.11.027. Disponível em: http://dx.doi.org/10.1016/j.watres.2012.11.027.

MICHAEL, Stella G. et al. Investigating the impact of UV-C/H2O2 and sunlight/H2O2 on the removal of antibiotics, antibiotic resistance determinants and toxicity present in urban wastewater. **Chemical Engineering Journal**, *[S. l.]*, v. 388, n. November 2019, p. 124383, 2020. DOI: 10.1016/j.cej.2020.124383. Disponível em: https://doi.org/10.1016/j.cej.2020.124383.

MICHAEL, Stella G.; MICHAEL-KORDATOU, Irene; BERETSOU, Vasiliki G.; JÄGER, Thomas; MICHAEL, Costas; SCHWARTZ, Thomas; FATTA-KASSINOS, Despo. Solar photo-Fenton oxidation followed by adsorption on activated carbon for the minimisation of antibiotic resistance determinants and toxicity present in urban wastewater. **Applied Catalysis B: Environmental**, *[S. l.]*, v. 244, n. September 2018, p. 871–880, 2019. DOI: 10.1016/j.apcatb.2018.12.030. Disponível em: https://doi.org/10.1016/j.apcatb.2018.12.030.

MIKLOS, David B.; REMY, Christian; JEKEL, Martin; LINDEN, Karl G.; DREWES, Jörg E.; HÜBNER, Uwe. Evaluation of advanced oxidation processes for water and wastewater treatment – A critical review. **Water Research**, *[S. l.]*, v. 139, p. 118–131, 2018. DOI: 10.1016/j.watres.2018.03.042.

MIŁOBEDZKA, Aleksandra et al. Monitoring antibiotic resistance genes in wastewater environments: The challenges of filling a gap in the One-Health cycle. **Journal of Hazardous Materials**, *[S. l.]*, v. 424, 2022. DOI: 10.1016/j.jhazmat.2021.127407.

MIRALLES-CUEVAS, S.; DAROWNA, D.; WANAG, A.; MOZIA, S.; MALATO, S.; OLLER, I. Comparison of UV/H2O2, UV/S2O82−, solar/Fe(II)/H2O2 and solar/Fe(II)/S2O82− at pilot plant scale for the elimination of micro-contaminants in natural water: An economic assessment. **Chemical Engineering Journal**, *[S. l.]*, v. 310, p. 514–524, 2017. DOI: 10.1016/j.cej.2016.06.121. Disponível em: http://dx.doi.org/10.1016/j.cej.2016.06.121.

MONTAÑA, Sabrina et al. The genetic analysis of an Acinetobacter Johnsonii clinical strain evidenced the presence of horizontal genetic transfer. **PLoS ONE**, *[S. l.]*, v. 11, n. 8, p. 1–20, 2016. DOI: 10.1371/journal.pone.0161528.

MONTEAGUDO, J. M.; DURÁN, A.; GONZÁLEZ, R.; EXPÓSITO, A. J. In situ chemical oxidation of carbamazepine solutions using persulfate simultaneously activated by heat energy, UV light, Fe2+ ions, and H2O2. **Applied Catalysis B: Environmental**, *[S. l.]*, v. 176–177, p. 120–129, 2015. DOI: 10.1016/j.apcatb.2015.03.055. Disponível em: http://dx.doi.org/10.1016/j.apcatb.2015.03.055.

MOREIRA, Nuno F. F. et al. Rethinking water treatment targets: bacteria regrowth under unprovable conditions. **Water Research**, *[S. l.]*, p. 117374, 2021. DOI: 10.1016/j.watres.2021.117374. Disponível em: https://doi.org/10.1016/j.watres.2021.117374.

MOREIRA, Nuno F. F.; NARCISO-DA-ROCHA, Carlos; POLO-LÓPEZ, M. Inmaculada; PASTRANA-MARTÍNEZ, Luisa M.; FARIA, Joaquim L.; MANAIA, Célia M.; FERNÁNDEZ-IBÁÑEZ, Pilar; NUNES, Olga C.; SILVA, Adrián M. T. Solar treatment (H2O2, TiO2-P25 and GO-TiO2 photocatalysis, photo-Fenton) of organic micropollutants, human pathogen indicators, antibiotic resistant bacteria and related genes in urban wastewater. **Water Research**, *[S. l.]*, v. 135, p. 195–206, 2018. DOI:

10.1016/j.watres.2018.01.064.

MORIN-CRINI, Nadia et al. **Removal of emerging contaminants from wastewater using advanced treatments. A review**. [s.l.] : Springer International Publishing, 2022. v. 20 DOI: 10.1007/s10311-021-01379-5. Disponível em: https://doi.org/10.1007/s10311-021-01379-5.

MOSTEO, Rosa; VARON LOPEZ, Angelica; MUZARD, David; BENITEZ, Norberto; GIANNAKIS, Stefanos; PULGARIN, Cesar. Visible light plays a significant role during bacterial inactivation by the photo-fenton process, even at sub-critical light intensities. **Water Research**, *[S. l.]*, v. 174, p. 115636, 2020. DOI: 10.1016/j.watres.2020.115636. Disponível em: https://doi.org/10.1016/j.watres.2020.115636.

MUNCK, Christian; ALBERTSEN, Mads; TELKE, Amar; ELLABAAN, Mostafa; NIELSEN, Per Halkjær; SOMMER, Morten O. A. Limited dissemination of the wastewater treatment plant core resistome. **Nature Communications**, *[S. l.]*, v. 6, p. 2–11, 2015. DOI: 10.1038/ncomms9452.

MUNOZ-PRICE, L. Silvia et al. Clinical epidemiology of the global expansion of Klebsiella pneumoniae carbapenemases. **The Lancet Infectious Diseases**, *[S. l.]*, v. 13, n. 9, p. 785–796, 2013. DOI: 10.1016/S1473-3099(13)70190-7. Disponível em: http://dx.doi.org/10.1016/S1473-3099(13)70190-7.

MURRAY, Aimee K.; ZHANG, Lihong; YIN, Xiaole; ZHANG, Tong; BUCKLING, Angus; SNAPE, Jason; GAZE, William H. Novel Insights into Selection for Antibiotic Resistance in Complex Microbial Communities. **bioRxiv**, *[S. l.]*, v. 9, n. 4, p. 1–12, 2018. DOI: 10.1101/323634.

NAHIM-GRANADOS, Samira; RIVAS-IBÁÑEZ, Gracia; ANTONIO SÁNCHEZ PÉREZ, José; OLLER, Isabel; MALATO, Sixto; POLO-LÓPEZ, María Inmaculada. Fresh-cut wastewater reclamation: Techno-Economical assessment of solar driven processes at pilot plant scale. **Applied Catalysis B: Environmental**, *[S. l.]*, v. 278, n. June, p. 119334, 2020. DOI: 10.1016/j.apcatb.2020.119334. Disponível em: https://doi.org/10.1016/j.apcatb.2020.119334.

NARCISO-DA-ROCHA, Carlos; ROCHA, Jaqueline; VAZ-MOREIRA, Ivone; LIRA, Felipe; TAMAMES, Javier; HENRIQUES, Isabel; MARTINEZ, José Luis; MANAIA, Célia M. Bacterial lineages putatively associated with the dissemination of antibiotic resistance genes in a full-scale urban wastewater treatment plant. **Environment International**, *[S. l.]*, v. 118, n. May, p. 179–188, 2018. DOI: 10.1016/j.envint.2018.05.040. Disponível em: https://doi.org/10.1016/j.envint.2018.05.040.

NEILL, Jim O. ’. Antimicrobial Resistance: Tackling a crisis for the health and wealth of nations The Review on Antimicrobial Resistance Chaired. *[S. l.]*, n. December, 2014.

NESME, Joseph; CÉCILLON, Sébastien; DELMONT, Tom O.; MONIER, Jean Michel; VOGEL, Timothy M.; SIMONET, Pascal. Large-scale metagenomic-based study of antibiotic resistance in the environment. **Current Biology**, *[S. l.]*, v. 24, n. 10, p. 1096–1100, 2014. DOI: 10.1016/j.cub.2014.03.036.

NGUYEN, Anh Q.; VU, Hang P.; NGUYEN, Luong N.; WANG, Qilin; DJORDJEVIC, Steven P.; DONNER, Erica; YIN, Huabing; NGHIEM, Long D. Monitoring antibiotic resistance genes in wastewater treatment: Current strategies and future challenges.

Science of The Total Environment, *[S. l.]*, v. 783, p. 146964, 2021. DOI: 10.1016/j.scitotenv.2021.146964. Disponível em: https://doi.org/10.1016/j.scitotenv.2021.146964.

NIHEMAITI, Maolida; YOON, Younggun; HE, Huan; DODD, Michael C.; CROUÉ, Jean Philippe; LEE, Yunho. Degradation and deactivation of a plasmid-encoded extracellular antibiotic resistance gene during separate and combined exposures to UV254 and radicals. **Water Research**, *[S. l.]*, v. 182, p. 1–11, 2020. DOI: 10.1016/j.watres.2020.115921.

NOGUEIRA, Raquel F. Pup.; OLIVEIRA, Mirela C.; PATERLINI, Willian C. Simple and fast spectrophotometric determination of H2O 2 in photo-Fenton reactions using metavanadate. **Talanta**, *[S. l.]*, v. 66, n. 1, p. 86–91, 2005. DOI: 10.1016/j.talanta.2004.10.001.

NOYOLA, Adalberto; PADILLA-RIVERA, Alejandro; MORGAN-SAGASTUME, Juan Manuel; GÜERECA, Leonor Patricia; HERNÁNDEZ-PADILLA, Flor. Typology of Municipal Wastewater Treatment Technologies in Latin America. **Clean - Soil, Air, Water**, *[S. l.]*, v. 40, n. 9, p. 926–932, 2012. DOI: 10.1002/clen.201100707.

NUMBERGER, Daniela; GANZERT, Lars; ZOCCARATO, Luca; MÜHLDORFER, Kristin; SAUER, Sascha; GROSSART, Hans Peter; GREENWOOD, Alex D. Characterization of bacterial communities in wastewater with enhanced taxonomic resolution by full-length 16S rRNA sequencing. **Scientific Reports**, *[S. l.]*, v. 9, n. 1, p. 1–14, 2019. DOI: 10.1038/s41598-019-46015-z.

O'LEARY, Nuala A. et al. Reference sequence (RefSeq) database at NCBI: Current status, taxonomic expansion, and functional annotation. **Nucleic Acids Research**, *[S. l.]*, v. 44, n. D1, p. D733–D745, 2016. DOI: 10.1093/nar/gkv1189.

OH, Wen Da; DONG, Zhili; LIM, Teik Thye. Generation of sulfate radical through heterogeneous catalysis for organic contaminants removal: Current development, challenges and prospects. **Applied Catalysis B: Environmental**, *[S. l.]*, v. 194, p. 169–201, 2016. DOI: 10.1016/j.apcatb.2016.04.003. Disponível em: http://dx.doi.org/10.1016/j.apcatb.2016.04.003.

OH, Junsik; SALCEDO, Dennis Espineli; MEDRIANO, Carl Angelo; KIM, Sungpyo. Comparison of different disinfection processes in the effective removal of antibiotic-resistant bacteria and genes. **Journal of Environmental Sciences (China)**, *[S. l.]*, v. 26, n. 6, p. 1238–1242, 2014. DOI: 10.1016/S1001-0742(13)60594-X.

OKSANEN, Author Jari et al. Vegan. **Encyclopedia of Food and Agricultural Ethics**, *[S. l.]*, p. 2395–2396, 2019. DOI: 10.1007/978-94-024-1179-9_301576.

OLEKHNOVICH, Evgenii I.; VASILYEV, Artem T.; ULYANTSEV, Vladimir I.; KOSTRYUKOVA, Elena S.; TYAKHT, Alexander V. MetaCherchant: Analyzing genomic context of antibiotic resistance genes in gut microbiota. **Bioinformatics**, *[S. l.]*, v. 34, n. 3, p. 434–444, 2018. DOI: 10.1093/bioinformatics/btx681.

OLIVER, James D. Recent findings on the viable but nonculturable state in pathogenic bacteria. **FEMS Microbiology Reviews**, *[S. l.]*, v. 34, n. 4, p. 415–425, 2010. DOI: 10.1111/j.1574-6976.2009.00200.x.

OLMEZ-HANCI, Tugba; ARSLAN-ALATON, Idil; DURSUN, Duygu. Investigation of the toxicity of common oxidants used in advanced oxidation processes and their

quenching agents. **Journal of Hazardous Materials**, *[S. l.]*, v. 278, p. 330–335, 2014. DOI: 10.1016/j.jhazmat.2014.06.021. Disponível em: http://dx.doi.org/10.1016/j.jhazmat.2014.06.021.

OSIŃSKA, Adriana; KORZENIEWSKA, Ewa; HARNISZ, Monika; FELIS, Ewa; BAJKACZ, Sylwia; JACHIMOWICZ, Piotr; NIESTĘPSKI, Sebastian; KONOPKA, Iwona. Small-scale wastewater treatment plants as a source of the dissemination of antibiotic resistance genes in the aquatic environment. **Journal of Hazardous Materials**, *[S. l.]*, v. 381, n. August 2019, p. 121221, 2020. DOI: 10.1016/j.jhazmat.2019.121221. Disponível em: https://doi.org/10.1016/j.jhazmat.2019.121221.

OTURAN, Mehmet A.; AARON, Jean Jacques. Advanced oxidation processes in water/wastewater treatment: Principles and applications. A review. **Critical Reviews in Environmental Science and Technology**, *[S. l.]*, v. 44, n. 23, p. 2577–2641, 2014. DOI: 10.1080/10643389.2013.829765.

PANG, Zheng; RAUDONIS, Renee; GLICK, Bernard R.; LIN, Tong Jun; CHENG, Zhenyu. Antibiotic resistance in Pseudomonas aeruginosa: mechanisms and alternative therapeutic strategies. **Biotechnology Advances**, *[S. l.]*, v. 37, n. 1, p. 177–192, 2019. DOI: 10.1016/j.biotechadv.2018.11.013. Disponível em: https://doi.org/10.1016/j.biotechadv.2018.11.013.

PARTRIDGE, Sally R.; TSAFNAT, Guy; COIERA, Enrico; IREDELL, Jonathan R. Gene cassettes and cassette arrays in mobile resistance integrons: Review article. **FEMS Microbiology Reviews**, *[S. l.]*, v. 33, n. 4, p. 757–784, 2009. DOI: 10.1111/j.1574-6976.2009.00175.x.

PATEL, Manvendra; KUMAR, Rahul; KISHOR, Kamal; MLSNA, Todd; PITTMAN, Charles U.; MOHAN, Dinesh. Pharmaceuticals of emerging concern in aquatic systems: Chemistry, occurrence, effects, and removal methods. **Chemical Reviews**, *[S. l.]*, v. 119, n. 6, p. 3510–3673, 2019. DOI: 10.1021/acs.chemrev.8b00299.

PAZDA, Magdalena; KUMIRSKA, Jolanta; STEPNOWSKI, Piotr; MULKIEWICZ, Ewa. Antibiotic resistance genes identified in wastewater treatment plant systems – A review. **Science of the Total Environment**, *[S. l.]*, v. 697, p. 134023, 2019. DOI: 10.1016/j.scitotenv.2019.134023. Disponível em: https://doi.org/10.1016/j.scitotenv.2019.134023.

PERRY, J. D.; FREYDIÈRE, A. M. The application of chromogenic media in clinical microbiology. **Journal of Applied Microbiology**, *[S. l.]*, v. 103, n. 6, p. 2046–2055, 2007. DOI: 10.1111/j.1365-2672.2007.03442.x.

PESAKHOV, Stella; BENISTY, Rachel; SIKRON, Noga; COHEN, Zvi; GOMELSKY, Pavel; KHOZIN-GOLDBERG, Inna; DAGAN, Ron; PORAT, Nurith. Effect of hydrogen peroxide production and the Fenton reaction on membrane composition of Streptococcus pneumoniae. **Biochimica et Biophysica Acta - Biomembranes**, *[S. l.]*, v. 1768, n. 3, p. 590–597, 2007. DOI: 10.1016/j.bbamem.2006.12.016.

PODSCHUN, R.; ULLMANN, U. Klebsiella spp. as nosocomial pathogens: Epidemiology, taxonomy, typing methods, and pathogenicity factors. **Clinical Microbiology Reviews**, *[S. l.]*, v. 11, n. 4, p. 589–603, 1998. DOI: 10.1128/cmr.11.4.589.

POLIANCIUC, Svetlana Iuliana; GURZĂU, Anca Elena; KISS, Bela; GEORGIA ȘTEFAN, Maria; LOGHIN, Felicia. Antibiotics in the environment: causes and consequences. **Medicine and Pharmacy Reports**, *[S. l.]*, v. 93, n. 3, p. 231–240, 2020. DOI: 10.15386/mpr-1742.

POLO-LÓPEZ, María Inmaculada; SÁNCHEZ PÉREZ, José Antonio. Perspectives of the solar photo-Fenton process against the spreading of pathogens, antibiotic-resistant bacteria and genes in the environment. **Current Opinion in Green and Sustainable Chemistry**, *[S. l.]*, v. 27, p. 100416, 2021. DOI: 10.1016/j.cogsc.2020.100416. Disponível em: https://doi.org/10.1016/j.cogsc.2020.100416.

POOLE, Andrew J. Treatment of biorefractory organic compounds in wool scour effluent by hydroxyl radical oxidation. **Water Research**, *[S. l.]*, v. 38, n. 14–15, p. 3458–3464, 2004. DOI: 10.1016/j.watres.2004.06.001.

QIAN, Yajie; ZHOU, Xuefei; ZHANG, Yalei; SUN, Peizhe; ZHANG, Weixian; CHEN, Jiabin; GUO, Xin; ZHANG, Xiao. Performance of α-methylnaphthalene degradation by dual oxidant of persulfate/calcium peroxide: Implication for ISCO. **Chemical Engineering Journal**, *[S. l.]*, v. 279, p. 538–546, 2015. DOI: 10.1016/j.cej.2015.05.053. Disponível em: http://dx.doi.org/10.1016/j.cej.2015.05.053.

QIU, Qianlinglin; LI, Guoxiang; DAI, Yi; XU, Yaoyang; BAO, Peng. Removal of antibiotic resistant microbes by Fe(II)-activated persulfate oxidation. **Journal of Hazardous Materials**, *[S. l.]*, v. 396, n. April, p. 122733, 2020. DOI: 10.1016/j.jhazmat.2020.122733. Disponível em: https://doi.org/10.1016/j.jhazmat.2020.122733.

QIU, Rui; ZHANG, Peng; FENG, Guojie; NI, Xinxin; MIAO, Zhu; WEI, Li; SUN, Hongwen. Enhanced thermal activation of persulfate by coupling hydrogen peroxide for efficient degradation of pyrene. **Chemosphere**, *[S. l.]*, v. 303, n. P3, p. 135057, 2022. DOI: 10.1016/j.chemosphere.2022.135057. Disponível em: https://doi.org/10.1016/j.chemosphere.2022.135057.

QUINTELA-BALUJA, Marcos; ABOUELNAGA, M.; ROMALDE, J.; SU, Jian Qiang; YU, Yongjie; GOMEZ-LOPEZ, Mariano; SMETS, B.; ZHU, Yong Guan; GRAHAM, David W. Spatial ecology of a wastewater network defines the antibiotic resistance genes in downstream receiving waters. **Water Research**, *[S. l.]*, v. 162, p. 347–357, 2019. DOI: 10.1016/j.watres.2019.06.075. Disponível em: https://doi.org/10.1016/j.watres.2019.06.075.

RAHIM POURAN, Shima; ABDUL AZIZ, A. R.; WAN DAUD, Wan Mohd Ashri. Review on the main advances in photo-Fenton oxidation system for recalcitrant wastewaters. **Journal of Industrial and Engineering Chemistry**, *[S. l.]*, v. 21, p. 53–69, 2015. DOI: 10.1016/j.jiec.2014.05.005. Disponível em: http://dx.doi.org/10.1016/j.jiec.2014.05.005.

RAHUBE, Teddie O.; VIANA, Laia Santiña; KORAIMANN, Günther; YOST, Christopher K. Characterization and comparative analysis of antibiotic resistance plasmids isolated from a wastewater treatment plant. **Frontiers in Microbiology**, *[S. l.]*, v. 5, n. OCT, p. 1–9, 2014. DOI: 10.3389/fmicb.2014.00558.

RANJAN, Ravi; RANI, Asha; METWALLY, Ahmed; MCGEE, Halvor S.; PERKINS, David L. Analysis of the microbiome: Advantages of whole genome shotgun versus 16S amplicon sequencing. **Biochemical and Biophysical Research**

Communications, *[S. l.]*, v. 469, n. 4, p. 967–977, 2016. DOI: 10.1016/j.bbrc.2015.12.083. Disponível em: http://dx.doi.org/10.1016/j.bbrc.2015.12.083.

RAZA, Shahbaz; JO, Hyejun; KIM, Jungman; SHIN, Hanseob; HUR, Hor Gil; UNNO, Tatsuya. Metagenomic exploration of antibiotic resistome in treated wastewater effluents and their receiving water. **Science of the Total Environment**, *[S. l.]*, v. 765, p. 142755, 2021. DOI: 10.1016/j.scitotenv.2020.142755. Disponível em: https://doi.org/10.1016/j.scitotenv.2020.142755.

RAZA, Shahbaz; SHIN, Hanseob; HUR, Hor Gil; UNNO, Tatsuya. Higher abundance of core antimicrobial resistant genes in effluent from wastewater treatment plants. **Water Research**, *[S. l.]*, v. 208, n. August 2021, p. 117882, 2022. DOI: 10.1016/j.watres.2021.117882. Disponível em: https://doi.org/10.1016/j.watres.2021.117882.

REN, Shaojie; BOO, Chanhee; GUO, Ning; WANG, Shuguang; ELIMELECH, Menachem; WANG, Yunkun. Photocatalytic Reactive Ultrafiltration Membrane for Removal of Antibiotic Resistant Bacteria and Antibiotic Resistance Genes from Wastewater Effluent. **Environmental Science and Technology**, *[S. l.]*, v. 52, n. 15, p. 8666–8673, 2018. DOI: 10.1021/acs.est.8b01888.

RIAZ, Luqman; ANJUM, Muzammil; YANG, Qingxiang; SAFEER, Rabia; SIKANDAR, Anila; ULLAH, Habib; SHAHAB, Asfandyar; YUAN, Wei; WANG, Qianqian. **Treatment technologies and management options of antibiotics and AMR/ARGs**. [s.l.] : Elsevier Inc., 2019. DOI: 10.1016/B978-0-12-818882-8.00023-1. Disponível em: http://dx.doi.org/10.1016/B978-0-12-818882-8.00023-1.

RICE, Eric W.; WANG, Phillip; SMITH, Adam L.; STADLER, Lauren B. Determining Hosts of Antibiotic Resistance Genes: A Review of Methodological Advances. **Environmental Science and Technology Letters**, *[S. l.]*, v. 7, n. 5, p. 282–291, 2020. DOI: 10.1021/acs.estlett.0c00202.

RIESENFELD, Christian S.; SCHLOSS, Patrick D.; HANDELSMAN, Jo. Metagenomics: Genomic analysis of microbial communities. **Annual Review of Genetics**, *[S. l.]*, v. 38, p. 525–552, 2004. DOI: 10.1146/annurev.genet.38.072902.091216.

RIZZO, L.; MANAIA, C.; MERLIN, C.; SCHWARTZ, T.; DAGOT, C.; PLOY, M. C.; MICHAEL, I.; FATTA-KASSINOS, D. Urban wastewater treatment plants as hotspots for antibiotic resistant bacteria and genes spread into the environment: A review. **Science of the Total Environment**, *[S. l.]*, v. 447, p. 345–360, 2013. DOI: 10.1016/j.scitotenv.2013.01.032. Disponível em: http://dx.doi.org/10.1016/j.scitotenv.2013.01.032.

RIZZO, Luigi. Bioassays as a tool for evaluating advanced oxidation processes in water and wastewater treatment. **Water Research**, *[S. l.]*, v. 45, n. 15, p. 4311–4340, 2011. DOI: 10.1016/j.watres.2011.05.035. Disponível em: http://dx.doi.org/10.1016/j.watres.2011.05.035.

RIZZO, Luigi et al. Consolidated vs new advanced treatment methods for the removal of contaminants of emerging concern from urban wastewater. **Science of the Total Environment**, *[S. l.]*, v. 655, n. October 2018, p. 986–1008, 2019. DOI: 10.1016/j.scitotenv.2018.11.265.

RIZZO, Luigi. Addressing main challenges in the tertiary treatment of urban wastewater: are homogeneous photodriven AOPs the answer? **Environmental Science: Water Research & Technology**, *[S. l.]*, 2022. DOI: 10.1039/d2ew00146b.

RIZZO, Luigi; GERNJAK, Wolfgang; KRZEMINSKI, Pawel; MALATO, Sixto; MCARDELL, Christa S.; PEREZ, Jose Antonio Sanchez; SCHAAR, Heidemarie; FATTA-KASSINOS, Despo. Best available technologies and treatment trains to address current challenges in urban wastewater reuse for irrigation of crops in EU countries. **Science of the Total Environment**, *[S. l.]*, v. 710, p. 136312, 2020. DOI: 10.1016/j.scitotenv.2019.136312. Disponível em: https://doi.org/10.1016/j.scitotenv.2019.136312.

ROBBINS, Cristian A.; DU, Xuewei; BRADLEY, Thomas H.; QUINN, Jason C.; BANDHAUER, Todd M.; CONRAD, Steven A.; CARLSON, Kenneth H.; TONG, Tiezheng. Beyond treatment technology: Understanding motivations and barriers for wastewater treatment and reuse in unconventional energy production. **Resources, Conservation and Recycling**, *[S. l.]*, v. 177, n. May 2021, p. 106011, 2022. DOI: 10.1016/j.resconrec.2021.106011. Disponível em: https://doi.org/10.1016/j.resconrec.2021.106011.

ROCHA, Jaqueline et al. Inter-laboratory calibration of quantitative analyses of antibiotic resistance genes. **Journal of Environmental Chemical Engineering**, *[S. l.]*, v. 8, n. 1, p. 102214, 2020. DOI: 10.1016/j.jece.2018.02.022. Disponível em: https://doi.org/10.1016/j.jece.2018.02.022.

RODRIGUES-SILVA, Fernando; MARIA, Maria Clara; AMORIM, Camila C. Challenges on solar oxidation as post-treatment of municipal wastewater from UASB systems: Treatment efficiency, disinfection and toxicity. **Science of the Total Environment**, *[S. l.]*, v. 850, n. August, p. 157940, 2022. DOI: 10.1016/j.scitotenv.2022.157940. Disponível em: https://doi.org/10.1016/j.scitotenv.2022.157940.

RODRÍGUEZ-CHUECA, Jorge et al. Assessment of full-scale tertiary wastewater treatment by UV-C based-AOPs: Removal or persistence of antibiotics and antibiotic resistance genes? **Science of the Total Environment**, *[S. l.]*, v. 652, p. 1051–1061, 2019. a. DOI: 10.1016/j.scitotenv.2018.10.223. Disponível em: https://doi.org/10.1016/j.scitotenv.2018.10.223.

RODRÍGUEZ-CHUECA, Jorge; GIANNAKIS, Stefanos; MARJANOVIC, Miloch; KOHANTORABI, Mona; GHOLAMI, Mohammad Reza; GRANDJEAN, Dominique; DE ALENCASTRO, Luiz Felippe; PULGARÍN, César. Solar-assisted bacterial disinfection and removal of contaminants of emerging concern by Fe2+-activated HSO5- vs. S2O82- in drinking water. **Applied Catalysis B: Environmental**, *[S. l.]*, v. 248, n. February, p. 62–72, 2019. b. DOI: 10.1016/j.apcatb.2019.02.018. Disponível em: https://doi.org/10.1016/j.apcatb.2019.02.018.

RODRÍGUEZ-CHUECA, Jorge; MOREIRA, Sónia I.; LUCAS, Marco S.; FERNANDES, José R.; TAVARES, Pedro B.; SAMPAIO, Ana; PERES, José A. Disinfection of simulated and real winery wastewater using sulphate radicals: Peroxymonosulphate/transition metal/UV-A LED oxidation. **Journal of Cleaner Production**, *[S. l.]*, v. 149, p. 805–817, 2017. DOI: 10.1016/j.jclepro.2017.02.135.

ROMANOWSKI, G.; LORENZ, M. G.; WACKERNAGEL, W. Adsorption of plasmid

DNA to mineral surfaces and protection against DNase I. **Applied and Environmental Microbiology**, *[S. l.]*, v. 57, n. 4, p. 1057–1061, 1991. DOI: 10.1128/aem.57.4.1057-1061.1991.

ROMMOZZI, Elena; GIANNAKIS, Stefanos; GIOVANNETTI, Rita; VIONE, Davide; PULGARIN, César. Detrimental vs. beneficial influence of ions during solar (SODIS) and photo-Fenton disinfection of E. coli in water: (Bi)carbonate, chloride, nitrate and nitrite effects. **Applied Catalysis B: Environmental**, *[S. l.]*, v. 270, n. December 2019, 2020. DOI: 10.1016/j.apcatb.2020.118877.

ROSANO, Germán L.; CECCARELLI, Eduardo A. Recombinant protein expression in Escherichia coli: Advances and challenges. **Frontiers in Microbiology**, *[S. l.]*, v. 5, n. APR, p. 1–17, 2014. DOI: 10.3389/fmicb.2014.00172.

ROWE, Will P. M.; WINN, Martyn D. Indexed variation graphs for efficient and accurate resistome profiling. **Bioinformatics**, *[S. l.]*, v. 34, n. 21, p. 3601–3608, 2018. DOI: 10.1093/bioinformatics/bty387.

RYAN, Michael P.; PEMBROKE, J. Tony. Brevundimonas spp: Emerging global opportunistic pathogens. **Virulence**, *[S. l.]*, v. 9, n. 1, p. 480–493, 2018. DOI: 10.1080/21505594.2017.1419116. Disponível em: https://doi.org/10.1080/21505594.2017.1419116.

SAIMA, Saima; FIAZ, Marium; ZAFAR, Rabeea; AHMED, Iftikhar; ARSHAD, Muhammad. **Dissemination of antibiotic resistance in the environment**. [s.l.] : Elsevier Inc., 2019. DOI: 10.1016/B978-0-12-818882-8.00006-1. Disponível em: http://dx.doi.org/10.1016/B978-0-12-818882-8.00006-1.

SAMBAZA, Shepherd Sundayi; NAICKER, Nisha. Contribution of wastewater to Antimicrobial Resistance- A Review article. **Journal of Global Antimicrobial Resistance**, *[S. l.]*, p. 0–27, 2023. DOI: 10.1016/j.jgar.2023.05.010. Disponível em: https://doi.org/10.1016/j.jgar.2023.05.010.

SAMREEN; AHMAD, Iqbal; MALAK, Hesham A.; ABULREESH, Hussein H. Environmental antimicrobial resistance and its drivers: a potential threat to public health. **Journal of Global Antimicrobial Resistance**, *[S. l.]*, v. 27, p. 101–111, 2021. DOI: 10.1016/j.jgar.2021.08.001.

SAN MILLAN, Alvaro. Evolution of Plasmid-Mediated Antibiotic Resistance in the Clinical Context. **Trends in Microbiology**, *[S. l.]*, v. 26, n. 12, p. 978–985, 2018. DOI: 10.1016/j.tim.2018.06.007. Disponível em: https://doi.org/10.1016/j.tim.2018.06.007.

SANSCHAGRIN, Sylvie; YERGEAU, Etienne. Next-generation sequencing of 16S ribosomal RNA gene amplicons. **Journal of Visualized Experiments**, *[S. l.]*, n. 90, p. 3–8, 2014. DOI: 10.3791/51709.

SBARDELLA, L.; VELO-GALA, I.; COMAS, J.; RODRÍGUEZ-RODA LAYRET, I.; FENU, A.; GERNJAK, W. The impact of wastewater matrix on the degradation of pharmaceutically active compounds by oxidation processes including ultraviolet radiation and sulfate radicals. **Journal of Hazardous Materials**, *[S. l.]*, v. 380, n. July, p. 120869, 2019. DOI: 10.1016/j.jhazmat.2019.120869. Disponível em: https://doi.org/10.1016/j.jhazmat.2019.120869.

SEGATA, Nicola; IZARD, Jacques; WALDRON, Levi; GEVERS, Dirk; MIROPOLSKY, Larisa; GARRETT, Wendy S.; HUTTENHOWER, Curtis. Segata-LEfSe-gb-2011. *[S.*

I.], 2011.

SENG, Piseth et al. Emerging role of Raoultella ornithinolytica in human infections: A series of cases and review of the literature. **International Journal of Infectious Diseases**, *[S. l.]*, v. 45, p. 65–71, 2016. DOI: 10.1016/j.ijid.2016.02.014.

SERNA-GALVIS, Efraim A.; TROYON, Jean Arnaud; GIANNAKIS, Stefanos; TORRES-PALMA, Ricardo A.; CARENA, Luca; VIONE, Davide; PULGARIN, C. Kinetic modeling of lag times during photo-induced inactivation of E. coli in sunlit surface waters: Unraveling the pathways of exogenous action. **Water Research**, *[S. l.]*, v. 163, p. 114894, 2019. DOI: 10.1016/j.watres.2019.114894. Disponível em: https://doi.org/10.1016/j.watres.2019.114894.

SHARMA, Virender K.; JOHNSON, Natalie; CIZMAS, Leslie; MCDONALD, Thomas J.; KIM, Hyunook. A review of the influence of treatment strategies on antibiotic resistant bacteria and antibiotic resistance genes. **Chemosphere**, *[S. l.]*, v. 150, p. 702–714, 2016. DOI: 10.1016/j.chemosphere.2015.12.084.

SHARMA, Virender K.; YU, Xin; MCDONALD, Thomas J.; JINADATHA, Chetan; DIONYSIOU, Dionysios D.; FENG, Mingbao. Elimination of antibiotic resistance genes and control of horizontal transfer risk by UV-based treatment of drinking water: A mini review. **Frontiers of Environmental Science and Engineering**, *[S. l.]*, v. 13, n. 3, 2019. DOI: 10.1007/s11783-019-1122-7.

SIDDIQUE, Yasir Hasan; ARA, Gulshan; AFZAL, Mohammad. Estimation of lipid peroxidation induced by hydrogen peroxide in cultured human lymphocytes. **Dose-Response**, *[S. l.]*, v. 10, n. 1, p. 1–10, 2012. DOI: 10.2203/dose-response.10-002.Siddique.

SILVA, Laís G. M.; MOREIRA, Francisca C.; SOUZA, Antônio A. U.; SOUZA, Selene M. A. G. U.; BOAVENTURA, Rui A. R.; VILAR, Vítor J. P. Chemical and electrochemical advanced oxidation processes as a polishing step for textile wastewater treatment: A study regarding the discharge into the environment and the reuse in the textile industry. **Journal of Cleaner Production**, *[S. l.]*, v. 198, p. 430–442, 2018. DOI: 10.1016/j.jclepro.2018.07.001.

SIMÕES, Joana; MOREIRA, Ana S. P.; DA COSTA, Elisabete; EVTYUGIN, Dmitry; DOMINGUES, Pedro; NUNES, Fernando M.; COIMBRA, Manuel A.; DOMINGUES, M. Rosário M. Oxidation of amylose and amylopectin by hydroxyl radicals assessed by electrospray ionisation mass spectrometry. **Carbohydrate Polymers**, *[S. l.]*, v. 148, p. 290–299, 2016. DOI: 10.1016/j.carbpol.2016.03.034. Disponível em: http://dx.doi.org/10.1016/j.carbpol.2016.03.034.

SINGH, Ashish Kumar; KAUR, Rajinder; VERMA, Shashikala; SINGH, Samer. Antimicrobials and Antibiotic Resistance Genes in Water Bodies: Pollution, Risk, and Control. **Frontiers in Environmental Science**, *[S. l.]*, v. 10, n. April, p. 1–13, 2022. DOI: 10.3389/fenvs.2022.830861.

SONG, Yue et al. Zero-valent iron activated persulfate remediation of polycyclic aromatic hydrocarbon-contaminated soils: An in situ pilot-scale study. **Chemical Engineering Journal**, *[S. l.]*, v. 355, n. August 2018, p. 65–75, 2019. DOI: 10.1016/j.cej.2018.08.126. Disponível em: https://doi.org/10.1016/j.cej.2018.08.126.

SONUNE, Amit; GHATE, Rupali. Developments in wastewater treatment methods.

Desalination, *[S. l.]*, v. 167, n. 1–3, p. 55–63, 2004. DOI: 10.1016/j.desal.2004.06.113.

SOUSA, José M.; MACEDO, Gonçalo; PEDROSA, Marta; BECERRA-CASTRO, Cristina; CASTRO-SILVA, Sérgio; PEREIRA, M. Fernando R.; SILVA, Adrián M. T.; NUNES, Olga C.; MANAIA, Célia M. Ozonation and UV254nm radiation for the removal of microorganisms and antibiotic resistance genes from urban wastewater. **Journal of Hazardous Materials**, *[S. l.]*, v. 323, p. 434–441, 2017. DOI: 10.1016/j.jhazmat.2016.03.096.

STANTON, Isobel C.; MURRAY, Aimee K.; ZHANG, Lihong; SNAPE, Jason; GAZE, William H. Evolution of antibiotic resistance at low antibiotic concentrations including selection below the minimal selective concentration. **Communications Biology**, *[S. l.]*, v. 3, n. 1, p. 1–11, 2020. DOI: 10.1038/s42003-020-01176-w. Disponível em: http://dx.doi.org/10.1038/s42003-020-01176-w.

STARLING, Maria Clara V. M.; AMORIM, Camila C.; LEÃO, Mônica Maria D. Occurrence, control and fate of contaminants of emerging concern in environmental compartments in Brazil. **Journal of Hazardous Materials**, *[S. l.]*, v. 372, n. October 2017, p. 17–36, 2019. DOI: 10.1016/j.jhazmat.2018.04.043. Disponível em: https://doi.org/10.1016/j.jhazmat.2018.04.043.

STARLING, Maria Clara V. M.; COSTA, Elizângela P.; SOUZA, Felipe A.; MACHADO, Elayne C.; ARAUJO, Juliana Calábria De; AMORIM, Camila C. Persulfate mediated solar photo-Fenton aiming at wastewater treatment plant effluent improvement at neutral PH : emerging contaminant removal , disinfection , and elimination of antibiotic-resistant bacteria. *[S. l.]*, 2021.

SU, Jian Qiang; AN, Xin Li; LI, Bing; CHEN, Qing Lin; GILLINGS, Michael R.; CHEN, Hong; ZHANG, Tong; ZHU, Yong Guan. Metagenomics of urban sewage identifies an extensively shared antibiotic resistome in China. **Microbiome**, *[S. l.]*, v. 5, n. 1, p. 1–15, 2017. DOI: 10.1186/s40168-017-0298-y.

SUN, Peizhe; TYREE, Corey; HUANG, Ching Hua. Inactivation of Escherichia coli, Bacteriophage MS2, and Bacillus Spores under UV/H2O2 and UV/Peroxydisulfate Advanced Disinfection Conditions. **Environmental Science and Technology**, *[S. l.]*, v. 50, n. 8, p. 4448–4458, 2016. DOI: 10.1021/acs.est.5b06097.

SZCZEPANOWSKI, Rafael; LINKE, Burkhard; KRAHN, Irene; GARTEMANN, Karl Heinz; GÜTZKOW, Tim; EICHLER, Wolfgang; PÜHLER, Alfred; SCHLÜTER, Andreas. Detection of 140 clinically relevant antibiotic-resistance genes in the plasmid metagenome of wastewater treatment plant bacteria showing reduced susceptibility to selected antibiotics. **Microbiology**, *[S. l.]*, v. 155, n. 7, p. 2306–2319, 2009. DOI: 10.1099/mic.0.028233-0.

TAGLIAFERRI, Thaysa Leite; GUIMARÃES, Natália Rocha; PEREIRA, Marcella de Paula Martins; VILELA, Liza Figueiredo Felicori; HORZ, Hans Peter; DOS SANTOS, Simone Gonçalves; MENDES, Tiago Antônio de Oliveira. Exploring the Potential of CRISPR-Cas9 Under Challenging Conditions: Facing High-Copy Plasmids and Counteracting Beta-Lactam Resistance in Clinical Strains of Enterobacteriaceae. **Frontiers in Microbiology**, *[S. l.]*, v. 11, n. April, p. 1–11, 2020. DOI: 10.3389/fmicb.2020.00578.

TAKEUCHI, Shotaro; HASHIZUME, Naoko; KINOSHITA, Takafumi; KAIDOH, Toshio; TAMURA, Yutaka. Detection of Clostridium septicum Hemolysin Gene by Polymerase

Chain Reaction. **Journal of Veterinary Medical Science**, *[S. l.]*, v. 59, n. 9, p. 853–855, 1997. DOI: 10.1292/jvms.59.853.

TIWARI, Bhagyashree; SELLAMUTHU, Balasubramanian; OUARDA, Yassine; DROGUI, Patrick; TYAGI, Rajeshwar D.; BUELNA, Gerardo. Review on fate and mechanism of removal of pharmaceutical pollutants from wastewater using biological approach. **Bioresource Technology**, *[S. l.]*, v. 224, p. 1–12, 2017. DOI: 10.1016/j.biortech.2016.11.042. Disponível em: http://dx.doi.org/10.1016/j.biortech.2016.11.042.

TORRES, Neusa F.; CHIBI, Buyisile; KUUPIEL, Desmond; SOLOMON, Vernon P.; MASHAMBA-THOMPSON, Tivani P.; MIDDLETON, Lyn E. The use of non-prescribed antibiotics; prevalence estimates in low-and-middle-income countries. A systematic review and meta-analysis. **Archives of Public Health**, *[S. l.]*, v. 79, n. 1, p. 1–15, 2021. DOI: 10.1186/s13690-020-00517-9.

VAZ-MOREIRA, Ivone; EGAS, Conceição; NUNES, Olga C.; MANAIA, Célia M. Culture-dependent and culture-independent diversity surveys target different bacteria: A case study in a freshwater sample. **Antonie van Leeuwenhoek, International Journal of General and Molecular Microbiology**, *[S. l.]*, v. 100, n. 2, p. 245–257, 2011. DOI: 10.1007/s10482-011-9583-0.

VAZ-MOREIRA, Ivone; NUNES, Olga C.; MANAIA, Célia M. Bacterial diversity and antibiotic resistance in water habitats: Searching the links with the human microbiome. **FEMS Microbiology Reviews**, *[S. l.]*, v. 38, n. 4, p. 761–778, 2014. DOI: 10.1111/1574-6976.12062.

VERBEL-OLARTE, Martha I.; SERNA-GALVIS, Efraim A.; SALAZAR-OSPINA, Lorena; JIMÉNEZ, J. Natalia; PORRAS, Jazmín; PULGARIN, Cesar; TORRES-PALMA, Ricardo A. Irreversible inactivation of carbapenem-resistant Klebsiella pneumoniae and its genes in water by photo-electro-oxidation and photo-electro-Fenton - Processes action modes. **Science of The Total Environment**, *[S. l.]*, v. 792, p. 148360, 2021. DOI: 10.1016/j.scitotenv.2021.148360. Disponível em: https://doi.org/10.1016/j.scitotenv.2021.148360.

VIKESLAND, Peter; GARNER, Emily; GUPTA, Suraj; KANG, Seju; MAILE-MOSKOWITZ, Ayella; ZHU, Ni. Differential Drivers of Antimicrobial Resistance across the World. **Accounts of Chemical Research**, *[S. l.]*, v. 52, n. 4, p. 916–924, 2019. a. DOI: 10.1021/acs.accounts.8b00643.

VIKESLAND, Peter; GARNER, Emily; GUPTA, Suraj; KANG, Seju; MAILE-MOSKOWITZ, Ayella; ZHU, Ni. Differential Drivers of Antimicrobial Resistance across the World. **Accounts of Chemical Research**, *[S. l.]*, v. 52, n. 4, p. 916–924, 2019. b. DOI: 10.1021/acs.accounts.8b00643.

VILELA, P. B.; DALALIBERA, A.; DUMINELLI, E. C.; BECEGATO, V. A.; PAULINO, A. T. Correction to: Adsorption and removal of chromium (VI) contained in aqueous solutions using a chitosan-based hydrogel (Environmental Science and Pollution Research, (2018), 10.1007/s11356-018-3208-3). **Environmental Science and Pollution Research**, *[S. l.]*, 2018. DOI: 10.1007/s11356-018-3372-5.

VILELA, Pâmela B.; MARTINS, Alessandra S.; STARLING, Maria Clara V. M.; DE SOUZA, Felipe A. R.; PIRES, Giovana F. F.; AGUILAR, Ananda P.; PINTO, Maria Eduarda A.; MENDES, Tiago A. O.; DE AMORIM, Camila C. Solar photon-Fenton

process eliminates free plasmid DNA harboring antimicrobial resistance genes from wastewater. **Journal of Environmental Management**, *[S. l.]*, v. 285, n. October 2020, 2021. a. DOI: 10.1016/j.jenvman.2021.112204.

VILELA, Pâmela B.; MENDONÇA NETO, Rondon P.; STARLING, Maria Clara V. M.; DA S. MARTINS, Alessandra; PIRES, Giovanna F. F.; SOUZA, Felipe A. R.; AMORIM, Camila C. Metagenomic analysis of MWWTP effluent treated via solar photo-Fenton at neutral pH: Effects upon microbial community, priority pathogens, and antibiotic resistance genes. **Science of The Total Environment**, *[S. l.]*, v. 801, p. 149599, 2021. b. DOI: 10.1016/j.scitotenv.2021.149599. Disponível em: https://doi.org/10.1016/j.scitotenv.2021.149599.

VILELA, Pâmela B.; V.M. STARLING, Maria Clara; MENDONÇA NETO, Rondon P.; DE SOUZA, Felipe A. R.; PIRES, Giovanna F. F.; AMORIM, Camila C. Solar photo-Fenton mediated by alternative oxidants for MWWTP effluent quality improvement: Impact on microbial community, priority pathogens and removal of antibiotic-resistant genes. **Chemical Engineering Journal**, *[S. l.]*, v. 441, n. March, p. 136060, 2022. a. DOI: 10.1016/j.cej.2022.136060.

VILELA, Pâmela B.; V.M. STARLING, Maria Clara; MENDONÇA NETO, Rondon P.; DE SOUZA, Felipe A. R.; PIRES, Giovanna F. F.; AMORIM, Camila C. Solar photo-Fenton mediated by alternative oxidants for MWWTP effluent quality improvement: Impact on microbial community, priority pathogens and removal of antibiotic-resistant genes. **Chemical Engineering Journal**, *[S. l.]*, v. 441, n. January, p. 136060, 2022. b. DOI: 10.1016/j.cej.2022.136060.

VON SPERLING, Marcos. Urban wastewater treatment in Brazil. **Minas Gerais Brazil**, *[S. l.]*, n. August, p. 27, 2016. Disponível em: www.iadb.org.

WACŁAWEK, Stanisław; LUTZE, Holger V.; GRÜBEL, Klaudiusz; PADIL, Vinod V. T.; ČERNÍK, Miroslav; DIONYSIOU, Dionysios D. Chemistry of persulfates in water and wastewater treatment: A review. **Chemical Engineering Journal**, *[S. l.]*, v. 330, n. June, p. 44–62, 2017. DOI: 10.1016/j.cej.2017.07.132.

WALKER, R. D. Standards for antimicrobial susceptibility testing. **American journal of veterinary research**, *[S. l.]*, v. 60, n. 9, p. 1034, 1999.

WANG, Feifei; VAN HALEM, Doris; LIU, Gang; LEKKERKERKER-TEUNISSEN, Karin; VAN DER HOEK, Jan Peter. Effect of residual H2O2 from advanced oxidation processes on subsequent biological water treatment: A laboratory batch study. **Chemosphere**, *[S. l.]*, v. 185, p. 637–646, 2017. a. DOI: 10.1016/j.chemosphere.2017.07.073. Disponível em: http://dx.doi.org/10.1016/j.chemosphere.2017.07.073.

WANG, Haichao; WANG, Jin; LI, Shuming; DING, Guoyu; WANG, Kun; ZHUANG, Tao; HUANG, Xue; WANG, Xiaoyue. Synergistic effect of UV/chlorine in bacterial inactivation, resistance gene removal, and gene conjugative transfer blocking. **Water Research**, *[S. l.]*, v. 185, p. 116290, 2020. a. DOI: 10.1016/j.watres.2020.116290. Disponível em: https://doi.org/10.1016/j.watres.2020.116290.

WANG, Jianlong; CHEN, Xiaoying. Removal of antibiotic resistance genes (ARGs) in various wastewater treatment processes: An overview. **Critical Reviews in Environmental Science and Technology**, *[S. l.]*, v. 0, n. 0, p. 1–60, 2020. DOI: 10.1080/10643389.2020.1835124. Disponível em:

https://doi.org/10.1080/10643389.2020.1835124.

WANG, Jianlong; CHEN, Xiaoying. Removal of antibiotic resistance genes (ARGs) in various wastewater treatment processes: An overview. **Critical Reviews in Environmental Science and Technology**, *[S. l.]*, v. 52, n. 4, p. 571–630, 2022. DOI: 10.1080/10643389.2020.1835124. Disponível em: https://doi.org/10.1080/10643389.2020.1835124.

WANG, Jianlong; CHU, Libing; WOJNÁROVITS, László; TAKÁCS, Erzsébet. Occurrence and fate of antibiotics, antibiotic resistant genes (ARGs) and antibiotic resistant bacteria (ARB) in municipal wastewater treatment plant: An overview. **Science of the Total Environment**, *[S. l.]*, v. 744, p. 140997, 2020. b. DOI: 10.1016/j.scitotenv.2020.140997. Disponível em: https://doi.org/10.1016/j.scitotenv.2020.140997.

WANG, Jianlong; WANG, Shizong. Activation of persulfate (PS) and peroxymonosulfate (PMS) and application for the degradation of emerging contaminants. **Chemical Engineering Journal**, *[S. l.]*, v. 334, n. October 2017, p. 1502–1517, 2018. DOI: 10.1016/j.cej.2017.11.059. Disponível em: https://doi.org/10.1016/j.cej.2017.11.059.

WANG, Li; PENG, Libin; XIE, Liling; DENG, Peiyan; DENG, Dayi. Compatibility of Surfactants and Thermally Activated Persulfate for Enhanced Subsurface Remediation. **Environmental Science and Technology**, *[S. l.]*, v. 51, n. 12, p. 7055–7064, 2017. b. DOI: 10.1021/acs.est.6b05477.

WANG, Manna; ATEIA, Mohamed; AWFA, Dion; YOSHIMURA, Chihiro. Regrowth of bacteria after light-based disinfection — What we know and where we go from here. **Chemosphere**, *[S. l.]*, v. 268, p. 128850, 2021. a. DOI: 10.1016/j.chemosphere.2020.128850. Disponível em: https://doi.org/10.1016/j.chemosphere.2020.128850.

WANG, Meng et al. Genomic insights into evolution of pathogenicity and resistance of multidrug-resistant Raoultella ornithinolytica WM1. **Annals of the New York Academy of Sciences**, *[S. l.]*, v. 1497, n. 1, p. 74–90, 2021. b. DOI: 10.1111/nyas.14595.

WANG, Pengxia; HE, Dongmei; LI, Baiyuan; GUO, Yunxue; WANG, Weiquan; LUO, Xiongjian; ZHAO, Xuanyu; WANG, Xiaoxue. Eliminating mcr-1-harbouring plasmids in clinical isolates using the CRISPR/Cas9 system. **Journal of Antimicrobial Chemotherapy**, *[S. l.]*, v. 74, n. 9, p. 2559–2565, 2019. a. DOI: 10.1093/jac/dkz246.

WANG, Wanjun; WANG, Hanna; LI, Guiying; AN, Taicheng; ZHAO, Huijun; WONG, Po Keung. Catalyst-free activation of persulfate by visible light for water disinfection: Efficiency and mechanisms. **Water Research**, *[S. l.]*, v. 157, p. 106–118, 2019. b. DOI: 10.1016/j.watres.2019.03.071. Disponível em: https://doi.org/10.1016/j.watres.2019.03.071.

WANG, Yafen; LIU, Chaoxing; HONG, Tingting; WU, Fan; YU, Shuyi; HE, Zhiyong; MAO, Wuxiang; ZHOU, Xiang. Application of Ammonium Persulfate for Selective Oxidation of Guanines for Nucleic Acid Sequencing. **Molecules (Basel, Switzerland)**, *[S. l.]*, v. 22, n. 7, p. 1–10, 2017. c. DOI: 10.3390/molecules22071222.

WEAR, Stephanie L.; ACUÑA, Vicenç; MCDONALD, Rob; FONT, Carme. Sewage pollution, declining ecosystem health, and cross-sector collaboration. **Biological**

Conservation, *[S. l.]*, v. 255, 2021. DOI: 10.1016/j.biocon.2021.109010.

WEI, Ziyan; FENG, Kai; LI, Shuzhen; ZHANG, Yu; CHEN, Hongrui; YIN, Huaqun; XU, Meiying; DENG, Ye. Exploring abundance, diversity and variation of a widespread antibiotic resistance gene in wastewater treatment plants. **Environment International**, *[S. l.]*, v. 117, n. May, p. 186–195, 2018. DOI: 10.1016/j.envint.2018.05.009. Disponível em: https://doi.org/10.1016/j.envint.2018.05.009.

WELLINGTON, Elizabeth M. H. et al. The role of the natural environment in the emergence of antibiotic resistance in Gram-negative bacteria. **The Lancet Infectious Diseases**, *[S. l.]*, v. 13, n. 2, p. 155–165, 2013. DOI: 10.1016/S1473-3099(12)70317-1. Disponível em: http://dx.doi.org/10.1016/S1473-3099(12)70317-1.

WILKINSON, John; HOODA, Peter S.; BARKER, James; BARTON, Stephen; SWINDEN, Julian. Occurrence, fate and transformation of emerging contaminants in water: An overarching review of the field. **Environmental Pollution**, *[S. l.]*, v. 231, p. 954–970, 2017. DOI: 10.1016/j.envpol.2017.08.032. Disponível em: https://doi.org/10.1016/j.envpol.2017.08.032.

WINGETT, Steven W.; ANDREWS, Simon. Fastq screen: A tool for multi-genome mapping and quality control [version 1; referees: 3 approved, 1 approved with reservations]. **F1000Research**, *[S. l.]*, v. 7, n. 0, p. 1–13, 2018. DOI: 10.12688/f1000research.15931.1.

WOEGERBAUER, Markus; BELLANGER, Xavier; MERLIN, Christophe. Cell-Free DNA: An Underestimated Source of Antibiotic Resistance Gene Dissemination at the Interface Between Human Activities and Downstream Environments in the Context of Wastewater Reuse. **Frontiers in Microbiology**, *[S. l.]*, v. 11, n. April, p. 1–11, 2020. DOI: 10.3389/fmicb.2020.00671.

WOOD, Derrick E.; LU, Jennifer; LANGMEAD, Ben. Improved metagenomic analysis with Kraken 2. **bioRxiv**, *[S. l.]*, p. 1–13, 2019. DOI: 10.1101/762302.

WORDOFA, Dawit N.; WALKER, Sharon L.; LIU, Haizhou. Sulfate Radical-Induced Disinfection of Pathogenic Escherichia coli O157:H7 via Iron-Activated Persulfate. **Environmental Science and Technology Letters**, *[S. l.]*, v. 4, n. 4, p. 154–160, 2017. DOI: 10.1021/acs.estlett.7b00035.

WU, Ya; FANG, Rongmiao; LI, Hao; LI, Jingyao; ZHAO, Dan; CHANG, Na Na; SUN, Huaming; SHI, Jun. Synergistic effect of ferrous ion-activated hydrogen peroxide and persulfate on the degradation of phthalates in aquatic environments by non-target analysis. **Chemical Engineering Journal**, *[S. l.]*, v. 451, n. August 2022, 2023. DOI: 10.1016/j.cej.2022.139100.

XIA, Yu; WEN, Xianghua; ZHANG, Bing; YANG, Yunfeng. Diversity and assembly patterns of activated sludge microbial communities: A review. **Biotechnology Advances**, *[S. l.]*, v. 36, n. 4, p. 1038–1047, 2018. DOI: 10.1016/j.biotechadv.2018.03.005. Disponível em: https://doi.org/10.1016/j.biotechadv.2018.03.005.

XIAO, Ruiyang et al. Inactivation of pathogenic microorganisms by sulfate radical: Present and future. **Chemical Engineering Journal**, *[S. l.]*, v. 371, n. March, p. 222–232, 2019. DOI: 10.1016/j.cej.2019.03.296.

XIE, Ning et al. Community composition and function of bacteria in activated sludge of municipal wastewater treatment plants. **Water (Switzerland)**, *[S. l.]*, v. 13, n. 6, p. 1–13, 2021. DOI: 10.3390/w13060852.

XIE, Shanshan; GU, April Z.; CEN, Tianyu; LI, Dan; CHEN, Jianmin. The effect and mechanism of urban fine particulate matter (PM2.5) on horizontal transfer of plasmid-mediated antimicrobial resistance genes. **Science of the Total Environment**, *[S. l.]*, v. 683, p. 116–123, 2019. DOI: 10.1016/j.scitotenv.2019.05.115. Disponível em: https://doi.org/10.1016/j.scitotenv.2019.05.115.

XU, Xiangjian; YANG, Yu; JIA, Yongfeng; LIAN, Xinying; ZHANG, Yan; FENG, Fan; LIU, Qiulong; XI, Beidou; JIANG, Yonghai. Heterogeneous catalytic degradation of 2,4-dinitrotoluene by the combined persulfate and hydrogen peroxide activated by the as-synthesized Fe-Mn binary oxides. **Chemical Engineering Journal**, *[S. l.]*, v. 374, n. January, p. 776–786, 2019. a. DOI: 10.1016/j.cej.2019.05.138. Disponível em: https://doi.org/10.1016/j.cej.2019.05.138.

XU, Ximeng; ZONG, Shaoyan; CHEN, Weiming; LIU, Dan. Heterogeneously catalyzed binary oxidants system with magnetic fly ash for the degradation of bisphenol A. **Chemical Engineering Journal**, *[S. l.]*, v. 360, n. October 2018, p. 1363–1370, 2019. b. DOI: 10.1016/j.cej.2018.10.192. Disponível em: https://doi.org/10.1016/j.cej.2018.10.192.

YADAV, Shailendra; KAPLEY, Atya. Antibiotic resistance: Global health crisis and metagenomics. **Biotechnology Reports**, *[S. l.]*, v. 29, p. e00604, 2021. DOI: 10.1016/j.btre.2021.e00604. Disponível em: https://doi.org/10.1016/j.btre.2021.e00604.

YAN, Ni; LIU, Fei; HUANG, Weiying. Interaction of oxidants in siderite catalyzed hydrogen peroxide and persulfate system using trichloroethylene as a target contaminant. **Chemical Engineering Journal**, *[S. l.]*, v. 219, p. 149–154, 2013. DOI: 10.1016/j.cej.2012.12.072. Disponível em: http://dx.doi.org/10.1016/j.cej.2012.12.072.

YANG, Chao; ZHANG, Wei; LIU, Ruihua; LI, Qiang; LI, Baobin; WANG, Shufang; SONG, Cunjiang; QIAO, Chuanling; MULCHANDANI, Ashok. Phylogenetic diversity and metabolic potential of activated sludge microbial communities in full-scale wastewater treatment plants. **Environmental Science and Technology**, *[S. l.]*, v. 45, n. 17, p. 7408–7415, 2011. DOI: 10.1021/es2010545.

YANG, Qi et al. Recent advances in photo-activated sulfate radical-advanced oxidation process (SR-AOP) for refractory organic pollutants removal in water. **Chemical Engineering Journal**, *[S. l.]*, v. 378, n. January, p. 122149, 2019. DOI: 10.1016/j.cej.2019.122149. Disponível em: https://doi.org/10.1016/j.cej.2019.122149.

YAZICI GUVENC, Senem. Optimization of COD removal from leachate nanofiltration concentrate using H2O2/Fe+2/heat – Activated persulfate oxidation processes. **Process Safety and Environmental Protection**, *[S. l.]*, v. 126, p. 7–17, 2019. DOI: 10.1016/j.psep.2019.03.034. Disponível em: https://doi.org/10.1016/j.psep.2019.03.034.

YIN, Huiyong; XU, Libin; PORTER, Ned A. Free radical lipid peroxidation: Mechanisms and analysis. **Chemical Reviews**, *[S. l.]*, v. 111, n. 10, p. 5944–5972, 2011. DOI: 10.1021/cr200084z.

YIN, Linning; WEI, Junyan; QI, Yumeng; TU, Zhengnan; QU, Ruijuan; YAN, Chao; WANG, Zunyao; ZHU, Feng. Degradation of pentachlorophenol in peroxymonosulfate/heat system: Kinetics, mechanism, and theoretical calculations. **Chemical Engineering Journal**, *[S. l.]*, v. 434, n. October 2021, p. 134736, 2022. DOI: 10.1016/j.cej.2022.134736. Disponível em: https://doi.org/10.1016/j.cej.2022.134736.

YIN, Xiaole; DENG, Yu; MA, Liping; WANG, Yulin; CHAN, Lilian Y. L.; ZHANG, Tong. Exploration of the antibiotic resistome in a wastewater treatment plant by a nine-year longitudinal metagenomic study. **Environment International**, *[S. l.]*, v. 133, n. November, p. 105270, 2019. DOI: 10.1016/j.envint.2019.105270. Disponível em: https://doi.org/10.1016/j.envint.2019.105270.

YIN, Xiaole; JIANG, Xiao Tao; CHAI, Benli; LI, Liguan; YANG, Ying; COLE, James R.; TIEDJE, James M.; ZHANG, Tong. ARGs-OAP v2.0 with an expanded SARG database and Hidden Markov Models for enhancement characterization and quantification of antibiotic resistance genes in environmental metagenomes. **Bioinformatics**, *[S. l.]*, v. 34, n. 13, p. 2263–2270, 2018. DOI: 10.1093/bioinformatics/bty053.

YIP, Alex Chi Kin; LAM, Frank Leung Yuk; HU, Xijun. Chemical-vapor-deposited copper on acid-activated bentonite clay as an applicable heterogeneous catalyst for the photo-fenton-like oxidation of textile organic pollutants. **Industrial and Engineering Chemistry Research**, *[S. l.]*, v. 44, n. 21, p. 7983–7990, 2005. DOI: 10.1021/ie050647y.

YOON, Younggun; CHUNG, Hay Jung; WEN DI, Doris Yoong; DODD, Michael C.; HUR, Hor Gil; LEE, Yunho. Inactivation efficiency of plasmid-encoded antibiotic resistance genes during water treatment with chlorine, UV, and UV/H2O2. **Water Research**, *[S. l.]*, v. 123, p. 783–793, 2017. DOI: 10.1016/j.watres.2017.06.056. Disponível em: http://dx.doi.org/10.1016/j.watres.2017.06.056.

YOON, Younggun; DODD, Michael C.; LEE, Yunho. Elimination of transforming activity and gene degradation during UV and UV/H2O2 treatment of plasmid-encoded antibiotic resistance genes. **Environmental Science: Water Research and Technology**, *[S. l.]*, v. 4, n. 9, p. 1239–1251, 2018. DOI: 10.1039/c8ew00200b.

ZANKARI, Ea; HASMAN, Henrik; COSENTINO, Salvatore; VESTERGAARD, Martin; RASMUSSEN, Simon; LUND, Ole; AARESTRUP, Frank M.; LARSEN, Mette Voldby. Identification of acquired antimicrobial resistance genes. **Journal of Antimicrobial Chemotherapy**, *[S. l.]*, v. 67, n. 11, p. 2640–2644, 2012. DOI: 10.1093/jac/dks261.

ZAPPI, Mark; WHITE, Kenneth; HWANG, Huey Min; BAJPAI, Rakesh; QASIM, Mohammad. The fate of hydrogen peroxide as an oxygen source for bioremediation activities within saturated aquifer systems. **Journal of the Air and Waste Management Association**, *[S. l.]*, v. 50, n. 10, p. 1818–1830, 2000. DOI: 10.1080/10473289.2000.10464207.

ZHANG, Chiqian; BROWN, Pamela J. B.; HU, Zhiqiang. Higher functionality of bacterial plasmid DNA in water after peracetic acid disinfection compared with chlorination. **Science of the Total Environment**, *[S. l.]*, v. 685, p. 419–427, 2019. DOI: 10.1016/j.scitotenv.2019.05.074. Disponível em: https://doi.org/10.1016/j.scitotenv.2019.05.074.

ZHANG, Guosheng; LI, Weiying; CHEN, Sheng; ZHOU, Wei; CHEN, Jiping. Problems of conventional disinfection and new sterilization methods for antibiotic resistance control. **Chemosphere**, *[S. l.]*, v. 254, p. 126831, 2020. a. DOI: 10.1016/j.chemosphere.2020.126831. Disponível em: https://doi.org/10.1016/j.chemosphere.2020.126831.

ZHANG, Houpu; ZHANG, Zihan; SONG, Jiajin; CAI, Lin; YU, Yunlong; FANG, Hua. Foam shares antibiotic resistomes and bacterial pathogens with activated sludge in wastewater treatment plants. **Journal of Hazardous Materials**, *[S. l.]*, v. 408, n. August 2020, p. 124855, 2021. a. DOI: 10.1016/j.jhazmat.2020.124855. Disponível em: https://doi.org/10.1016/j.jhazmat.2020.124855.

ZHANG, Huaicheng; CHANG, Fangyu; SHI, Peng; YE, Lin; ZHOU, Qing; PAN, Yang; LI, Aimin. Antibiotic Resistome Alteration by Different Disinfection Strategies in a Full-Scale Drinking Water Treatment Plant Deciphered by Metagenomic Assembly. **Environmental Science and Technology**, *[S. l.]*, v. 53, n. 4, p. 2141–2150, 2019. a. DOI: 10.1021/acs.est.8b05907.

ZHANG, Lingling; JIN, Hui; MA, Hongkun; GREGORY, Kelvin; QI, Zhongwei; WANG, Chenxi; WU, Wentong; CANG, Daqiang; LI, Zifu. Oxidative damage of antibiotic resistant E. coli and gene in a novel sulfidated micron zero-valent activated persulfate system. **Chemical Engineering Journal**, *[S. l.]*, v. 381, n. 30, p. 122787, 2020. b. DOI: 10.1016/j.cej.2019.122787. Disponível em: https://doi.org/10.1016/j.cej.2019.122787.

ZHANG, Menglu; CHEN, Sheng; YU, Xin; VIKESLAND, Peter; PRUDEN, Amy. Degradation of extracellular genomic, plasmid DNA and specific antibiotic resistance genes by chlorination. **Frontiers of Environmental Science and Engineering**, *[S. l.]*, v. 13, n. 3, 2019. b. DOI: 10.1007/s11783-019-1124-5.

ZHANG, Ye; GU, April Z.; HE, Miao; LI, Dan; CHEN, Jianmin. Subinhibitory Concentrations of Disinfectants Promote the Horizontal Transfer of Multidrug Resistance Genes within and across Genera. **Environmental Science and Technology**, *[S. l.]*, v. 51, n. 1, p. 570–580, 2017. DOI: 10.1021/acs.est.6b03132.

ZHANG, Yingying; ZHUANG, Yao; GENG, Jinju; REN, Hongqiang; XU, Ke; DING, Lili. Reduction of antibiotic resistance genes in municipal wastewater effluent by advanced oxidation processes. **Science of the Total Environment**, *[S. l.]*, v. 550, p. 184–191, 2016. DOI: 10.1016/j.scitotenv.2016.01.078.

ZHANG, Yiqing; XIAO, Yongjun; ZHONG, Yang; LIM, Teik Thye. Comparison of amoxicillin photodegradation in the UV/H2O2 and UV/persulfate systems: Reaction kinetics, degradation pathways, and antibacterial activity. **Chemical Engineering Journal**, *[S. l.]*, v. 372, n. April, p. 420–428, 2019. c. DOI: 10.1016/j.cej.2019.04.160. Disponível em: https://doi.org/10.1016/j.cej.2019.04.160.

ZHANG, Yiting; ZHANG, Menglu; YE, Chengsong; FENG, Mingbao; WAN, Kun; LIN, Wenfang; SHARMA, Virender K.; YU, Xin. Mechanistic insight of simultaneous removal of tetracycline and its related antibiotic resistance bacteria and genes by ferrate(VI). **Science of the Total Environment**, *[S. l.]*, v. 786, p. 147492, 2021. b. DOI: 10.1016/j.scitotenv.2021.147492. Disponível em: https://doi.org/10.1016/j.scitotenv.2021.147492.

ZHOU, Chun shuang et al. Removal of antibiotic resistant bacteria and antibiotic resistance genes in wastewater effluent by UV-activated persulfate. **Journal of**

Hazardous Materials, *[S. l.]*, v. 388, n. January, p. 122070, 2020. DOI: 10.1016/j.jhazmat.2020.122070. Disponível em: https://doi.org/10.1016/j.jhazmat.2020.122070.

ZHOU, Chun shuang; CAO, Guang li; WU, Xiu Kun; LIU, Bing feng; QI, Qing Yue; MA, Wan Li. Removal of antibiotic resistant bacteria and genes by nanoscale zero-valent iron activated persulfate: Implication for the contribution of pH decrease. **Journal of Hazardous Materials**, *[S. l.]*, v. 452, n. March, p. 131343, 2023. DOI: 10.1016/j.jhazmat.2023.131343. Disponível em: https://doi.org/10.1016/j.jhazmat.2023.131343.